THE COLLISION AVOIDANCE PROBLEM: METHODS AND ALGORITHMS

by

Francisco Javier Martín Campo

Supervisors:

Laureano F. Escudero and **Antonio Alonso Ayuso**

November, 2010

Department of Statistics and Operations Research

Rey Juan Carlos University

Don Laureano F. Escudero, Catedrático de la Universidad Rey Juan Carlos del Departamento de Estadística e Investigación Operativa y don Antonio Alonso Ayuso, Profesor Titular de la Universidad Rey Juan Carlos del Departamento de Estadística e Investigación Operativa AUTORIZAN:

La presentación de la Tesis Doctoral titulada ***The Collision Avoidance Problem: Methods and Algorithms*** realizada por Don Francisco Javier Martín Campo bajo nuestra inmediata dirección y supervisión en el Departamento de Estadística e Investigación Operativa y que presenta para la obtención del grado de Doctor por la Universidad Rey Juan Carlos.

En Móstoles, a 5 de Noviembre de 2010

Laureano F. Escudero Antonio Alonso Ayuso

Don Antonio Alonso Ayuso, Profesor Titular de Universidad y director del Departamento de Estadística e Investigación Operativa de la Universidad Rey Juan Carlos INFORMA:

Que la Tesis Doctoral titulada ***The Collision Avoidance Problem: Methods and Algorithms*** ha sido realizada por Don Francisco Javier Martín Campo bajo la dirección y supervisión de Don Laureano F. Escudero y Don Antonio Alonso Ayuso y que el Departamento ha dado su conformidad para que sea presentada ante la Comisión de Doctorado.

En Móstoles, a 5 de Noviembre de 2010

Antonio Alonso Ayuso

A mis padres, mi hermana,

familiares y amigos.

To my parents, my sister,

my family and friends.

Contents

List of Tables

List of Figures

Agradecimientos

“Agradece a la llama su luz, pero no olvides el pie del candil que, constante y paciente, la sostiene en la sombra” (Rabindranath Tagore).

Quiero aprovechar la oportunidad de agradecer todo el apoyo constante recibido durante la realización de este trabajo. No existe nada de tal valor que pueda pagar el impulso de mis padres, mi hermana y Nieves, que me hicieron aprender que todo en la vida es posible si uno se enfrenta a ello con valentía, haciendo que las cumbres jamás soñadas acaben rendidas a nuestros pies. El calor del hogar, a veces desde la distancia, supuso una recarga de energía en los momentos en los que parecía que todo el trabajo se detenía o incluso daba la sensación de dar marcha atrás, haciendo que nuevos caminos surgieran de la nada frente a mí.

Sin duda, esta tesis no habría llegado a su fin sin la colaboración sin medida de mis directores Antonio, y sobre todo Laureano, ya que gracias a su experiencia y conocimientos en el campo de la Investigación Operativa lograron que mi entusiasmo por esta disciplina aumentaran día a día. No podré olvidar cómo lograron inculcar en mí la puesta en práctica de los valores de la *constancia*, reflejado en el tan repetido lema “lo queremos para ayer”, y de la *paciencia* ante los obstáculos que iban surgiendo, apostando por el lema “todo trabajo bien hecho finalmente da su fruto”.

Todavía recuerdo los primeros pasos andados en el departamento, que me acogió con los brazos abiertos desde el primer instante. Con todos ellos estoy en deuda, ya que hicieron idóneo el entorno en el cual he desarrollado mi actividad docente e investigadora, sintiéndome uno más y compartiendo luchas y alegrías.

En último lugar, y no por ello menos importantes, son los agradecimientos a mis amigos, por su constante interés en la evolución de mi tesis, sus fervientes ánimos y por la

celebración que nos espera si todo termina bien. Especialmente quisiera agradecer a Carlos Javier la generosidad al compartir sus conocimientos y pasión por la aviación.

Acknowledgements

"Be grateful to the flame for its light, but do not forget the base of the lamp that, constant and patient, holds it up in the shadow" (Rabindranath Tagore).

I would like to take advantage of this opportunity say thank you for the constant support received during my work on this project. There is nothing so valuable that ever could repay the encouragement of my parents, my sister and Nieves, who made me learn that everything in life is possible if one confronts it with bravery, making undreamed of heights fall defeated at our feet. The warmth of home, sometimes from a distance, meant a charge of energy at times when it seemed that the whole project was coming to a standstill or even when it seemed to be going backward, making it so that new paths came out of nowhere to open in front of me.

Without a doubt, this thesis would not have seen the light of day without the invaluable collaboration of my advisors Laureano and Antonio. Thanks to their experience and knowledge in the field of operations research they managed to steadily increase my enthusiasm for this discipline. I will not be able to forget how they were able to instill in me the values of *perseverance*, reflected in the oft-repeated motto, "we want it for yesterday' and of *patience* in the face of obstacles that came up, putting faith in the motto "all work well done eventually bears fruit".

I still remember my first steps in the department, which accepted me with open arms from the very beginning. I am in debt to all of them, since they created an ideal environment in which I have developed my teaching and research skills, feeling like one of them and sharing joys and struggles.

Last but not least are the acknowledgements for my friends, for their constant interest in the evolution of my thesis, their passionate encouragement and for the celebration

that awaits us if everything ends well. I would especially like to thank Carlos Javier and his generosity in sharing his knowledge and passion for aviation.

Resumen

Introducción

La detección y resolución de conflictos aéreos es actualmente un tema de gran interés para muchas compañías de servicios aéreos que se preocupan por dar respuesta a la siguiente cuestión: Dado un conjunto de aeronaves y sus trayectorias previstas, ¿qué estrategia debería llevarse a cabo por medio de los pilotos y controladores aéreos para prevenir que los aviones entren en conflicto debido a que las trayectorias de los mismos intersequen entre sí?

Se han elaborado varios métodos para mantener la separación entre aviones en el espacio aéreo actual a partir de las características de rutas estructuradas y procedimientos desarrollados. El factor humano es un elemento esencial en este proceso debido a la habilidad de integrar información, analizarla y tomar las decisiones oportunas. No obstante, debido a que pueden producirse errores operacionales, los sistemas autómatas han empezado a tomar posesión tanto en la cabina de pilotos como en las bases de control aéreo para ofrecer una decisión y servir como sistemas de alerta de conflictos. Estos sistemas usan un sensor de datos para predecir conflictos entre aviones, alertar de ellos al factor humano y ofrecer un conjunto de instrucciones a seguir para resolver dichos conflictos. Los métodos de prevención de conflictos relativamente sencillos han formado parte del control automático de tráfico aéreo varios años, y el sistema de prevención de colisiones ha tomado lugar en el transporte aéreo, dentro de las cabinas de las aeronaves, desde principios de los 90. Juntos, estos sistemas automáticos ofrecen una red de procedimientos y acciones entre controlador y piloto que hacen mantener las separaciones mínimas establecidas.

Recientemente, ha crecido el interés hacia el desarrollo de sistemas automáticos más avanzados para detectar conflictos en tráfico aéreo y poder ofrecer asistencia a su resolución.

Estos sistemas podrían hacer uso de tecnologías futuras, tales como información sobre planes actuales de vuelo, para mejorar así la seguridad y permitir nuevos procedimientos para aumentar la eficiencia del flujo de tráfico aéreo.

Con el incremento de la demanda en el campo aéreo, hay una necesidad urgente de implementar este tipo de sistemas para asistir a los controladores aéreos en el manejo de las cargas de tráfico y mejorar la eficiencia del flujo aéreo.

En la literatura se han propuesto varios métodos para tratar la detección y resolución de conflictos en el espacio aéreo. Estos métodos se han estudiado no solamente para fines aeroespaciales, sino también para vehículos de tierra, en robótica y aplicaciones marítimas, dado que las cuestiones fundamentales de prevención de conflictos son similares a otros medios de transporte. Un resumen de la investigación reciente sobre el problema de detección y resolución de conflictos aéreos, sugiere que el entorno actual debe ser tal que en él debe darse una solución aproximada al problema y ejecutada, normalmente a través de un conjunto de ejemplos simplificados. No obstante, en este trabajo se presenta una modelización y algoritmia que permite avanzar en el estado-del-arte de la investigación en el problema.

Para comenzar, es necesario tener una definición clara y concisa de un conflicto. Un conflicto es una situación en la cual dos o más aviones experimentan una pérdida de separación mínima. En otras palabras, la distancia entre los aviones viola un criterio de separación establecido. Un criterio frecuentemente utilizado es una distancia mínima de 5 millas náuticas respecto a la distancia horizontal y al menos 1000 pies de separación vertical. El resultado es una zona protegida o un volumen de espacio alrededor de cada avión que no debe ser infringido en ningún instante de tiempo por cualquier otro vehículo. El espacio protegido podría ser definido también como una región más pequeña (por ejemplo, una esfera de 500 pies de diámetro) en el caso de sistemas de alerta de conflictos en entornos más tácticos, o incluso en términos de otros parámetros que no sean distancias (como por ejemplo, el tiempo). En cualquier caso, las funciones subyacentes del problema son similares, aunque los modelos específicos y los umbrales de alerta serían diferentes.

El objetivo de los sistemas automáticos es predecir la ocurrencia de un conflicto en el futuro, asistir en la resolución del mismo y, en algunos casos, comunicar el conflicto detectado a un operador humano.

Se requiere un modelo dinámico en el cual se tenga en cuenta el tiempo para ayudar a predecir las diferentes posiciones de los aviones en el futuro y así poder deducir si tendrá lugar un conflicto o no. Esta predicción debería estar basada únicamente en la información

del estado actual del avión (una extrapolación a través de una línea recta del vector de velocidad actual) o en información adicional tal como un plan de vuelo, ya que, con la información del estado actual del avión, puede no ser del todo fiable la estimación de la trayectoria futura debido a la incertidumbre que rodea al modelo.

La información, en lo que respecta a los estados actual y futuro del avión, puede ser analizada conjuntamente para una mejor toma de decisiones finales. Algunos análisis incluyen una mínima separación pronosticada o el tiempo estimado al punto más cercano propuesto. Mientras que los estados actual y futuro pueden generalmente ser estimados independientemente de cada avión, el análisis del conflicto requiere el estudio conjunto de los distintos vehículos envueltos en él.

Son muchos los medios que se han estudiado para la resolución de este problema en el campo de la aviación. Un resumen de gran parte de la bibliografía existente en el tema que nos concierne, puede ser estudiada en el primer capítulo de esta memoria. Sin embargo, el trabajo presentado utiliza como herramienta principal la optimización matemática, definida dentro del campo de la Investigación Operativa. La razón principal para tomar esta decisión, ha sido la estructura que posee un modelo de optimización matemática, en el que forman parte una o varias funciones objetivo y un conjunto de restricciones. En este problema, la función objetivo pierde protagonismo frente al conjunto de restricciones que es la parte más importante del modelo matemático en este trabajo. Si se consigue modelar matemáticamente las restricciones que envuelven a cada aeronave (distancia que deben mantener, tanto horizontal como vertical, velocidades y alturas dentro de sus cotas, etc.), ofreciendo en segundo plano un objetivo a conseguir, que se verá reflejado en la función objetivo del modelo, el problema podría abordarse usando las algoritmias de optimización matemática desarrolladas hasta el momento, clasificando previamente el modelo en las subcategorías establecidas dentro de la optimización matemática (lineal, no lineal, entera, continua, etc.)

Objetivos

El objetivo principal de este trabajo consiste en la creación de un modelo matemático capaz de resolver el problema de la prevención de conflictos en una porción de espacio aéreo determinado previamente, así como el uso de las herramientas necesarias para su resolución e interpretación de los parámetros correspondientes.

Para ello es necesaria una serie de parámetros iniciales que conforman la configuración inicial de cada una de las aeronaves bajo consideración. A partir de esta configuración, el modelo propuesto debe en primer lugar tener en cuenta esta serie de parámetros iniciales y, en segundo lugar, ofrecer una solución adecuada al problema que se está tratando para, finalmente, expresar dicha solución en términos que sean comprensibles para cualquier controlador aéreo.

Por último, se ha de desarrollar una experiencia computacional suficiente para el conocimiento de la calidad de las soluciones propuestas y el conjunto de recursos (hardware, software, tiempo computacional, etc.) necesitado.

Metodología

Para llevar a cabo los objetivos propuestos anteriormente se ha desarrollado el siguiente plan de trabajo:

En primer lugar, se ha realizado una revisión intensiva de la literatura existente hasta el momento relacionada con el problema a resolver, como un punto de partida hacia el adecuado conocimiento del problema. Dentro de esta literatura se enfatizó en el estudio de aquéllos trabajos que utilizaban técnicas basadas en optimización matemática, eligiendo como pilar de los modelos que se proponen en la tesis doctoral, el trabajo propuesto por Pallottino et al. en 2002 [85]. Este trabajo propone dos modelos basados en optimización lineal entera mixta para la resolución de conflictos aéreos. El primero de ellos es denominado “Velocity Changes”, VC, (i.e., cambios de velocidad), que se presentaba incompleto al verse incapaz de resolver numerosos casos que pueden darse en casos realísticos, además de presentar inestabilidad en casos en los que no se tiene en cuenta un posible denominador nulo. El segundo modelo que proponían los autores es el denominado “Heading Angle Changes”, HAC, (cambios de dirección de vuelo), que no puede ser aceptado para su implementación real al considerar una hipótesis muy fuerte, que no se da en casos reales, por la cual todos los aviones deben volar a la misma velocidad constante. Por esta razón, no se consideró esta parte del trabajo en el desarrollo de los modelos propuestos en la tesis doctoral.

Por tanto, tomando como sustento el modelo VC, el siguiente paso fue el desarrollo de un modelo capaz de tomar las ventajas del VC sin dejar de contemplar los numerosos casos que éste es incapaz de resolver, como los citados a continuación:

- “Frente a frente”.
- Cercanía entre las dos aeronaves.
- Persecución entre dos aeronaves, siguiendo la misma trayectoria, donde la velocidad de la aeronave perseguida es considerablemente menor.
- Inestabilidad en situaciones en las que existe un denominador nulo.

Ante los tres primeros casos, se optó por la inclusión de maniobras verticales (i.e., cambios de altura), de tal modo que con la simple realización de esta maniobra se resuelven los conflictos. Sin embargo, para el último caso era necesario un estudio más profundo de estas situaciones peculiares, resolviéndose finalmente mediante el giro del sistema de referencia de los parámetros de configuración de las aeronaves implicadas, evitando de este modo el denominador nulo.

El resultado de todas estas consideraciones es el modelo matemático denominado “Velocity and Altitude Changes”, VAC, (i.e., cambios de velocidad y altura), basado en optimización lineal entera mixta y que se presenta detalladamente en el capítulo 2.

A pesar de la eficiencia del modelo, se determinó la conveniencia de ampliar el mismo, de tal modo que se incluyera en el nuevo modelo el horizonte temporal. De este modo surge el modelo matemático denominado “Velocity Changes with Time Periods”, VCTP, (i.e., cambios de velocidad con períodos de tiempo), basado en optimización no lineal 0-1 mixta, y que se presenta detalladamente en el capítulo 3.

Las ventajas que aporta este modelo al modelo anterior son:

- Consideración de horizonte temporal.
- Continuidad en las maniobras de velocidad.
- Detección temprana de conflictos lejanos.

La principal ventaja de este último modelo es la consideración de un horizonte temporal tan amplio como se desee, de modo que pueden detectarse conflictos lejanos con tiempo suficiente de modo que el impacto de la maniobra de velocidad a realizar es menor. Otra ventaja es la consideración de un término de aceleración, haciendo que los cambios realizados se produzcan de manera continua en el tiempo. Ante el gran tiempo de ejecución

necesario para resolver el problema para casos de dimensiones no muy grandes, se vio la necesidad de integrar un método metaheurístico de modo que la resolución se realizara en menor tiempo. El tipo de algoritmia utilizado es el de "búsqueda de entorno variable" (VNDS, del inglés *Variable Neighbourhood Decomposition Search*), ofreciendo soluciones que a priori se presentan eficientes. Cabe destacar que en este problema prima la seguridad (es decir, una solución factible), sobre la optimalidad (maniobras menos eficientes). Como línea de investigación futura se realizará la inclusión de esquemas basados en relajación Lagrangiana, de modo que se pueda medir la eficiencia de las soluciones a partir de la diferencia ponderada entre la cota superior (ofrecida por la metaheurística de búsqueda de entorno variable) y la cota inferior (ofrecida por el esquema Lagrangiano) de la función objetivo elegida.

Resultados

Tras la depuración de cada modelo, se ha realizado una extensa experiencia computacional para cada uno de ellos, valorando la consecución de los objetivos prefijados de antemano (detección y prevención de conflictos, tiempo de ejecución razonable, etc)

Para el primer modelo que se presenta en este trabajo, la experiencia computacional ofreció grandes resultados en cuanto a la resolución de los conflictos se refiere, así como a su tiempo de ejecución, realmente impresionante, ya que para casos realistas el software estado-del-arte empleado para su resolución logra la solución óptima en cuestión de centésimas de segundo, pudiéndose aplicar este modelo en tiempo real, ayudando al agente encargado de la supervisión del tráfico aéreo a tomar la decisión final sobre la resolución de cada conflicto. Además de estos impresionantes resultados, se logró el objetivo de cubrir todos los frentes que el modelo VC dejó abiertos: inestabilidad frente a la existencia de denominadores nulos, casos que no pueden ser resueltos, etc. Por tanto, el modelo diseñado puede entrar en la categoría matemática de "modelos fuertes de optimización".

En el segundo modelo el objetivo se centró en realizar la detección y resolución de conflictos en un horizonte de planificación más extenso, tratando de extender el primer modelo propuesto, ofreciendo resultados más reales aún al incorporar al modelo un término de aceleración, haciendo que los cambios en velocidad puedan ser contemplados de modo continuo. Las primeras experiencias computacionales realizadas sobre el modelo VCTP, trantándolo directamente como un problema de optimización no lineal 0-1 mixta no fueron

muy satisfactorios, ya que debido a la existencia de raíces cuadradas y fracciones en determinadas restricciones del modelo, las distintas plataformas para resolución de problemas de esta envergadura no iniciaban sus algoritmos. Por tanto, se decidió resolver el problema mediante aproximaciones lineales sucesivas de las restricciones del modelo, y afrontar su resolución usando plataformas específicas para resolver problemas sucesivos de optimización matemática 0-1 mixta. Aun así, los tiempos de resolución no fueron suficientemente brillantes debido a la complejidad algorítmica del método de "ramificación y corte" que se emplea para la resolución de este tipo de problemas, haciendo lenta la resolución para problemas de tamaño medio-largo. Sin embargo, las soluciones factibles que se obtenían cumplían con los objetivos pretendidos por el modelo.

Para la consecución de mejores resultados, en cuanto a tiempo de resolución se refiere, se optó por la utilización de esquemas metaheurísticos. Este tipo de algoritmia tiene su mayor inconveniente en no poder asegurar la optimalidad de la solución final obtenida, pero posee la gran ventaja de ofrecer soluciones muy buenas en tiempos muy cortos. En este tipo de problema prima la seguridad por encima de la optimalidad, por tanto, la consecución de soluciones cercanas a la óptima pero que aseguran en todo caso ser factibles, no supone una importante debilidad. La algoritmia metaheurística elegida fue VNDS, como previamente se ha indicado, junto a una algoritmia de "ramificación local" en modelos de optimización matemática entera mixta. De este modo, no se dejó de un lado el modelo matemático desarrollado. La experiencia computacional aportada en este trabajo revela que los resultados son bastante buenos, ya que la consecución de soluciones factibles se realiza en tiempos cortos. Como último paso queda medir la calidad de estas soluciones obtenidas, ya que son cotas superiores de la función objetivo del problema (el objetivo es minimización), siendo importante la implementación de esquemas que aporten buenas cotas inferiores, como han demostrado ser los esquemas de Relajación Lagrangiana. Una vez que estos métodos estén implementados será posible medir la calidad de las soluciones obtenidas a través de la diferencia tipificada entre ambas cotas conseguidas en la función objetivo.

Conclusiones

Como conclusiones del trabajo realizado destacan las siguientes:

- Tras una fuerte revisión bibliográfica, el problema de prevención de conflictos ha sido abordado desde diferentes disciplinas. En la mayoría de los casos, o bien las hipótesis

de partida, o bien las dimensiones del problema, o bien las soluciones obtenidas no eran las adecuadas para abordar el problema desde la realidad, resaltando la dificultad del problema a tratar. La optimización matemática se adapta bien al problema a tratar, ya que si se modelan adecuadamente las restricciones del problema, se obtiene un modelo teórico ajustable a la realidad. Sin embargo, en numerosos casos la existencia de no linealidad en el modelo desarrollado, hace que el coste computacional sea excesivo.

- Se ha desarrollado un modelo basado en optimización lineal entera mixta, VAC, ofreciendo soluciones óptimas a bajo coste computacional, de modo que este modelo puede ser aplicado en tiempo real. Este modelo matemático absorbe como caso particular el modelo VC propuesto anteriormente, resolviendo aquéllos casos que éste último es incapaz de resolver y dando solución a casos particulares en los que un denominador nulo hacen inestable el modelo.

- Se ha desarrollado otro modelo matemático basado en optimización no lineal 0-1 mixta, el VCTP, que aporta como novedad la inclusión de un horizonte temporal tan amplio como se desee. Aprovechando la discretización del espacio temporal en períodos de tiempo, se ha incluido un término de aceleración al modelo aportando continuidad a los cambios de velocidad.

- Debido al alto coste computacional al resolver el modelo VCTP mediante algoritmias que garantizan la optimalidad de la solución, se ha implementado un esquema metaheurístico basado en "búsqueda de entorno variable", de tal modo que se obtienen soluciones buenas en tiempo razonable. El inconveniente de este tipo de algoritmia es que no dispone de herramientas necesarias para evaluar la calidad de la solución obtenida. Sin embargo, esto no supone una debilidad, ya que sí se asegura la factibilidad de la solución obtenida, de modo que la seguridad en el espacio aéreo no se ve disminuida.

Difusión de resultados

Los resultados de este trabajo han sido presentados en los siguientes eventos:

- XXXI Congreso Nacional de la SEIO. *On the collision avoidance for air traffic management problem* (Agustín, A.; Alonso-Ayuso, A.; Escudero, L. F.; Martín-Campo,

F. J.; Olaso, P.; Pizarro, C.). Murcia. Febrero 2009.

- The Advanced School on Mathematical Modeling. *On the collision avoidance problem* (Martín-Campo, F. J.). Sevilla (España). Junio 2009.

- XXIII Congreso de EURO. *A short term approach for the collision avoidance for air traffic management problem* (Martín-Campo, F. J.; Agustín, A.; Pizarro, C.). Bonn (Alemania). Julio 2009.

- XXIII Congreso de EURO. *On the collision avoidance for air traffic management problem, a large scale mixed 0-1 program approach* (Olaso, P.; Pizarro, C.; Martín-Campo, F. J.). Bonn (Alemania). Julio 2009.

- Advanced Course on Optimization: Theory, Methods and Applications. *On the collision avoidance for air traffic management problem* (Martín-Campo, F. J.). Barcelona. Julio 2010.

- Workshop on Mixed Integer Nonlinear Programming. *Collision avoidance for the ATM problem: A mixed 0-1 nonlinear model* (Martín-Campo, F. J.; Alonso-Ayuso, A.; Escudero, L. F.). Marsella (Francia). Abril 2010.

- XXIII Conferencia ECCO. *A mixed 0-1 nonlinear approach for the collision avoidance for the Air Traffic Management Problem* (Martín-Campo, F. J.; Alonso-Ayuso, A.; Escudero, L. F.). Málaga. Mayo 2010.

- XXIV Congreso EURO. *Collision avoidance for the ATM problem: A mixed 0-1 nonlinear approach* (Martín-Campo, F. J.; Alonso-Ayuso, A.; Escudero, L. F.). Lisboa (Portugal). Julio 2010.

- XXXII Congreso Nacional de la SEIO. *A mixed 0-1 nonlinear approach for the collision avoidance problem* (Martín-Campo, F. J.; Alonso-Ayuso, A.; Escudero, L. F.). A Coruña. Septiembre 2010.

Además de la presentación del trabajo en los eventos enumerados anteriormente, parte del trabajo realizado ha sido aceptado para publicación, y ya se ha publicado online, como puede observarse en las referencias bibliográficas [7, 8, 9]

Líneas de investigación futura

El trabajo que a continuación se presenta, ofrece un nuevo punto de vista al tratamiento del problema de prevención de conflictos aéreos. Sin embargo, nuevas líneas de investigación se abren para el desarrollo de modelos más precisos capaces de resolver el problema de forma eficiente en un tiempo computacional adecuado. Algunas líneas de investigación futura son:

- En primer lugar, una de las deficiencias del modelo VAC descrito en el capítulo 2 es la consideración de cambios instantáneos en velocidad y altura. No es una deficiencia grave, ya que los tiempos que un avión necesita para la realización de tales maniobras no excede los diez segundos en el caso de los cambios de velocidad (considerando el paso de la velocidad mínima a la máxima). En el caso de la altura el problema es menor, ya que los conflictos son detectados con tiempo suficiente para realizar las maniobras verticales oportunas. Sin embargo, la obtención de un modelo capaz de integrar la continuidad en los cambios, mejoraría los resultados obtenidos con el modelo VAC. Una línea de investigación futura es, por tanto, la obtención de un modelo, quizá bietápico, capaz de incluir la continuidad en las maniobras en el modelo matemático, creando un modelo intermedio entre los modelos matemáticos VAC y VCTP.

- Es necesario el estudio de la cota inferior en el modelo propuesto VCTP, en el capítulo 3, ya que con el tipo de algoritmia metaheurística empleada, VNDS, se obtiene una buena cota superior del valor de la función objetivo, pero hay que dar medida a la calidad de la cota, y para ello es importante el estudio de la cota inferior. Con la obtención de estas dos cotas, estudiando la diferencia entre ambas dentro de las magnitudes del problema, es posible determinar si la solución obtenida con el modelo VCTP es realmente buena o no. Para la obtención de esta cota inferior es necesaria la implementación de esquemas de Relajación Lagrangiana, ya que es sabido que éstos aportan cotas inferiores fuertes a la solución óptima de los problemas tratados.

- Otro frente que queda abierto tras la implementación del modelo VCTP es la inclusión en el mismo de maniobras verticales, a ser posible de modo continuo aprovechando los intervalos de tiempo usados en el modelo matemático. De este modo, se afrontarían los conflictos con dos maniobras distintas, aportando un mayor espacio de soluciones factibles y evitando situaciones infactibles si sólo se contemplan las

maniobras en velocidad (casos como “frente a frente”, persecución de un avión a otro en la misma trayectoria pero con velocidad menor en el avión perseguido, etc.)

- Para los dos modelos estudiados en el trabajo presentado, es importante la mejora de la función objetivo, en la cual pueden incluirse otras consideraciones no estudiadas que, sin embargo, sean importantes para la resolución del problema.

- Finalmente, es importante poder introducir en los modelos presentados la última posibilidad de maniobra, consistente en cambios de dirección en las aeronaves. Su estudio puede implicar la posibilidad de ecuaciones no lineales, debido a la naturaleza no lineal de estas maniobras. Sin embargo, estas maniobras deberían realizarse sólo en aquellos casos en los que los cambios de velocidad o altura sean insuficientes para evitar los conflictos, ya que suponen un incremento en la distancia recorrida que repercute directamente en posibles retrasos sobre los planes iniciales del vuelo.

Preface

Presentation and motivation

The aim of the presented work is the intensive study of an important problem in the aviation field, such as air traffic management. Due to the increase in the demand along the last years, the implementation of new techniques that make a more efficient management of the air traffic is very important. One of the future objectives is the elimination of the air ways, providing more independence and autonomy to the pilots, and allowing the incorporation of the very known "free flight". This ambitious proposal is very complex in a field where the security is the most important aspect to take into account.

Working together in a common project, called ATLANTIDA, with the company GMV and the Rey Juan Carlos Universtiy, three important objectives were fixed:

- Optimal air flow management, taking into account the possible delays in the air as well as ground holding delays.
- Optimal trajectories for each aircraft taking into account all physical elements that take place in the aircraft engineering.
- Detection and resolution of the possible conflicts in the airspace between different aircraft.

As far as this work is concerned, the study of the third objective is the main aim to tackle. Several conflict situations can happen in the airspace between some aircraft, being those ones the loss of the minimum separation between the aircraft involved. Briefly, the goal of the work is deciding the best strategy for the new aircraft configurations where no conflicts exist. This problem has been studied from different points of view in several

scientific fields. The proposal in this work is raising this problem by using mathematical optimization. The nature of the problem description has the same structure as a traditional problem in mathematical optimization, where a set of constraints and an objective function take place. In this problem, the set of constraints has to be such that all the equations together implement the main aspects of the problem.

Thesis objectives

In this work, two different models based on mathematical optimization have been developed, via mixed integer linear and mixed 0-1 nonlinear optimization, respectively. For the resolution of the first one, exact schemes have been used, whereas for the second model, exact and metaheuristic schemes are needed for the resolution.

Thesis outline

The thesis is structured as follows:

- Chapter 1 presents an overview about the main contributions for the collision avoidance problem as well as a compact summary in a table of the studied bibliography.
- Chapter 2 is devoted to study a previous model based on mixed integer linear optimization so called “Velocity Changes” (VC) proposed by Pallottino et al. (2002). In this model an interesting geometric construction is studied and a mathematical optimization model based on this construction is developed. Despite the interest of this model, several important weak points have to be solved. The aim of this chapter is extending this mathematical model including important aspects that the authors did not take into account and, then, developing a new mathematical model based on mixed integer linear optimization so called “Velocity and Altitude Changes” (VAC).
- Chapter 3 presents an extension of the VAC model including a larger time horizon divided in time periods that will be useful for the inclusion of the acceleration term, making the velocity changes continuous in time. The result of this extension is the so called “Velocity Changes with Time Periods” (VCTP), being this one based on mixed 0-1 nonlinear optimization. The difficulty to solve this problem by using exact schemes culminated in the linearization of the nonlinear constraints to solve the mo-

del by using mixed 0-1 linear schemes. Due to the big computing times for solving medium-large dimensional problems, a metaheuristic algoritmia based on "Variable Neighbourhood Decomposition Search" was implemented to solve the model achieving good results in short computing time.

- Chapter 4 presents the main conclusions, important contributions and the open future research lines.

Original contributions

The Collision Avoidance Problem has been studied from different points of view and research fields. It can be found in the thesis the following original contributions:

- A mathematical model based on mixed integer linear optimization is developed, extending the VC model proposed by Pallottino et al. (2002) [85], solving efficiently the weak points of the model and with very short execution times, making this model able to be applied in real time, helping the air traffic controllers decision making.
- Additionally, a mathematical model based on mixed 0-1 nonlinear optimization is developed, introducing a large horizon time that allows velocity changes to be continuous. Different ways to solve the problem are presented, using firstly exact schemes and after metaheuristic ones.
- A simple visual application was implemented in JAVA with the help of a master student for easing to see the efficiency of the VAC model.

Part of the developed work in this thesis has been accepted for publication:

- IEEE, Transactions on Intelligent Transportation Systems [8].
- Submitted for publication in the Proceedings of the 9th Innovative Research Workshop & Exhibition [9].
- Proceedings of the European Workshop on Mixed Integer Nonlinear Programming [7].

The main results of this thesis have been presented in several national and international meetings:

- XXXI SEIO. *On the collision avoidance for air traffic management problem* (Agustín, A.; Alonso-Ayuso, A.; Escudero, L. F.; Martín-Campo, F. J.; Olaso, P.; Pizarro, C.). Murcia (Spain). February 2009.

- The Advanced School on Mathematical Modeling. *On the collision avoidance problem* (Martín-Campo, F. J.). Seville (Spain). June 2009.

- XXIII EURO. *A short term approach for the collision avoidance for air traffic management problem* (Martín-Campo, F. J.; Agustín, A.; Pizarro, C.). Bonn (Germany). July 2009.

- XXIII EURO. *On the collision avoidance for air traffic management problem, a large scale mixed 0-1 program approach* (Olaso, P.; Pizarro, C.; Martín-Campo, F. J.). Bonn (Germany). July 2009.

- Advanced Course on Optimization: Theory, Methods and Applications. *On the collision avoidance for air traffic management problem* (Martín-Campo, F. J.). Barcelona (Spain). July 2010.

- Workshop on Mixed Integer Nonlinear Programming. *Collision avoidance for the ATM problem: A mixed 0-1 nonlinear model* (Martín-Campo, F. J.; Alonso-Ayuso, A.; Escudero, L. F.). Marseille (France). April 2010.

- XXIII ECCO. *A mixed 0-1 nonlinear approach for the collision avoidance for the Air Traffic Management Problem* (Martín-Campo, F. J.; Alonso-Ayuso, A.; Escudero, L. F.). Málaga (Spain). May 2010.

- XXIV EURO. *Collision avoidance for the ATM problem: A mixed 0-1 nonlinear approach* (Martín-Campo, F. J.; Alonso-Ayuso, A.; Escudero, L. F.). Lisbon (Portugal). July 2010.

- XXXII SEIO. *A mixed 0-1 nonlinear approach for the collision avoidance problem* (Martín-Campo, F. J.; Alonso-Ayuso, A.; Escudero, L. F.). A Coruña (Spain). September 2010.

Chapter 1

State of the art

1.1 Introduction

Aircraft conflict detection and resolution is currently attracting the interest of many air transportation service providers and is concerned with the following question: Given a set of airborne aircraft and their intended trajectories, what control strategy should be followed by the pilots and the air traffic service provider to prevent the aircraft from coming too close to each other?

There have been built methods for maintaining separation between aircraft in the current airspace system. Humans are an essential element in this process due to their ability to integrate information and make judgments. However, because failures and operational errors can occur, automated systems have begun to appear both in the cockpit and on the ground to provide decision support and to serve as traffic conflict alerting systems. These systems use sensor data to predict conflicts between aircraft and alert humans to a conflict and can provide commands or guidance to resolve the conflict. Relatively simple conflict predictors have been a part of air traffic control automation for several years, and the traffic alert and collision avoidance system (TCAS) has been in place onboard domestic transport aircraft since the early 1990s. Together, these automated systems provide a safety net that should provide normal procedures to help controller and pilot when human actions fail to keep aircraft separated beyond established minimums.

Recently, interest has grown toward developing more advanced automation tools to detect traffic conflicts and assist in their resolution. These tools could make use of future technologies, such as a data link of current aircraft flight plan information, to enhance safety

and enable new procedures to improve traffic flow efficiency.

With the growth of airspace congestion, there is an emerging need to implement these types of tools to assist the human operators in handling the expanding traffic loads and improve flow efficiency.

Different methods have been proposed by various researchers to address airborne conflict detection and resolution (CDR). These methods have been developed not only for aerospace, but also for ground vehicle, robotics, and maritime applications because the fundamental conflict avoidance issues are similar across transportation modes. A review of recent CDR research suggests that the current state-of-the-art is one in which a given solution approach to the problem is proposed and exercised, typically through a set of constrained and simplified examples.

To begin with, it is necessary to have a clear definition of a conflict. A conflict is an event in which two or more aircraft experience a loss of minimum separation. In other words, the distance between aircraft violates a criterion what is considered undesirable. One example criterion is a minimum of 5 nmi of horizontal distance between aircraft or at least 1000 ft of vertical separation (the current en-route separation standard at lower altitudes). The result is a protected zone (PZ) or volume of airspace surrounding each aircraft that should not be infringed upon by another vehicle. The PZ could also be defined as a much smaller region (e.g., a sphere 500 ft in diameter) in the case of tactical collision alerting systems, or even in terms of parameters other than distance (e.g., time). In any case, the underlying CDR functions are similar, although the specific models and alerting thresholds would likely be different.

The goal for the CDR system consists of predicting that a conflict is going to occur in the future, assist in the resolution of the conflict situation and, in some cases, communicate the detected conflict to a human operator.

A dynamic trajectory model is required to project the states into the future in order to predict whether a conflict will occur. This projection can be based solely on current state information (e.g., a straight-line extrapolation of the current velocity vector) or it can also be based on additional, procedural information such as a flight plan. In both situations there is generally some uncertainty in the estimate of the future trajectory.

Information regarding the current and predicted states can then be combined to derive metrics used to make traffic management decisions. Some example metrics include pre-

dicted minimum separation or the estimated time to the closest point of approach. Whereas the current and projected states can generally be estimated independently for each aircraft, the conflict metrics require some form of aggregation of the states between the different vehicles involved.

Traditionally, absolute 4D trajectory-based air traffic management and control and relative aircraft-to-aircraft-based spacing concepts have been investigated as alternative pathways. Prevot et al. (2003) [91] describe research in European programs, such as the Program for Harmonized ATC Research in Europe (PHARE) and Co-space, and in USA, programs such as Distributed Air/Ground Traffic Management (DAG-TM). Finally, it was suggested to investigate combinations of these elements.

A recent paper by EUROCONTROL (2009) [35] aimed to specify the required capabilities of Medium-Term conflict Detection (MTCD) for Air Traffic Management Systems (ATMS). The MTCD system is required to detect and notify to the controller of probable loss of the required separation between two aircraft, or aircraft penetrating restricted airspace, or aircraft blocking airspace that might have been used by the other. This paper considers that although flight data and trajectories are provided to the MTCD, some uncertainty is likely on the trajectories. It distinguishes too about tactical and planned trajectories.

Dimarogonas and Kyriakopoulos (2003) [25] review different methods from optimal control, non-cooperative game theory, optimization and others that have been proposed to deal with the problem of conflict avoidance. The most efficient approaches to probabilistic Conflict Detection and Resolution Problem until 2003 were reviewed, where the major contributor to the uncertainty is the wind.

An important aspect to have into account in the problem is how the conflicts in the frontier can be modeled when aircraft, that have taken off or have landed, reach the point in which they have to continue their flights leaving the remote control by the airport controller. Magister (2002 and 2004) [75, 76] models this problem for the sake of facilitating the free-flight concept, using geometric constructions that are included in kinematical equations. Magister in [75] presents two different models: The first one is applied to conflict detection in which a closed interval of conflicting time is calculated, but it does not automatically mean that the aircraft are in conflict, however it is necessary to obtain the final conflict relations. The second one is related to conflict resolution solving the conflict by descending one of the two aircraft in conflict. In this resolution, the author does not take into account the case in which there are more than two aircraft. In [76], Magister describes

the conflict resolution problem in great detail and makes a quantitative analysis of avoidance procedures.

The remainder of the chapter is organized as follows. Section 1.2 is devoted to the most interesting papers existing in the literature on Collision Detection. Section 1.3 is devoted to the main categories of Collision Resolution.

1.2 Collision Detection

Conflict (or Collision) Detection (CD) is the process of detecting conflicts among two or more aircraft, or between an aircraft and some other airspace constraint such as restricted airspace or regions of bad weather.

Let two aircraft be moving on the same horizontal plane, each following its individual flight plan. The flight plan is assumed to consist of a sequence of way points on the plane and a sequence of speeds for moving between them. One can then define the probability of conflict (PC) as the probability that two aircraft will be within an unsafe distance from one another (typically, 5 nm outside the TRACON - Terminal Radar Approach Control - and 3 nautical miles inside the TRACON). Conflict detection consists of estimating PC when it is high.

An earlier work from Chiang et al. (1997) [19] use Delaunay and Voronoi Diagrams to the conflict detection. With this research, they reduce the conflict resolution algorithm from $\mathcal{O}(n^2)$ to $\mathcal{O}(n \log n)$. A contemporary work, by Erzberger et al. (1997) [34] combines deterministic trajectory prediction and stochastic conflict analysis to achieve reliable conflict detection. They formulate error models for trajectory prediction, and describe an efficient algorithm for estimating the conflict probability as a function of encounter geometry.

Prandini et al. [89] deal with aircraft conflict detection at the mid-range and short range levels of the ATMS. Starting from an empirically motivated probabilistic description of the aircraft motion, stochastic models are proposed for mid-term and short term prediction of the aircraft positions, thus, allowing the corresponding criticality measures to take into account the various sources of uncertainty inherent in the environment. Although they focus on the planar case, the extension to the 3-D case is straightforward suggested. However, it is considerably harder to get meaningful bounds for the error of such approximations.

Prandini et al. [90] outline a framework for conflict detection and resolution for pairs of aircraft moving on the same horizontal plane, and the focuss on the prediction component is made. They propose a probabilistic framework, thus allowing uncertainty in the aircraft positions, and solve the problem resorting to appropriate randomized algorithms.

Gandhi et al. (2000) [42] describe approaches to detect airborne obstacles on the collision course and crossing trajectories in video images captured from an airborne aircraft. The crossing target detection algorithm was also implemented on a pipelined architecture from DataCube and runs in real time. Their work has been successfully tested on flight tests conducted by NASA.

Hu et al. (2003) [58] study the problem of evaluating if the flight plan assigned to an aircraft is safe. They introduce a kinematic model of the aircraft motion in a three dimensional wind field with spatially correlated random perturbations. An iterative algorithm based on a Markov chain approximation scheme is also proposed in this work. The same authors (2005) [59] introduce a model of a two-aircraft encounter with a random field term to address correlation of the wind perturbations to the aircraft motions. Based on this model, they estimate the probability of conflict by using a Markov chain approximation scheme.

One of the most recent works, due to Jardin (2005) [68], presents some algorithms for strategic conflict detection, based on the use of a 4-dimensional space and time grid to represent the airspace. This approach to compute conflict detection was previously introduced by Jardin in his PhD thesis (2003) [67], and in [66], where he used a 3-dimensional grid (two horizontal spatial dimensions and time).

Prandini and Hu (2008) [88] present a stochastic approximation scheme to estimate the probability that a single aircraft will enter a forbidden area of the airspace within a finite time horizon. They obtain a weak approximation of the switching diffusion through a Markov chain and, then, develop a numerical algorithm for computing an estimate of the probability that the aircraft enters an unsafe region of the airspace or come too close to another aircraft.

1.3 Collision Resolution

There are several methods by which a solution to a conflict is generated. Kuchar and Yang (2000) [71] present a survey of CDR modeling methods with their own classification.

Dowek and Muñoz (2007) [28] present a mathematical framework for the formal specification and analysis of conflict detection and resolution algorithms and their properties. For this state-of-the-art four categories have been picked up, namely, Prescribed, Optimized, Force field and Manual, as well as the works presented in the two most recent conferences of aviation that took place in 2009.

1.3.1 Prescribed

This type of studies gives the standard maneuvers that aircraft are able to carry out to avoid simple conflicts in the airspace. Resolution maneuvers are fixed during system design based on a set of predefined procedures. NASA (1996) [82] and Carpenter and Kuchar (1997) [16] assume that a fixed climbing-turn maneuver is always performed to avoid traffic on a parallel runway approach. Prescribed maneuvers may have the benefit that operators can be trained to perform them reflexively. This can decrease response time when a conflict alert is issued. However, prescribed maneuvers are less effective, in general, than maneuvers that are computed in real time since there is no opportunity to modify the resolution maneuver. In many conflicts, it will be necessary to adapt the resolution maneuver to account for unexpected events in the environment, or to reduce the aggressiveness of the maneuver.

1.3.2 Optimization

This type of approaches typically combine a kinematic model with a set of cost metrics. An optimal resolution strategy is then determined by solving for the trajectories with the lowest cost. TCAS (1983) [96], for example, searches through a set of potential climb or descent maneuvers and selects the least-aggressive maneuver that still provides adequate protection. This requires the definition of appropriate cost functions, typically projected separation, or fuel or time, but costs could also cover workload. Developing costs may be fairly straightforward for economic values but difficult when modeling subjective human utilities. Since current interest in this field is generally centered on strategic resolution of conflicts before immediate tactical evasion is required, economic costs and operator workload will be important to the system design.

Some of the models denoted are using optimized conflict resolution apply schemes such as game theory, genetic algorithms, expert systems, or fuzzy control to the problem.

Expert system methods use rule bases to categorize conflicts and decide whether to alert and/or resolve a conflict. These models can be complex and would require a large number of rules to completely cover all possible encounter situations. Additionally, it can be difficult to certify that the system will always operate as intended, and the "experts" used to develop or training the system may in fact not use the best strategy in resolving conflicts. However, a rule base, by design, can be easier for a human to understand or explain than it is an abstract mathematical algorithm.

Krozel and Peters (1997) [70] analyze the collision avoidance problem in free flight context, taking economics features into consideration. They use relative motion of two aircraft in a horizontal plane and vectorial and probabilistic calculations, to detect if a conflict occurs so the model is non-deterministic. To solve the collision avoidance problem, first of all, they consider economic factors, like fuel consumption, and time factors, like time required to execute the maneuver and return back to course. The authors also order the different possible maneuvers relative to the cost of these ones, being altitude changes the most economical, and speed changes the worst economical. However, the order is reversed in comfort terms, as it can be seen in [39] presented below.

Shewchun et al. (1997) [99] propose a method to analyze conflicts between two aircraft, given their intended trajectories and uncertainty about their behavior. The method provided guaranteed lower bounds on miss distances beetween the aircraft over a given time horizon. The approach could handle very complex uncertain behaviors at a very efficient (polynomial) time using linear matrix inequalities and positive semi-definite optimization.

Frazzoli et al. (1999) [39] solve a planar, multi-aircraft conflict resolution problem, formulating it as a nonconvex, quadratically constrained quadratic program, and then approximating it by a convex, semidefinite program. The optimal solution to this convex program is then used to randomly generate feasible and locally optimal conflict resolution maneuvers. Every individual aircraft should then be able to express its preferences at regular time intervals; they are always given conflict-free, straight paths.

Bilimoria (2000) [15] presents a geometric optimization approach for the conflict resolution, utilizing information on current positions and velocity vectors. The resolution runs well for two aircraft, but the resolution is sequential for more than two, with each aircraft resolving its most immediate conflict at each update cycle.

An optimal air traffic resolution is proposed by Galdino et al. (2001) [40] based on an algorithm so called KB2D, that computes the resolution maneuvers where only one

component of the velocity vector (ground speed or heading) is modified. This algorithm considers pairs of aircraft, and then, the domino effect can happen.

Dowek et al. (2001) [27] present an algorithm for the conflict detection and resolution where the maneuvers can be based on speed or vertical changes, but only one of them at the same moment. The conflict is predicted by using a linear projection of the aircraft states.

Mao et al. (2001) [78] set out geometric constructions to solve the problem, including one by one aircraft until obtaining the total number of them, taking the previous aircraft as obstacles, and making a sequential process. They analyze problems involving aircraft flows, since interactions occurring within a finite set of aircraft can only have a finite duration.

A geometric approach for the conflict detection and resolution is proposed by Geser and Muñoz (2002) [45], where the concept of recovery course is introduced. It redirects the ownship to its original target waypoint without introducing new conflicts, in a geometric optimal way. In this method only a pair of aircraft is considered.

Hu has devoted a series of papers and two thesis, to this problem. Particularly, in [56] Hu et al. (2002) study the problem of designing optimal conflict-free maneuvers (a maneuver is defined to be a continuous and piecewise C^1 map) for multi-aircraft encounters in a three dimensional environment, proposing an algorithm for solving the resultant constrained optimization problem in the two aircraft case. When more than two aircraft are involved, they consider what they call two-legged maneuvers (i.e., a maneuver consisting of two stages, moving at constant velocity and through a straight line in both stages). The original optimization problem is then reduced to a finite dimensional convex optimization problem with linearly approximated conflict-free constraints on the waypoints (with quadratic objective function). Path flyability is taken into account by introducing maximum speed and turning angle constraints, what can be expressed using second order cone constraints. Therefore, the optimization problem together with the speed and the simplified turning angle constraints becomes a Second Order Cone Programming (SOCP) problem.

However, the assumptions considered at the beginning (every aircraft departures and arrives at the same time, all aircraft move linearly except for one heading angle change in the two-legged maneuver, etc.) make necessary to apply the model recursively, what could make it unaffordable to resort to it in most of the practical cases, due to the non-linearity of its constraints and objective function. In [57], Hu et al. (2003) study the same problem

as above, although constrained to the plane, proposing for the general multi-agent case, a randomized convex optimization algorithm to find the optimal multi-legged maneuvers (with an arbitrary number of stages) numerically.

Pallottino et al. (2002) [85] propose an approach based on Mixed Integer Linear Programming (MILP) to detect and solve conflict problems. They consider two different maneuvers in two different models, velocity changes problem (VC) and heading angle change problem (HAC) in the same plane, i.e., this model does not consider to climb or descend the aircraft. The VC problem consists of aircraft flying along given fixed directions that can maneuver only once with a velocity variation called q_i that can be positive (acceleration), negative (deceleration) or null (no velocity variation) into an upper bound ($v_{i,max}$) and a lower bound ($v_{i,min}$). A geometric approach is proposed for studying non-conflict conditions and defining the set of constraints. The model does not always obtain a solution for the conflict problem, because in the case of head to head conflict, a change of velocity is not enough to avoid the conflict. The other model is the HAC problem, that is based on geometric arguments again to define the set of constraints. The model assumes that the velocity is the same for all the aircraft, and each one can maneuver only once with an instantaneous heading angle deviation called p_i that can be positive (left turn), negative (right turn) or null (no deviation). It does not consider returning to the original route, nor it explains how the aircraft reaches its destination after a maneuver.

The aim of this work consists of developing a new model by including the aspects that Pallottino et al. (2002) [85] did not solve. The first possibility is including the heading angle change model in the velocity change model, but this new problem will not be linear since the constraints will include nonlinear functions (sines and cosines). However, it can be solved by using e.g. in CPLEX [63] the S2 sets mechanism, that allows to approximate a separable nonlinear function by a piece-wise function with linear segments up to the desired approximation. However the strongest hypothesis for the HAC model that all aircraft fly with the same velocity, does not make this alternative very interesting to work with.

Obstacle avoidance using the linearized constrained Uninhabited Aerial Vehicle (UAV) dynamic has been modeled by Richards and How (2002) [93]. As the authors refer to, Centralized Model Predictive Control has been widely developed for constrained systems with many results concerning robustness and has been applied to the co-operative control of multiple vehicles. By augmenting the system with a binary ”target state”, that indicates whether the target set is reached or not, the authors end up with a hybrid system at hand. Task completion is then guaranteed by imposing a hard terminal equality constraint

on the target state. See also (2003) [94].

Schouwenaars et al. (2005) [97] discuss the implementation, by using the state-of-the-art optimization engine, of a guidance system based on MILP on a modified, autonomous T-33 aircraft equipped with Boeing's UCAV avionics package. The formulation is presented for safe, real-time trajectory generation in a partially-known, cluttered environment.

Christodoulou and Costoulakis (2004) [20] also propose a Mixed Integer Non Linear Programming (MINLP) to solve the conflict problem. The method allows velocity changes and heading angle control to solve all potential conflicts by using standard optimization software, but it can require more computational effort than what it could be affordable.

Ma and Miller (2005) [74] present in a MILP Trajectory Generation model applied to a rotorcraft performing nap-of-the-earth flight in challenging terrain with multiple known surface threats, i.e. they work on a specific application of optimal path planning for one autonomous vehicle in an obstacle field in three dimensions.

Mao et al. (2005) [79] tackle the problem by using instantaneous heading changes as maneuvers between two aircraft, but this action does not generate cascaded diverging conflict-avoidance behavior in neighboring aircraft. This paper extends the results of Mao et al. (2001) [78] in which the maneuvers described in the document are not physically realistic. In [79], the authors prove the closed-loop stability of two intersecting flows of aircraft under decentralized sequential conflict-resolution schemes, but the cost of the computational calculations is more complex than those required by the original document.

The MINLP model proposed by Christodoulou and Kodaxakis (2006) [21] with linear objective function and nonlinear constraints functions, locate conflicts and solve them by using optimization software. This method only allows velocity changes as maneuvers. Pannequin et al. (2007) [86] present an approach to the problem of deconflicting aircraft paths through severe weather by using Nonlinear Model Predictive Control (NMPC).

Treleaven (2007) [102] assumes that aircraft travel at the same altitude and with the same speed, and uses only horizontal maneuvers for the conflict resolution. This analysis is extended to consider two, three and multiple intersecting flows.

Rebollo et al. (2008) [92] consider collision avoidance by changing the velocity of the vehicles by using a two step algorithm. The first step is an heuristic initialization and

the second one uses a Linear Programming (LP) model.

In Alonso-Ayuso et al. (2010) [8, 9] we propose a MILP approach by using velocity and altitude changes for the conflict resolution and extending the work developed by Pallottino et al. [85]. This work will be developed detailed in Chapter 2, page 21. Furthermore, in Alonso-Ayuso et al. (2010) [7] we propose a new model based on Mixed 0-1 Nonlinear Programing to be used in a large term, avoiding all conflicts in the air traffic considering only one altitude level but all velocity changes being continuous by using an acceleration term. This work will be also developed in Chapter 3, page 77.

Alonso-Ayuso et al. (2010) propose two integer LP models for aircraft conflict avoidance between any number of aircraft. The first one is a pure 0–1 LP which avoid aircraft conflicts by means of altitude changes, and the second one is a mixed 0–1 LP whose strategy is based on velocity and altitude changes for the medium term Conflict Detection and Resolution.

Finally, Hu (1999) [54], Hu and Sastry (2001) [62], Hu (2002) [55], Hu et al. (2005) [60] and Hu et al. (2007) [61] study the more general problem of optimal collision avoidance and optimal formation switching for multiple agents moving on a Riemannian manifold.

1.3.3 Force field

This type of approaches treat each aircraft as a charged particle and use modified electrostatic equations to generate resolution maneuvers. The repulsive forces between aircraft are used to define the maneuver that each performs to avoid a collision. A force field method, while attractive in the sense that a conflict resolution solution is continuously available by using relatively simple equations, may have some pathologies that require additional consideration before they can be used in operation. For example, force field methods may assume that aircraft continuously maneuver in response to the changing force field, or that aircraft can vary their speed over a wide range. This requires a high level of guidance on the flight deck and increases complexity beyond issuing simple heading vectors, for example. Additionally, sharp discontinuities in the commanded resolution maneuvers may occur that require additional processing or filtering to arrive at physically feasible solutions. Several human-in-the-loop implementations of the force field method, however, appear to have resolved these problems and have shown that the force field based on resolution can be effective when properly applied. See Duong and Hoffman (1997) [30], Hoekstra, Van Gent

and Ruigrok (1998) [53] and Zeghal and Hoffman (1999) [103].

It has also been suggested that potencial fields can be used in Unmanned Aerial Vehicle (UAV) navigation for obstacle and collision avoidance applications. Sigurd and How (2003) [100] proposed a method that provides a way for groups of UAVs to use the gradient of a potencial field to navigate through heavily populated areas safely while still aggressively approaching their targets.

1.3.4 Manual

Some models allow the user to generate potential conflict resolution solutions and obtain feedback as to whether the trial solution is acceptable. These models are denoted as handling a manual solution in the table. The benefit of a manual solution is that it is generally more flexible in the sense that it is based on human intuition, by using information that may not be available to the automation. For example, weather information that is not available to the CDR system may be important when considering a conflict resolution maneuver. Automated solutions that do not take relevant environmental information into account will likely produce nuisance solutions that the human finds unacceptable.

1.3.5 Neural Networks

In the fifties, artificial neural networks began to be applied to many fields in artificial intelligence like analysis and adaptive control, speech and pattern recognition and classification, etc. These networks are based on statistical estimation and optimization and control theory. This field has been used in the collision avoidance problem together with other heuristics schemes like genetic algorithms, but it is not possible to determine exactly if the final solution is the optimum, normally being this one a good approximation.

Durand et al. (2000) [32] have built a neural network with unsupervised learning to compute new trajectories that are near to the optimal trajectory in conflicts with two aircraft. This 3-layer neural network modifies only the heading direction (not more than 45 degrees) of the aircraft if there is a conflict between them. To help the training of the neural network, the authors use a genetic algorithm. This network is not valid for conflicts involving more than two aircraft, however they provide some schemes to solve conflicts involving three aircraft, but not more.

Alam et al. (2005) [3] have constructed a neural network that computes near optimal trajectories to solve two aircraft conflicts in a 2D free flight environment, allowing only heading changes maneuvers, since they assume that the aircraft fly with constant speed. A three layer artificial neural network architecture and is used to lead the aircraft to the destination point. This neural network does not confront more than two aircraft in a same conflict, and it is not valid in a 3D environment. These are important drawbacks for the problem.

Doshi (2005) [26] presents a neural network to predict the position of the aircraft by using event history, being a long history a better choice than a short history since it reduces noise in the model. With this neural network, the conflict detection is obtained by computing separation distances between points of the prediction. An algorithm for determining the incursion distance between two aircraft is presented. It is based on trigonometric analysis and yields SD values useful for danger detection, but it only detects danger conflicts.

Christodoulou and Kontogeorgou (2008) [22] present a neural network to predict the optimal speed change for two aircraft in order to avoid an imminent conflict in a 3D environment. The algorithm combines the neural network with non-linear optimization to obtain the optimal speed change. For each conflict case there is an unique model based on non-linear optimization and it is solved in a 3D environment, but only speed changes are allowed. Vertical maneuvers are not considered since it is assumed that aircraft can fly out of a space divided in layers. It is also assumed that aircraft fly with constant speed and the motion direction is linear what is a simplification of the problem. It is also assumed that a conflict occurs if the two aircraft are separated by less than 9 kilometers.

Cetek (2009) [17] presents a model that takes into account many physical features like wind speed, relative density at the given flight altitude, gravitational acceleration, mass of the aircraft, aerodynamic drag force, etc. The model is non-linear and it is necessary a great effort to solve the problem, in fact the computational experience that is reported shows very large resolution times (more than 10 minutes), and it is not valid neither for imminent conflicts (short term) nor medium term. In this model, vertical and heading maneuvers are not contemplated, being “head to head” conflicts impossible to solve, since a speed change is not enough to avoid the conflict.

1.3.6 Last important conferences in aviation

In 2009 two important conferences in the aviation field took place, the *8th USA-Europe Air Traffic Management Research and Development Seminar* (ATM) and the *8th Innovative Research Workshop & Exhibition* (INO), where the most recent research about different lines for air traffic was presented. The contributions about the Collision Avoidance problem that were presented in these conferences are detailed below.

In the ATM conference refered to above, Durand and Alliot (2009) [31] presented a work based on an ant colony optimization for the resolution of the problem. This metaheuristic was implemented since the authors found that the resolution by using classical mathematical optimization is very difficult for big instances, say up to 30 aircraft, on which we do not completely agree. The ants model considers different aircraft trajectories and the problem is solved in the horizontal plane by executing the algorithm iteratively.

Barnier and Allignol (2009) [11] developed a constrained optimization model of the large scale combinatorial optimization problem. This work considers a 4D trajectory, i.e., the time horizon is assumed.

On the other hand, Drogoul et al. (2009) [29] present a summarize of the analysis of the En Route Air Traffic Soft Management Ultimate System (ERASMUS) for its validation.

In the INO conference, Chaloulos et al. (2009) [18] presented a work based on the recent advances in the fields of robotics and control and used navigation functions to resolve conflicts arising in the short term, while in medium term they use another algorithm. These algorithms were only applied in the horizontal plane.

Gaukrodger et al. (2009) [43] made a 2D plan-view radar display for the collision avoidance, helping the air traffic controllers to visualize the aircraft in the aerial sector as well as the possible conflicts and their simple resolutions.

Alam et al. (2009) [2] analyzed the sensitive of the medium term conflict detection algorithms to detect false alarms and missed detects, by using two given proved methods.

In the *European Control Conference*, Roussos et al. (2009) [95] presented a navigation function based on control strategy for multiple 3-dimensional non-holonomic aircraft-like agents. The use of navigation functions provides guaranteed global convergence and collision avoidance together.

Zhong and Xuejun (2009) [104], in the *9th International Conference on Electronic Measurement & Instruments* developed a geometric approach for the conflict resolution when some noise take place, by using projective geometry.

1.3.7 Others

Chiang et al. (1997) [19] solve the conflict problem by using their so-called Space-Time Flow (STF) Method. It is based on an iterative procedure for adding tubes (aircraft) by using a graph search in a discretized space-time to route each tube amongst the already routed tubes, which are considered to be obstacles.

The work presented by Erzberger and Paielli (1997) [33] is based on probability estimation for the conflict problem. The conflict prediction is based on the calculation of the probability that a conflict will occur, given a pair of predicted trajectories and their levels of uncertainty. For the validation of the algorithm Monte Carlo numerical examples are used.

Tomlin et al. (1998) [101] develop a method to solve the conflict problem by using both speed and heading changes. The algorithm is based on Lie algebra and Hamilton-Jacobi-Isaacs equations.

Bicchi and Pallottino (2000) [14] use optimal control and game theory to solve the problem. The model assumes that linear velocity is constant and allows to maneuver all the aircraft including airspeed, several angles, heading angle, longitude and latitude as parameters.

Goodchild et al. (2000) [46] propose a cooperative optimal conflict resolution algorithm based on distributed artificial intelligence, by using a dynamic optimization algorithm.

Bayen et al. (2005) [12] propose a Lagrangian model where the maneuvers are simple instructions such as turn to heading angle, fly direct to a concrete point and speed increase. The model permits aircraft to fly at different altitudes, but not to climb or descend. This model permits a shortcut or detour maneuver that could either shorten or lengthen the flight plan.

Alam et al. (2009) [5] present a set of algorithms to detect aircraft conflicts defining a set of rules for each algorithm and then, decide what is the best algorithm to solve a particular conflict detection problem by using data mining schemes to identify the patterns

in the probe characteristics where the conflict detection algorithms missed or falsely identified a conflict. The objective is to reduce the number of missed detects and false alarms by choosing the most efficient algorithm from several ones in different specific problems. They chose three algorithms: Dowek et al. (2001) [27], that is a extension of Bilimoria (2000) [15]; Erzberger and Paielly (1997) [33], being a probabilistic algorithm; and, Gazit (1996), that gave the worst results in the experimentation that was reported.

Peng and Lin (2010) [87] present a study based on two different models for solving the collision avoidance by using only independent horizontal maneuvers (i.e. only speed changes or heading angle changes are allowed). They propose two algorithms for the horizontal plane for TCAS.

1.4 Similar problems

On the one hand there exists two similar problems: The first one is the development of an en route descent advisor that avoids conflicts while an aircraft is descending for landing that was proposed by Coppenbarger et al. (2004) [23]. The second one is applied in military aircraft is presented by Sharma et al. (2007) [98], whose model considers aircraft flying in close proximity to terrain and all fixed obstacles like mountains have to be avoided. The problem is modeled in a 3D environment by using a minimax optimal control nonlinear optimization model. This model has a nonsmooth cost function that is transformed into a smooth cost by introducing additional inequality constraints. These works can be used in collision avoidance applied to aircraft when a zone in the airspace is closed due to atmospheric conditions or zones in which the flight of aircraft is restricted.

On the other hand, there are others problems treated in the literature that are related to collision avoidance applied in other fields like underwater or automobile routs where the machine have to avoid fixed obstacles in its path. Neural networks have been used to tackle this type of problems, see Ishi et al. (2003) [1], Nishida et al. (2006) [83] and Ishi et al. (2002) [65] applying the results to an underwater robot. Mukai et al. (2007 and 2008) [80] and [81] use their results to generate a new path avoiding the collision with a fixed obstacle by using MILP. Finally, Kim et al. (2005) [69] model the same problem as a MILP model but by using a piecewise polynomial approach which is a class of the hybrid dynamical system.

In Table 1.1 the main features of the literature that has been previously reviewed

are presented. The Collision Detection Problem (CDP) and Collision Resolution Problem (CRP) are distinguished. With regard to the type of maneuver three types of maneuvers are classified: Horizontal (H), Vertical (V) and Speed changes (S).

Table 1.1: Review literature

Reference	CDP	CRP	Maneuvers	Number of aircraft	Dimension
[2]	X			N	
[3]	X	X	H	2	2D
[4]	X			N	3D
[8]	X	X	VS	N	3D
[9]	X	X	VS	N	3D
[7]	X	X	S	N	2D
[10]	X	X	VS	N	3D
[11]	X	X	HV	N	3D
[12]	X			N	2D
[14]	X	X	H	N	2D
[15]	X	X	H,V	N	2D
[16]	X	X	H,V	2	2D
[17]	X	X	S	2	2D
[18]	X	X	H	N	2D
[19]	X	X	HV	N	3D
[20]	X	X	HS	N	2D
[21]	X	X	S	N	3D
[22]	X	X	S	N	3D
[24]		X	S,V	N	1D
[26]	X			N	2D
[27]	X	X	S,V,H	N	3D
[28]	X	X	H,S,V	N	3D
[29]	X	X		N	
[31]	X	X	H	N	2D
[32]		X	H	2	2D
[33]	X			2	2D
[34]	X	X	H,S,V	N	3D
[40]	X	X	H,S	2	2D
[42]	X			1	2D

(It is continued in the next page)

Review literature continuation.

Reference	CDP	CRP	Maneuvers	Number of aircraft	Dimension
[43]	X	X		N	2D
[45]	X	X	H,V	2	3D
[46]		X	S	N	2D
[54]		X	H,S	N	2D
[55]		X	H,S,V	N	3D
[56]		X	H,S,V	N	3D
[57]		X	H,S	N	2D
[58]	X			2	3D
[59]	X			2	3D
[60]		X	H,S,V	N	3D
[61]		X	H,S,V	N	3D
[62]		X	H,S,V	N	3D
[66]	X	X	H	N	3D
[67]		X	H,S,V	N	3D
[68]	X			N	4D
[70]	X	X	H, V, S	N	3D
[74]	X	X	H,S,V	1	3D
[77]		X	H,S	3	2D
[78]		X	H	N	2D
[79]		X	H	N	2D
[82]	X	X	H,V	2	2D
[85]	X	X	H, S	N	2D
[86]		X	H,S,V	N	3D
[87]	X	X	H,S	2	2D
[88]	X			1	2D
[89]	X			N	2D
[90]	X			2	2D
[91]		X	H	N	3D
[92]		X	S	N	3D
[93]	X	X	H,V	N	2D
[94]		X	H,V	N	2D
[95]	X	X	H,V	N	3D
[100]		X	H	N	2D

(It is continued in the next page)

Review literature continuation.

Reference	CDP	CRP	Maneuvers	Number of aircraft	Dimension
[101]		X	H	2,3	2D
[104]	X	X	H,V	2	2D

(Table end.)

1.5 Problem description

Collision Avoidance has been broadly studied in the literature as it can be seen in this chapter. There are several ways to solve the problem, including three different maneuvers: velocity, altitude and heading angle changes to avoid conflicts. In principle, only two maneuvers, velocity and altitude changes will be contemplated in this work to avoid conflicts, but other alternatives to consider independently heading angle changes will be taken into account as future research. Heading angle changes have a nonlinear nature, and most of the models are nonlinear ones, although Pallottino et al. (2002) [85] (presented above) solve the problem with heading angle changes by using MILP, but this model does not return aircraft to initial direction. The difficulty with nonlinear models is that the computing of the new direction may require more time than it is affordable.

In this work, two models are presented. The first one is based on MILP to solve the collision avoidance problem, by using only two maneuvers to avoid conflicts: velocity and altitude changes. The second one is based on MINLP, by using only velocity changes (including an acceleration term to do this changes continuous), but altitude changes will be introduced as future research, making this model more effective in real-life cases. This second model will be linearized by using Taylor polynomials and will be solved by using standard MILP schemes and “Variable Neighbourhood Search” (VNS) in a second step, since the execution time by using schemes that provide the optimal solution are very large.

Chapter 2

The static model: Velocity and altitude changes

2.1 Introduction

In this chapter a model for the collision avoidance problem is presented, based on Pallottino [84] and Pallottino et al. (2002) [85], by permitting aircraft to fly at different altitudes and to climb and descend in a fixed flight sector. The model that is proposed as a first step is based on MILP, whose resolution may require short computing time.

The model permits aircraft to fly at different altitudes and change their velocity to avoid conflicts, especially "head to head" conflicts and others that will be studied below. Any number of aircraft can be taken into account and each of them is given a set of fixed parameters (namely, coordinates, altitude, angle and number of changes in altitude and velocity in the sector). The objective consists of deciding the flight level and velocity that each aircraft must have at every execution, guaranteeing that collisions are avoided, while at the same time minimizing the fuel consumption cost of the velocity and altitude changes since the velocity changes will be smoothed.

The proposal is to optimize the model when an aircraft comes in or comes out the aerial sector, i.e., when there are important changes in the status of the set of aircraft in the aerial sector (being a portion of airspace managed by an Air Traffic Controller, ATC). The short changes in the initial direction of motion during the route force the optimization of the model in fixed time periods, but this is not an inconvenience since the computing time is very short, being able to solve real-life examples in real time (less than one second).

The objective of this model consists of avoiding all conflicts in a certain aerial sector, minimizing the number of velocity and altitude changes and returning to the initial conditions in the minimum possible time. The model is restricted to one aerial sector, since it will be applied for a short period and will help ATC decision-making. This aspect will be also useful for reducing the problem's dimensions, but it is also valid for the whole of airspace. Analyzing the airspace divided in aerial sectors is proposed to solve the problems separately, but exchanging all obtained parameters between the sectors when an aircraft changes its sector by any other.

The model avoids all conflicts by changing velocity, and it avoids some infeasible cases in Pallottino (2002) [85] by introducing vertical maneuvers with altitude changes. Furthermore, the model updates the number of velocity and altitude changes, as well as the velocity of each aircraft if it has avoided all conflicts by returning to the initial configuration.

The main contribution of this chapter consists of improving the basic model proposed by Pallottino et al. (2002) by including level changes to avoid infeasible situations like "head to head" cases, aircraft flying in the same direction where one of them has a faster velocity than the other one, aircraft flying nearby and their velocity bounds preventing a feasible solution, special cases due to a null denominator, etc. A continuous algorithm has also been constructed which solves the model in several time periods, minimizing the number of changes in each aircraft, and complex maneuvers like ascending or descending more than one level at once. In this algorithm, a preprocessing step is performed by filtering aircraft that will be in conflict in the sector, fixing some variables to relax the model, helping to solve the problem quickly, because it only considers aircraft that are getting closer each other, etc.

The model has been tested by using different examples with many conflicts between aircraft (20-50), and the execution time has been very short (less than 5 sec. in the most complicated instances).

2.1.1 Notation

Sets

$\mathcal{F}$, set of flights in the sector $(1, \ldots, F)$.

$\mathcal{Z}^f$, set of admissible flight levels for aircraft $f \in \mathcal{F}$, $(\underline{z}_f, \ldots, \overline{z}_f)$.

Parameters

t, current time.

e, fixed distance, such that if two different aircraft are further apart than this distance, the corresponding pair of aircraft is not considered in the model.

w_n, weight (between 0 and 1) for each objective function term for $n = 1, \ldots, 5$.

ϑ, random angle to turn aircraft configurations in case of null denominators.

For all $f \in \mathcal{F}$:

x_f, y_f, position (abscissa and ordinate) of aircraft f.

x_f^1, y_f^1, out of sector position (abscissa and ordinate) of aircraft f.

v_f, current velocity in time t of aircraft f.

v_f^*, initial velocity configuration for aircraft f.

z_f, current flight level in time t of aircraft f.

z_f^*, initial flight level configuration for aircraft f.

$\underline{v}_f, \overline{v}_f$, minimum and maximum velocity allowed for aircraft f.

$\underline{z}_f, \overline{z}_f$, minimum and maximum altitude level allowed for aircraft f.

m_f^*, initial direction of motion in $(-\pi, \pi]$ for aircraft f.

r_f, safety radius for each aircraft f, usually 2.5 nautical miles (nm).

n_f^v, n_f^a, number of changes in velocity and altitude in the sector for aircraft f until the new execution, respectively.

t_f^1, exit time from the aerial sector for aircraft f.

$c_f^{q^+}, c_f^{q^-}$, costs for positive and negative velocity changes for aircraft f, respectively.

c_f^j, cost for number of levels that aircraft f changes.

c_f^v, c_f^a, costs for changing velocity and altitude for aircraft f, respectively.

$c_f^{\hat{v}}$, cost for different velocity with respect to the initial flight plan for aircraft f.

$c_f^{z^*}$, cost for different altitude level with respect to the initial flight plan for aircraft f.

Data preprocessing

For all $f \in \mathcal{F}$:

$\widehat{v}_f$, optimal velocity configuration to arrive at the final sector point at the predicted time for aircraft f.

For all $i, j \in \mathcal{F} : i < j$:

$g_{ij}, l_{ij}, \alpha_{ij}$, angles in the geometric construction for conflict detection.

ω_{ij}, angle between the line that joins the aircraft and the abscissa axis.

$\hat{\omega}_{ij}$, angle between aircraft i and j that depends on the quadrant in which j lies considering aircraft i centered in the origin.

hth_{ij}, 0-1 parameter that determines if there is a "head to head" conflict for aircraft i and j.

sc_{ij}, 0-1 parameter that determines if two aircraft i and j are separated by less than distance $r_i + r_j$.

pc_{ij}, 0-1 parameter that determines if there is an "anomalous case" between aircraft i and j.

fc_{ij}, 0-1 parameter that detects if there is a "false conflict" between aircraft i and j.

ip_{ij}, intersection point between the straight line trajectories for aircraft i and j if the trajectories are not parallel or coincident.

d_{ij}, distance between aircraft i and j.

d_{ij}^1, distance between aircraft position i and ip_{ij}.

d_{ij}^2, distance between points $\left(x_i + \cos(m_i^*), y_i + \sin(m_i^*)\right)$ and ip_{ij} for aircraft i and j.

p_{ij}, 0-1 parameter that will be one if the couple of aircraft i and j will not be taken into account for the conflict resolution. This parameter depends on the criterion decided by the ATC. Notice that this parameter will be one if $fc_{ij} = 1$.

Variables

For all $f \in F$:

q_f, velocity variation for aircraft f. This variable is real, and it is divided into two nonnegative variables, for example q_f^+ and q_f^-, such that $q_f = q_f^+ - q_f^-$ as it is standard in optimization, where q_f^+ and q_f^- are the positive and negative velocity variation for aircraft f, respectively.

a_f, 0-1 variable that takes value 1 if aircraft f changes its velocity in the resolution and, otherwise, it is zero.

b_f, 0-1 variable that takes value 1 if aircraft f changes its altitude in the resolution and, otherwise, it is zero.

ρ_f, nonnegative integer variable that shows the number of levels that aircraft f ascends or descends.

β_f, auxiliary nonnegative continuous variable that models the absolute value of the difference between current velocities and initial velocities as a linear function for aircraft f.

For all $f \in F$ and $z \in \mathcal{Z}$:

ν_f^z, 0-1 variable that takes value 1 if aircraft f is at altitude level z in the resolution and, otherwise, it is zero.

For all $i, j \in \mathcal{F} : i < j$ and $z \in \mathcal{Z}^i \cup \mathcal{Z}^j$ and $n = 1, \ldots, 5$:

δ_{ijz}^n, auxiliary 0-1 variables to model or constraints.

2.2 The Velocity Changes (VC) model

The first model that is proposed in this thesis is based on the Velocity Changes problem (VC) developed by Pallottino (2002) [84] and Pallottino et al. (2002) [85] with velocity as well as altitude changes. The execution time of the VC model is very short; for example, for 11 aircraft the reported execution time is 1.13 seconds on a typical PC

in 2002. This model cannot avoid some infeasible situations (which will be studied later) where velocity changes are not sufficient. Altitude changes are proposed to avoid these situations as long as the execution time does not increase considerably. The proposal is creating an algorithm that runs when there is a new change in one sector (a new aircraft enters or an aircraft exits). Additionally, it runs in a continuous way to avoid new conflicts due to heading angle changes of each aircraft route, or if it is desired to return to the initial configuration after the conflict is avoided and the aircraft are moving far away from each other.

2.2.1 Geometric construction

This model is based on a geometric construction by using simple considerations. Let two aircraft have the initial parameters (x_i, y_i, m_i^*, v_i) and (x_j, y_j, m_j^*, v_j), respectively, where x and y are the coordinates of each aircraft, m^* is the initial direction of motion and v is the initial velocity. With these velocities, each velocity vector can be built with abscissa and ordinate components as follows,

$$\vec{v}_i = \begin{pmatrix} (v_i + q_i)\cos(m_i^*) \\ (v_i + q_i)\sin(m_i^*) \end{pmatrix},$$

$$\vec{v}_j = \begin{pmatrix} (v_j + q_j)\cos(m_j^*) \\ (v_j + q_j)\sin(m_j^*) \end{pmatrix},$$

where q is the velocity variation in the new configuration (after avoiding conflict situations). Now the difference vector, which is the relative velocity vector, is constructed as follows,

$$\vec{v}_i - \vec{v}_j = \begin{pmatrix} (v_i + q_i)\cos(m_i^*) - (v_j + q_j)\cos(m_j^*) \\ (v_i + q_i)\sin(m_i^*) - (v_j + q_j)\sin(m_j^*) \end{pmatrix}.$$

This new vector shows the relative velocity from one aircraft with respect to the other as it can be seen in Fig. 2.1. With this vector, it is easy to know when a conflict occurs by comparing its tangent with the tangent of two new angles that will be constructed below.

The two parallel lines to $\vec{v}_1 - \vec{v}_j$ that are tangent to aircraft j localize a segment on the straight line over the direction of motion of the aircraft i (see Fig. 2.2(a)): This segment will be referred as the *shadow* of aircraft j along the aircraft i direction. Then a conflict occurs if aircraft i with its safe disc intersects the shadow generated by aircraft j, or vice-versa since $\vec{v}_i - \vec{v}_j$ and $\vec{v}_j - \vec{v}_i$ are the same vector with opposite orientation. It can

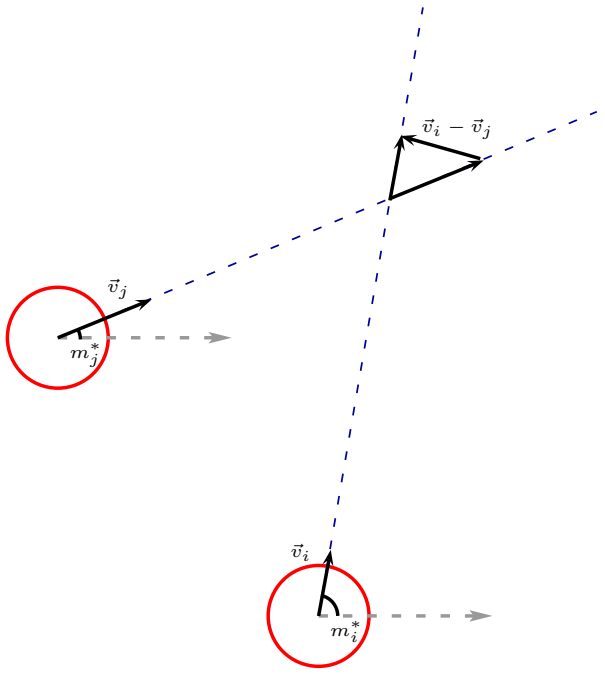

Figure 2.1: Construction of difference vector

be seen in Fig. 2.2(a) a no conflict situation, and in Fig. 2.2(b) a conflict situation, since the intersection between the shadow segment and the safety circle of aircraft i is not empty.

Let the two nonparallel straight lines be tangent to the discs of both aircraft, and let l_{ij} and g_{ij} be the angles between these two straight lines and the horizontal axis. As it can be seen in Fig. 2.3, $l_{ij} = \omega_{ij} + \alpha$ and $g_{ij} = \omega_{ij} - \alpha$, by using rules based on the angles of a triangle. Let r_f be the safety radius for each aircraft $f \in \mathcal{F}$, such that $r_f = \frac{s}{2} \quad \forall f \in \mathcal{F}$. Notice that $\alpha = \arcsin\left(\frac{r_i + r_j/2}{d_{ij}/2}\right) = \arcsin\left(\frac{r_i}{d_{ij}}\right)$ or $\arcsin\left(\frac{r_j}{d_{ij}}\right)$ (all safety radii are considered the same) as can be seen in Fig. 2.4, since the radius from the tangency point to the circle center is perpendicular to the tangential straight line. Notice that the radius of the circle must be normalized to 1 to obtain the $\arcsin$.

Let d_{ij} be the Euclidean distance between the two aircraft, which can be obtained by using the following expression: $\sqrt{(x_i - x_j)^2 + (y_i - y_j)^2}$; and ω_{ij} is the angle between the line that joins the aircraft and the horizontal axis. Notice that ω_{ij} can be calculated as $\omega_{ij} = \arctan\left(\frac{y_i - y_j}{x_i - x_j}\right)$, as shown in Fig. 2.3.

By using these preliminary concepts, no conflict situations happen if the following

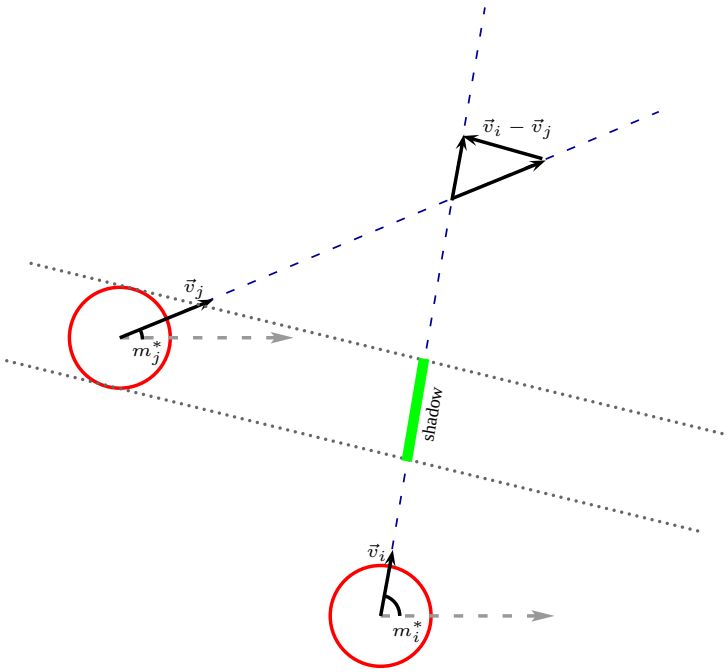

(a) No conflict situation

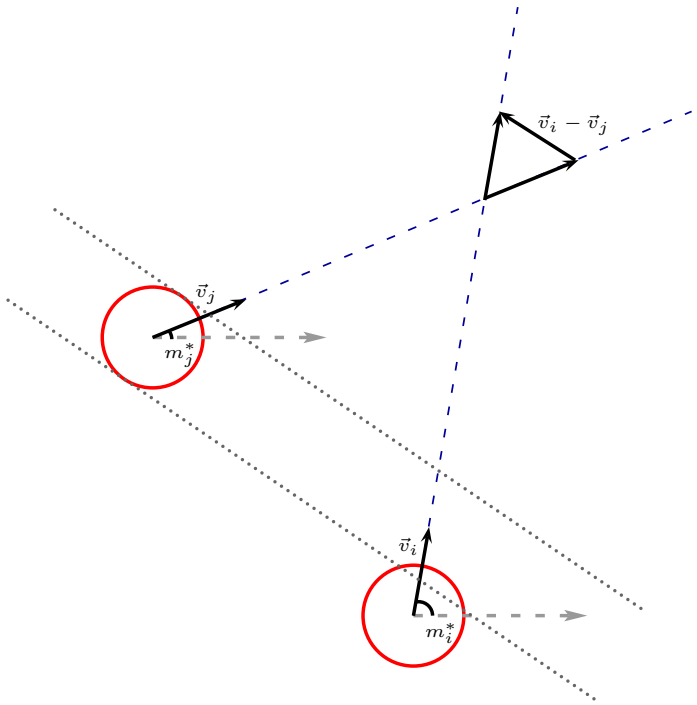

(b) Conflict situation

Figure 2.2: Geometric construction for conflict avoidance constraints

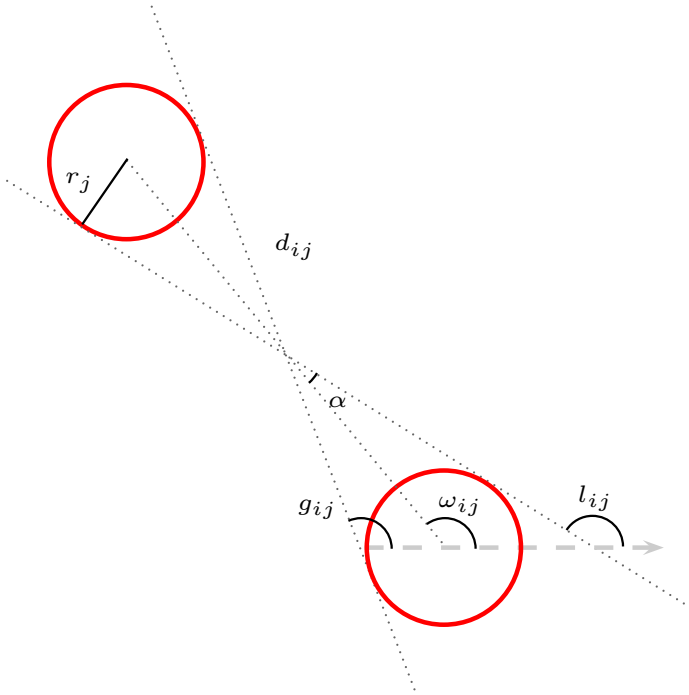

Figure 2.3: The two nonparallel straight lines tangent to the safety discs of radius $r_i = s/2$ for two aircraft at distance d_{ij}

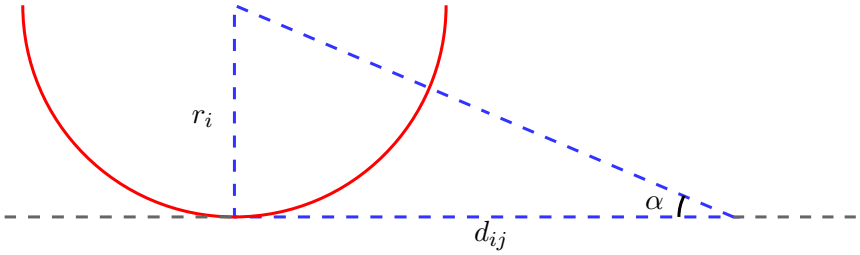

Figure 2.4: α angle construction

conditions are verified:

$$\begin{aligned} \tan(\vec{v}_i - \vec{v}_j) &\geqslant \tan(l_{ij}) \\ &\text{or} \\ \tan(\vec{v}_i - \vec{v}_j) &\leqslant \tan(g_{ij}) \end{aligned}$$

i.e.,

$$\frac{(v_i+q_i)\sin(m_i^*)-(v_j+q_j)\sin(m_j^*)}{(v_i+q_i)\cos(m_i^*)-(v_j+q_j)\cos(m_j^*)} \geqslant \tan(l_{ij}) \quad (2.1a)$$

or

$$\frac{(v_i+q_i)\sin(m_i^*)-(v_j+q_j)\sin(m_j^*)}{(v_i+q_i)\cos(m_i^*)-(v_j+q_j)\cos(m_j^*)} \leqslant \tan(g_{ij}). \quad (2.1b)$$

This affirmation is easy to see. Notice that if $\tan(\vec{v_i}-\vec{v_j})=\tan(g_{ij})$ or $\tan(\vec{v_i}-\vec{v_j})=\tan(l_{ij})$, the two circumferences slide cross the tangent straight line that joins them, without a conflict situation. This situation occurs when the tangent of the relative velocity vector is bigger or smaller than the tangent of the angles l and g, respectively. However, if these conditions are not satisfied, a conflict situation will take place between these two aircraft.

Now the non-conflict constraints will be constructed for all pairs of aircraft in the aerial sector. Making these conditions linear is a previous step, since there are two possible cases to consider: $(v_i+q_i)\cos(m_i^*)-(v_j+q_j)\cos(m_j^*)<0$ and $(v_i+q_i)\cos(m_i^*)-(v_j+q_j)\cos(m_j^*)>0$. Notice that they can change the direction of the inequalities depending on the sign of the denominator, when it is moved to the other side of the inequality. To simplify the notation, let the following parameters be as follows,

$$\begin{aligned} h_i &= \tan(l_{ij})\cos(m_i^*)-\sin(m_i^*) \\ h_j &= \tan(l_{ij})\cos(m_j^*)-\sin(m_j^*) \\ k_i &= \tan(g_{ij})\cos(m_i^*)-\sin(m_i^*) \\ k_j &= \tan(g_{ij})\cos(m_j^*)-\sin(m_j^*). \end{aligned}$$

If $(v_i+q_i)\cos(m_i^*)-(v_j+q_j)\cos(m_j^*)>0$ the constraints (2.1) can be rewritten as follows,

$$\begin{aligned} (v_j+q_j)h_j &\geqslant (v_i+q_i)h_i \\ (v_i+q_i)k_i &\geqslant (v_j+q_j)k_j \end{aligned}$$

and, if $(v_i + q_i)\cos(m_i^*) - (v_j + q_j)\cos(m_j^*) < 0$:

$$(v_i + q_i)h_i \geqslant (v_j + q_j)h_j$$
$$(v_j + q_j)k_j \geqslant (v_i + q_i)k_i$$

from where the following groups of constraints are obtained:

Case 1: $(v_i + q_i)\cos(m_i^*) - (v_j + q_j)\cos(m_j^*) < 0$

$$\begin{cases} \cos(m_i^*)q_i - \cos(m_j^*)q_j & \leqslant -v_i\cos(m_i^*) + v_j\cos(m_j^*) \\ -h_iq_i + h_jq_j & \leqslant v_ih_i - v_jh_j \end{cases} \tag{2.2a}$$

or

$$\begin{cases} \cos(m_i^*)q_i - \cos(m_j^*)q_j & \leqslant -v_i\cos(m_i^*) + v_j\cos(m_j^*) \\ k_iq_i - k_jq_j & \leqslant -v_ik_i + v_jk_j \end{cases} \tag{2.2b}$$

Case 2: $(v_i + q_i)\cos(m_i^*) - (v_j + q_j)\cos(m_j^*) > 0$

$$\begin{cases} -\cos(m_i^*)q_i + \cos(m_j^*)q_j & \leqslant v_i\cos(m_i^*) - v_j\cos(m_j^*) \\ h_iq_i - h_jq_j & \leqslant -v_ih_i + v_jh_j \end{cases} \tag{2.2c}$$

or

$$\begin{cases} -\cos(m_i^*)q_i + \cos(m_j^*)q_j & \leqslant v_i\cos(m_i^*) - v_j\cos(m_j^*) \\ -k_iq_i + k_jq_j & \leqslant v_ik_i - v_jk_j \end{cases} \tag{2.2d}$$

All these constraints are linear in the velocity variation variables q_f, for $f \in \mathcal{F}$.

2.2.2 The VC formulation

To represent the constraints in a MILP scheme, it is necessary to transform these logic expressions in linear constraints as it is shown in appendix A.1.1, page 141. Then, the full model for the VC problem is constructed by using the auxiliary 0-1 variables $\delta_{ij}^1, \delta_{ij}^2, \delta_{ij}^3, \delta_{ij}^4$ as it is described in (A.1.1) for equations (2.2) and $\forall i < j$. The new ex-

pressions are as follows,

$$(v_i + q_i)\cos(m_i^*) - (v_j + q_j)\cos(m_j^*) \leqslant M_1(1 - \delta_{ij}^1) \tag{2.3a}$$
$$-(v_i + q_i)h_i + (v_j + q_j)h_j \leqslant M_2(1 - \delta_{ij}^1) \tag{2.3b}$$
$$(v_i + q_i)\cos(m_i^*) - (v_j + q_j)\cos(m_j^*) \leqslant M_3(1 - \delta_{ij}^2) \tag{2.3c}$$
$$(v_i + q_i)k_i - (v_j + q_j)k_j \leqslant M_4(1 - \delta_{ij}^2) \tag{2.3d}$$
$$-(v_i + q_i)\cos(m_i^*) + (v_j + q_j)\cos(m_j^*) \leqslant M_5(1 - \delta_{ij}^3) \tag{2.3e}$$
$$(v_i + q_i)h_i - (v_j + q_j)h_j \leqslant M_6(1 - \delta_{ij}^3) \tag{2.3f}$$
$$-(v_i + q_i)\cos(m_i^*) + (v_j + q_j)\cos(m_j^*) \leqslant M_7(1 - \delta_{ij}^4) \tag{2.3g}$$
$$-(v_i + q_i)k_i + (v_j + q_j)k_j \leqslant M_8(1 - \delta_{ij}^4) \tag{2.3h}$$
$$\delta_{ij}^1 + \delta_{ij}^2 + \delta_{ij}^3 + \delta_{ij}^4 = 1, \tag{2.3i}$$

where $M_1 = M_3 = M_5 = M_7 = (\overline{v}_i + \overline{v}_j)$ are, respectively, the upper bounds of

$$(v_i + q_i)\cos(m_i^*) - (v_j + q_j)\cos(m_j^*)$$
$$(v_i + q_i)\cos(m_i^*) - (v_j + q_j)\cos(m_j^*)$$
$$-(v_i + q_i)\cos(m_i^*) + (v_j + q_j)\cos(m_j^*)$$
$$-(v_i + q_i)\cos(m_i^*) + (v_j + q_j)\cos(m_j^*),$$

$M_2 = M_6 = \overline{v}_i|h_i| + \overline{v}_j|h_j|$ are, respectively, the upper bounds of

$$-(v_i + q_i)h_i + (v_j + q_j)h_j$$
$$(v_i + q_i)h_i - (v_j + q_j)h_j$$

and $M_4 = M_8 = \overline{v}_i|k_i| + \overline{v}_j|k_j|$ are, respectively, the upper bounds of

$$(v_i + q_i)k_i - (v_j + q_j)k_j$$
$$-(v_i + q_i)k_i + (v_j + q_j)k_j.$$

These bounds are important as they can affect both the model feasibility and the computing time, since the make the model stronger.

As case 1 and case 2 are disjoint ones, the number of activated constraints is only one; and as the sign of the denominator can be positive or negative, one constraint in each case must be activated, then, the sum of the δ variables has to be equal to one.

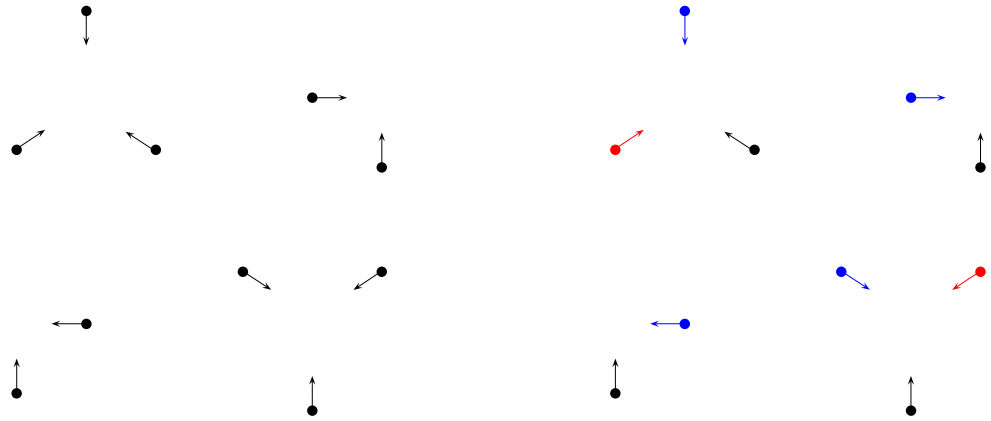

(a) Initial situation in the VC problem. (b) Solution for the initial situation.

Figure 2.5: Example for the VC problem

2.2.3 Illustrative instances

In this section several examples are presented in order to check the validity of the VC model. The first instance presents a situation where the VC solves the problem efficiently, whereas the second gives the particular cases that are not solved by the VC model.

In the example shown in Fig. 2.5 all aircraft fly with the same velocity, and there are four conflicts, and in two of them two aircraft are involved. After the resolution of the VC problem, six velocity changes have been made, see the right side of the figure: The red aircraft have accelerated and the blue ones have decelerated, whereas the black aircraft have not changed their configurations. With these changes, the set of aircraft do not have any conflicts any more.

Four different cases are presented in Fig. 2.6, such that the VC model cannot solve their conflicts. The first one shown in Fig. 2.6(a) is called “head to head”. It is easy to see that, in this case no sort of velocity change will be enough to avoid the conflict situation. The second one shown in Fig. 2.6(b) is a pursuit, where one aircraft flies in the same direction than another one with a higher velocity that will imply a conflict situation. The third one shown in Fig. 2.6(c) is the case where two aircraft are too much close to each other that whatever velocity change, into its bounds, will not be enough to avoid the conflict. The fourth one shown in Fig. 2.6(d) is a particular case that will be called “anomalous case” in the rest of the text, and it is the result of a denominator equal to zero. It causes a physical crash in the computational experience realized for testing the VC model.

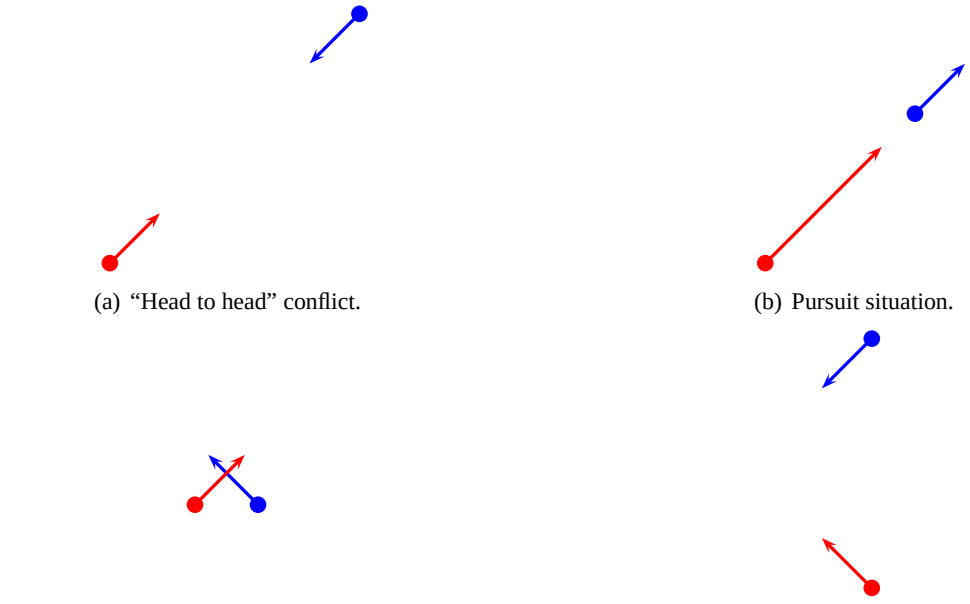

(a) "Head to head" conflict.

(b) Pursuit situation.

(c) Insufficient margin to avoid conflict by velocity changes.

(d) Anomalous case.

Figure 2.6: Non solved examples by the VC model

There is also a particular case that will be called "false conflict". It will be solved by changing the velocity in some aircraft that are not in conflict and it is explained in Section 2.3.4.

The purpose of this thesis consists of developing a new mathematical model that extends the VC formulation, where the cases shown in Fig. 2.6 and "false conflicts" can be contemplated and solved with only one execution.

2.3 The Velocity and Altitude Changes (iVAC) model: Initial approach

A solution for the conflict problem does not always exist in the VC model, see the cases shown in Fig. 2.6 that cannot be solved only using velocity changes. To avoid these situations, an extension for the VC problem including altitude changes is proposed, obtaining the initial Velocity and Altitude Changes model (iVAC).

Some important aspects are included in this model. First of all, the wind factor is included by extending the safety radius of some aircraft. Altitude changes are also included

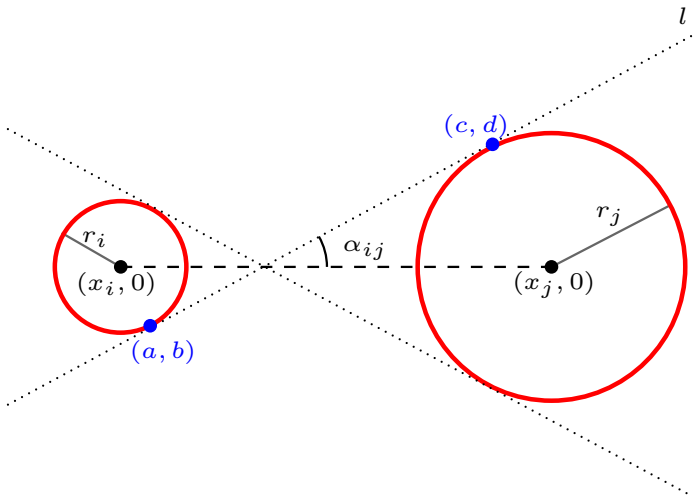

Figure 2.7: Interior tangent straight lines construction

to solve some situations that the VC model cannot, as shown in Fig. 2.6 whose most important case is the "head to head" situation that is described in the following. With this model all maneuvers, velocity and altitude are counted with the aim of penalizing those aircraft that have made more maneuvers. And, finally, more terms will be included in the objective function.

2.3.1 Different safety radius of aircraft

The VC problem considers that all safety radii of the aircraft have the same value $r_f = \frac{s}{2}$ where s is 5 nautical miles. With this consideration, it constructs all α angles, which are based on symmetric geometry. Allowing different safety radii is a good approximation to the realistic problem, since each aircraft has a different configuration that depends on the aircraft weight, the aerodynamic aspects, the aircraft size, etc. If different safety radii of the aircraft are considered, it is necessary to find the two interior tangent straight lines between two circumferences as shown in Fig. 2.7 and, then, calculate the slope of one of them.

Developing all the steps shown in Appendix A.2, page 143, the expression for angle α considering aircraft $i, j \in \mathcal{F}$ is as follows,

$$\alpha_{ij} = \arctan\left(\frac{r_i + r_j}{\sqrt{d_{ij}^2 - (r_i + r_j)^2}} \right). \tag{2.4}$$

If an aircraft has an unstable trajectory, the safety radius can be extended to avoid

possible conflicts with other aircraft. If it is preferred, this α angle can be taken to calculate the new l angle or the g angle. This is useful for considering the wind factor if takes place.

This calculation is only valid if the distance between the two aircraft is greater than $r_i + r_j$. If the distance is equal to $r_i + r_j$, the slope is infinity, since the denominator of the expression (2.4) is zero and, in this case, there is only one tangent point. If the distance is less than $r_i + r_j$, the two circles have a non empty intersection, and only exterior tangent straight lines can exist. In these last two cases, the first aircraft is near to the second one; they will be considered in the section 2.3.3 in the sc parameter.

2.3.2 Changes in the VC model considered in the iVAC model

When the VC model is expanded by considering altitude changes, it can solve the case where two different aircraft have a conflict that a velocity change is not enough to avoid the conflict situation, as shown in Fig. 2.6.

If altitude changes are considered, first the δ variables have to be modified including the dimension of the altitude, i.e., the subindex z is introduced with the variables written as δ_{ijz}. Therefore, the variables to be included in the model are as follows: δ^1_{ijz}, δ^2_{ijz}, δ^3_{ijz} and δ^4_{ijz}.

Additionally, a new variable δ^5_{ijz} will be included in the model to avoid infeasible situations in the δ variables constraints (2.3i). This new variable will take the value zero if a conflict exists between the aircraft i and j at the same level z; and this variable will take the value 1 if there is not a conflict at the same level between these aircraft or if there is a conflict at the same level that cannot be solved with a feasible velocity change. This new variable has the advantage of detecting infeasible situations in the velocity bounds if two different aircraft are nearby or an aircraft flies faster than other one for instance.

All the constraints of the VC model must include the dimension z in the δ variables, and the constraints of the sum of the δ variables must be as follows (including the δ^5 variable):

$$\sum_{n=1}^{5} \delta^n_{ijz} = 1 \quad \forall i < j \in \mathcal{F}, z \in \mathcal{Z}^i \cap \mathcal{Z}^j,$$

Now, if two different aircraft fly at different levels, variable δ^5_{ijz} will be forced to take value 1, i.e., if $\nu^z_i + \nu^z_j \leqslant 1 \Rightarrow \delta^5_{ijz} = 1$, and if $\nu^z_i + \nu^z_j \geqslant 2 \Rightarrow \delta^5_{ijz} = 0$. So, let the

following constraints,

$$\begin{aligned} \nu_i^z + \nu_j^z &\geqslant \delta_{ijz}^5 - 1 && \forall i < j \in \mathcal{F}, \forall z \in \mathcal{Z}^i \cap \mathcal{Z}^j \\ \nu_i^z + \nu_j^z &\leqslant 2 - \delta_{ijz}^5 && \forall i < j \in \mathcal{F}, \forall z \in \mathcal{Z}^i \cap \mathcal{Z}^j. \end{aligned}$$

It is easy to check that if $\delta_{ijz}^5 = 1$ then aircraft i and j fly at different levels since $\nu_i^z + \nu_j^z \leqslant 1$, and if $\delta_{ijz}^5 = 0$ the previous sum is greater than -1 and smaller than 2, i.e., the sum is not restricted.

This argument helps to fix the value of some δ^5 variables and makes the model stronger. This aspect is important for the execution time in the resolution with the optimization engine, since it reinforces the iVAC model.

2.3.3 Fixing some variables in preprocessing

The preprocessing phase is important when the main concern is fixing some variables in the previous model to the execution of the optimization engine, since it reinforces the model and it makes the search of the optimal solution faster.

"Head to head" situations

"Head to head" situations happen when two different aircraft are flying with the same direction but opposite sense, bringing closer to each other. As shown in Fig. 2.6, this situation cannot be solved with a velocity change. It is proposed in this work that when a "head to head" situation occurs, the flights of the aircraft that experience this conflict should be forced to stay at different altitude levels. As a first step, the preprocessing can detect a "head to head" situation and, then, a parameter called hth can be fixed to value 1, and the rest of the hth parameters will be fixed to value 0.

It can be determined if there is a "head to head" situation between two aircraft by using the α angle from the VC model or from section 2.3.1 (where different radii were considered). First, the angle between the abscissa axis and the straight line that joins aircraft i and j, has to be considered, for $i, j \in \mathcal{F}$. The ω_{ij} angle is in the range $(\frac{-\pi}{2}, \frac{\pi}{2}]$ and the angle in range $(-\pi, \pi]$ must be considered. An auxiliary angle called $\widehat{\omega}_{ij}$ will be considered with the properties that are depicted in Fig. 2.8, by using the ω angle calculated by the

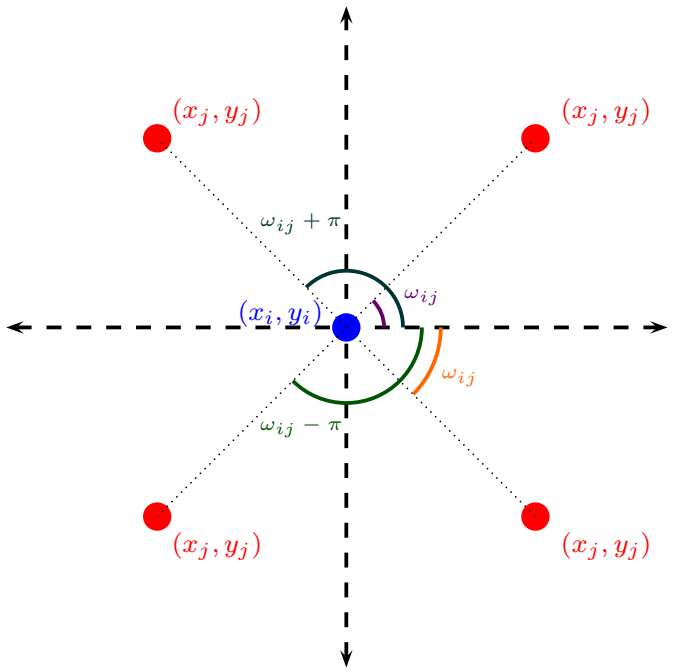

Figure 2.8: Angle between two aircraft for detecting a “head to head” situation

arctangent between the coordinates of each aircraft.

All “head to head” cases between every pair of aircraft can be detected in preprocessing. They occur when the following conditions are satisfied (see Fig. 2.9):

$$\widehat{\omega}_{ij} - \alpha_{ij} \leqslant m_i^* \leqslant \widehat{\omega}_{ij} + \alpha_{ij}$$
$$\widehat{\omega}_{ji} - \alpha_{ji} \leqslant m_j^* \leqslant \widehat{\omega}_{ji} + \alpha_{ji}.$$

It can be seen in Fig. 2.9(a) that a “head to head” situation will occur when the two circumferences will cross one of the two tangent straight lines that join them. If the previous condition is not satisfied, there is no “head to head” situation as it can be seen in Fig. 2.9(b). In this situation the parameter hth_{ij} is fixed to 1, forcing the two involved aircraft to fly at different altitude levels, since previously the δ^5 variables can be fixed to 1 in this situation. The definition of the hth parameter is as follows,

$$hth_{ij} = \begin{cases} 1 & \text{if } \widehat{\omega}_{ij} - \alpha_{ij} \leqslant m_i^* \leqslant \widehat{\omega}_{ij} + \alpha_{ij} \wedge \widehat{\omega}_{ji} - \alpha_{ji} \leqslant m_j^* \leqslant \widehat{\omega}_{ji} + \alpha_{ji} \\ 0 & \text{otherwise.} \end{cases}$$

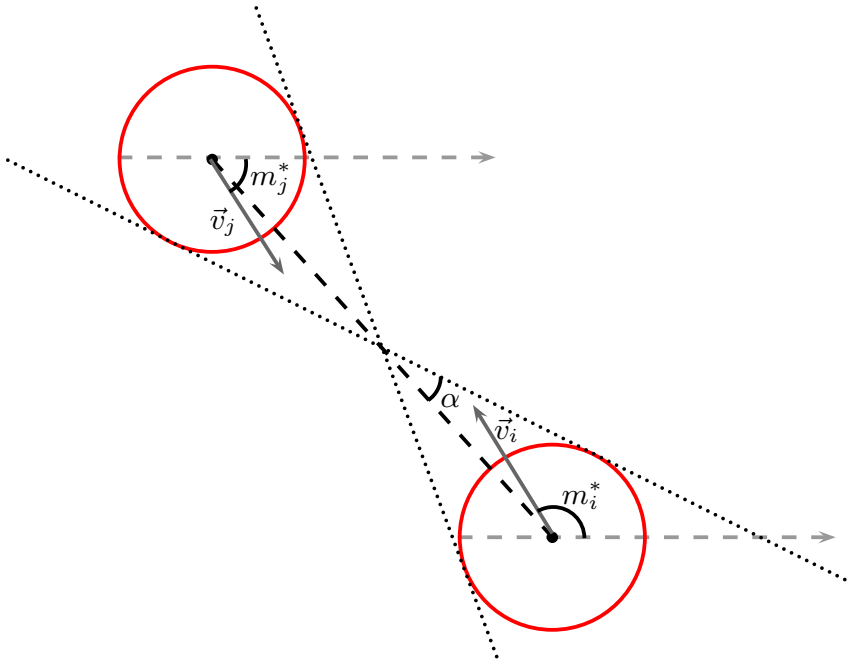

(a) "Head to head" situation.

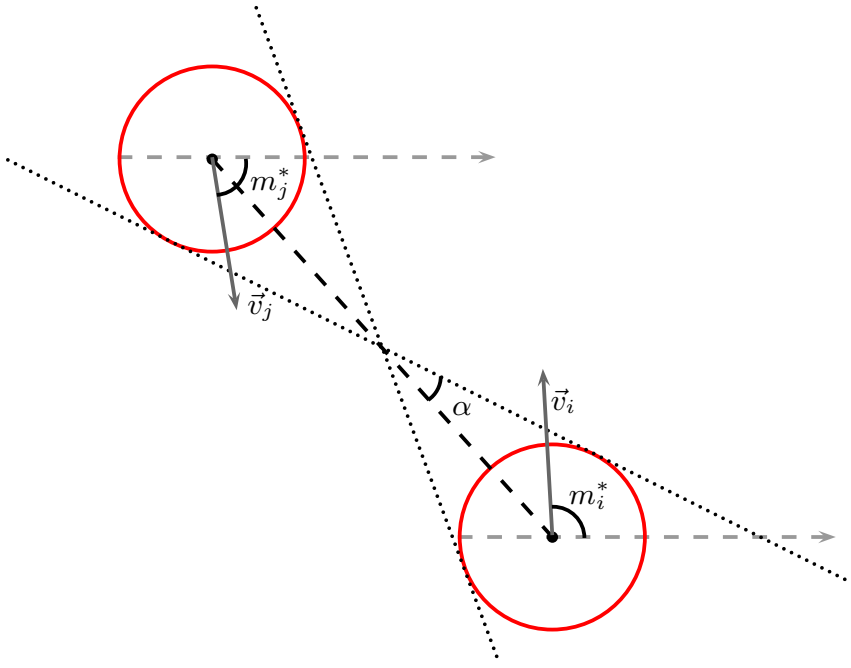

(b) No "Head to head" situation.

Figure 2.9: Study of "head to head" situations

The new altitude configuration will be saved in the ν variables. The following constraints ensure that each aircraft flies at only one level:

$$\sum_{z \in \mathcal{Z}^f} \nu_f^z = 1 \quad \forall f \in \mathcal{F}. \tag{2.5}$$

Now, when a "head to head" situation occurs the iVAC model forces the two aircraft in conflict to fly at different altitude levels as follows,

$$\delta_{ijz}^5 = 1 \quad \text{if } hth_{ij} = 1, \forall i < j \in \mathcal{F}, \forall z \in \mathcal{Z}^i \cap \mathcal{Z}^j.$$

Similar coordinates

It is possible for two aircraft to have similar coordinates, so, they must fly at different altitude levels to avoid collisions since a velocity change, within its bounds, is not enough to avoid the conflict situation. The parameter sc_{ij} will take the value 1 if the distance between two different aircraft is less or equal to $r_i + r_j$ (the safety distance) and, otherwise, 0. The expression for the parameter sc is as follows,

$$sc_{ij} = \begin{cases} 1 & \text{if } d_{ij} \leqslant r_i + r_j \\ 0 & \text{otherwise.} \end{cases}$$

Then, the δ^5 variables can be fixed to 1 in the preprocessing phase as follows,

$$\delta_{ijz}^5 = 1 \quad \text{if } sc_{ij} = 1, \forall i < j \in \mathcal{F}, \forall z \in \mathcal{Z}^i \cap \mathcal{Z}^j.$$

Fixing variables

These previous constraints are used to fix some δ^5 variables to help the execution of the optimization engine, but they are not indispensable for the model, since it is autonomous to detect infeasible situations. Notice that the two constraints can be joined into one as follows,

$$\delta_{ijz}^5 = 1 \quad hth_{ij} + sc_{ij} \geqslant 1, \forall i < j \in \mathcal{F}, \forall z \in \mathcal{Z}^i \cap \mathcal{Z}^j.$$

The altitude changes are the cheapest ones in economic terms for the cost in fuel, but they are the most expensive ones in terms of comfort for passengers, see Frazzoli et al.

(1999) [39]. As a first step, the iVAC model can force aircraft to climb or descend only one level. To avoid a change of more than one altitude level, let the constraints be as follows,

$$\nu_f^z \leqslant 0 \quad \forall f \in \mathcal{F}, \forall z \in \mathcal{Z}^f | z \neq z_f, z \neq z_f \pm 1. \tag{2.6}$$

The constraints (2.6) can cause infeasible situations if the airspace is very busy, and only one change in altitude level is not enough to solve the problem efficiently. A new variable will be included in the model to count the number of levels that an aircraft climbs or descends, and in the objective function this variable will be penalized, see Section 2.3.5.

2.3.4 False conflicts in the VC model

False conflicts can occur in the VC model where two aircraft that are not in conflict are forced by the VC model to change their velocities owing to the fact that the geometric construction permits this situation as it is depicted in Fig. 2.10. In these cases the expressions (2.1) indicate that there is a conflict situation but the velocity vectors show the contrary. To avoid this situation the following parameter is used only when the two straight lines (aircraft trajectories) are secant. Notice that in parallel or in the same straight line either there is no conflict or there is a "head to head" or a "pursuit" situation, then fc_{ij} will be one in the first case:

$$fc_{ij} = \begin{cases} 1 & \text{if } d_{ij}^2 - d_{ij}^1 > 0 \wedge d_{ji}^2 - d_{ji}^1 > 0 \wedge sc_{ij}, hth_{ij} \neq 1 \\ 0 & \text{otherwise,} \end{cases}$$

where $d_{ij}^1 = \text{dist}\{(x_i, y_i), ip_{ij}\}$ and $d_f^2 = \text{dist}\{\big(x_i + \cos(m_i^*), y_i + \sin(m_i^*)\big), ip_{ij}\}$ being ip_{ij} the intersection point between the two straight lines under consideration (the trajectories of aircraft i and j), which can be calculated during the first step of the algorithm. Notice that with this notation, $ip_{ij} = ip_{ji}$.

If $fc_{ij} = 1$ the sum of the δ variables is forced to be zero, since if a "false conflict" happens it is not necessary to make a velocity or altitude maneuver. Notice that the fc parameter detects if two aircraft are getting far away from each other.

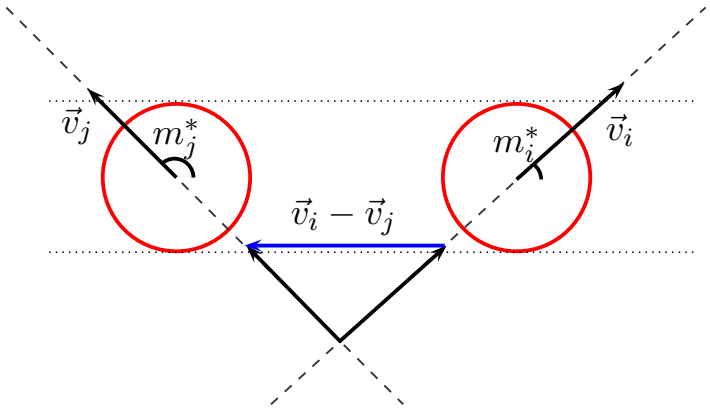

Figure 2.10: False conflict case between aircraft i and j

2.3.5 Limits on the number of altitude level changes

In busy airspace, it is possible for the iVAC model to have infeasible situations when aircraft cannot change more than one level. In these cases, the aircraft are allowed to change two or more altitude levels, but forcing these changes to be as seldom as possible.

To this effect, a new variable, $\rho_f, \forall f \in \mathcal{F}$, will be included in the model. It will take the value of the number of altitude levels that an aircraft climbs or descends. This number of changes can be greater than one and it will avoid infeasible situations in busy airspace. The number of altitude levels changed by an aircraft can be modeled as follows,

$$\rho_f = \Big| \sum_{z \in \mathcal{Z}^f} z\nu_f^z - z_f \Big|.$$

The first addend in the absolute value function gives the new level in which the aircraft must be after the optimization, since all ν variables take the value 0 except the ν variable in level $z \in \mathcal{Z}^f$ in which the aircraft flies after the resolution. The second addend gives the initial level in which the aircraft flies before the optimization. The absolute value makes the previous expression positive, but notice that this function is not linear, so, it has to be transformed. For this purpose, the maximum function can be taken between the differences $\sum_{z \in \mathcal{Z}^f} z\nu_f^z - z_f$ and $z_f - \sum_{z \in \mathcal{Z}^f} z\nu_f^z$ as shown in Appendix A.1.2, page 141, being this expression as follows,

$$\rho_f = \Big| \sum_{z \in \mathcal{Z}^f} z\nu_f^z - z_f \Big| = \max \Big\{ \sum_{z \in \mathcal{Z}^f} z\nu_f^z - z_f, z_f - \sum_{z \in \mathcal{Z}^f} z\nu_f^z \Big\}.$$

The maximum function is also nonlinear, but it can be linearized as shown in A.1.2, being as follows,

$$\rho_f \geqslant \sum_{z \in \mathcal{Z}^f} z\nu_f^z - z_f, \quad \forall f \in \mathcal{F} \tag{2.7a}$$

$$\rho_f \geqslant z_f - \sum_{z \in \mathcal{Z}^f} z\nu_f^z, \quad \forall f \in \mathcal{F}. \tag{2.7b}$$

The constraints (2.7) force ρ_f to be the maximum between the two expressions above, since ρ_f must be higher or equal than the two expressions, and ρ_f can only be greater than or equal to one expression, except if there is not a level change since the absolute value is 0. Now, these constraints are linear ones.

2.3.6 Updating the number of changes in velocity and altitude

In the iVAC model, one objective consists of minimizing the number of velocity and altitude changes executed by each aircraft, but as the algorithm will be iteratively executed it is necessary to update the number of changes of each aircraft to avoid situations in which it has to make several maneuvers whereas others have made none.

Velocity

As a first step the number of velocity changes will be counted. According to the following constraints, variable a_f takes the value 1 if a velocity change happens, and this occurs if $|q_f| \neq 0$. The absolute value is a nonlinear function to be modelized as a linear function as a traditional way in LP: $|q_f| = q_f^+ + q_f^-$ where $q_f^+ = \max\{q_f, 0\}$ is the positive component of q_f and $q_f^- = \max\{-q_f, 0\}$ is the negative component of q_f. These two new variables are positive and $q_f^+ + q_f^- \neq 0$ is equivalent to $q_f^+ + q_f^- > 0$.

$$\begin{aligned} M_1(1 - a_f) + \varepsilon &\leqslant q_f^+ + q_f^- && \forall f \in \mathcal{F} \\ q_f^+ + q_f^- &\leqslant M_2 a_f && \forall f \in \mathcal{F}, \end{aligned}$$

where $M_1 = -\varepsilon$ is the lower bound of

$$q_f^+ + q_f^- - \varepsilon$$

and $M_2 = \overline{v}_f - \underline{v}_f$ is the upper bound of

$$q_f^+ + q_f^-,$$

where ε is an infinitesimal parameter.

It is easy to prove that if there is a velocity change for aircraft $f \in \mathcal{F}$, then $q_f^+ + q_f^- \neq 0$, and the second constraints force a_f to take the value 1. On the other hand, if there is not a velocity change for aircraft $f \in \mathcal{F}$, then $q_f^+ + q_f^- = 0$, and the first constraints force a_f to take the value 0.

Altitude

The next step is to modify the value of b_f from 0 to 1 if there is an altitude change. With the following constraints, the number of altitude changes is updated:

$$b_f = 1 - \nu_f^{z_f^*} \quad \forall f \in \mathcal{F},$$

since if aircraft f flies at the same level before and after the current execution, then the variable $\nu_f^{z_f^*}$ will take value 1 and the difference will be 0, i.e., the aircraft does not change its altitude level. On the other hand, if aircraft f flies at different altitude levels before and after the current execution, $\nu_f^{z_f^*}$ will be 0 and b_f will take the value 1, i.e., the aircraft changes its altitude level.

2.3.7 Different terms for the objective function

The objective function will include all factors and different terms that are important for the problem. They are detailed below.

Velocity variations

The first objective consists of minimizing the velocity change's absolute value, such that the velocity changes and an early or delayed arrival to destination point in the aerial sector for each aircraft are smoothed. In [85] this term was considered by maximizing the velocity variations. It does not make sense when aircraft fly with an intermediate velocity and have to be accelerated due to this objective function. To make the number early arrivals

or arrival delays as small as possible, it is proposed, in this thesis, the minimization of the velocity variations by using the absolute value function to avoid major changes in the initial flight plan as follows,

$$\min \sum_{f \in \mathcal{F}} |q_f| = \min \sum_{f \in \mathcal{F}} (c_f^{q^+} q_f^+ + c_f^{q^-} q_f^-).$$

Different objective terms are considered, but with different magnitudes. All magnitudes involved in velocity changes expressions are normalized (between 0 and 1) as follows,

$$\min \sum_{f \in \mathcal{F}} \Big(\frac{c_f^{q^+} q_f^+}{\overline{v}_f - \underline{v}_f} + \frac{c_f^{q^-} q_f^-}{\overline{v}_f - \underline{v}_f} \Big).$$

Only q_f^+ or q_f^- will take a value greater than zero, and the objective function will make one of these variables equal to zero. Notice that $\overline{v}_f - \underline{v}_f$ is the upper bound of a velocity variation for an aircraft $f \in \mathcal{F}$.

Altitude levels

In case of very congested airspace, an aircraft may need to climb or descend more than one level, thus provoking infeasible situations in the model. Therefore, a new term is introduced in the objective function to avoid infeasibility. This option is modeled by adding the following term to the objective function such that the constraints (2.5) will be removed,

$$\min \sum_{f \in \mathcal{F}} c_f^j \rho_f. \tag{2.8}$$

Aircraft number of changes

Another term to include in the objective function to minimize is the number of velocity and altitude changes made by each aircraft in the aerial sector. Notice that the cost will increase when several changes are made in the same aircraft. The function is as follows,

$$\min \sum_{f \in \mathcal{F}} (c_f^v n_f^v a_f + c_f^a n_f^a b_f).$$

Returning to the initial configuration

Returning all aircraft configurations to their initial state both in velocity and altitude is desirable. A new term can be included so that the aircraft return to their initial configurations as soon as they are not in conflict.

Velocity First, the return to the initial velocity configuration is modeled, where there are two valid alternatives. The first alternative is to return to the initial velocity configuration, which is easy to model as follows,

$$\min \sum_{f \in \mathcal{F}} c_f^{v^*} |v_f + q_f - v_f^*|. \tag{2.9}$$

This function is nonlinear, but it can be modeled as a linear one by using the maximum-function as is explained in A.1.2, page 141. The addend is descomposed as $\beta_f = v_f + q_f - v_f^* = (v_f + q_f^+) - (q_f^- + v_f^*)$, with its use two additional constraints are necessary,

$$\begin{aligned} &\min \sum_{f \in \mathcal{F}} c_f^{v^*} \beta_f \\ s.t. : \beta_f &\geqslant (v_f + q_f^+) - (q_f^- + v_f^*) \quad \forall f \in \mathcal{F} \\ \beta_f &\geqslant (q_f^- + v_f^*) - (v_f + q_f^+) \quad \forall f \in \mathcal{F}. \end{aligned}$$

The second option is to force the aircraft to arrive at the destination point at the predicted time. Some notes about geometric constructions are necessary, taking Fig. 2.11 as support and the corresponding detailed explanation in Appendix A.3, page 147. The result is the following expression for the optimal velocity such that the aircraft $f \in \mathcal{F}$ goes out the sector at the predicted time,

$$\widehat{v}_f = \frac{\sqrt{(x_f^1 - x_f)^2 + (y_f^1 - y_f)^2}}{t_1 - t}.$$

Therefore, the difference between the current velocity and the optimal velocity to

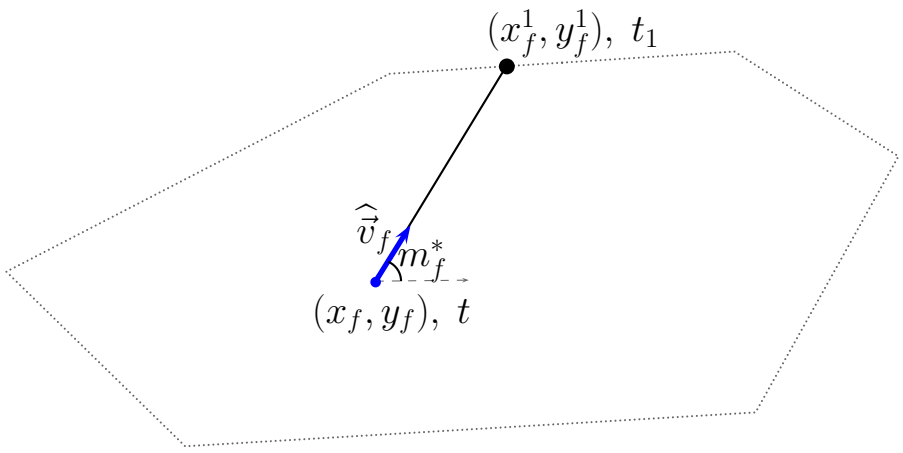

Figure 2.11: Return to the initial configuration time

arrive at the destination point at the predicted time is penalized as follows,

$$\min \sum_{f \in \mathcal{F}} c_f^{\hat{v}} |v_f + q_f - \widehat{v_f}|. \tag{2.10}$$

This function is nonlinear, but it can be modeled as a linear one by using the maximum function as it is detailed in Appendix A.1.2. The addend can be descomposed as $\beta_f = v_f + q_f - \widehat{v_f} = (v_f + q_f^+) - (q_f^- + \widehat{v_f})$, and by using this, two additional constraints are necessary as follows,

$$\begin{aligned} \min & \sum_{f \in \mathcal{F}} c_f^{\hat{v}} \beta_f \\ s.t. : \beta_f &\geqslant (v_f + q_f^+) - (q_f^- + \widehat{v_f}) \\ \beta_f &\geqslant (q_f^- + \widehat{v_f}) - (v_f + q_f^+). \end{aligned}$$

Altitude A term to penalize the difference between the current and initial level configurations is added by using the ν variable. An aircraft takes its initial level configuration if $\nu_f^{z_f^*} = 1$; therefore, the new objective function will be as follows,

$$\max \sum_{f \in \mathcal{F}} c_f^{z^*} \nu_f^{z_f^*}.$$

Notice that all previous terms for the objective function have to be minimized, therefore, it is necessary to change maximization by minimization by changing the sign of the addend

as follows,

$$\min \sum_{f \in \mathcal{F}} -c_f^{z^*} \nu_f^{z_f^*}.$$

Costs

Besides the above terms in the objective function, new costs to model other preferences like fuel consumption can be added and, finally, any linear combination of terms can be chosen, taking into account that (2.9) and (2.10) cannot be chosen at the same time since each considers disjoint objectives.

The penalization parameters $c_f^{q^+}$, $c_f^{q^-}$, c_f^j, c_f^v, c_f^a, $c_f^{v^*}$, $c_f^{\hat{v}}$ and $c_f^{z^*}$ can be used in the corresponding term of the objective function that will be used. Also, any linear combination is possible, just as considering weights w_n for each objective function term $n = 1, \ldots, 5$ to attribute the importance given to each one being $\sum_{n=1}^{5} w_n = 1$.

Then, the full objective function will be as follows,

$$\min w_1 \sum_{f \in \mathcal{F}} \left(\frac{c_f^{q^+} q_f^+}{\overline{v}_f - \underline{v}_f} + \frac{c_f^{q^-} q_f^-}{\overline{v}_f - \underline{v}_f} \right) + w_2 \sum_{f \in \mathcal{F}} c_f^j \rho_f + w_3 \sum_{f \in \mathcal{F}} (c_f^v n_f^v a_f + c_f^a n_f^a b_f) + w_4 \sum_{f \in \mathcal{F}} c_f^{v^*} \beta_f - w_5 \sum_{f \in \mathcal{F}} c_f^{z^*} \nu_f^{z_f^*}$$

if the first method is chosen to return to the initial configuration, and

$$\min w_1 \sum_{f \in \mathcal{F}} \left(\frac{c_f^{q^+} q_f^+}{\overline{v}_f - \underline{v}_f} + \frac{c_f^{q^-} q_f^-}{\overline{v}_f - \underline{v}_f} \right) + w_2 \sum_{f \in \mathcal{F}} c_f^j \rho_f + w_3 \sum_{f \in \mathcal{F}} (c_f^v n_f^v a_f + c_f^a n_f^a b_f) + w_4 \sum_{f \in \mathcal{F}} c_f^{\hat{v}} \beta_f - w_5 \sum_{f \in \mathcal{F}} c_f^{z^*} \nu_f^{z_f^*}$$

if the second method to go out from the aerial sector in the predicted time is chosen.

2.3.8 The iVAC formulation

To summarize all of the previous concepts the full iVAC model is as follows,

$$\min w_1 \sum_{f\in\mathcal{F}} \Big(\frac{c_f^{q^+} q_f^+}{\overline{v}_f - \underline{v}_f} + \frac{c_f^{q^-} q_f^-}{\overline{v}_f - \underline{v}_f}\Big) + w_2 \sum_{f\in\mathcal{F}} c_f^j \rho_f + w_3 \sum_{f\in\mathcal{F}} (c_f^v n_f^v a_f + c_f^a n_f^a b_f) + w_4 \sum_{f\in\mathcal{F}} c_f^{v^*} \beta_f - w_5 \sum_{f\in\mathcal{F}} c_f^{z^*} \nu_f^{z_f^*} \quad (2.11a)$$

or

$$\min w_1 \sum_{f\in\mathcal{F}} \Big(\frac{c_f^{q^+} q_f^+}{\overline{v}_f - \underline{v}_f} + \frac{c_f^{q^-} q_f^-}{\overline{v}_f - \underline{v}_f}\Big) + w_2 \sum_{f\in\mathcal{F}} c_f^j \rho_f + w_3 \sum_{f\in\mathcal{F}} (c_f^v n_f^v a_f + c_f^a n_f^a b_f) + w_4 \sum_{f\in\mathcal{F}} c_f^{\hat{v}} \beta_f - w_5 \sum_{f\in\mathcal{F}} c_f^{z^*} \nu_f^{z_f^*} \quad (2.11b)$$

subject to

$$\underline{v}_f \leqslant v_f + q_f \leqslant \overline{v}_f \quad \forall f \in \mathcal{F} \quad (2.12)$$

$\forall i,j \in \mathcal{F} : i < j, \forall z \in \mathcal{Z}^i \cap \mathcal{Z}^j \wedge p_{ij} = 0$

$$(v_i + q_i)\cos(m_i^*) - (v_j + q_j)\cos(m_j^*) \leqslant (\overline{v}_i + \overline{v}_j)(1 - \delta_{ijz}^1) \quad (2.13a)$$
$$-(v_i + q_i)h_i + (v_j + q_j)h_j \leqslant (\overline{v}_i|h_i| + \overline{v}_j|h_j|)(1 - \delta_{ijz}^1) \quad (2.13b)$$
$$(v_i + q_i)\cos(m_i^*) - (v_j + q_j)\cos(m_j^*) \leqslant (\overline{v}_i + \overline{v}_j)(1 - \delta_{ijz}^2) \quad (2.13c)$$
$$(v_i + q_i)k_i - (v_j + q_j)k_j \leqslant (\overline{v}_i|k_i| + \overline{v}_j|k_j|)(1 - \delta_{ijz}^2) \quad (2.13d)$$
$$-(v_i + q_i)\cos(m_i^*) + (v_j + q_j)\cos(m_j^*) \leqslant (\overline{v}_i + \overline{v}_j)(1 - \delta_{ijz}^3) \quad (2.13e)$$
$$(v_i + q_i)h_i - (v_j + q_j)h_j \leqslant (\overline{v}_i|h_i| + \overline{v}_j|h_j|)(1 - \delta_{ijz}^3) \quad (2.13f)$$
$$-(v_i + q_i)\cos(m_i^*) + (v_j + q_j)\cos(m_j^*) \leqslant (\overline{v}_i + \overline{v}_j)(1 - \delta_{ijz}^4) \quad (2.13g)$$
$$-(v_i + q_i)k_i + (v_j + q_j)k_j \leqslant (\overline{v}_i|k_i| + \overline{v}_j|k_j|)(1 - \delta_{ijz}^4) \quad (2.13h)$$
$$\delta_{ijz}^1 + \delta_{ijz}^2 + \delta_{ijz}^3 + \delta_{ijz}^4 + \delta_{ijz}^5 = 1 \quad (2.13i)$$

$\forall i,j \in \mathcal{F} : i < j, \forall z \in \mathcal{Z}^i \cap \mathcal{Z}^j$

$$\delta_{ijz}^5 = 1 \qquad \text{if } hth_{ij} = 1 + sc_{ij} \geqslant 1 \quad (2.14a)$$
$$\nu_i^z + \nu_j^z \geqslant \delta_{ijz}^5 - 1 \quad (2.14b)$$

$$\nu_i^z + \nu_j^z \leqslant 2 - \delta_{ijz}^5 \tag{2.14c}$$

$\forall f \in \mathcal{F}$

$$\sum_{z \in \mathcal{Z}^f} \nu_f^z = 1 \tag{2.15}$$

$$\nu_f^z = 0 \qquad \forall z \in \mathcal{Z}^f | z \neq z_f, z_f \pm 1 \tag{2.16}$$

$$\sum_{z \in \mathcal{Z}^f} z\nu_f^z - z_f \leqslant \rho_f \tag{2.17a}$$

$$z_f - \sum_{z \in \mathcal{Z}^f} z\nu_f^z \leqslant \rho_f \tag{2.17b}$$

$$-\varepsilon(1 - a_f) + \varepsilon \leqslant q_f^+ + q_f^- \tag{2.18a}$$

$$q_f^+ + q_f^- \leqslant (\overline{v}_f - \underline{v}_f)a_f \tag{2.18b}$$

$$1 - \nu_f^{z_f} = b_f \tag{2.18c}$$

$$(v_f + q_f^+) - (q_f^- + v_f^*) \leqslant \beta_f \tag{2.19a}$$

$$(q_f^- + v_f^*) - (v_f + q_f^+) \leqslant \beta_f \tag{2.19b}$$

$$(v_f + q_f^+) - (q_f^- + \widehat{v_f}) \leqslant \beta_f \tag{2.20a}$$

$$(q_f^- + \widehat{v_f}) - (v_f + q_f^+) \leqslant \beta_f \tag{2.20b}$$

$\forall f \in \mathcal{F}$

$$q_f \in \mathbb{R} \tag{2.21a}$$

$$q_f^+, q_f^-, \beta_f \in \mathbb{R}^+ \tag{2.21b}$$

$$\rho_f \in \mathbb{Z}^+ \tag{2.21c}$$

$\forall f, i, j \in \mathcal{F} : i < j, \forall z \in \mathcal{Z}$

$$\nu_f^z, a_f, b_f, \delta_{ijz}^1, \delta_{ijz}^2, \delta_{ijz}^3, \delta_{ijz}^4, \delta_{ijz}^5 \in \{0, 1\}. \tag{2.21d}$$

The objective function (2.11) can be any linear combination of the alternatives that were considered in Section 2.3.7. Only one of the functions (2.11a) or (2.11b) can be chosen with the corresponding set of constraints (2.16) or (2.17), respectively. The constraints (2.12) avoid setting new aircraft velocities above or below two fixed bounds, say, $\overline{v}_f$ and $\underline{v}_f$, respectively, where $q_i = q_i^+ - q_i^-$ is the velocity variation, q_i^+ is its positive part and q_i^- is its negative part, both positive variables. If $q_i > 0$ then $q_i^+ > 0$ and $q_i^- = 0$; If $q_i < 0$ then $q_i^+ = 0$ and $q_i^- > 0$; If $q_i = 0$ then $q_i^+ = 0$ and $q_i^- = 0$. The constraints (2.12) and (2.13) are the VC model adapted for the iVAC, as can be seen in (2.3i), including the δ^5 variables in order to allow altitude level changes in the infeasible situations shown in Fig. 2.6. The parameter p_{ij} is used in constraints (2.13) to consider only the pairs of aircraft that are interesting (see Section 2.3.4 for information on false conflicts and Section 2.3.9 for the explanation of the p_{ij} parameter). Constraints (2.14a) fix the δ^5 variables to 1 if there is a "head to head" or a "similar coordinate" situation between two different aircraft i and j. These constraints can be used to reduce the execution time. However, if it is desirable not to use them, there is not an inconvenience, since the iVAC model is autonomous in avoiding infeasible situations by using constraints (2.14b) and (2.14c). These constraints force two different aircraft to fly at different altitudes if $\delta^5 = 1$, i.e., if different situations occur like the "head to head" case, infeasibility in velocity bounds as two aircraft have similar coordinates or velocity bounds prevent aircraft avoid a conflict, an aircraft flies faster than another one in the same direction, etc. Moreover, these constraints help to have a tighter LP relaxation of the model. Constraints (2.15) force each aircraft to fly at only one level, as it was shown in (2.5). Constraints (2.16) force each aircraft to change only one level if it is necessary, as noticed in (2.6). They must not be used jointly with constraints (2.17). Constraints (2.17) are used to minimize the number of levels that the aircraft change, to avoid infeasible situations in busy airspace where one level change is not enough to avoid a conflict, as was considered in Section 2.3.5. Constraints (2.18) count the number of velocity changes in constraints (2.18a) and (2.18b) and the number of altitude changes in constraints (2.18c), respectively. These constraints must be used jointly with the term (2.8) of the objective function and constraints (2.21c). Constraints (2.19) model the absolute value of the term (2.9) of the objective function as a linear function, and must be used jointly with it. Constraints (2.20) model the absolute value of the term (2.10) of the objective function as a

Table 2.1: Dimensions of the VAC model

Variables q_f^+: F	Variables q_f^-: F
Variables ν_f^z: FZ	Variables a_f: F
Variables b_f: F	Variables ρ_f: F
Variables β_f: F	Variables δ_{ijz}^n: $5Z\frac{(F-1)F}{2}$

(a) Number of variables

C. (2.12): $2F$	C. (2.13): $9Z\frac{F(F-1)}{2}$
C. (2.14a): $Z\frac{F(F-1)}{2}$	C. (2.14b)-(2.14c): $ZF(F-1)$
C. (2.15): F	C. (2.16): $3F$
C. (2.17): $2F$	C. (2.18a)-(2.18b): $2F$
C. (2.18c): F	C. (2.19) or (2.20): $2F$

(b) Number of constraints

linear function, and must be used jointly with it. Constraints (2.21) give the variables' type.

Model dimensions

Table 2.1 shows the summary of the recount of all variables and constraints for the iVAC model. The total number of variables in the iVAC model depends on the choice of the objective function, and it will be the sum of the corresponding values. It also shows the number of constraints for the iVAC model. (Notice that it also depends on the objective function of choice, and it will be the sum of the corresponding values).

2.3.9 Computational experience

In this section a computational experience is presented in order to test the validity of the iVAC model.

Preprocessing

A careful preprocessing in order to fix variables that will help to simplify the model and reduce the execution time must be performed.

First, it is necessary to fix the coordinates, the current velocity, maximum and minimum velocity, the motion angle of each aircraft, and the security distance between aircraft (usually 5 nautical miles), or if different radii are considered, each aircraft radius. With this

information, the angle ω_{ij} must be fixed to $\pi/2$ if $x_i = x_j$ or 0 if $y_i = y_j$. Otherwise, it should be calculated by using the arctangent expression. The next step consists of calculating the distance between all aircraft and α angles. In order to simplify the notation, l_{ij}, g_{ij}, h_i, h_j, k_i, k_j can be calculated previously as well as all the bounds in the model.

Now, it should be determined whether two aircraft are in a "head to head" situation, see parameter hth in Section 2.3.3. If there is a "head to head" situation the parameter hth_{ij} is fixed to 1, otherwise, it will be fixed to 0. It is possible for two aircraft to have the same or similar coordinates x and y, i.e., the distance between them is 0 or they are close to each other, but they fly at different altitude levels. This case must be included in the model for, on the one hand, avoiding the calculation of the arctangent has the denominator equal to 0 and, on the other hand, forcing the parameter sc_{ij} to take the value 1 and, then, forcing the aircraft to fly at different levels, see parameter sc in Section 2.3.3.

In the preprocessing phase some δ^5 variables can be fixed, which will make the computing time for the optimal solution of the model shorter. If preferred, the number of variables in the model can be reduced if the intersection between the trajectories of two aircraft is out of the sector.

The calculation of the intersection point is presented in Appendix A.4, page 149, such that it can be as follows,

$$\left(\frac{y_j - \frac{v_j^2}{v_j^1} x_j - y_i + \frac{v_i^2}{v_i^1} x_i}{\frac{v_i^2}{v_i^1} - \frac{v_j^2}{v_j^1}} \quad , \frac{\frac{v_i^2}{v_i^1}\left(y_j - \frac{v_j^2}{v_j^1} x_j\right) - \frac{v_j^2}{v_j^1}\left(y_i - \frac{v_i^2}{v_i^1} x_i\right)}{\frac{v_i^2}{v_i^1} - \frac{v_j^2}{v_j^1}} \right)$$

where (x_i, y_i), (x_j, y_j), $\vec{v_i} = (v_i^1, v_j^2)$ and $\vec{v_j} = (v_j^1, v_j^2)$ are the initial points and the direction vectors of the two different aircraft i and j.

All aircraft that have an intersection point inside the aerial sector must be considered, since a conflict can occur between them. All previous calculations are based on the assumption that altitude levels do not exist, since new conflicts can exist in other altitude levels and it is desired to restrict all these possible cases.

The auxiliary parameter p_{ij} can also be used to include only the pair of aircraft that whose intersection point is not far away from the aircraft positions, in order to consider only the pair of aircraft that are near each other. If this parameter is used in the model it is

necessary to take into account all pairs of aircraft. The parameter is as follows,

$$p_{ij} = \begin{cases} 1 \text{ if } dist(p, p_i) > e \text{ and } dist(p, p_j) > e \vee fc_{ij} = 1 \\ 0 \text{ otherwise,} \end{cases}$$

where p is the intersection point between aircraft i and j; p_i and p_j are the aircraft positions of i and j respectively; and e is the parameter that represents the minimum distance to consider for comparing two aircraft in the model. This parameter will also be one if aircraft i and j are in false conflict, see Section 2.3.4.

By using this preprocessing, the number of variables and constraints in the model is reduced, and additionally, some variables are forced to be zero so that the resolution of the model will be faster than considering all aircraft in the sector.

The model has to be solved by using an optimization engine, such as the commercial engines CPLEX [63], GUROBI [49] and XPRESS-MP [36] among others, or the free software SCIP [105] and COIN-OR [64], among others.

Illustrative instances

The iVAC model has been initially tested with the example shown in Fig. 2.12, by using the weights $w_1 = w_2 = 0.5$ in the objective function. Then, the velocity variations and the number of levels that the aircraft have to change are minimized. In this objective function, $c_f^{q^+} = 1$, $c_f^{q^-} = 1$ and $c_f^j = 1$, and the rest of the costs will be $0 \; \forall f \in \mathcal{F}$. The parameter p_{ij} is not considered; therefore, all pairs of aircraft are taken into account, since this is of interest in testing the full model.

The computational experiment was made using the following HW/SW platform: Intel Core 2 DUO P8400, 2.26GHz, 2GB RAM; Microsoft Windows 7 Professional SO.

The velocities of all aircraft are the same: velocity 9, maximum velocity 10 and minimum velocity 8, except for aircraft (c), whose configuration is velocity 100, maximum velocity 101 and minimum velocity 99, forcing this aircraft to descend two levels in order to avoid a “head to head” conflict and a pursuit situation.

In this example there are many interrelated conflicts to solve such as (1) “head to head” situations that will force aircraft to change their levels, (2) cases (a) and (b) where same or similar coordinate situations will force involved aircraft to fly at different levels and

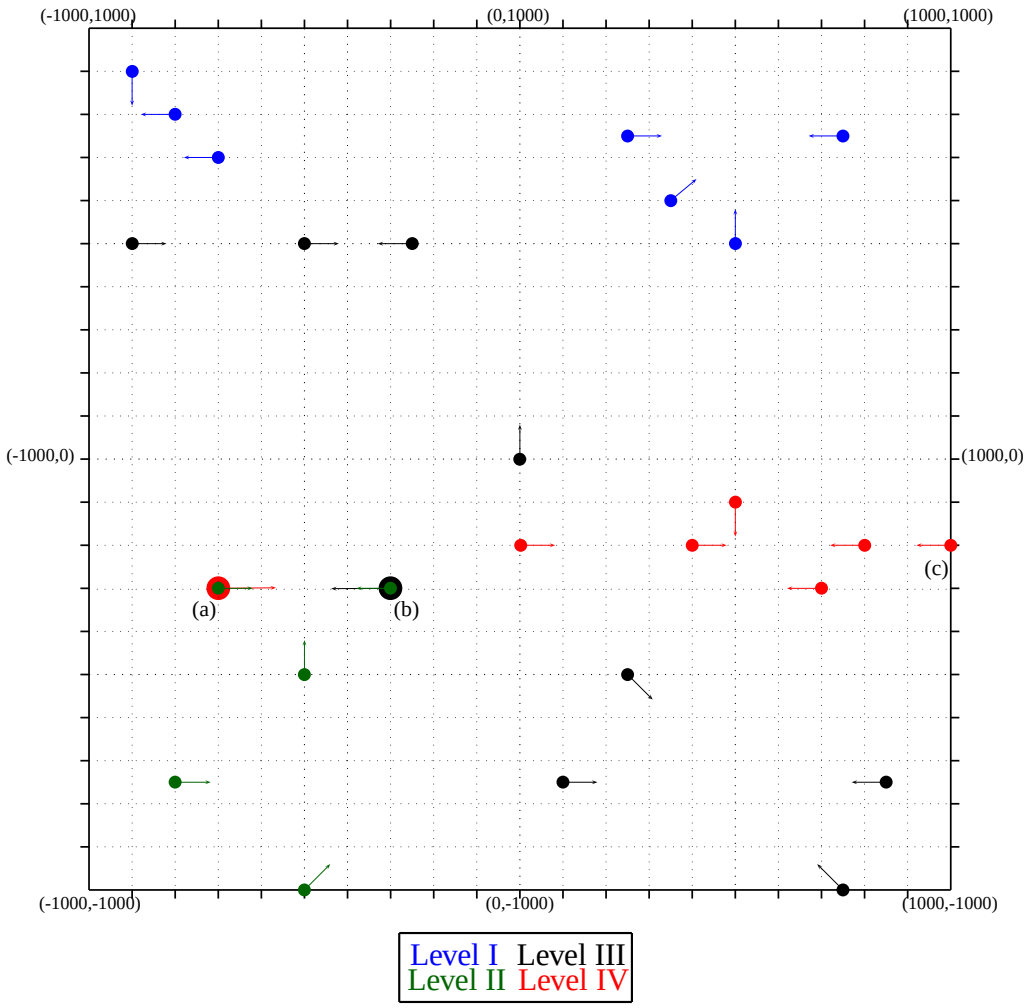

Figure 2.12: 1st illustrative instance for testing the iVAC model. Initial situation

(3) case (c) in which an aircraft flies faster than another one in the same direction to force them to fly at different levels, one of them descending two levels due to “head to head” conflict with other one.

The main results of executing the iVAC model for the instance are as follows:

- Five velocity changes have been made, see Fig. 2.13. The dotted line circles denote the positive variation of velocity (in two aircraft), and the dashed line circle denotes the negative variation of velocity (in three aircraft). In this case, all velocity changes are negative (deceleration), since the same costs in the objective function are considered, and multiple solutions with the same value in the objective function are obtained.

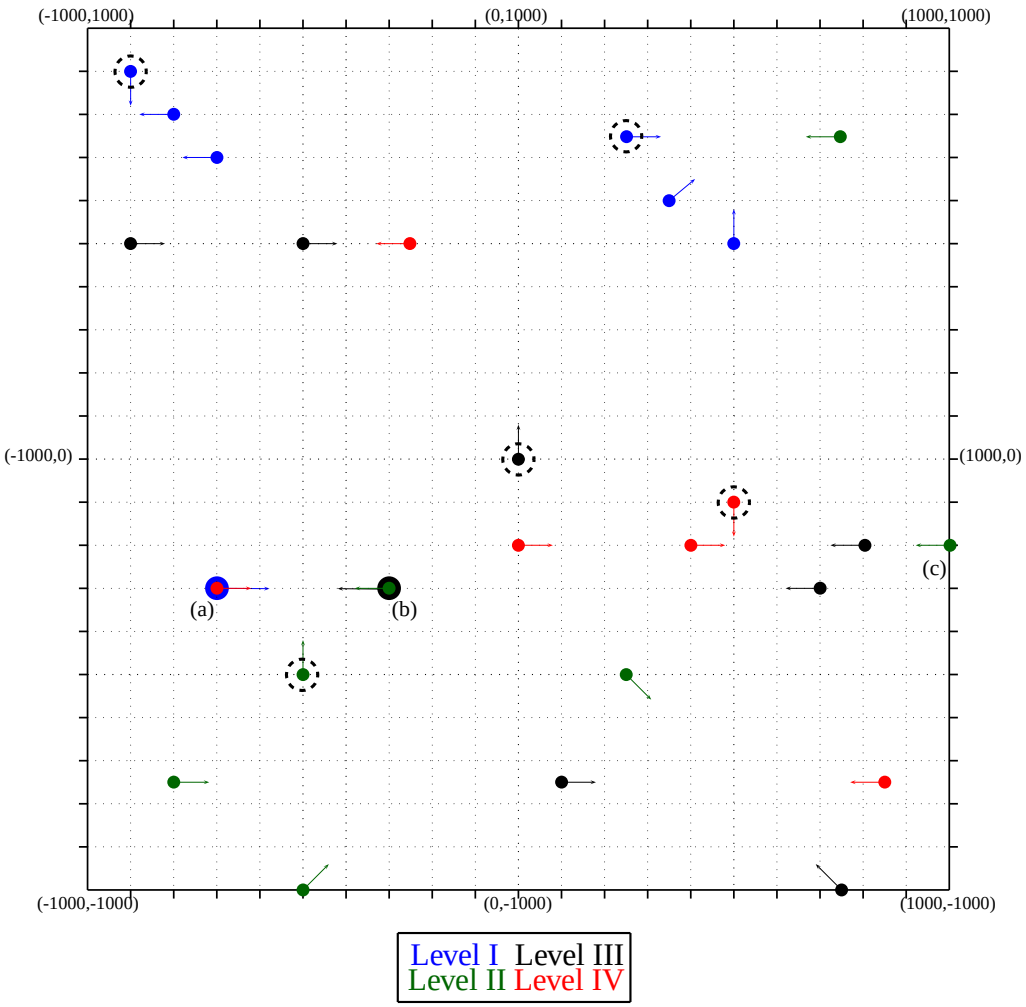

Figure 2.13: 1st illustrative instance for testing the iVAC model. Resolution

- There are eight altitude level changes, three positive and five negative changes, one of which descends two levels. The final configuration of all aircraft can be seen in Fig. 2.13.
- The objective function value is 10.001750.
- The execution time has been 3.60 seconds by using CPLEX v.12.1 [63] (with the default options).

In this example, all conflicts have been avoided satisfactorily. However, the iVAC model does not solve some particular cases, like those with a null denominator. In the

example shown in Fig. 2.14, some new aircraft have been added where the resolution does not solve all the conflict situations.

In this second illustrative instance the velocities of all aircraft are the same as in the first: velocity 9, maximum velocity 10 and minimum velocity 8, except for aircraft (c) and (d) whose configurations are velocity 100, maximum velocity 101 and minimum velocity 99. It will force aircraft (c) to descend two levels, since it is involved in a "head to head" situation with two other aircraft and will force aircraft (d) to avoid the "head to head" cases in the vertical axis. There are many crossing conflicts to solve in this example, such as "head to head" situations in order to force aircraft to change their levels and conflicts where the involved aircraft have similar coordinates, to force (a) and (b) to fly at different levels. Aircraft (e), (f), (g) and (h) have been included to take into account "false conflict" situations.

The resolution of the instance without fixed variables by using parameters sc and hth is as follows:

- Five velocity changes have been made, see Fig. 2.15. The dotted line circles denote the positive variation of velocity (in two aircraft), and the dashed line circle denotes the negative variation of velocity (in three aircraft). In this case, all velocity changes are negative (deceleration).
- There are nine altitude level changes, two positive and seven negative, one of which descends two levels. The final configuration of all aircraft can be seen in Fig. 2.15.
- The aircraft (e), (f), (g) and (h) have not changed their velocities since they are in a "false conflict".
- The objective function value is 10.9601.
- The execution time has been 3.43 seconds by using CPLEX v.12.1 (with the default options).

It can be seen in the example that there are two aircraft, (i) and (j), that do not avoid the collision situation, since they have the same velocity after the resolution. The aircraft (d), (k), (l) and (m) do not avoid the conflicts due to the null denominator in expression (2.1), making this situation unstable and causing the physical collision between the two aircraft.

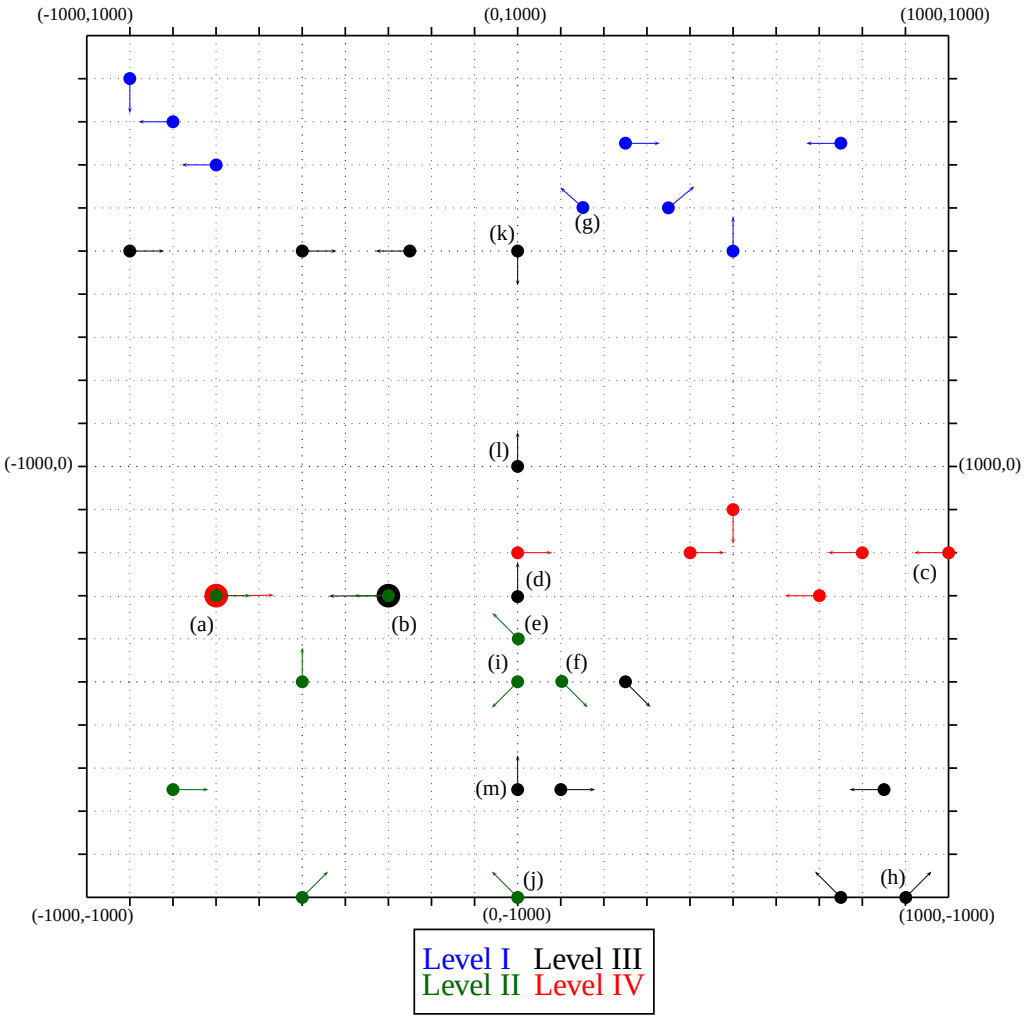

Figure 2.14: 2nd illustrative instance for testing the iVAC model. Initial situation

If the δ^5 variables are fixed in preprocessing, one of the "head to head" conflicts between aircraft (d), (k), (l) and (m) is avoided, but there is a "head to head" conflict that is not avoided, caused by the higher velocity of aircraft (d).

The results of the example with fixed variables, where parameters sc and hth are used, are as follows:

- Five velocity changes have been made, see Fig. 2.16. The dotted line circles denote the positive variation of velocity (in two aircraft), and the dashed line circle denotes the negative variation of velocity (in three aircraft). In this case, all velocity changes are negative (deceleration).

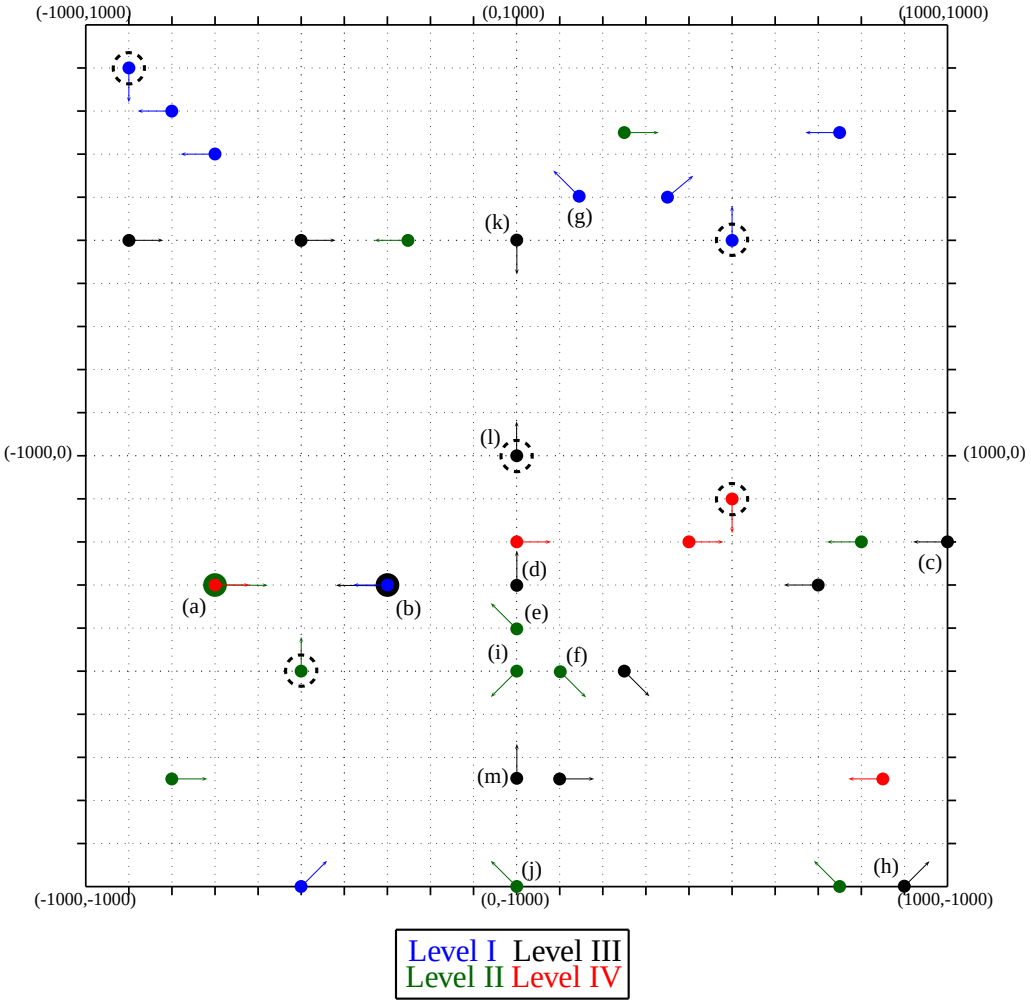

Figure 2.15: Resolution of the 2nd. illustrative instance for testing the iVAC model without preprocessing

- There are ten altitude level changes, four positive and six negative, one of which descends two levels. The final configuration of all aircraft can be seen in Fig. 2.16.
- The aircraft (e), (f), (g) and (h) have not changed their velocities since they are in a "false conflict".
- The objective function value is 11.9601.
- The execution time was 4.26 seconds by using CPLEX v.12.1 (with the default options).

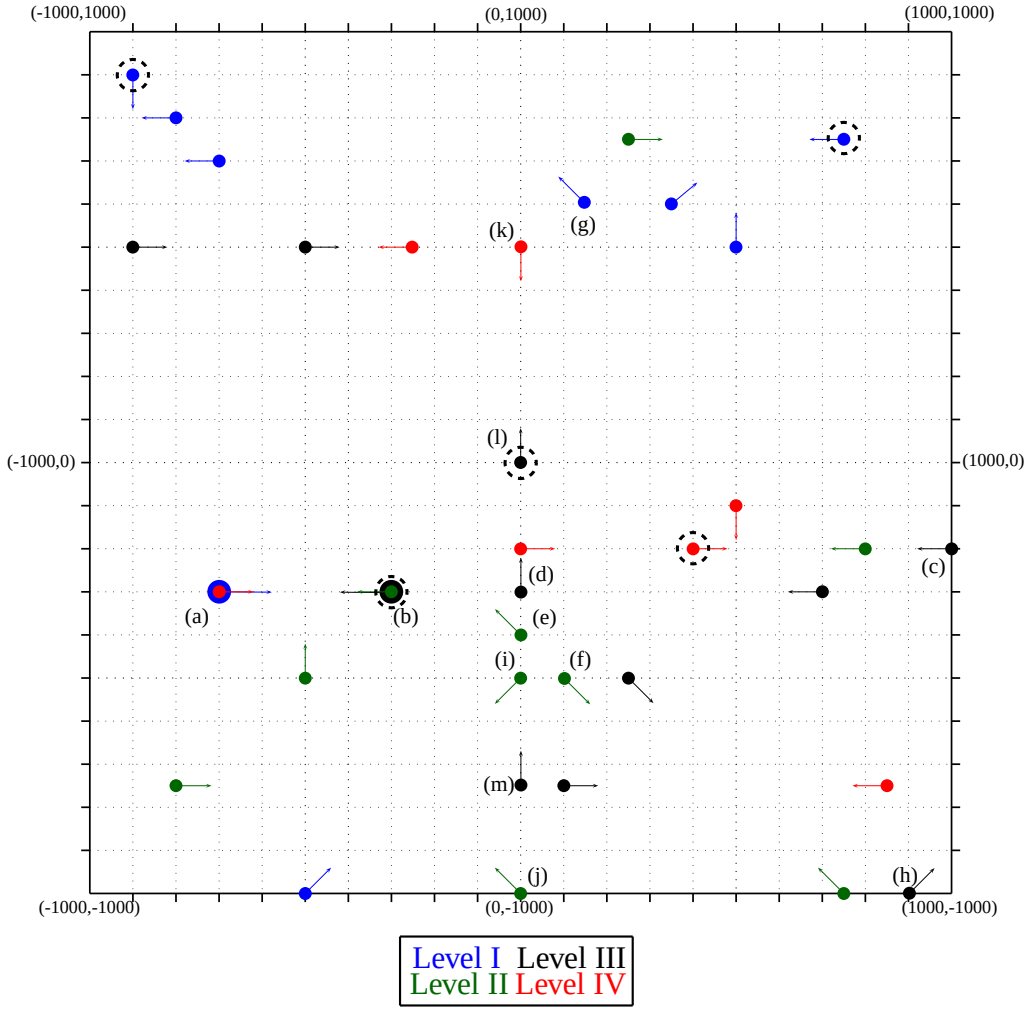

Figure 2.16: Resolution of the 2nd illustrative instance for testing the iVAC model by using preprocessing

It can be seen in the instance that there are two aircraft, (i) and (j), that do not avoid a collision situation with neither velocity changes nor altitude changes. It is due to the fact that the denominator in expression (2.1) is equal to zero and the situation is unstable, causing the collision between the two aircraft. The aircraft (d) and (l) do not avoid the conflict due to the null denominator and a pursuit situation not solved.

The first resolution (without fixed variables) is not autonomous when “anomalous cases” caused by a null denominator take place, whereas the second resolution (with fixed variables) allows changing the altitude in “head to head” cases.

This inconvenience can be remedied by first calculating the denominator of the expression (2.1) for all obtained solutions for all $i < j$, and, second, if there exists a null denominator, by making a rotation of the airspace such that the denominator is not zero. This problem is invariant with respect to rotational transformations of the flight plan since Euclidean distances are considered. The rotation matrix in two dimensions with a random angle ϑ is used to rotate, which can be simulated, as follow,

$$\begin{pmatrix} \cos(\vartheta) & -\sin(\vartheta) \\ \sin(\vartheta) & \cos(\vartheta) \end{pmatrix}.$$

All coordinates of the aircraft have to be rotated around the origin point in the reference system, and adding ϑ to all angles by using the rotation matrix as follows,

$$\begin{pmatrix} \cos(\vartheta) & -\sin(\vartheta) \\ \sin(\vartheta) & \cos(\vartheta) \end{pmatrix} \begin{pmatrix} x_i \\ y_i \end{pmatrix}.$$

The new coordinates are:

$$\begin{aligned} x_i' &= x_i \cos(\vartheta) - y_i \sin(\vartheta) \\ y_i' &= x_i \sin(\vartheta) + y_i \sin(\vartheta). \end{aligned}$$

By using these expressions the model can be solved again and then, proving again if all denominators with the new solution are different from zero.

This point of view is proposed in [84, 85] and is not advisable since many cycles can occur without reaching all non-zero denominators, and the execution time will increase. In the next section the final version of the VAC model with the resolution of the anomalous cases is presented.

2.4 The Velocity and Altitude Changes (VAC) model: Full version

In this section the most important contribution of this chapter is presented. As shown in the previous section, some cases are not solved by the VC and iVAC models, due to the existence of possible null denominators in the relative velocity vectors. These cases

have been called “anomalous cases”, since the resolution gives a configuration where the two involved aircraft will crash physically, causing unstable situations.

2.4.1 Anomalous cases

The main motivation behind implementing the anomalous cases in the VAC model consists of detecting them in the preprocessing phase. Then, if there is an anomalous case between aircraft i and j, turning the aircraft configuration in the model is proposed, but only between these aircraft, since the model considers each pair of aircraft independently, for avoiding conflicts, in each set of constraints, but all maneuvers as a whole.

In order to detect possible anomalous cases between two aircraft in preprocessing, a 0-1 parameter is used. This parameter will be 1 if the tangent of the relative velocity vector can be infinity and, otherwise, it will be zero. Only the pairs of aircraft where the difference between their abscissas is less than the sum of the safety radii are considered. The formal definition of the parameter is as follows,

$$pc_{ij} = \begin{cases} 1 & \text{if } |x_i - x_j| \leqslant r_i + r_j \\ 0 & \text{otherwise.} \end{cases} \tag{2.22}$$

All conflicts where the abscissa of the positions are similar in both aircraft of the pair will be taken into account since the denominator can be zero. In these cases, the configuration (direction of motion and consequently angles l and g) of the aircraft i and j with $i, j \in \mathcal{F}$, is turned $\frac{\pi}{2}$ radians, considering the same velocity.

This parameter will be included in the VAC model, so that all anomalous cases will be avoided and it will not be necessary to detect if there is a denominator equal to zero and solve again in the affirmative case, so, reducing the computational cost.

If pc_{ij} is equal to 1, the parameters of the initial configuration of aircraft i and j will be turned $\frac{\pi}{2}$ radians, otherwise, the initial configuration will not be changed. For the first constraints in each case of the iVAC model (the one that detects if the denominator is positive or negative), the new expression will be as follows,

$$(v_i+q_i)\big(\cos(m_i^*)(1-pc_{ij})-\sin(m_i^*)pc_{ij}\big)-(v_j+q_j)\big(\cos(m_j^*)(1-pc_{ij})-\sin(m_j^*)pc_{ij}\big) \leqslant M_m(1-\delta_{ijz}^n),$$

where $\cos(m_i^* + \frac{\pi}{2}) = -\sin(m_i^*)$ and $M_m = (\overline{v}_i + \overline{v}_j)$ is the upper bound of

$$(v_i+q_i)\big(\cos(m_i^*)(1-pc_{ij})-\sin(m_i^*)pc_{ij}\big)-(v_j+q_j)\big(\cos(m_j^*)(1-pc_{ij})-\sin(m_j^*)pc_{ij}\big).$$

For the second constraints in each case, the new expression will be as follows,

$$-(v_i+q_i)\big(h_i(1-pc_{ij})+h_i'pc_{ij}\big)+(v_j+q_j)\big(h_j(1-pc_{ij})+h_j'pc_{ij}\big)\leqslant M_m(1-\delta_{ijz}^n),$$

where h_i' and h_j' are the terms h_i and h_j with the new turned parameters and M_m, in these constraints, will be as follows,

$$M_m = (\overline{v}_i|h_i| + \overline{v}_j|h_j|)(1-pc_{ij}) + (\overline{v}_i|h_i'| + \overline{v}_j|h_j'|)pc_{ij}.$$

Notice that for constraints where parameter k is involved, the expression in the VAC model is analogue.

The parameters when an anomalous case happens h_i, h_j, k_i, k_j will be as follows,

$$\begin{aligned}
h_i' &= -\tan(l_{ij})\sin(m_i^*) - \cos(m_i^*)\\
h_j' &= -\tan(l_{ij})\sin(m_j^*) - \cos(m_j^*)\\
k_i' &= -\tan(g_{ij})\sin(m_i^*) - \cos(m_i^*)\\
k_j' &= -\tan(g_{ij})\sin(m_j^*) - \cos(m_j^*).
\end{aligned}$$

2.4.2 The VAC formulation

Next, the full VAC model is presented, where all unstable situations caused by anomalous cases are considered and solved.

$$\min w_1 \sum_{f\in\mathcal{F}}\Big(\frac{c_f^{q^+}q_f^+}{\overline{v}_f-\underline{v}_f}+\frac{c_f^{q^-}q_f^-}{\overline{v}_f-\underline{v}_f}\Big)+w_2\sum_{f\in\mathcal{F}}c_f^j\rho_f+w_3\sum_{f\in\mathcal{F}}(c_f^v n_f^v a_f+c_f^a n_f^a b_f)+ \\ w_4\sum_{f\in\mathcal{F}}c_f^{v^*}\beta_f - w_5\sum_{f\in\mathcal{F}}c_f^{z^*}\nu_f^{z_f^*} \quad (2.23a)$$

or

$$\min w_1 \sum_{f\in\mathcal{F}} \Big(\frac{c_f^{q^+} q_f^+}{\overline{v}_f - \underline{v}_f} + \frac{c_f^{q^-} q_f^-}{\overline{v}_f - \underline{v}_f}\Big) + w_2 \sum_{f\in\mathcal{F}} c_f^j \rho_f + w_3 \sum_{f\in\mathcal{F}} (c_f^v n_f^v a_f + c_f^a n_f^a b_f) + w_4 \sum_{f\in\mathcal{F}} c_f^{\hat{v}} \beta_f - w_5 \sum_{f\in\mathcal{F}} c_f^{z^*} \nu_f^{z_f^*} \quad (2.23b)$$

subject to

$$\underline{v}_f \leqslant v_f + q_f \leqslant \overline{v}_f \quad \forall f \in \mathcal{F} \quad (2.24)$$

$\forall i, j \in \mathcal{F} | i < j, \forall z \in \mathcal{Z}^i \cap \mathcal{Z}^j \wedge p_{ij} = 0$

$$(v_i + q_i)\big(\cos(m_i^*)(1 - pc_{ij}) - \sin(m_i^*) pc_{ij}\big) - (v_j + q_j)\big(\cos(m_j^*)(1 - pc_{ij}) - \sin(m_j^*) pc_{ij}\big) \leqslant (\overline{v}_i + \overline{v}_j)(1 - \delta_{ijz}^1) \quad (2.25a)$$

$$-(v_i + q_i)\big(h_i(1 - pc_{ij}) + h_i' pc_{ij}\big) + (v_j + q_j)\big(h_j(1 - pc_{ij}) + h_j' pc_{ij}\big) \leqslant \big((\overline{v}_i|h_i| + \overline{v}_j|h_j|)(1 - pc_{ij}) + (\overline{v}_i|h_i'| + \overline{v}_j|h_j'|) pc_{ij}\big)(1 - \delta_{ijz}^1) \quad (2.25b)$$

$$(v_i + q_i)\big(\cos(m_i^*)(1 - pc_{ij}) - \sin(m_i^*) pc_{ij}\big) - (v_j + q_j)\big(\cos(m_j^*)(1 - pc_{ij}) - \sin(m_j^*) pc_{ij}\big) \leqslant (\overline{v}_i + \overline{v}_j)(1 - \delta_{ijz}^2) \quad (2.25c)$$

$$(v_i + q_i)\big(k_i(1 - pc_{ij}) + k_i' pc_{ij}\big) - (v_j + q_j)\big(k_j(1 - pc_{ij}) + k_j' pc_{ij}\big) \leqslant \big((\overline{v}_i|k_i| + \overline{v}_j|k_j|)(1 - pc_{ij}) + (\overline{v}_i|k_i'| + \overline{v}_j|k_j'|) pc_{ij}\big)(1 - \delta_{ijz}^2) \quad (2.25d)$$

$$-(v_i + q_i)\big(\cos(m_i^*)(1 - pc_{ij}) - \sin(m_i^*) pc_{ij}\big) + (v_j + q_j)\big(\cos(m_j^*)(1 - pc_{ij}) - \sin(m_j^*) pc_{ij}\big) \leqslant (\overline{v}_i + \overline{v}_j)(1 - \delta_{ijz}^3) \quad (2.25e)$$

$$(v_i + q_i)\big(h_i(1 - pc_{ij}) + h_i' pc_{ij}\big) - (v_j + q_j)\big(h_j(1 - pc_{ij} + h_j' pc_{ij})\big) \leqslant \big((\overline{v}_i|h_i| + \overline{v}_j|h_j|)(1 - pc_{ij}) + (\overline{v}_i|h_i'| + \overline{v}_j|h_j'|) pc_{ij}\big)(1 - \delta_{ijz}^3) \quad (2.25f)$$

$$-(v_i+q_i)\big(\cos(m_i^*)(1-pc_{ij})-\sin(m_i^*)pc_{ij}\big)+$$
$$(v_j+q_j)\big(\cos(m_j^*)(1-pc_{ij})-\sin(m_j^*)pc_{ij}\big)\leqslant(\overline{v}_i+\overline{v}_j)(1-\delta^4_{ijz}) \quad (2.25g)$$

$$-(v_i+q_i)\big(k_i(1-pc_{ij})+k_i'pc_{ij}\big)+(v_j+q_j)\big(k_j(1-pc_{ij})+k_j'pc_{ij}\big)$$
$$\leqslant\big((\overline{v}_i|k_i|+\overline{v}_j|k_j|)(1-pc_{ij})+(\overline{v}_i|k_i'|+\overline{v}_j|k_j'|)pc_{ij}\big)(1-\delta^4_{ijz}) \quad (2.25h)$$

$$\delta^1_{ijz}+\delta^2_{ijz}+\delta^3_{ijz}+\delta^4_{ijz}+\delta^5_{ijz}=1 \quad (2.25i)$$

$\forall i<j\in\mathcal{F},\forall z\in\mathcal{Z}^i\cap\mathcal{Z}^j$

$$\delta^5_{ijz}=1 \qquad \text{if } hth_{ij}+sc_{ij}\geqslant 1 \quad (2.26a)$$
$$\nu_i^z+\nu_j^z\geqslant\delta^5_{ijz}-1 \quad (2.26b)$$
$$\nu_i^z+\nu_j^z\leqslant 2-\delta^5_{ijz} \quad (2.26c)$$

$\forall f\in\mathcal{F}$

$$\sum_{z\in\mathcal{Z}^f}\nu_f^z=1 \quad (2.27)$$
$$\nu_f^z=0 \qquad \forall z\in\mathcal{Z}^f|z\neq z_f,z_f\pm 1 \quad (2.28)$$

$$\sum_{z\in\mathcal{Z}^f}z\nu_f^z-z_f\leqslant\rho_f \quad (2.29a)$$
$$z_f-\sum_{z\in\mathcal{Z}^f}z\nu_f^z\leqslant\rho_f \quad (2.29b)$$

$$-\varepsilon(1-a_f)+\varepsilon\leqslant q_f^++q_f^- \quad (2.30a)$$
$$q_f^++q_f^-\leqslant(\overline{v}_f-\underline{v}_f)a_f \quad (2.30b)$$
$$1-\nu_f^z=b_f \quad (2.30c)$$

$$(v_f+q_f^+)-(q_f^-+v_f^*)\leqslant\beta_f \quad (2.31a)$$
$$(q_f^-+v_f^*)-(v_f+q_f^+)\leqslant\beta_f \quad (2.31b)$$

$$(v_f + q_f^+) - (q_f^- + \widehat{v_f}) \leqslant \beta_f \tag{2.32a}$$
$$(q_f^- + \widehat{v_f}) - (v_f + q_f^+) \leqslant \beta_f \tag{2.32b}$$

$\forall f \in \mathcal{F}$

$$q_f \in \mathbb{R} \qquad \forall f \in \mathcal{F} \tag{2.33a}$$
$$q_f^+, q_f^-, \beta_f \in \mathbb{R}^+ \qquad \forall f \in \mathcal{F} \tag{2.33b}$$
$$\rho_f \in \mathbb{Z}^+ \qquad \forall f \in \mathcal{F} \tag{2.33c}$$

$\forall f, i, j \in \mathcal{F} : i < j, \forall z \in \mathcal{Z}$

$$\nu_f^z, a_f, b_f, \delta_{ijz}^1, \delta_{ijz}^2, \delta_{ijz}^3, \delta_{ijz}^4, \delta_{ijz}^5 \in \{0, 1\} \tag{2.33d}$$

The objective function (2.23) takes into account the terms presented in Section 2.3.7. Constraints (2.24) give the velocity bounds. Constraints (2.25) detect conflicts that can be solved by making velocity changes. Constraints (2.26) include altitude changes in the model. Constraints (2.27) force aircraft to fly at only one altitude level. Constraints (2.28) are used if variable ρ is not considered. Constraints (2.29) are related to the number of altitude levels that an aircraft climbs or descends. Constraints (2.30) update the number of changes in velocity and altitude. Constraints (2.31a) force aircraft to fly with the velocity from the initial flight plan after avoiding conflict situations. Constraints (2.32) force aircraft to exit from the aerial sector at the predicted time. Constraints (2.33) give the type of variables in the model.

Model dimensions

The dimensions of the VAC model are the same as the dimensions of the iVAC model, shown in Table 2.1, since neither new variables nor new constraints are added.

2.4.3 Computational experience

Illustrative instance

The final version of the VAC model has been initially tested with the case shown in Fig. 2.14 by using weights $w_1 = w_2 = 0.5$ and $w_3 = w_4 = w_5 = 0$, where velocity variations and the levels that the aircraft have to change are minimized. In this objective function, $c_f^{q^+} = 1$, $c_f^{q^-} = 1$ and $c_f^j = 1$, $\forall f \in \mathcal{F}$. The parameter p_{ij} is not considered, unless the "false conflict" situation occurs, therefore all pairs of aircraft are taken into account. The case is bigger than the realistic ones, since notice that $F = 37$ aircraft in possible conflicts are considered. Also notice that there are two aircraft in both points (a) and (b). All aircraft fly with the same velocity, except aircraft (c) and (d) that fly with a higher velocity to test "pursuit cases". Aircraft (e), (f), (g) and (h) are in "false conflict" that implies an unnecessary velocity change. Aircraft (i), (j), (k), (l) and (m) are in an anomalous case.

Fig. 2.17 depicts the results of applying the VAC model for collision avoidance in the case depicted in Fig. 2.14 as follows:

- Seven velocity changes have been performed. The dotted line circles in the figure denote the positive variation of velocity, and the dashed line circle denotes the negative variation of velocity. In this case, all velocity changes are negative (slowdown). This is due to the same value of the costs $c_f^{q^+}$ and $c_f^{q^-}$.
- The points (a) and (b) still have two aircraft each, but the conflict has been avoided.
- The aircraft (e), (f), (g) and (h) have not changed their velocities, since they are in a "false conflict".
- There are eleven altitude level changes, four positive and seven negative, one of which descends two levels.
- The number of constraints, continuous and 0-1 variables in the reduced MIP have been 2998, 37 and 1963, respectively.
- The objective function value is 13.1124.
- The execution time was 8.42 seconds using the optimization engine CPLEX v.12.1 [63] (with the default options) in the following HW/SW platform: Intel Core 2 DUO P8400, 2.26GHz, 2GB RAM; Microsoft Windows 7 Professional SO.

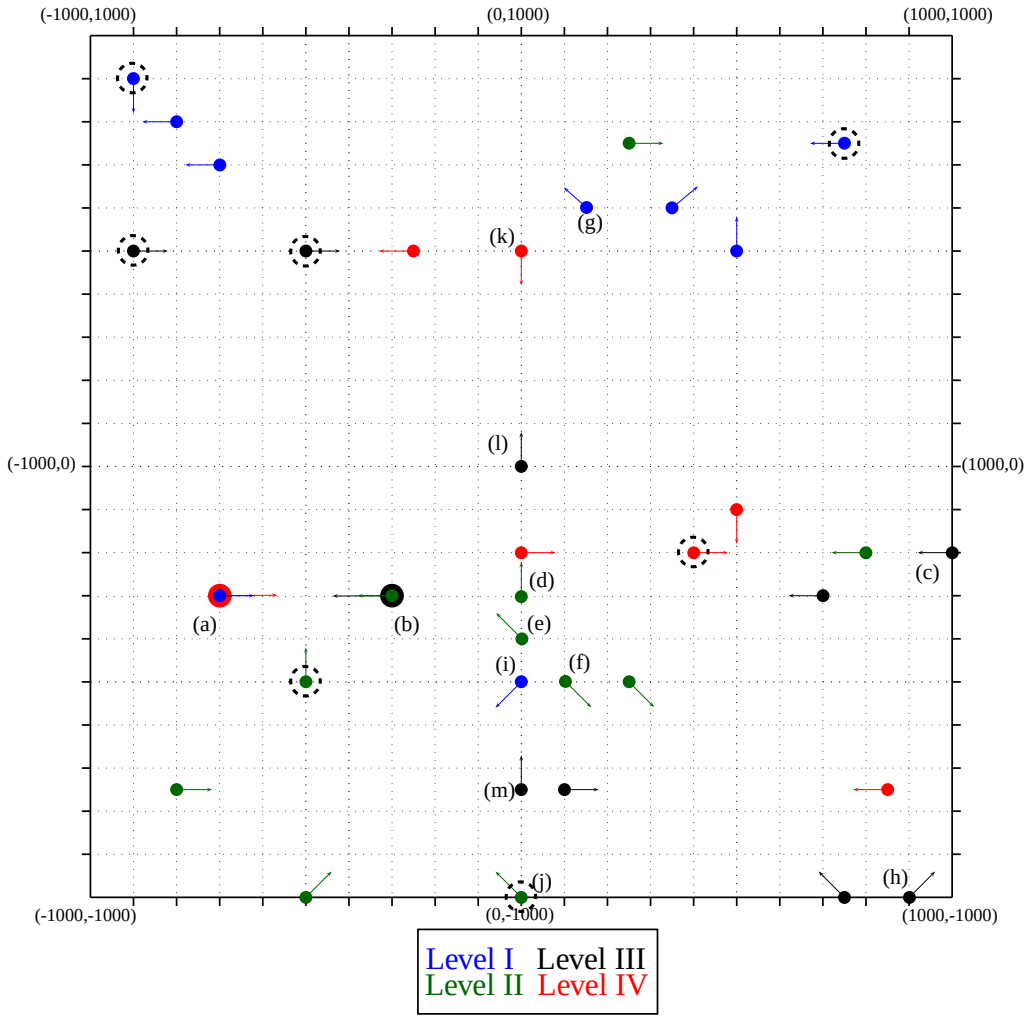

Figure 2.17: Illustrative instance for testing the VAC model. Resolution

Extensive computational experience

Next, some computational experience for the VAC model is reported. 25 random simulations are performed for each dimensional case, and the resulting averages are presented. For the simulation the following technical aspects were taken into account:

- The number of aircraft, altitude levels and velocity bounds were fixed.
- The abscissas and ordinates of aircraft were generated by using a Uniform distribution between the bounds for each axis.
- The altitude level of each aircraft was generated by using a Uniform distribution

between 0 and the considered altitude levels.

- The initial altitude level configuration was generated by taking probability 0.1 for an aircraft flying in altitude level different from the initial flight plan.
- The number of altitude level changes made by each aircraft until the resolution was 0 with probability 0.8, 1 with probability 0.15 and 2 with probability 0.05.
- The direction of motion was generated by taking only eight possible angles (dividing the circumference in eight parts) trying to force aircraft to have "head to head" conflicts.
- The velocity of each aircraft was generated by using an Uniform distribution between the bounds allowed for each aircraft.
- The initial velocity configuration was generated by taking the same value of the previous velocity generated with probability 0.9 and, otherwise, generating another velocity by using an Uniform distribution again.
- The number of velocity changes made by each aircraft until the execution was 0 with probability 0.8, 1 with probability 0.15 and 2 with probability 0.5.
- The safety radius was 2.5 with probability 0.85, and 2.6, 2.7, 2.8, 2.9 and 3 with probability 0.03 each case.

The VAC model is solved by using preprocessing in the computational experience although the full VAC model is autonomous in order to detect all conflicts. The only one difference can be the final resolution times. After this simulation, the resolution of the 525 cases studied was as follows.

Table 2.2 shows the average of the dimensions of the model before and after the presolve made by CPLEX where the headings are as follows:

- *Case*: Gives the case configuration: CAAA-ZZ denotes number of aircraft (AAA) and levels (ZZ).
- m: Number of constraints.
- n: Number of variables.
- d: Constraints matrix density.

Table 2.2: Case dimensions

Case	m	n	d	m^*	n^*	d^*
C020-05	10650.0	4970.0	0.0009	1377.1	843.1	0.0053
C020-07	14830.0	6910.0	0.0007	1838.8	1121.3	0.0041
C020-10	21100.0	9820.0	0.0005	2643.1	1587.1	0.0029
C025-05	16750.0	7775.0	0.0006	1996.8	1205.4	0.0037
C025-07	23350.0	10825.0	0.0004	2866.4	1683.6	0.0027
C025-10	33250.0	15400.0	0.0003	4203.2	2446.6	0.0019
C030-05	24225.0	11205.0	0.0004	3054.0	1777.4	0.0025
C030-07	33795.0	15615.0	0.0003	3931.2	2292.7	0.0020
C030-10	48150.0	22230.0	0.0002	5403.9	3157.4	0.0015
C035-05	33075.0	15260.0	0.0003	3960.6	2290.1	0.0020
C035-07	46165.0	21280.0	0.0002	5411.5	3119.7	0.0015
C035-10	65800.0	30310.0	0.0002	7206.3	4132.8	0.0011
C040-05	43300.0	19940.0	0.0002	5453.7	3088.5	0.0015
C040-07	60460.0	27820.0	0.0002	6812.5	3919.8	0.0012
C040-10	86200.0	39640.0	0.0001	9981.9	5677.5	0.0008
C045-05	54900.0	25245.0	0.0002	6157.8	3505.6	0.0013
C045-07	76680.0	35235.0	0.0001	9035.1	5088.6	0.0009
C045-10	109350.0	50220.0	0.0001	12474.6	6998.8	0.0007
C050-05	67875.0	31175.0	0.0001	7663.0	4326.1	0.0010
C050-07	94825.0	43525.0	0.0001	10831.9	6077.8	0.0008
C050-10	135250.0	62050.0	0.0001	16204.9	9009.2	0.0005

- m^*, n^* and d^*: the number of constraints, variables and constraints matrix density, respectively, after the preprocessing made by CPLEX [63].

The first computational observation that can be made in Table 2.2 is the strength of the CPLEX preprocessing by comparing the columns m and m^* and n and n^*. Moreover, the dimensions m^* and n^* are still very big.

Table 2.3 shows the most important results (averages) where the headings are as follows:

- *Case*: Gives the case configuration: CAAA-ZZ denotes number of aircraft (AAA) and levels (ZZ).
- z_{lp}: Value of the objective function in the continuous linear relaxation.
- z_s: Value of the bound after performing the CPLEX cut identification and appending at node 0
- z_{ip}: Value of the objective function for the optimal solution of the problem.

- GAP_{lp}: $\frac{z_{ip}-z_{lp}}{z_{ip}}$
- GAP_s: $\frac{z_{ip}-z_s}{z_{ip}}$
- nb: Number of times that there is branching
- nn: Number of CPLEX branch-and-cut nodes
- t_{lp}: Time (secs.) to obtain the z_{lp} value
- t_s: Time (secs.) to obtain the z_s value.
- t_{ip}: Time (secs.) to obtain the z_{ip} value.
- nc: Total number of cuts performed by CPLEX.

Notice that the minimum, average and maximum GAPs are reported in Table 2.3.

In Table 2.3 the very small GAP_s for all the instances can be observed, showing the tightness of the model plus the CPLEX cuts. (Notice that nb is small for most of the instances) and, then, the elapsed time is very short.

And finally, Table 2.4 shows the average of the number of cuts that CPLEX executed to solve the VAC model, where the headings are as follows:

- *Case*: Gives the case configuration: CAAA-ZZ denotes number of aircraft (AAA) and levels (ZZ).
- Clique: Number of clique cuts.
- Cover: Number of Cover cuts.
- Implied: Number of Implied cuts.
- Flow: Number of Flow cuts.
- MIR: Number of Mixed Integer Rounding cuts.
- Zero-Half: Number of Zero-half cuts.
- Gomory: Number of Gomory cuts.
- Total: Total number of cuts.

Table 2.3: Computational results

Case	z_{lp}	z_s	z_{ip}	GAP_{lp}	GAP_s	nb	nn	t_{lp}	t_s	t_{ip}	nc
C020-05	6.1179	6.3687	6.3787	0.00 4.09 100.00	0.00 0.16 1.74	0	0.00	0.06	0.70	0.67	11.0
C020-07	5.1651	5.4827	5.5090	0.00 6.24 24.54	0.00 0.48 11.62	2	3.50	0.07	0.81	1.03	34.0
C020-10	4.1421	4.2673	4.2951	0.00 3.56 12.41	0.00 0.65 4.78	4	15.75	0.09	1.20	1.12	18.6
C025-05	9.7815	10.5495	10.6043	0.00 7.76 52.36	0.00 0.52 3.48	3	71.33	0.08	0.86	1.03	53.1
C025-07	5.2982	5.4847	5.4943	0.00 3.57 41.63	0.00 0.17 1.50	2	18.00	0.10	1.14	1.31	36.7
C025-10	7.7335	8.1448	8.1726	0.00 5.37 42.96	0.00 0.34 2.06	1	20.00	0.14	1.38	1.63	45.3
C030-05	9.3827	10.6330	10.6904	0.00 12.23 100.00	0.00 0.54 67.79	7	14.29	0.11	1.39	1.40	102.5
C030-07	6.2307	6.9418	6.9917	0.00 10.88 100.00	0.00 0.71 7.50	3	14.33	0.14	1.60	2.02	62.4
C030-10	5.0408	5.3576	5.3877	0.00 6.44 79.61	0.00 0.56 60.63	4	11.00	0.19	1.81	2.09	53.7
C035-05	12.1933	13.6538	13.7500	0.00 11.32 57.01	0.00 0.70 7.19	11	25.91	0.14	1.64	1.85	188.9
C035-07	10.8919	12.2413	12.3179	0.00 11.58 100.00	0.00 0.62 8.95	3	11.33	0.19	2.29	2.08	139.8
C035-10	9.8494	10.5813	10.6036	0.00 7.11 41.72	0.00 0.21 9.42	3	2.00	0.24	2.54	2.57	132.5
C040-05	13.3918	15.7756	15.9059	0.00 15.81 76.51	0.00 0.82 7.32	7	124.43	0.18	1.87	2.49	215.0
C040-07	12.1882	13.9940	14.1239	0.00 13.71 85.95	0.00 0.92 5.49	7	21.57	0.24	2.62	2.90	263.9
C040-10	8.0451	8.9137	8.9472	0.00 10.08 47.74	0.00 0.38 6.26	6	8.83	0.32	3.18	2.82	218.4
C045-05	9.5783	12.4885	12.6698	0.00 24.40 100.00	0.00 1.43 9.95	12	33.42	0.22	2.32	2.73	334.4
C045-07	7.3346	9.2790	9.4741	0.00 22.58 100.00	0.00 2.06 13.55	11	26.64	0.29	3.17	3.59	281.8
C045-10	11.7084	12.9528	12.9969	0.00 9.91 93.13	0.00 0.34 3.06	4	16.75	0.40	4.06	4.30	241.6
C050-05	12.5373	15.7431	15.9704	0.00 21.50 100.00	0.00 1.42 90.51	15	80.67	0.26	3.02	3.85	325.5
C050-07	12.4788	14.9265	15.0525	0.00 17.10 100.00	0.00 0.84 5.21	7	50.00	0.36	3.32	3.98	342.6
C050-10	9.1112	10.9923	11.0690	0.00 17.69 100.00	0.00 0.69 35.34	5	121.60	0.49	5.59	5.83	389.7

Table 2.4: Cuts identified and appended

Case	Clique	Cover	Implied	Flow	MIR	Zero-Half	Gomory	Total
C020-05	0.5	3.2	3.1	1.6	0.2	0.2	2.2	11.0
C020-07	2.4	10.4	8.2	2.9	0.4	0.2	9.4	34.0
C020-10	1.7	6.2	3.4	1.2	0.3	0.3	5.5	18.6
C025-05	3.6	15.2	12.5	6.9	0.2	0.7	14.0	53.1
C025-07	4.5	11.5	6.9	2.8	0.0	0.2	10.7	36.7
C025-10	7.5	15.1	6.8	1.5	0.2	0.2	14.1	45.3
C030-05	9.3	29.7	24.8	11.5	0.6	1.5	25.1	102.5
C030-07	6.5	18.2	14.8	5.6	0.4	0.8	16.0	62.4
C030-10	9.1	19.0	6.9	2.3	0.3	0.3	15.8	53.7
C035-05	19.8	53.6	46.2	19.4	0.4	2.1	47.4	188.9
C035-07	14.8	45.2	26.8	9.4	0.4	0.8	42.4	139.8
C035-10	12.9	49.7	22.0	4.3	0.2	0.2	43.2	132.5
C040-05	20.6	65.5	48.6	21.8	0.8	2.6	55.0	215.0
C040-07	31.2	81.7	52.0	17.8	0.5	1.1	79.6	263.9
C040-10	31.1	74.5	32.2	11.1	0.3	0.4	68.6	218.4
C045-05	27.5	106.2	78.2	30.8	0.4	3.7	87.6	334.4
C045-07	33.2	90.8	50.1	22.2	0.3	2.2	83.0	281.8
C045-10	27.2	85.7	39.7	9.0	0.2	0.6	79.2	241.6
C050-05	25.5	96.0	82.4	35.9	0.3	5.0	80.4	325.5
C050-07	42.8	111.2	64.1	21.3	0.5	1.8	101.0	342.6
C050-10	53.4	135.8	62.2	17.2	0.4	1.6	119.2	389.7

In Appendix A.5, page 151, more detailed tables for the particular cases of study are shown, and the whole computational experience is presented in the extended version of the thesis on the enclosed CD.

It is worth pointing out the impressive elapsed time that was obtained. Given the extensive computational experience that has been reported, it can be concluded that the model can be used for real-time execution.

Also notice that the results presented in this thesis are different (in terms of time) than the results that we presented in Alonso-Ayuso et al. [8]. The computational experience in both cases was performed on the same computer but with different Operative Systems: For the results of the paper, Windows XP Professional was used whereas for the results reported in the thesis Windows 7 Professional was used. Notice that the performance by using Windows 7 is worse than that of Windows XP.

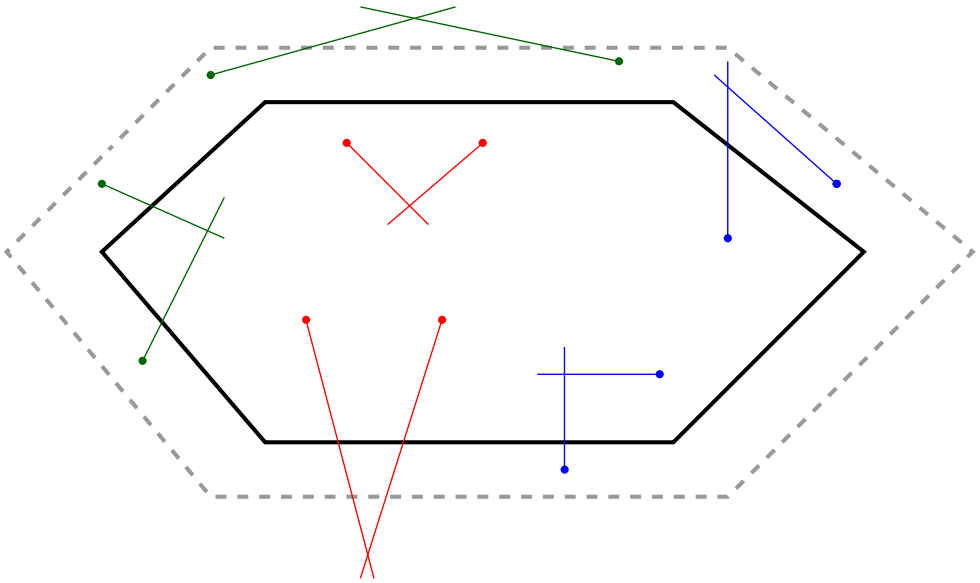

Figure 2.18: Cases on the border

2.5 Extensions: Conflicts in the frontier

The iVAC and VAC models do not consider the conflicts on the border where an immediate conflict can take place.

To avoid these situations, a ring around the aerial sector can be taken into account with the aircraft that are in the frontier. Then, the following parameter:

$$os_f = \begin{cases} 1 & \text{if the aircraft } f \text{ is out of the aerial sector} \\ 0 & \text{otherwise} \end{cases} \tag{2.34}$$

can distinguish if an aircraft is in or out the sector.

Four cases can occur as shown in Fig. 2.18:

- Case 1: $os_i = os_j = 0, \quad \forall i, j \in \mathcal{F} : i < j$. This is the case of the red aircraft, where both os parameters are equal to zero. In this case the model is optimized and the ATC should make the proposed changes suggested by the model.
- Case 2: $os_i = 1$ and $os_j = 0, \quad \forall i, j \in \mathcal{F} : i < j$ or vice-versa. This is the case of the blue aircraft, where one of them is out of the aerial sector. In this case the model is optimized in each aerial sector, and the ATC should reach an agreement choosing

the best change.

- Case 3: $os_i = os_j = 1, \quad \forall i, j \in \mathcal{F} : i < j$. This is the case of the green aircraft, where both os parameters are equal to one. In this case the ATC of the considered aerial sector should warn the ATC in the aerial sector where the conflict will take place that there is a conflict between two aircraft in their area of responsibility.

It is point out that the costs in the objective function can be greater for $os = 1$, penalizing all changes in the frontier and favoring the changes on aircraft in the aerial sector. A cooperative system could be constructed for the coordination between the different ATC to help them to make better decisions.

2.5.1 Conflicts during an altitude change

If an aircraft has to change its altitude level, while the maneuver is being realized this aircraft is taking up more than one altitude levels, and the conflicts in these zones have to be avoided. For this purpose the following parameter is added to the model,

$$ca_f = \begin{cases} +a & \text{if the aircraft } f \text{ is changing its altitude climbing } a \text{ altitude levels} \\ -a & \text{if the aircraft } f \text{ is changing its altitude descending } a \text{ altitude levels} \\ 0 & \text{otherwise.} \end{cases}$$

First, all possible changes (q_f^+, q_f^-, a_f, b_f, ρ_f) of the aircraft f, which is changing its altitude level, are fixed to zero:

$$q_f^+, q_f^-, a_f, b_f, \rho_f = 0 \quad \text{if } ca \neq 0.$$

Now, constraints (2.15) of the iVAC model and (2.27) of the VAC model have to be replaced with the following constraints:

$$\sum_{n \in \mathcal{Z}^f} \nu_f^n = 1 + |ca_f| \quad \forall f \in \mathcal{F},$$

where situations for an aircraft to ascend several levels simultaneously is allowed.

Additionally the following constraints have to be added to the model,

$$\nu_f^{z_f^*+n\text{sign}(ca_f)} = 1 \quad \text{if } ca_f \neq 0 \text{ and } \forall f \in \mathcal{F} \text{ and } \forall n = 0, \ldots, |ca_f|,$$

where the variables ν are fixed to 1 in the altitude levels that the aircraft take up, due to the fact that this one is climbing or descending.

Chapter 3

The dynamic model: Velocity changes through time periods

3.1 Introduction

In the previous chapter a first approximation for the Collision Avoidance Problem has been presented. In the related iVAC and VAC models it was supposed trajectories along a straight line, instantaneous changes in velocity and altitude, without regard to the acceleration and, reduced airspace, since the models are used in an aerial sector. In this chapter the VC model will be replaced with the Velocity Changes through Time Periods (VCTP) model, where a time horizon will be studied by using Uniformly Accelerated Linear Motion (UALM).

In this chapter we propose a dynamic model in order to avoid aircraft conflicts considering a big airspace where several aircraft take place and dividing the time horizon in time periods. The geometric idea proposed by Pallottino et al. (2002) [85] is behind the model but considering dynamic changes of the main angles considered for the conflict detection. For solving this model, it is supposed that the aircraft trajectories as well as the configuration in several time points are known. The result is a model based on Mixed 0–1 Nonlinear Programming. Due to the hard nonlinear inequalities, an algorithmic approach will be needed in order to linearize the nonlinear inequalities and, by iteratively, solving simpler mixed 0–1 linear problems. The algorithmic approach is based on approximations by using Taylor polynomials. After a hard preprocessing and the corresponding algorithmic approach for linearizing the model, the VCTP model solves instances in a reasonable time for medium term (less than 10 minutes). This model has the same weak point than

the VC since "head to head" conflicts are not solved with this model, but this is the first step to construct a complete model where altitude changes are considered, like in the VAC philosophy.

It is supposed that the preliminary trajectories of the F aircraft are known and it can be extracted the aircraft configurations in T fixed time points. In these points the velocity and the position (abscissa and ordinate) of each aircraft in each point and the motion angles between two points are known. With these data a new model to decide the optimal configuration by changing the aircraft accelerations and avoiding all conflicts between the aircraft will be designed. To change the aircraft accelerations the equations relating to the UALM will be used, as follows,

$$v(t) = v_0 + at \tag{3.1a}$$

$$x(t) = x_0 + v_0 t + \frac{1}{2}at^2, \tag{3.1b}$$

where a is a constant that represents the acceleration.

It is supposed that in the VCTP model the aircraft positions are variables resulting, finally, a nonlinear model since trigonometric functions involving variables take place.

3.1.1 Notation

Let the following notation for the elements in the formulation of the model:

Sets

$\mathcal{F} = \{1, \ldots, F\},$ set of aircraft in the airspace.

$\mathcal{T} = \{0, \ldots, T\},$ set of time periods.

Parameters

$s,$ safety distance between aircraft, usually, 2.5 nautical miles.

$e,$ distance bound to consider a pair of aircraft.

$w_1, w_2,$ weight (between 0 and 1) for each objective function term.

$div,$ integer parameter greater than 1 to be considered for the bounds of some variables.

For all $t \in \mathcal{T}$:

$I_t,$ length of the time period between times instants $t-1$ and t.

For all $f \in \mathcal{F}$ and $t \in \mathcal{T}$:

$x_f^{*t}, y_f^{*t},$ initial configuration of position, abscissa and ordinate, for aircraft f in time period t, respectively.

$d_f^{*t},$ covered distance for aircraft f during time period t in the initial configuration.

$v_f^{*t},$ initial velocity configuration for aircraft f in time period t.

$a_f^{*t},$ initial acceleration configuration for aircraft f in time period t.

$r_f^t,$ safety radius for each aircraft f in time period t, usually 2.5 nautical miles (nm).

$\underline{v}_f^t, \overline{v}_f^t,$ minimum and maximum velocities allowed for aircraft f in time period t, respectively.

$\underline{a}_f^t, \overline{a}_f^t,$ minimum and accelerations allowed for aircraft f in time period t, respectively.

$m_f^{*t},$ direction of motion in $(-\pi, \pi]$ for aircraft f in time period t.

$\hat{x}_f^t, \hat{y}_f^t,$ position parameters to be updated in the Taylor approximation for aircraft f in time period t.

$\hat{d}_f^t,$ distance parameter to be updated in the Taylor approximation for aircraft f in time period t.

$\hat{v}_f^t,$ velocity parameter to be updated in the Taylor approximation for aircraft f in time period t.

$c_{ft}^{a^+}, c_{ft}^{a^-},$ costs for positive and negative acceleration changes for aircraft f in time period t, respectively.

$c_{ft}^{v},$ costs for the difference between the initial and optimal velocity configuration for aircraft f in time period t.

c_{ft}^{d}, costs for the difference between the initial and optimal covered distance for aircraft f in time period t.

For all $f \in \mathcal{F}$:

$x_f^{*t_f^d}, y_f^{*t_f^d}, x_f^{*t_f^r}, y_f^{*t_f^r}$, departure and arrival positions (abscissa and ordinate) for aircraft f.

d_f^{tot}, total length of the polygonal of the trajectory for aircraft f.

t_f^d, t_f^r, scheduled departure and arrival times for flight f.

Data preprocessing

For all $f \in \mathcal{F}$ and $t \in \mathcal{T}$:

$\overline{x}_f^t, \overline{y}_f^t, \overline{d}_f^t$, upper bounds for variables x, y and d, respectively.

$\underline{x}_f^t, \underline{y}_f^t$, lower bounds for variables x and y, respectively.

For all $i, j \in \mathcal{F} : i < j$, for all $t \in \mathcal{T} : t = \left\{ \max\{t_i^d, t_j^d\} + 1, \ldots, \min\{t_i^r, t_j^r\} - 1 \right\}$:

fc_{ij}^t, 0-1 parameter that detects if there is a "false conflict" between aircraft i and j in time period t.

p_{ij}^t, 0-1 parameter that will be 1 if the pair of aircraft i and j will not be taken into account in time period t for conflict resolution. This parameter depends on the criterion decided by the ATC. Notice that this parameter will be 1 if $fc_{ij}^t = 1$.

ip_{ijt}, intersection point between the straight line trajectories of the corresponding polygonal segment for time period t for aircraft i and j, if the trajectories are not parallel o coincident.

d_{ijt}^1, distance between the i aircraft position and ip_{ijt} in time period t.

d_{ijt}^2, distance between points $\left(x_i^t + \cos(m_i^{*t}), y_i^t + \sin(m_i^{*t})\right)$ and ip_{ijt} for aircraft i and j in time period t.

Variables

For all $f \in \mathcal{F}$ and for all $t \in \mathcal{T}$:

$x_f^t, y_f^t,$ the position, abscissa and ordinate, of aircraft f in time period t, for $f \in \mathcal{F}$ and $t \in \mathcal{T}$, respectively.

$a_f^t,$ acceleration variation for aircraft f in time period t, for $f \in \mathcal{F}$ and $t \in \mathcal{T}$. This variable is real and can be divided in two positive variables, say, a_f^{t+} and a_f^{t-}, such that $a_f^t = a_f^{t+} - a_f^{t-}$ as a traditional way in LP.

$a_f^{t+},$ positive acceleration variation for aircraft f in time period t, for $f \in \mathcal{F}$ and $t \in \mathcal{T}$.

$a_f^{t-},$ negative acceleration variation for aircraft f in time period t, for $f \in \mathcal{F}$ and $t \in \mathcal{T}$.

$v_f^t,$ velocity for aircraft f in time period t, for $f \in F$ and $t \in T$.

$d_f^t,$ covered distance for aircraft f during time period t, for $f \in \mathcal{F}$ and $t \in \mathcal{T}$.

$\gamma_{ft}^1, \gamma_{ft}^2, \gamma_{ft}^3, \gamma_{ft}^4, \gamma_f^t$ auxiliary 0-1 variables to model the case of early or delay for aircraft f in time period t, for $f \in \mathcal{F}$ and $t \in \mathcal{T}$.

For all $i, j \in \mathcal{F} : i < j$, for all $t \in \mathcal{T} : t = \left\{ \max\{t_i^d, t_j^d\} + 1, \ldots, \min\{t_i^r, t_j^r\} - 1 \right\}$ and $n = 1, \ldots, 8$:

$\delta_{ijt}^n,$ auxiliary 0-1 variables for modeling the or constraints.

3.2 The Velocity Changes through Time Periods (VCTP) model: Preliminaries

In this section the changes in the VC model are presented to adapt it to the new hypothesis that have to be included in the model, resulting the so called VCTP model. The most important hypothesis consists of including an acceleration term to make continuous the changes in velocity. This term will allow to include time periods in the model, useful for the medium-large consideration.

3.2.1 Continuous velocity changes

The continuity in the velocity changes is the first purpose of this new model. To implement the continuity in the velocity changes, an acceleration term is necessary as well

as a time horizon divided in time periods. In this model an UALM is assumed for the implementation of continuous velocity changes.

Firstly, constraints (2.24) on page 64 have to be adjusted to the new requirements. Beforehand the length of the time periods I_t is known, and can be different for each $t \in \mathcal{T}$. The aircraft velocities are also known for each time period $t \in \mathcal{T}$. If the velocities are accelerated, by using equation (3.1a) and taking into account the acceleration of the aircraft resourcefully in each time period $t \in \mathcal{T}$, it results,

$$v_f^t = v_f^{t-1} + a_f^t I_t = v_f^{t-2} + a_f^{t-1} I_{t-1} + a_f^t I_t = \ldots = \\ v_f^{t_f^d} + a_f^1 I_1 + a_f^2 I_2 + \ldots + a_f^t I_t = v_f^{t_f^d} + \sum_{\ell=t_f^d}^{t} a_f^\ell I_\ell. \quad (3.2)$$

Therefore, constraints (2.24) can be modeled as follows,

$$\underline{v}_f^t \leqslant v_f^{t-1} + a_f^t I_t \leqslant \overline{v}_f^t \quad \forall f \in \mathcal{F}, t = t_f^d, \ldots, t_f^r, \quad (3.3)$$

or only the initial velocity configuration can be taken into account

$$\underline{v}_f^t \leqslant v_f^{t_f^d} + \sum_{\ell=t_f^d}^{t} a_f^\ell I_\ell \leqslant \overline{v}_f^t, \forall f \in \mathcal{F}, t = t_f^d, \ldots, t_f^r.$$

In the final model the variables v_f^t are considered instead of the initial velocity configuration, since it will be more appropiate for the linear approximation to be implemented by using Taylor polynomials. Notice that the derivatives with respect to variables a_f^t have not to be considered. On the other hand, if the variables v_f^t are considered, only the derivative with respect to the variable v_f^t has to be taken into account jointly with (3.3).

Furthermore, the acceleration must be included between its bounds

$$\underline{a}_f^t \leqslant a_f^t \leqslant \overline{a}_f^t \quad \forall f \in \mathcal{F}, t = t_f^d + 1, \ldots, t_f^r.$$

Constraints for the geometric construction

For modeling the constraints (2.25a), (2.25c), (2.25e) and (2.25g) on page 64, time periods and the acceleration variable are included, resulting the new constraints $\forall i < j \in \mathcal{F}$

and $t = \left\{ \max\{t_i^d, t_j^d\} + 1, \ldots, \min\{t_i^r, t_j^r\} - 1 \right\}$

$$\begin{aligned} v_i^t \cos(m_i^{*t}) - v_j^t \cos(m_j^{*t}) &\leqslant M_1(1 - \delta_{ijt}^1) \\ v_i^t \cos(m_i^{*t}) - v_j^t \cos(m_j^{*t}) &\leqslant M_2(1 - \delta_{ijt}^2) \\ -v_i^t \cos(m_i^{*t}) + v_j^t \cos(m_j^{*t}) &\leqslant M_3(1 - \delta_{ijt}^3) \\ -v_i^t \cos(m_i^{*t}) + v_j^t \cos(m_j^{*t}) &\leqslant M_4(1 - \delta_{ijt}^4), \end{aligned}$$

where $M_1 = M_2 = M_3 = M_4 = (\overline{v}_i^t + \overline{v}_j^t)$ are respectively the upper bounds of

$$\begin{aligned} v_i^t \cos(m_i^{*t}) - v_j^t \cos(m_j^{*t}) \\ v_i^t \cos(m_i^{*t}) - v_j^t \cos(m_j^{*t}) \\ -v_i^t \cos(m_i^{*t}) + v_j^t \cos(m_j^{*t}) \\ -v_i^t \cos(m_i^{*t}) + v_j^t \cos(m_j^{*t}). \end{aligned}$$

Now the most difficult part of the VCTP model is confronted, since the constraints that have the nonlinear trigonometric functions have to be modeled. In the VC model the angles ω_{ij}, l_{ij} and g_{ij} are known, whereas in the VCTP model, the aircraft positions are considered as variables and it is necessary to know these angles to calculate the parameters $h_i^t, h_j^t, k_i^t, k_j^t$ that depend on $\tan l_{ij}^t$ and $\tan g_{ij}^t$ in each time period $t \in \mathcal{T}$. The final expressions for $\tan l_{ij}^t$ and $\tan g_{ij}^t$ are presented below and the trigonometric properties and the respective proofs can be found in Appendix B.1, page 159.

$$\begin{aligned} \tan l_{ij}^t &= \frac{(x_i^t - x_j^t)s + (y_i^t - y_j^t)\sqrt{(x_i^t - x_j^t)^2 + (y_i^t - y_j^t)^2 - s^2}}{(x_i^t - x_j^t)\sqrt{(x_i^t - x_j^t)^2 + (y_i^t - y_j^t)^2 - s^2} - (y_i^t - y_j^t)s} \\ \tan g_{ij}^t &= \frac{-(x_i^t - x_j^t)s + (y_i^t - y_j^t)\sqrt{(x_i^t - x_j^t)^2 + (y_i^t - y_j^t)^2 - s^2}}{(x_i^t - x_j^t)\sqrt{(x_i^t - x_j^t)^2 + (y_i^t - y_j^t)^2 - s^2} + (y_i^t - y_j^t)s}. \end{aligned}$$

Therefore, the terms $h_i^t, h_j^t, k_i^t, k_j^t$ can be expressed:

$$h_i^t = \frac{(x_i^t - x_j^t)s + (y_i^t - y_j^t)\sqrt{(x_i^t - x_j^t)^2 + (y_i^t - y_j^t)^2 - s^2}}{(x_i^t - x_j^t)\sqrt{(x_i^t - x_j^t)^2 + (y_i^t - y_j^t)^2 - s^2} - (y_i^t - y_j^t)s} \cos(m_i^{*t}) - \sin(m_i^{*t}) \tag{3.4a}$$

$$h_j^t = \frac{(x_i^t - x_j^t)s + (y_i^t - y_j^t)\sqrt{(x_i^t - x_j^t)^2 + (y_i^t - y_j^t)^2 - s^2}}{(x_i^t - x_j^t)\sqrt{(x_i^t - x_j^t)^2 + (y_i^t - y_j^t)^2 - s^2} - (y_i^t - y_j^t)s} \cos(m_j^{*t}) - \sin(m_j^{*t}) \tag{3.4b}$$

$$k_i^t = \frac{-(x_i^t - x_j^t)s + (y_i^t - y_j^t)\sqrt{(x_i^t - x_j^t)^2 + (y_i^t - y_j^t)^2 - s^2}}{(x_i^t - x_j^t)\sqrt{(x_i^t - x_j^t)^2 + (y_i^t - y_j^t)^2 - s^2} + (y_i^t - y_j^t)s} \cos(m_i^{*t}) - \sin(m_i^{*t}) \tag{3.4c}$$

$$k_j^t = \frac{-(x_i^t - x_j^t)s + (y_i^t - y_j^t)\sqrt{(x_i^t - x_j^t)^2 + (y_i^t - y_j^t)^2 - s^2}}{(x_i^t - x_j^t)\sqrt{(x_i^t - x_j^t)^2 + (y_i^t - y_j^t)^2 - s^2} + (y_i^t - y_j^t)s} \cos(m_j^{*t}) - \sin(m_j^{*t}). \tag{3.4d}$$

The constraints (2.25b), (2.25d), (2.25f) and (2.25h) on page 64 for the VAC model are written in the VCTP model as follows,

$$\begin{aligned} -v_i^t h_i^t + v_j^t h_j^t &\leqslant M_1(1 - \delta_{ijt}^1) \\ v_i^t k_i^t - v_j^t k_j^t &\leqslant M_2(1 - \delta_{ijt}^2) \\ v_i^t h_i^t - v_j^t h_j^t &\leqslant M_3(1 - \delta_{ijt}^3) \\ -v_i^t k_i^t + v_j^t k_j^t &\leqslant M_4(1 - \delta_{ijt}^4), \end{aligned}$$

where $M_1 = M_3 = \overline{v}_i^t|h_i^t| + \overline{v}_j^t|h_j^t|$ are, respectively, the upper bounds of

$$\begin{aligned} -v_i^t h_i^t + v_j^t h_j^t \\ v_i^t h_i^t - v_j^t h_j^t \end{aligned}$$

and $M_2 = M_4 = \overline{v}_i^t|k_i^t| + \overline{v}_j^t|k_j^t|$ are, respectively, the upper bounds of

$$\begin{aligned} v_i^t k_i^t - v_j^t k_j^t \\ -v_i^t k_i^t + v_j^t k_j^t \end{aligned}$$

The terms $|h_i^t|$, $|h_j^t|$, $|k_i^t|$ and $|k_j^t|$ can be infinity, for anomalous cases, see Section 2.4.1, page 62. To avoid anomalous cases in the VCTP model, new constraints will be studied in Section 3.2.2.

Constraints (2.25i) on page 65 will be modified in the subindex of the δ variables

since the time period $t \in \mathcal{T}$ has to be aggregated. Firstly, there are four δ variables, since in the VCTP model altitude changes will not be aggregated for the time being.

Only the conflicts that can occur in a short time period can be modeled, as a first step, by ruling out the aircraft whose intersection point of the trajectories is remote. For this purpose the following auxiliary parameter was chosen,

$$p_{ij}^t = \begin{cases} 1 \text{ if } dist(p^t, p_i^t) > e \text{ and } dist(p^t, p_j^t) > e \\ 0 \text{ otherwise,} \end{cases}$$

where p^t is the intersection point between the aircraft trajectories p_i^t, p_j^t in time period $t \in \mathcal{T}$. See that it can be calculated by using equation (A.7) on page 149) and i^t, j^t are the aircraft positions in time period $t \in \mathcal{T}$. Notice that the angles of motion can be different in each time period, and then, all intersection points have to be calculated.

Therefore, if $p_{ij}^t = 1$, the pair of aircraft (i, j) will not be considered in time period $t \in \mathcal{T}$, and all δ variables must be zero; otherwise, the pair will be considered in time period $t \in \mathcal{T}$, and only one of the δ variables must be one.

3.2.2 Anomalous cases

The denominators of the expressions (3.4) can be zero if and only if $s = |x_i^t - x_j^t|$. This situation is an anomalous case as in the VC model, and can be detected in the preprocessing phase by using the initial configuration parameters.

It is easy to see that if $|x_i^{*t} - x_j^{*t}| \leqslant s$, an anomalous case involves aircraft i and $j \in \mathcal{F}$ in time period $t \in \mathcal{T}$ and, then, parameter pc_{ij}^t will be 1. The formal definition of the pc parameter is analogue to the pc parameter defined in Section 2.4.1, page 62, such that

$$pc_{ij}^t = \begin{cases} 1 & \text{if } |x_i^{*t} - x_j^{*t}| \leqslant r_i^t + r_j^t \\ 0 & \text{otherwise.} \end{cases}$$

For the anomalous cases an implicit turn of $\pi/2$ degrees of the angles involved in aircraft i and j configurations is needed as was done in Section 2.4.1. To do this, the

following trigonometric properties will be used

$$\cos(x) = \sin(x + \pi/2)$$
$$\sin(x) = -\cos(x + \pi/2).$$

To avoid anomalous cases, the following constraints related to constraints (2.25b), (2.25d), (2.25f) and (2.25h), on page 64, are considered, adding variables δ^n_{ijt} for $n = 5, \ldots, 8$:

$$\begin{aligned}
-v_i^t \sin(m_i^{*t}) + v_j^t \sin(m_j^{*t}) &\leqslant M_1(1 - \delta^5_{ijt}) \\
-v_i^t \sin(m_i^{*t}) + v_j^t \sin(m_j^{*t}) &\leqslant M_2(1 - \delta^6_{ijt}) \\
v_i^t \sin(m_i^{*t}) - v_j^t \sin(m_j^{*t}) &\leqslant M_3(1 - \delta^7_{ijt}) \\
v_i^t \sin(m_i^{*t}) - v_j^t \sin(m_j^{*t}) &\leqslant M_4(1 - \delta^8_{ijt}),
\end{aligned}$$

where $M_1 = M_2 = M_3 = M_4 = (\overline{v}_i^t + \overline{v}_j^t)$ are, respectively, the upper bounds of,

$$\begin{aligned}
-v_i^t \sin(m_i^{*t}) + v_j^t \sin(m_j^{*t}) \\
-v_i^t \sin(m_i^{*t}) + v_j^t \sin(m_j^{*t}) \\
v_i^t \sin(m_i^{*t}) - v_j^t \sin(m_j^{*t}) \\
v_i^t \sin(m_i^{*t}) - v_j^t \sin(m_j^{*t}).
\end{aligned}$$

For the constraints (2.25a), (2.25c), (2.25e) and (2.25g), page 64, the parameters $h_i^{'t}$, $h_j^{'t}$, $k_i^{'t}$ and $k_j^{'t}$ are as follows, considering $\tan(x) = -\cot(x + \pi/2)$. (See Appendix B.1, page 159),

$$h_i^{'t} = \frac{(x_i^t - x_j^t)s + (y_i^t - y_j^t)\sqrt{(x_i^t - x_j^t)^2 + (y_i^t - y_j^t)^2 - s^2}}{(x_i^t - x_j^t)\sqrt{(x_i^t - x_j^t)^2 + (y_i^t - y_j^t)^2 - s^2} - (y_i^t - y_j^t)s} \sin(m_i^{*t}) - \cos(m_i^{*t})$$

$$h_j^{'t} = \frac{(x_i^t - x_j^t)s + (y_i^t - y_j^t)\sqrt{(x_i^t - x_j^t)^2 + (y_i^t - y_j^t)^2 - s^2}}{(x_i^t - x_j^t)\sqrt{(x_i^t - x_j^t)^2 + (y_i^t - y_j^t)^2 - s^2} - (y_i^t - y_j^t)s} \sin(m_j^{*t}) - \cos(m_j^{*t})$$

$$k_i^{'t} = \frac{-(x_i^t - x_j^t)s + (y_i^t - y_j^t)\sqrt{(x_i^t - x_j^t)^2 + (y_i^t - y_j^t)^2 - s^2}}{(x_i^t - x_j^t)\sqrt{(x_i^t - x_j^t)^2 + (y_i^t - y_j^t)^2 - s^2} + (y_i^t - y_j^t)s} \sin(m_i^{*t}) - \cos(m_i^{*t})$$

$$k_j^{'t} = \frac{-(x_i^t - x_j^t)s + (y_i^t - y_j^t)\sqrt{(x_i^t - x_j^t)^2 + (y_i^t - y_j^t)^2 - s^2}}{(x_i^t - x_j^t)\sqrt{(x_i^t - x_j^t)^2 + (y_i^t - y_j^t)^2 - s^2} + (y_i^t - y_j^t)s} \sin(m_j^{*t}) - \cos(m_j^{*t}).$$

Then, the following constraints are considered after the implicit turn,

$$\begin{aligned} -v_i^t h_i^{'t} + v_j^t h_j^{'t} &\leqslant M_1(1 - \delta_{ijt}^5) \\ v_i^t k_i^{'t} - v_j^t k_j^{'t} &\leqslant M_2(1 - \delta_{ijt}^6) \\ v_i^t h_i^{'t} - v_j^t h_j^{'t} &\leqslant M_3(1 - \delta_{ijt}^7) \\ -v_i^t k_i^{'t} + v_j^t k_j^{'t} &\leqslant M_4(1 - \delta_{ijt}^8), \end{aligned}$$

where $M_1 = M_3 = \overline{v}_i^t|h_i^{'t}| + \overline{v}_j^t|h_j^{'t}|$ are, respectively, the upper bounds of

$$\begin{aligned} -v_i^t h_i^{'t} + v_j^t h_j^{'t} \\ v_i^t h_i^{'t} - v_j^t h_j^{'t} \end{aligned}$$

and $M_2 = M_4 = \overline{v}_i^t|k_i^{'t}| + \overline{v}_j^t|k_j^{'t}|$ are, respectively, the upper bounds of,

$$\begin{aligned} v_i^t k_i^{'t} - v_j^t k_j^{'t} \\ -v_i^t k_i^{'t} + v_j^t k_j^{'t}. \end{aligned}$$

Notice that $|h_i^t|$, $|h_j^t|$, $|k_i^t|$ and $|k_j^t|$ can be infinity, but only when an anomalous case in the vertical axis happens. This last set of constraints will only be used when an anomalous case in the horizontal axis has occurred, and if an anomalous case also happens in the vertical axis, the two involved aircraft i and j are in similar coordinates in time period $t \in \mathcal{T}$. This case have no sense since the two aircraft are sufficient near to suffer an irreparable collision.

Finally, as there are eight δ variables, the sum of them must be 1, so the eight or-constraints (see Appendix A.1.1, page 141) are linear ones, as follows,

$$\sum_{n=1}^{8} = \delta_{ijt}^n = 1.$$

3.2.3 False conflicts

The formulation of the VC model has an important inconvenience for the conflict resolution when false conflicts take place (see Section 2.3.4, page 41). To avoid these situations in the VCTP model, the following new parameter fc_{ij}^t must be considered

$$fc_{ij}^t = \begin{cases} 1 & \text{if } d_{ijt}^2 - d_{ijt}^1 > 0 \wedge d_{jit}^2 - d_{jit}^1 > 0 \\ 0 & \text{otherwise,} \end{cases}$$

where $d_{ijt}^1 = \text{dist}\{(x_i^{*t}, y_i^{*t}), ip_{ijt}\}$ and $d_f^2 = \text{dist}\{\big(x_i^{*t} + \cos(m_i^{*t}), y_i^{*t} + \sin(m_i^{*t})\big), ip_{ijt}\}$, being ip_{ijt} the intersection point between the two considered straight lines (i.e., the corresponding segments of the polygonal trajectories for aircraft i and j). This point has to be calculated in the first step of the algorithm. Notice that with this notation, $ip_{ijt} = ip_{jit}$.

Notice that the dimensions of the model can be reduced by using this parameter, since the constraints, where the pairs of aircraft (in each time period) are going away each other, are not considered in the model.

3.2.4 Updating and projecting new positions in the polygonal trajectory. First approximation

Previously, it was shown that a polygonal is considered for each aircraft trajectory for taking into account nonlinear ones. The aircraft positions have to be updated in each time period $t \in \mathcal{T}$ by using the equations (3.1b) related to the UALM. Firstly, the VCTP model should include the following four constraints that makes a consistent model for the position variables x, y relating the departure and arrival times and the current time period, respectively, if all time periods are considered,

$$\begin{aligned} x_f^t &= x_f^{*t_f^d}, \quad \forall t < t_f^d \\ y_f^t &= y_f^{*t_f^d}, \quad \forall t < t_f^d \\ x_f^t &= x_f^{*t_f^r}, \quad \forall t > t_f^r \\ y_f^t &= y_f^{*t_f^r}, \quad \forall t > t_f^r. \end{aligned}$$

Notice that these constraints will not be considered, provided that the pair of aircraft flying between times $\max\{t_i^d, t_j^d\} + 1$ and $\min\{t_i^r, t_j^r\} - 1$.

Model assumptions

For designing a robust model when the bounds of some constraints have to be considered, some important assumptions must be done. In the next section, some bounds M, upper or lower, will be considered, taking into account their importance in the execution times in the resolution of the model. These bounds help the solver software to be faster since the lower bound of the objective function (in case of minimization) grows quicker and the optimality can be proved when this lower bound is equal to the upper bound of the objective function.

In the first computational tests reported in this thesis, big values for the upper bounds and small values for the lower bounds M showed very large execution times. This was due to the fact that the lower bound of the objective function did not grow enough and whereas the upper bound of the objective function did not modify its value after some execution time, the solver software could not prove that the optimal solution was found. In the illustrative instance that will be shown below, the solver software was not able to prove the optimality of the upper bound of the objective function after one hour of execution since the gap between the upper and lower bounds was around 90%. Finally, the solver finished the resolution due to memory out. That is, the model was very weak.

Once the importance of the M bounds has been noticed, it should be realized that the distance that can be covered by an aircraft $f \in \mathcal{F}$ in each time period $t \in \mathcal{T}$, d_f^t cannot be greater than the predicted covered distance d_f^{*t} plus a quantity of $\frac{d_f^{*t}}{div}$, being div an integer value greater than one. Analogously, the covered distance d_f^t cannot be less than $d_f^{*t} - \frac{d_f^{*t}}{div}$. Then, some variable bounds can be calculated, so a tighter model can be used,

$$\begin{aligned}
\underline{d}_f^t = d_f^{*t} - \frac{d_f^{*t}}{div} \leqslant \quad & d_f^t \quad \leqslant d_f^{*t} + \frac{d_f^{*t}}{div} = \overline{d}_f^t \\
\underline{x}_f^t = x_f^{*t} - \frac{d_f^{*t}}{div}\cos(m_f^{*t-1}) \leqslant \quad & x_f^t \quad \leqslant x_f^t + \frac{d_f^{*t}}{div}\cos(m_f^{*t}) = \overline{x}_f^t \\
\underline{y}_f^t = y_f^{*t} - \frac{d_f^{*t}}{div}\sin(m_f^{*t-1}) \leqslant \quad & y_f^t \quad \leqslant y_f^t + \frac{d_f^{*t}}{div}\sin(m_f^{*t}) = \overline{y}_f^t.
\end{aligned}$$

Other aspect that the VCTP model assumes consists of fixing the position variables in the last time period to the initial configuration in order to force aircraft to arrive to the destination in the predicted time. Of course, this constraints can be relaxed but it is a good

starting point to force aircraft to reach the final point in the predicted time,

$$x_f^{t_f^r} = x_f^{*t_f^r}$$
$$y_f^{t_f^r} = y_f^{*t_f^r}.$$

Consequently, the sum of the d variables will be the total length of the trajectory polygonal

$$\sum_{\ell=t_f^d}^{t_f^r} d_f^\ell = d_f^{tot} \quad \forall f \in \mathcal{F}.$$

Arrival to the predicted point cases

The VCTP model has a set of fixed "waypoints" in certain time points, and a set of variables which are the new aircraft positions after the conflict resolution. It can occur that these variables and parameters do not coincide, and it should be decided what criterion has to be used for cover the trajectories, so, the polygonal of the nonlinear trajectory in the fixed time points, is considered in this thesis, and the criterion to cover the trajectory to force the aircraft to fly along the polygonal. If this criterion is used, there are four cases to be taken into account:

- *Excess-Excess position situation:* The aircraft arrives earlier to the $t-1$ and t time periods.
- *Defect-Defect position situation:* The aircraft arrives later to the $t-1$ and t time periods.
- *Defect-Excess position situation:* The aircraft arrives later to the $t-1$ time period, and arrives earlier to the t time period.
- *Excess-Defect position situation:* The aircraft arrives earlier to the $t-1$ time period, and arrives later to the t time period.

For detecting the case whose the aircraft is located, the parameters d_f^{*t-1}, d_f^{*t} can be used, storing the covered distance on the polygonal until the time periods $t-1$ and $t \in \mathcal{T}$, respectively, as well as the the variables d_f^{t-1}, d_f^t, that store the covered distance on the polygonal until the time period $t \in \mathcal{T}$ after the conflict resolution. Comparing these parameters with the respective variables, it results the following situations,

- *Excess-Excess position situation:*

$$\begin{aligned} \sum_{\ell=1}^{t-1} d_f^{\ell} &\geqslant \sum_{\ell=1}^{t-1} d_f^{*\ell} \\ &\text{and} \\ \sum_{\ell=1}^{t} d_f^{\ell} &\geqslant \sum_{\ell=1}^{t} d_f^{*\ell}. \end{aligned}$$

- *Defect-Defect position situation:*

$$\begin{aligned} \sum_{\ell=1}^{t-1} d_f^{\ell} &\leqslant \sum_{\ell=1}^{t-1} d_f^{*\ell} \\ &\text{and} \\ \sum_{\ell=1}^{t} d_f^{\ell} &\leqslant \sum_{\ell=1}^{t} d_f^{*\ell}. \end{aligned}$$

- *Defect-Excess position situation:*

$$\begin{aligned} \sum_{\ell=1}^{t-1} d_f^{\ell} &\leqslant \sum_{\ell=1}^{t-1} d_f^{*\ell} \\ &\text{and} \\ \sum_{\ell=1}^{t} d_f^{\ell} &\geqslant \sum_{\ell=1}^{t} d_f^{*\ell}. \end{aligned}$$

- *Excess-Defect position situation:*

$$\begin{aligned} \sum_{\ell=1}^{t-1} d_f^{\ell} &\geqslant \sum_{\ell=1}^{t-1} d_f^{*\ell} \\ &\text{and} \\ \sum_{\ell=1}^{t} d_f^{\ell} &\leqslant \sum_{\ell=1}^{t} d_f^{*\ell}. \end{aligned}$$

Each case will be differentiated in the VCTP model by using the auxiliary 0-1 variables γ_{ft}^{n}, for $n = 1, \ldots, 4$.

First, the variables d_f^t and d_f^{t-1} must be modeled correctly by using the equation (3.1b). Therefore, the following expression is considered,

$$d_f^t = v_f^{t-1} I_t + \frac{1}{2} a_f^t I_t^2 \quad \forall t = t_f^d + 1, \ldots, t_f^r.$$

Forcing each aircraft to follow the polygonal, the procedure used in this thesis for each case described above. First, the positions $\tilde{x}_f^t$ and $\tilde{y}_f^t$ must be established, according to the situation and, then, a translation of the point (x_f^{*t}, y_f^{*t}) or (x_f^{*t-1}, y_f^{*t-1}) to the origin must be done, if the aircraft in time period $t-1$ arrives later or earlier, respectively. With this translation, the point $(\tilde{x}_f^t, \tilde{y}_f^t)$ or $(\tilde{x}_f^{t-1}, \tilde{y}_f^{t-1})$ has to be turned around the origin to the point (x_f^t, y_f^t) or (x_f^{t-1}, y_f^{t-1}), respectively, by using the turn matrix and the angle $m_f^{*t-1} - m_f^{*t}$ or $m_f^{*t-2} - m_f^{*t-1}$, respectively and, then, undoing the translation.

Excess-excess situation For the "Excess-Excess" position situation shown in Fig. 3.1, the point (x_f^{*t}, y_f^{*t}) is centered to the origin, and the point $(\tilde{x}_f^t, \tilde{y}_f^t)$ is turned clockwise around the origin $m_f^{*t-1} - m_f^{*t}$ degrees and undoing the translation, so that the new aircraft position is as follows,

$$x_f^t = \left(x_f^{t-1} + d_f^t \cos(m_f^{*t-1}) - x_f^{*t}\right) \cos(m_f^{*t-1} - m_f^{*t}) + \left(y_f^{t-1} + d_f^t \sin(m_f^{*t-1}) - y_f^{*t}\right) \sin(m_f^{*t-1} - m_f^{*t}) + x_f^{*t}$$

$$y_f^t = -\left(x_f^{t-1} + d_f^t \cos(m_f^{*t-1}) - x_f^{*t}\right) \sin(m_f^{*t-1} - m_f^{*t}) + \left(y_f^{t-1} + d_f^t \sin(m_f^{*t-1}) - y_f^{*t}\right) \cos(m_f^{*t-1} - m_f^{*t}) + y_f^{*t}.$$

The operations can be seen more detailed in appendix B.2, page 163.

For modeling an auxiliary 0-1 variable γ_{ft}^1 has to be used in the six conditions for this case, since there will be two conditions to distinguish the position situation case, two conditions to model the equality of variable x_f^t, dividing this one in two inequalities ($\leqslant$ and $\geqslant$), and two conditions to model the equality of variable y_f^t as the x_f^t variable. Therefore,

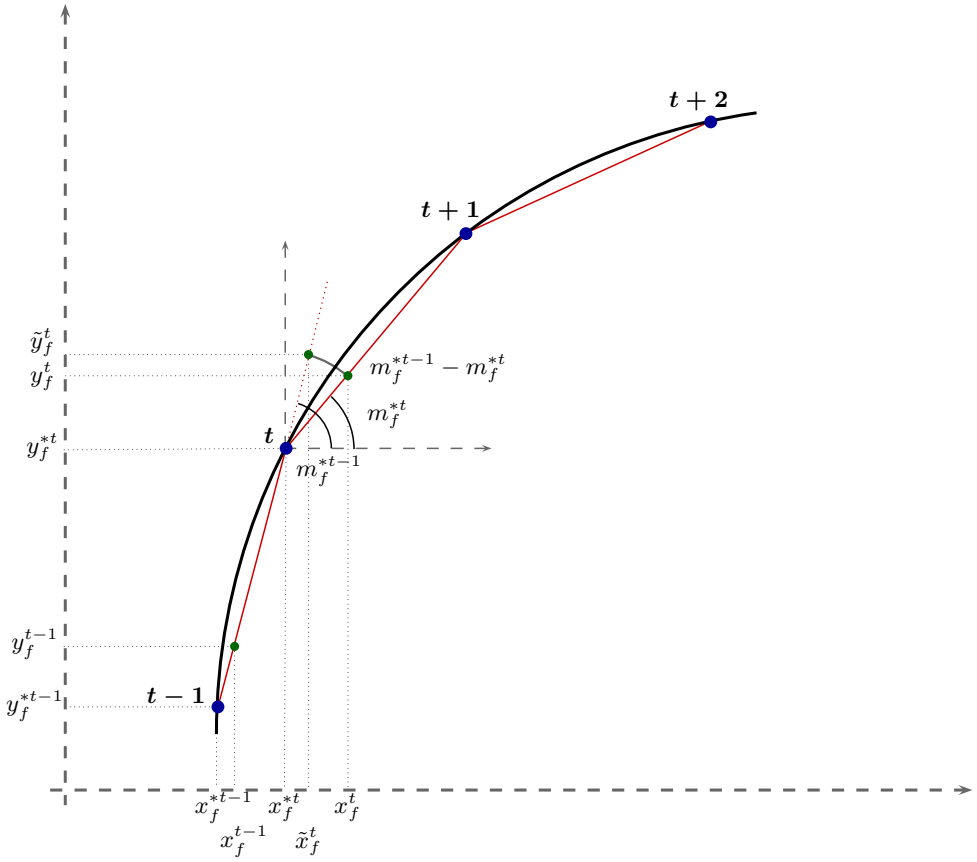

Figure 3.1: Excess-Excess position situation

the constraints to model this case will be as follows $\forall t = t_f^d + 1, \ldots, t_f^r$,

$$\sum_{\ell=t_f^d}^{t-1} d_f^{*\ell} - \sum_{\ell=t_f^d}^{t-1} d_f^{\ell} \leqslant M_1(1-\gamma_{ft}^1)$$

$$\sum_{\ell=t_f^d}^{t} d_f^{*\ell} - \sum_{\ell=t_f^d}^{t} d_f^{\ell} \leqslant M_2(1-\gamma_{ft}^1)$$

$$x_f^t - \left(x_f^{t-1} + d_f^t \cos(m_f^{*t-1}) - x_f^{*t}\right)\cos(m_f^{*t-1} - m_f^{*t}) -$$
$$\left(y_f^{t-1} + d_f^t \sin(m_f^{*t-1}) - y_f^{*t}\right)\sin(m_f^{*t-1} - m_f^{*t}) - x_f^{*t} \leqslant M_3(1-\gamma_{ft}^1)$$

$$x_f^t - \left(x_f^{t-1} + d_f^t \cos(m_f^{*t-1}) - x_f^{*t}\right)\cos(m_f^{*t-1} - m_f^{*t}) - \left(y_f^{t-1} + d_f^t \sin(m_f^{*t-1}) - y_f^{*t}\right)\sin(m_f^{*t-1} - m_f^{*t}) - x_f^{*t} \geqslant M_4(1 - \gamma_{ft}^1)$$

$$y_f^t + \left(x_f^{t-1} + d_f^t \cos(m_f^{*t-1}) - x_f^{*t}\right)\sin(m_f^{*t-1} - m_f^{*t}) - \left(y_f^{t-1} + d_f^t \sin(m_f^{*t-1}) - y_f^{*t}\right)\cos(m_f^{*t-1} - m_f^{*t}) - y_f^{*t} \leqslant M_5(1 - \gamma_{ft}^1)$$

$$y_f^t + \left(x_f^{t-1} + d_f^t \cos(m_f^{*t-1}) - x_f^{*t}\right)\sin(m_f^{*t-1} - m_f^{*t}) - \left(y_f^{t-1} + d_f^t \sin(m_f^{*t-1}) - y_f^{*t}\right)\cos(m_f^{*t-1} - m_f^{*t}) - y_f^{*t} \geqslant M_6(1 - \gamma_{ft}^1).$$

where

$$M_1 = d_f^{*t-1}/div$$
$$M_2 = d_f^{*t}/div$$

are, respectively, the upper bounds of

$$\sum_{\ell=t_f^d}^{t-1} d_f^{*\ell} - \sum_{\ell=t_f^d}^{t-1} d_f^{\ell}$$
$$\sum_{\ell=t_f^d}^{t} d_f^{*\ell} - \sum_{\ell=t_f^d}^{t} d_f^{\ell},$$

$$M_3 = \overline{x}_f^t + \overline{x}_f^{t-1} + 2\overline{d}_f^t + \overline{y}_f^{t-1} - 2x_f^{*t} - y_f^{*t}$$
$$M_4 = \underline{x}_f^t - \overline{x}_f^{t-1} - 2\overline{d}_f^t - \overline{y}_f^{t-1} + y_f^{*t}$$

are, respectively, the upper and lower bounds of

$$x_f^t - \left(x_f^{t-1} + d_f^t \cos(m_f^{*t-1}) - x_f^{*t}\right)\cos(m_f^{*t-1} - m_f^{*t}) - \left(y_f^{t-1} + d_f^t \sin(m_f^{*t-1}) - y_f^{*t}\right)\sin(m_f^{*t-1} - m_f^{*t}) - x_f^{*t},$$

$$M_5 = \overline{y}_f^t + \overline{x}_f^{t-1} + 2\overline{d}_f^t + \overline{y}_f^{t-1} - 2y_f^{*t} - x_f^{*t}$$
$$M_6 = \underline{y}_f^t - \overline{x}_f^{t-1} - 2\overline{d}_f^t - \overline{y}_f^{t-1} + x_f^{*t}$$

are, respectively, the upper and lower bounds of

$$y_f^t + \left(x_f^{t-1} + d_f^t \cos(m_f^{*t-1}) - x_f^{*t}\right) \sin(m_f^{*t-1} - m_f^{*t}) - \\ \left(y_f^{t-1} + d_f^t \sin(m_f^{*t-1}) - y_f^{*t}\right) \cos(m_f^{*t-1} - m_f^{*t}) - y_f^{*t}.$$

Notice that $\overline{x}_f^t$, $\overline{y}_f^t$ and $\overline{d}_f^t$ are, respectively, the upper bounds of the variables x_f^t, y_f^t and d_f^t, whereas $\underline{x}_f^t$ and $\underline{y}_f^t$ are, respectively, the lower bounds of the variables x_f^t and y_f^t.

Defect-defect situation In the "Defect-Defect" position situation (see Fig. 3.2), the point (x_f^{*t-1}, y_f^{*t-1}) is centered to the origin, and the point $(\tilde{x}_f^t, \tilde{y}_f^t)$ is turned clockwise around the origin $m_f^{*t-2} - m_f^{*t-1}$ degrees and undoing the translation, as in the first case, so that the new aircraft position is as follows,

$$x_f^t = \left(x_f^{t-1} + d_f^t \cos(m_f^{*t-2}) - x_f^{*t-1}\right) \cos(m_f^{*t-2} - m_f^{*t-1}) + \\ \left(y_f^{t-1} + d_f^t \sin(m_f^{*t-2}) - y_f^{*t-1}\right) \sin(m_f^{*t-2} - m_f^{*t-1}) + x_f^{*t-1}$$

$$y_f^t = -\left(x_f^{t-1} + d_f^t \cos(m_f^{*t-2}) - x_f^{*t-1}\right) \sin(m_f^{*t-2} - m_f^{*t-1}) + \\ \left(y_f^{t-1} + d_f^t \sin(m_f^{*t-2}) - y_f^{*t-1}\right) \cos(m_f^{*t-2} - m_f^{*t-1}) + y_f^{*t-1}.$$

As in the previous case, the constraints in the VCTP model are designed by using the auxiliary 0-1 variable γ_{ft}^2, such that $\forall t = t_f^d + 2, \ldots, t_f^r$,

$$\sum_{\ell=t_f^d}^{t-1} d_f^\ell - \sum_{\ell=t_f^d}^{t-1} d_f^{*\ell} \leqslant M_1(1 - \gamma_{ft}^2)$$
$$\sum_{\ell=t_f^d}^{t} d_f^\ell - \sum_{\ell=t_f^d}^{t} d_f^{*\ell} \leqslant M_2(1 - \gamma_{ft}^2)$$

$$x_f^t - \left(x_f^{t-1} + d_f^t \cos(m_f^{*t-2}) - x_f^{*t-1}\right) \cos(m_f^{*t-2} - m_f^{*t-1}) - \\ \left(y_f^{t-1} + d_f^t \sin(m_f^{*t-2}) - y_f^{*t-1}\right) \sin(m_f^{*t-2} - m_f^{*t-1}) - x_f^{*t-1} \leqslant M_3(1 - \gamma_{ft}^2)$$

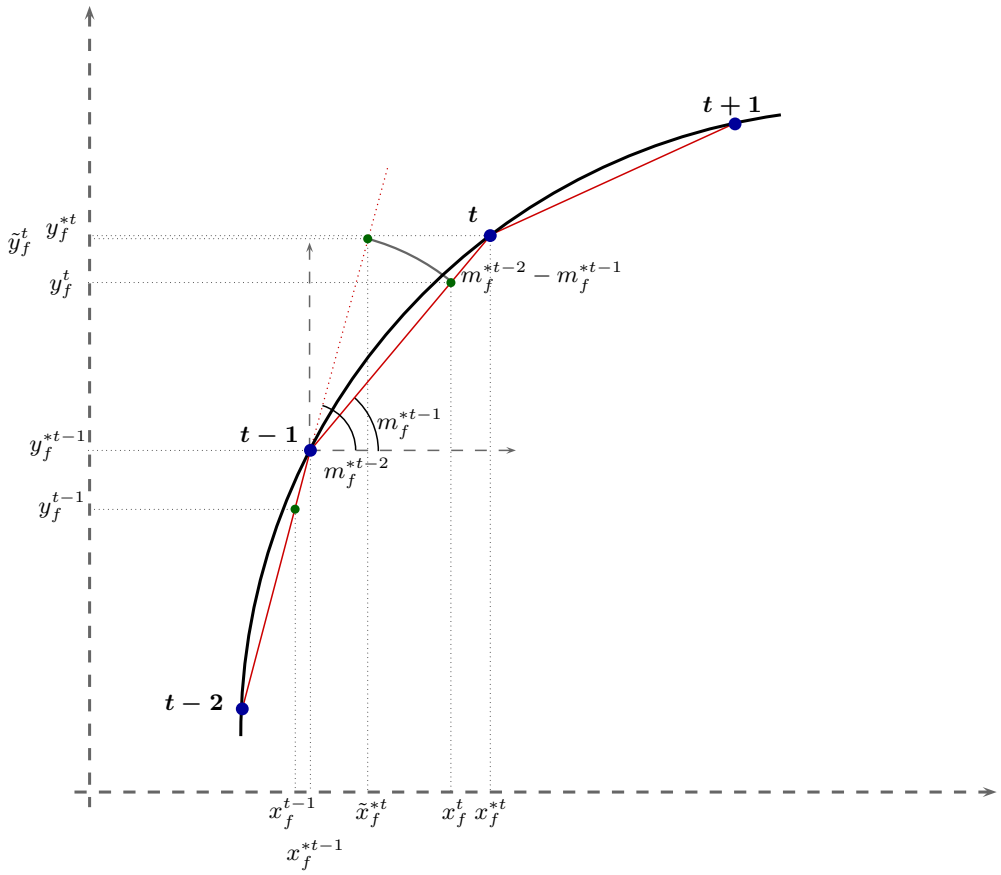

Figure 3.2: Defect-Defect position situation

$$x_f^t - \left(x_f^{t-1} + d_f^t \cos(m_f^{*t-2}) - x_f^{*t-1}\right) \cos(m_f^{*t-2} - m_f^{*t-1}) -$$
$$\left(y_f^{t-1} + d_f^t \sin(m_f^{*t-2}) - y_f^{*t-1}\right) \sin(m_f^{*t-2} - m_f^{*t-1}) - x_f^{*t-1} \geqslant M_4(1 - \gamma_{ft}^2)$$

$$y_f^t + \left(x_f^{t-1} + d_f^t \cos(m_f^{*t-2}) - x_f^{*t-1}\right) \sin(m_f^{*t-2} - m_f^{*t-1}) -$$
$$\left(y_f^{t-1} + d_f^t \sin(m_f^{*t-2}) - y_f^{*t-1}\right) \cos(m_f^{*t-2} - m_f^{*t-1}) - y_f^{*t-1} \leqslant M_5(1 - \gamma_{ft}^2)$$

$$y_f^t + \left(x_f^{t-1} + d_f^t \cos(m_f^{*t-2}) - x_f^{*t-1}\right) \sin(m_f^{*t-2} - m_f^{*t-1}) -$$
$$\left(y_f^{t-1} + d_f^t \sin(m_f^{*t-2}) - y_f^{*t-1}\right) \cos(m_f^{*t-2} - m_f^{*t-1}) - y_f^{*t-1} \geqslant M_6(1 - \gamma_{ft}^2),$$

where

$$M_1 = d_f^{*t-1}/div$$
$$M_2 = d_f^{*t}/div$$

are, respectively, the upper bounds of

$$\sum_{\ell=t_f^d}^{t-1} d_f^{*\ell} - \sum_{\ell=t_f^d}^{t-1} d_f^{\ell}$$
$$\sum_{\ell=t_f^d}^{t} d_f^{*\ell} - \sum_{\ell=t_f^d}^{t} d_f^{\ell},$$

$$M_3 = \overline{x}_f^t + \overline{x}_f^{t-1} + 2\overline{d}_f^t + \overline{y}_f^{t-1} - 2x_f^{*t-1} - y_f^{*t-1}$$
$$M_4 = \underline{x}_f^t - \overline{x}_f^{t-1} - 2\overline{d}_f^t - \overline{y}_f^{t-1} + y_f^{*t-1}$$

are, respectively, the upper and lower bounds of

$$x_f^t - \left(x_f^{t-1} + d_f^t \cos(m_f^{*t-2}) - x_f^{*t}\right)\cos(m_f^{*t-2} - m_f^{*t-1}) - \left(y_f^{t-1} + d_f^t \sin(m_f^{*t-2}) - y_f^{*t}\right)\sin(m_f^{*t-2} - m_f^{*t-1}) - x_f^{*t},$$

$$M_5 = \overline{y}_f^t + \overline{x}_f^{t-1} + 2\overline{d}_f^t + \overline{y}_f^{t-1} - 2y_f^{*t-1} - x_f^{*t-1}$$
$$M_6 = \underline{y}_f^t - \overline{x}_f^{t-1} - 2\overline{d}_f^t - \overline{y}_f^{t-1} + x_f^{*t-1}$$

are, respectively, the upper and lower bounds of

$$y_f^t + \left(x_f^{t-1} + d_f^t \cos(m_f^{*t-2}) - x_f^{*t}\right)\sin(m_f^{*t-2} - m_f^{*t-1}) - \left(y_f^{t-1} + d_f^t \sin(m_f^{*t-2}) - y_f^{*t}\right)\cos(m_f^{*t-2} - m_f^{*t-1}) - y_f^{*t}.$$

Defect-excess situation The "Defect-Excess" position situation is more difficult than the two cases studied above, since it is necessary to have two turns. The case is shown in Fig. 3.3. First, the point $(\tilde{x}_f^t, \tilde{y}_f^t)$ is used and after the translation and the turn clockwise around of the origin $m_f^{*t-2} - m_f^{*t-1}$ degrees, a second point $(\hat{x}_f^t, \hat{x}_f^t)$ is used and it must be turned clockwise $m_f^{*t-1} - m_f^t$ degrees and undoing the new translation, such that the new aircraft

position is as follows,

$$x_f^t = \Big\{ \big(\tilde{x}_f^t - x_f^{*t-1}\big)\cos(m_f^{*t-2} - m_f^{*t-1}) + \big(\tilde{y}_f^t - y_f^{*t-1}\big)\sin(m_f^{*t-2} - m_f^{*t-1}) + x_f^{*t-1} - x_f^{*t} \Big\} \cos(m_f^{*t-1} - m_f^{*t}) + \Big\{ -\big(\tilde{x}_f^t - x_f^{*t-1}\big)\sin(m_f^{*t-2} - m_f^{*t-1}) + \big(\tilde{y}_f^t - y_f^{*t-1}\big)\cos(m_f^{*t-2} - m_f^{*t-1}) + y_f^{*t-1} - y_f^{*t} \Big\} \sin(m_f^{*t-1} - m_f^{*t}) + x_f^{*t}$$

$$y_f^t = -\Big\{ \big(\tilde{x}_f^t - x_f^{*t-1}\big)\cos(m_f^{*t-2} - m_f^{*t-1}) + \big(\tilde{y}_f^t - y_f^{*t-1}\big)\sin(m_f^{*t-2} - m_f^{*t-1}) + x_f^{*t-1} - x_f^{*t} \Big\} \sin(m_f^{*t-1} - m_f^{*t}) + \Big\{ -\big(\tilde{x}_f^t - x_f^{*t-1}\big)\sin(m_f^{*t-2} - m_f^{*t-1}) + \big(\tilde{y}_f^t - y_f^{*t-1}\big)\cos(m_f^{*t-2} - m_f^{*t-1}) + y_f^{*t-1} - y_f^{*t} \Big\} \cos(m_f^{*t-1} - m_f^{*t}) + y_f^{*t},$$

where

$$\begin{aligned} \tilde{x}_f^t &= x_f^{t-1} + d_f^t \cos(m_f^{*t-2}) \\ \tilde{y}_f^t &= y_f^{t-1} + d_f^t \sin(m_f^{*t-2}) \end{aligned}$$

As in the previous cases, the constraints in the VCTP model are designed by including the auxiliary 0-1 variable γ_{ft}^3 such that they result $\forall t = t_f^d + 1, \ldots, t_f^r$ as follows,

$$\begin{aligned} \sum_{\ell=t_f^d}^{t-1} d_f^\ell - \sum_{\ell=t_f^d}^{t-1} d_f^{*\ell} &\leqslant M_1(1-\gamma_{ft}^3) \\ \sum_{\ell=t_f^d}^{t} d_f^{*\ell} - \sum_{\ell=t_f^d}^{t} d_f^\ell &\leqslant M_2(1-\gamma_{ft}^3) \end{aligned}$$

$$x_f^t - \Big\{ \big(\tilde{x}_f^t - x_f^{*t-1}\big)\cos(m_f^{*t-2} - m_f^{*t-1}) + \big(\tilde{y}_f^t - y_f^{*t-1}\big)\sin(m_f^{*t-2} - m_f^{*t-1}) + x_f^{*t-1} - x_f^{*t} \Big\} \cos(m_f^{*t-1} - m_f^{*t}) - \Big\{ -\big(\tilde{x}_f^t - x_f^{*t-1}\big)\sin(m_f^{*t-2} - m_f^{*t-1}) + \big(\tilde{y}_f^t - y_f^{*t-1}\big)\cos(m_f^{*t-2} - m_f^{*t-1}) + y_f^{*t-1} - y_f^{*t} \Big\} \sin(m_f^{*t-1} - m_f^{*t}) - x_f^{*t} \leqslant M_3(1-\gamma_{ft}^3)$$

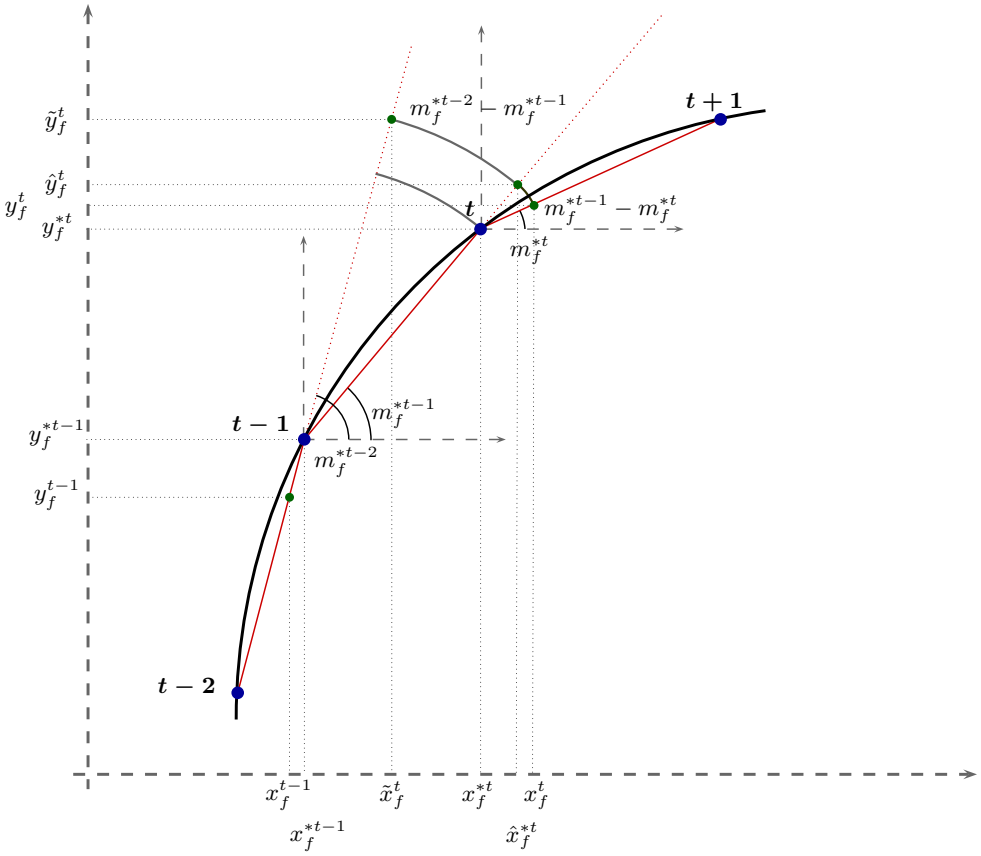

Figure 3.3: Defect-Excess position situation

$$x_f^t - \Big\{\big(\tilde{x}_f^t - x_f^{*t-1}\big)\cos(m_f^{*t-2} - m_f^{*t-1}) + \big(\tilde{y}_f^t - y_f^{*t-1}\big)\sin(m_f^{*t-2} - m_f^{*t-1}) + x_f^{*t-1} - x_f^{*t}\Big\}\cos(m_f^{*t-1} - m_f^{*t}) - \Big\{-\big(\tilde{x}_f^t - x_f^{*t-1}\big)\sin(m_f^{*t-2} - m_f^{*t-1}) + \big(\tilde{y}_f^t - y_f^{*t-1}\big)\cos(m_f^{*t-2} - m_f^{*t-1}) + y_f^{*t-1} - y_f^{*t}\Big\}\sin(m_f^{*t-1} - m_f^{*t}) - x_f^{*t} \geqslant M_4(1-\gamma_{ft}^3)$$

$$y_f^t + \Big\{\big(\tilde{x}_f^t - x_f^{*t-1}\big)\cos(m_f^{*t-2} - m_f^{*t-1}) + \big(\tilde{y}_f^t - y_f^{*t-1}\big)\sin(m_f^{*t-2} - m_f^{*t-1}) + x_f^{*t-1} - x_f^{*t}\Big\}\sin(m_f^{*t-1} - m_f^{*t}) - \Big\{-\big(\tilde{x}_f^t - x_f^{*t-1}\big)\sin(m_f^{*t-2} - m_f^{*t-1}) + \big(\tilde{y}_f^t - y_f^{*t-1}\big)\cos(m_f^{*t-2} - m_f^{*t-1}) + y_f^{*t-1} - y_f^{*t}\Big\}\cos(m_f^{*t-1} - m_f^{*t}) - y_f^{*t} \leqslant M_5(1-\gamma_{ft}^3)$$

$$y_f^t + \Big\{ \big(\tilde{x}_f^t - x_f^{*t-1}\big)\cos(m_f^{*t-2} - m_f^{*t-1}) + \big(\tilde{y}_f^t - y_f^{*t-1}\big)\sin(m_f^{*t-2} - m_f^{*t-1}) + x_f^{*t-1} - x_f^{*t} \Big\} \sin(m_f^{*t-1} - m_f^{*t}) - \Big\{ - \big(\tilde{x}_f^t - x_f^{*t-1}\big)\sin(m_f^{*t-2} - m_f^{*t-1}) + \big(\tilde{y}_f^t - y_f^{*t-1}\big)\cos(m_f^{*t-2} - m_f^{*t-1}) + y_f^{*t-1} - y_f^{*t} \Big\} \cos(m_f^{*t-1} - m_f^{*t}) - y_f^{*t} \geqslant M_6(1-\gamma_{ft}^3),$$

where

$$M_1 = d_f^{*t-1}/div$$
$$M_2 = d_f^{*t}/div$$

are, respectively, the upper bounds of

$$\sum_{\ell=t_f^d}^{t-1} d_f^{*\ell} - \sum_{\ell=t_f^d}^{t-1} d_f^{\ell}$$
$$\sum_{\ell=t_f^d}^{t} d_f^{*\ell} - \sum_{\ell=t_f^d}^{t} d_f^{\ell},$$

$$M_3 = \overline{x}_f^t + 2\overline{x}_f^{t-1} + 2\overline{y}_f^{t-1} + 4\overline{d}_f^t - 2x_f^{*t} - x_f^{*t-1} - y_f^{*t} - y_f^{*t-1}$$
$$M_4 = \underline{x}_f^t - 2\overline{x}_f^{t-1} - 2\overline{y}_f^{t-1} - 4\overline{d}_f^t + x_f^{*t-1} + y_f^{*t} + y_f^{*t-1}$$

are, respectively, the upper and lower bounds of

$$x_f^t - \Big\{ \big(\tilde{x}_f^t - x_f^{*t-1}\big)\cos(m_f^{*t-2} - m_f^{*t-1}) + \big(\tilde{y}_f^t - y_f^{*t-1}\big)\sin(m_f^{*t-2} - m_f^{*t-1}) + x_f^{*t-1} - x_f^{*t} \Big\} \cos(m_f^{*t-1} - m_f^{*t}) - \Big\{ - \big(\tilde{x}_f^t - x_f^{*t-1}\big)\sin(m_f^{*t-2} - m_f^{*t-1}) + \big(\tilde{y}_f^t - y_f^{*t-1}\big)\cos(m_f^{*t-2} - m_f^{*t-1}) + y_f^{*t-1} - y_f^{*t} \Big\} \sin(m_f^{*t-1} - m_f^{*t}) - x_f^{*t},$$

$$M_5 = 2\overline{x}_f^{t-1} + \overline{y}_f^t + 2\overline{y}_f^{t-1} + 4\overline{d}_f^t - x_f^{*t} - x_f^{*t-1} - 2y_f^{*t} - y_f^{*t-1}$$
$$M_6 = -2\overline{x}_f^{t-1} + \underline{y}_f^t - 2\overline{y}_f^{t-1} - 4\overline{d}_f^t + x_f^{*t} + x_f^{*t-1} + y_f^{*t-1}$$

are, respectively, the upper and lower bounds of

$$y_f^t + \Big\{ \big(\tilde{x}_f^t - x_f^{*t-1}\big)\cos(m_f^{*t-2} - m_f^{*t-1}) + \big(\tilde{y}_f^t - y_f^{*t-1}\big)\sin(m_f^{*t-2} - m_f^{*t-1}) + x_f^{*t-1} - x_f^{*t} \Big\} \sin(m_f^{*t-1} - m_f^{*t}) - \Big\{ -\big(\tilde{x}_f^t - x_f^{*t-1}\big)\sin(m_f^{*t-2} - m_f^{*t-1}) + \big(\tilde{y}_f^t - y_f^{*t-1}\big)\cos(m_f^{*t-2} - m_f^{*t-1}) + y_f^{*t-1} - y_f^{*t} \Big\} \cos(m_f^{*t-1} - m_f^{*t}) - y_f^{*t}.$$

Excess-defect situation Finally, the last case "Excess-Defect" position situation is the easiest one, since no turn must be done, as it is shown in Fig. 3.4. The new aircraft position will be as follows,

$$\begin{aligned} x_f^t &= x_f^{t-1} + d_f^t \cos(m_f^{*t-1}) \\ y_f^t &= y_f^{t-1} + d_f^t \sin(m_f^{*t-1}) \end{aligned}$$

As in the previous cases, the constraints in the VCTP model are designed by using the auxiliary 0-1 variable γ_{ft}^4, such that they result $\forall t = t_f^d + 1, \ldots, t_f^r$ as follows,

$$\begin{aligned} \sum_{\ell=t_f^d}^{t-1} d_f^{*\ell} - \sum_{\ell=t_f^d}^{t-1} d_f^{\ell} &\leqslant M_1(1-\gamma_{ft}^4) \\ \sum_{\ell=t_f^d}^{t} d_f^{\ell} - \sum_{\ell=t_f^d}^{t} d_f^{*\ell} &\leqslant M_2(1-\gamma_{ft}^4) \\ x_f^t - x_f^{t-1} - d_f^t \cos(m_f^{*t-1}) &\leqslant M_3(1-\gamma_{ft}^4) \\ x_f^t - x_f^{t-1} - d_f^t \cos(m_f^{*t-1}) &\geqslant M_4(1-\gamma_{ft}^4) \\ y_f^t - y_f^{t-1} - d_f^t \sin(m_f^{*t-1}) &\leqslant M_5(1-\gamma_{ft}^4) \\ y_f^t - y_f^{t-1} - d_f^t \sin(m_f^{*t-1}) &\geqslant M_6(1-\gamma_{ft}^4), \end{aligned}$$

where

$$\begin{aligned} M_1 &= d_f^{*t-1}/div \\ M_2 &= d_f^{*t}/div \end{aligned}$$

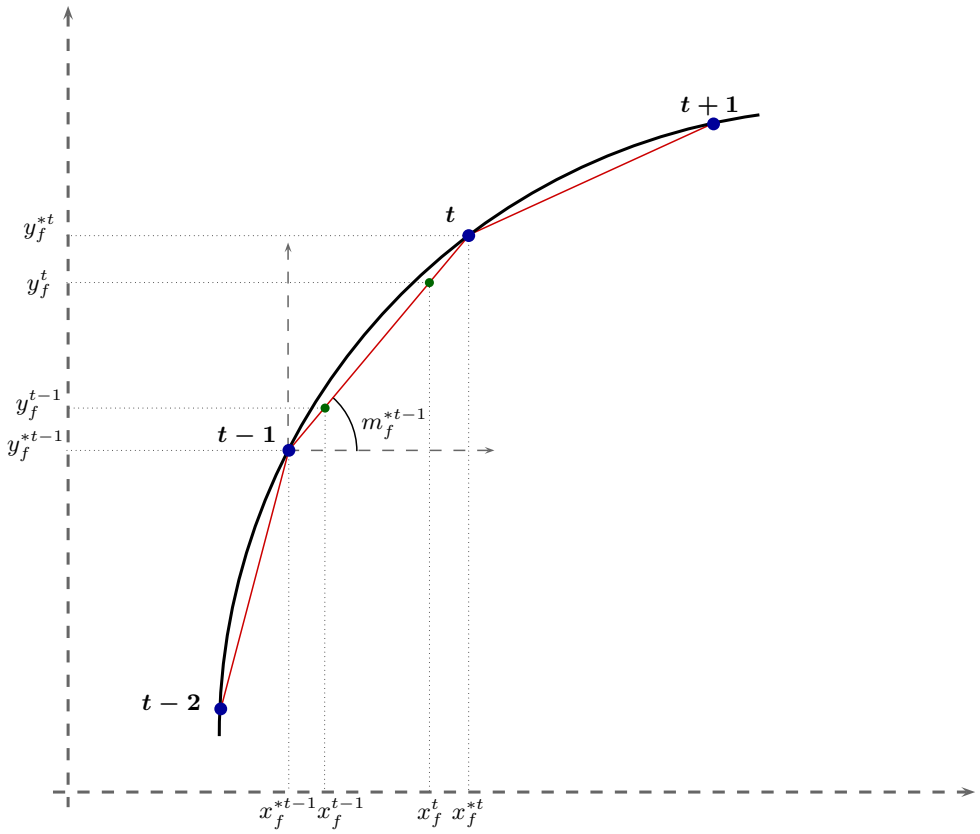

Figure 3.4: Excess-Defect position situation

are, respectively, the upper bounds of

$$\sum_{\ell=t_f^d}^{t-1} d_f^{*\ell} - \sum_{\ell=t_f^d}^{t-1} d_f^{\ell}$$

$$\sum_{\ell=t_f^d}^{t} d_f^{*\ell} - \sum_{\ell=t_f^d}^{t} d_f^{\ell},$$

$$M_3 = \overline{x}_f^t - \underline{x}_f^{t-1} + \overline{d}_f^t$$

$$M_4 = \underline{x}_f^t - \overline{x}_f^{t-1} - \overline{d}_f^t$$

are, respectively, the upper and lower bounds of

$$x_f^t - x_f^{t-1} - d_f^t \cos(m_f^{*t-1}),$$

$$M_5 = \overline{y}_f^t - \underline{y}_f^{t-1} + \overline{d}_f^t$$
$$M_6 = \underline{y}_f^t - \overline{y}_f^{t-1} - \overline{d}_f^t$$

are, respectively, the upper and lower bounds of

$$y_f^t - y_f^{t-1} - d_f^t \sin(m_f^{*t-1}).$$

Finally, the sum of the γ variables must be one, since one of the four cases has to be satisfied, (see Appendix A.1.1, page 141), so

$$\gamma_{ft}^1 + \gamma_{ft}^2 + \gamma_{ft}^3 + \gamma_{ft}^4 = 1.$$

3.2.5 Different terms for the objective function

The final step for designing the VCTP model consists of constructing an objective function to optimize, in order to solve the conflicts by considering certain requests. As in the previous chapter, where the VAC was presented, different terms in the objective function can be considered as it is shown below.

Acceleration variations

As the VAC model presented above, the first term in the objective function can be minimizing the sum of the acceleration variations. In this manner, the conflicts are solved since the constraints are satisfied and the velocity changes have to be smoothed. It can be done by minimizing the sum of the absolute values of the a_f^t variables as follows,

$$\min \sum_{f \in \mathcal{F}} \sum_{t \in \mathcal{T}} |a_f^t|$$

and it can be lineally modeled by using the nonnegative variables a_f^{t+} and a_f^{t-} as follows,

$$\min \sum_{f \in \mathcal{F}} \sum_{t \in \mathcal{T}} (a_f^{t+} + a_f^{t-}).$$

Each term a_f^{t+} and a_f^{t-} can be normalized between 0 and 1, such that they are penalized by the cost parameters $c_{ft}^{a^+}$ and $c_{ft}^{a^-}$, respectively, resulting the following objective function,

$$\min \sum_{f \in \mathcal{F}} \sum_{t \in \mathcal{T}} \left(\frac{c_{ft}^{a^+} a_f^{t+}}{\overline{a}_f^t - \underline{a}_f^t} + \frac{c_{ft}^{a^-} a_f^{t-}}{\overline{a}_f^t - \underline{a}_f^t} \right).$$

Differences between the predicted and final configurations

Some other terms to be optimized can be the difference between the initial and the final configurations for each aircraft. In order to model this other term, the differences in velocity and covered distances, are penalized for each time period, as it will be seen below.

Velocity differences The first difference between the initial and the final aircraft configuration that can be considered is the velocities in the intermediate points of the flight. Then, the sum of the absolute values of the velocities differences can be minimized as follows,

$$\min \sum_{f \in \mathcal{F}} \sum_{t \in \mathcal{T}} |v_f^t - v_f^{*t}|.$$

As this objective function is not linear, it can be linearized by considering an auxiliary 0-1 variable β_f^t, two additional constraints (see Appendix A.1.2, page 141) and a penalization cost c_{ft}^v as follows,

$$\begin{aligned} \min & \sum_{f \in \mathcal{F}} \sum_{t \in \mathcal{T}} c_{ft}^v \beta_f^t \\ \text{s.t.: } & \beta_f^t \geqslant v_f^t - v_f^{*t} \\ & \beta_f^t \geqslant v_f^{*t} - v_f^t. \end{aligned}$$

This objective function forces aircraft to change the velocity twice to avoid a conflict. The first change avoids the conflict and the second one forces aircraft to arrive to the next position (after the conflict is solved) in the predicted time, since the differences

between the velocities in each time period $t \in \mathcal{T}$ are penalized.

It can be noticed that the objective function shows unstable solutions, in the sense that an aircraft is accelerated and decelerated in consecutive time periods before the conflict is solved. Then, it will not be considered in the computational experience reported in this thesis.

Covered distances The other difference that can be penalized is in covered distance terms. The sum of the absolute values of the covered distances in each time period should be minimized, being $\sum_{\ell=1}^{t} d_f^{*\ell}$ and $\sum_{\ell=1}^{t} d_f^{\ell}$ the predicted and final covered distances for aircraft $f \in \mathcal{F}$ in time period $t \in \mathcal{T}$. Then,

$$\min \sum_{f \in \mathcal{F}} \sum_{t \in \mathcal{T}} \Big| \sum_{\ell=1}^{t} d_f^{\ell} - \sum_{\ell=1}^{t} d_f^{*\ell} \Big|.$$

In the same way as above, the linearized objective function must consider an auxiliary 0-1 variable β_f^t, two additional constraints and a penalization cost c_{ft}^d as follows,

$$\begin{aligned} \min & \sum_{f \in \mathcal{F}} \sum_{t \in \mathcal{T}} c_{ft}^d \beta_f^t \\ \text{s.t.: } \beta_f^t & \geqslant \sum_{\ell=1}^{t} d_f^{\ell} - \sum_{\ell=1}^{t} d_f^{*\ell} \\ \beta_f^t & \geqslant \sum_{\ell=1}^{t} d_f^{*\ell} - \sum_{\ell=1}^{t} d_f^{\ell}. \end{aligned}$$

Finally, new terms can be added to take into account the fuel consumption or other aspects like the total number of velocity changes made by an aircraft.

3.3 The VCTP model: Compact version

3.3.1 Dimension reduction in detection and resolution constraints

The constraints for the conflict detection and resolution were presented in Section 3.2.1, being eight different cases if the anomalous ones are considered. As in the VAC model, the anomalous cases in the initial situation can be detected and then, the model

can be reduced considerably in the number of constraints and variables. Then, by using the parameter pc, the eight constraints considered in Section 3.2.1 can be reduced to four constraints by including the parameter pc in the constraints formulation as follows,

$$v_i^t\big(\cos(m_i^{*t})(1-pc_{ij}^t)-\sin(m_i^{*t})pc_{ij}^t\big)-v_j^t\big(\cos(m_j^{*t})(1-pc_{ij}^t)-\sin(m_j^{*t})pc_{ij}^t\big)\leqslant (\overline{v}_i^t-\overline{v}_j^t)(1-\delta_{ijt}^1)$$

$$-v_i^t\big(h_i^t(1-pc_{ij}^t)+h_i^{'t}pc_{ij}^t\big)+v_j^t\big(h_j^t(1-pc_{ij}^t)+h_j^{'t}pc_{ij}^t\big)\leqslant \Big(\big(\overline{v}_i^t|h_i^t|+\overline{v}_j^t|h_j^t|\big)(1-pc_{ij}^t)+\big(\overline{v}_i^t|h_i^{'t}|+\overline{v}_j^t|h_j^{'t}|\big)pc_{ij}^t\Big)(1-\delta_{ijt}^1)$$

$$v_i^t\big(\cos(m_i^{*t})(1-pc_{ij}^t)-\sin(m_i^{*t})pc_{ij}^t\big)-v_j^t\big(\cos(m_j^{*t})(1-pc_{ij}^t)-\sin(m_j^{*t})pc_{ij}^t\big)\leqslant (\overline{v}_i^t-\overline{v}_j^t)(1-\delta_{ijt}^2)$$

$$v_i^t\big(k_i^t(1-pc_{ij}^t)+k_i^{'t}pc_{ij}^t\big)-v_j^t\big(k_j^t(1-pc_{ij}^t)+k_j^{'t}pc_{ij}^t\big)\leqslant \Big(\big(\overline{v}_i^t|k_i^t|+\overline{v}_j^t|k_j^t|\big)(1-pc_{ij}^t)+\big(\overline{v}_i^t|k_i^{'t}|+\overline{v}_j^t|k_j^{'t}|\big)pc_{ij}^t\Big)(1-\delta_{ijt}^2)$$

$$-v_i^t\big(\cos(m_i^{*t})(1-pc_{ij}^t)-\sin(m_i^{*t})pc_{ij}^t\big)+v_j^t\big(\cos(m_j^{*t})(1-pc_{ij}^t)-\sin(m_j^{*t})pc_{ij}^t\big)\leqslant (\overline{v}_i^t-\overline{v}_j^t)(1-\delta_{ijt}^3)$$

$$v_i^t\big(h_i^t(1-pc_{ij}^t)+h_i^{'t}pc_{ij}^t\big)-v_j^t\big(h_j^t(1-pc_{ij}^t)+h_j^{'t}pc_{ij}^t\big)\leqslant \Big(\big(\overline{v}_i^t|h_i^t|+\overline{v}_j^t|h_j^t|\big)(1-pc_{ij}^t)+\big(\overline{v}_i^t|h_i^{'t}|+\overline{v}_j^t|h_j^{'t}|\big)pc_{ij}^t\Big)(1-\delta_{ijt}^3)$$

$$-v_i^t\big(\cos(m_i^{*t})(1-pc_{ij}^t)-\sin(m_i^{*t})pc_{ij}^t\big)+v_j^t\big(\cos(m_j^{*t})(1-pc_{ij}^t)-\sin(m_j^{*t})pc_{ij}^t\big)\leqslant (\overline{v}_i^t-\overline{v}_j^t)(1-\delta_{ijt}^4)$$

$$-v_i^t\big(k_i^t(1-pc_{ij}^t)+k_i^{'t}pc_{ij}^t\big)+v_j^t\big(k_j^t(1-pc_{ij}^t)+k_j^{'t}pc_{ij}^t\big)\leqslant \Big(\big(\overline{v}_i^t|k_i^t|+\overline{v}_j^t|k_j^t|\big)(1-pc_{ij}^t)+\big(\overline{v}_i^t|k_i^{'t}|+\overline{v}_j^t|k_j^{'t}|\big)pc_{ij}^t\Big)(1-\delta_{ijt}^4).$$

If $pc_{ij}^t = 0$, the first four cases are considered in each set of constraints, otherwise, the last four cases must be considered. Notice that the bounds M of the initial constraints are included, and in the cases where the two different bounds take place (i.e. when terms h, k, h' and k' are in the constraints), these bounds are multiplied by pc and $1 - pc$ for taking into account the corresponding bound.

Then, the initial eight cases are reduced to four, and consequently, the number of δ variables will be reduced to four as well, from where it results,

$$\delta_{ijt}^1 + \delta_{ijt}^2 + \delta_{ijt}^3 + \delta_{ijt}^4 = 1.$$

3.3.2 Dimension reduction in updating position constraints

In the constraints for updating the aircraft positions was considered for time periods t and $t-1$ then, the dimensions of the model are increased. For having a tighter model, the assumptions make in Section 3.2.4 are conceptually changed. Notice that what happened in the past does not influence the present, i.e., only the earlier or later arrival in the present time period $t \in \mathcal{T}$ is important.

As two different cases are considered (earlier or later arrival, see Fig. 3.5), only one 0-1 variable γ_f^t has to be considered. First of all, an earlier or later arrival case has to be detected by using the terms $\sum_{\ell=1}^t d_f^{*\ell}$ and $\sum_{\ell=1}^t d_f^{\ell}$, i.e., the predicted and final covered distances for aircraft $f \in \mathcal{F}$ in the given time period $t \in \mathcal{T}$. The logic relation that will be considered is that $\gamma_f^t = 0$ if and only if a later arrival to the predicted position in time period $t \in \mathcal{T}$ happens. Then, two implications have to be modeled, in the two senses. For the implication $\gamma_f^t = 0 \Rightarrow \sum_{\ell=1}^t d_f^{\ell} \leqslant \sum_{\ell=1}^t d_f^{*\ell}$, the following constraints must be added,

$$\sum_{\ell=1}^{t} d_f^{\ell} - \sum_{\ell=1}^{t} d_f^{*\ell} \leqslant M\gamma_f^t,$$

where $M = \frac{d_f^{*t}}{div}$ is the upper bound of $\sum_{\ell=1}^t d_f^{\ell} - \sum_{\ell=1}^t d_f^{*\ell}$.

It is easy to prove that if $\gamma_f^t = 0$ then $\sum_{\ell=1}^t d_f^{\ell} \leqslant \sum_{\ell=1}^t d_f^{*\ell}$ and, otherwise, nothing happens.

For the other sense of the logic relation, i.e., $\sum_{\ell=1}^t d_f^{\ell} \leqslant \sum_{\ell=1}^t d_f^{*\ell} \Rightarrow \gamma_f^t = 0$, let

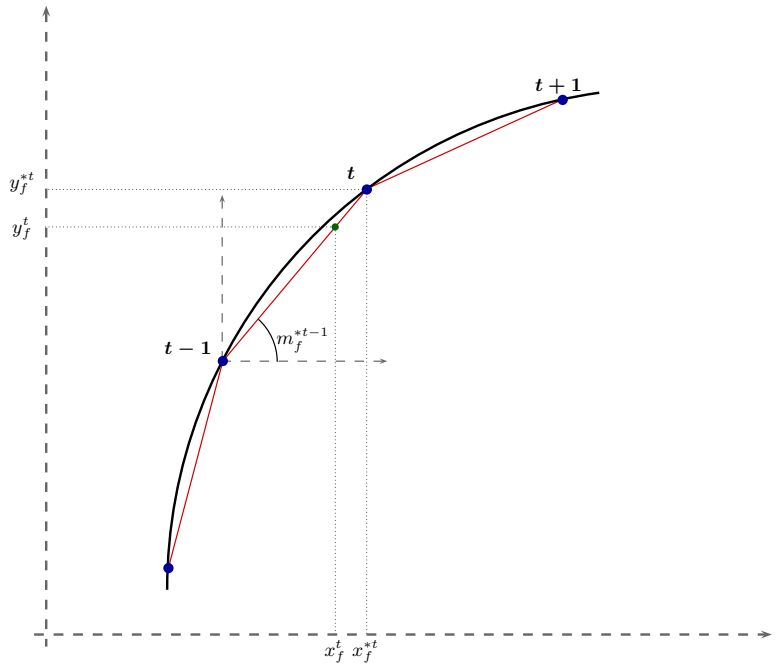

(a) Later arrival case

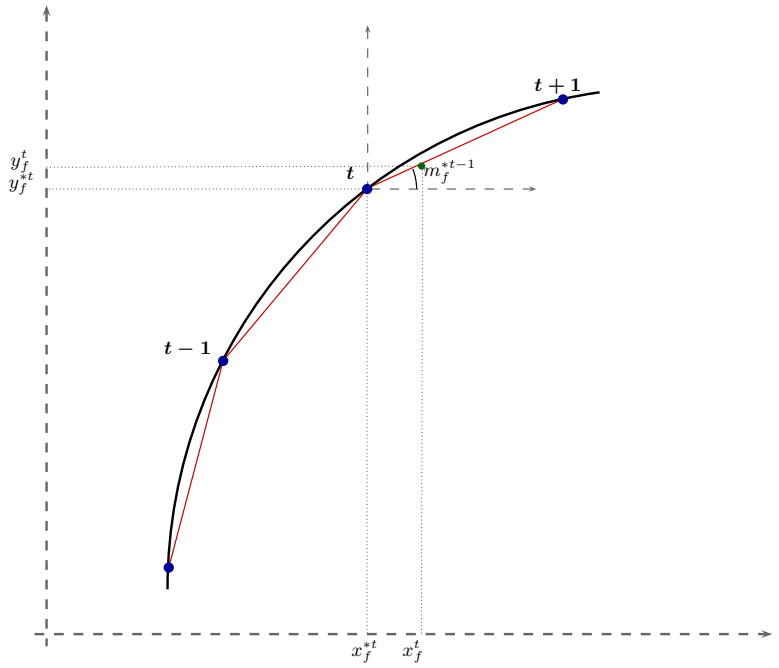

(b) Earlier arrival case

Figure 3.5: Cases of arrival to the predicted position in the predicted time $t \in \mathcal{T}$

the following constraints be as follows,

$$\sum_{\ell=1}^{t} d_f^{\ell} - \sum_{\ell=1}^{t} d_f^{*\ell} - \varepsilon \geqslant (M - \varepsilon)(1 - \gamma_f^t),$$

where $M = -\frac{d_f^{*t}}{div}$ is the lower bound of $\sum_{\ell=1}^{t} d_f^{\ell} - \sum_{\ell=1}^{t} d_f^{*\ell} - \varepsilon$ and ε is an enough positive number.

It can be proved that if $\sum_{\ell=1}^{t} d_f^{\ell} \leqslant \sum_{\ell=1}^{t} d_f^{*\ell}$ then $\gamma_f^t = 0$.

Then, the two senses have been modeled as linear constraints.

Earlier arrival positions In the case of earlier arrival to the predicted point in time period $t \in \mathcal{T}$, the new positions (abscissa and ordinate) will be as follows,

$$x_f^t = x_f^{*t} + \Big(\sum_{\ell=1}^{t} d_f^{\ell} - \sum_{\ell=1}^{t} d_f^{*\ell}\Big)\cos(m_f^{*t})$$
$$y_f^t = y_f^{*t} + \Big(\sum_{\ell=1}^{t} d_f^{\ell} - \sum_{\ell=1}^{t} d_f^{*\ell}\Big)\sin(m_f^{*t}).$$

In order to have the appropriate effect of these constraints, for $\gamma_f^t = 1$, four additional constraints are needed as follows,

$$x_f^t - x_f^{*t} - \Big(\sum_{\ell=1}^{t} d_f^{\ell} - \sum_{\ell=1}^{t} d_f^{*\ell}\Big)\cos(m_f^{*t}) \leqslant M_1(1 - \gamma_f^t)$$
$$x_f^t - x_f^{*t} - \Big(\sum_{\ell=1}^{t} d_f^{\ell} - \sum_{\ell=1}^{t} d_f^{*\ell}\Big)\cos(m_f^{*t}) \geqslant M_2(1 - \gamma_f^t)$$
$$y_f^t - y_f^{*t} - \Big(\sum_{\ell=1}^{t} d_f^{\ell} - \sum_{\ell=1}^{t} d_f^{*\ell}\Big)\sin(m_f^{*t}) \leqslant M_3(1 - \gamma_f^t)$$
$$y_f^t - y_f^{*t} - \Big(\sum_{\ell=1}^{t} d_f^{\ell} - \sum_{\ell=1}^{t} d_f^{*\ell}\Big)\sin(m_f^{*t}) \geqslant M_4(1 - \gamma_f^t),$$

where $M_1 = \overline{x}_f^t - x_f^{*t} + \frac{d_f^{*t}}{div}$ and $M_2 = \underline{x}_f^t - x_f^{*t} - \frac{d_f^{*t}}{div}$ are, respectively, the upper and lower bounds of

$$x_f^t - x_f^{*t} - \Big(\sum_{\ell=1}^{t} d_f^{\ell} - \sum_{\ell=1}^{t} d_f^{*\ell}\Big)\cos(m_f^{*t})$$

and $M_3 = \overline{y}_f^t - y_f^{*t} + \frac{d_f^{*t}}{div}$ and $M_4 = \underline{y}_f^t - y_f^{*t} - \frac{d_f^{*t}}{div}$ are, respectively, the upper and lower bounds of

$$y_f^t - y_f^{*t} - \Big(\sum_{\ell=1}^{t} d_f^{\ell} - \sum_{\ell=1}^{t} d_f^{*\ell}\Big)\sin(m_f^{*t}).$$

Later arrival positions For the later arrival to the predicted point in time period $t \in \mathcal{T}$, the new positions will be as follows,

$$x_f^t = x_f^{*t-1} + \Big(\sum_{\ell=1}^{t} d_f^{\ell} - \sum_{\ell=1}^{t-1} d_f^{*\ell}\Big)\cos(m_f^{*t-1})$$
$$y_f^t = y_f^{*t-1} + \Big(\sum_{\ell=1}^{t} d_f^{\ell} - \sum_{\ell=1}^{t-1} d_f^{*\ell}\Big)\sin(m_f^{*t-1}).$$

In order to have the appropriate effect of these constraints for $\gamma_f^t = 0$, four additional constraints are needed as follows,

$$x_f^t - x_f^{*t-1} - \Big(\sum_{\ell=1}^{t} d_f^{\ell} - \sum_{\ell=1}^{t-1} d_f^{*\ell}\Big)\cos(m_f^{*t-1}) \leqslant M_1\gamma_f^t$$
$$x_f^t - x_f^{*t-1} - \Big(\sum_{\ell=1}^{t} d_f^{\ell} - \sum_{\ell=1}^{t-1} d_f^{*\ell}\Big)\cos(m_f^{*t-1}) \geqslant M_2\gamma_f^t$$
$$y_f^t - y_f^{*t-1} - \Big(\sum_{\ell=1}^{t} d_f^{\ell} - \sum_{\ell=1}^{t-1} d_f^{*\ell}\Big)\sin(m_f^{*t-1}) \leqslant M_3\gamma_f^t$$
$$y_f^t - y_f^{*t-1} - \Big(\sum_{\ell=1}^{t} d_f^{\ell} - \sum_{\ell=1}^{t-1} d_f^{*\ell}\Big)\sin(m_f^{*t-1}) \geqslant M_4\gamma_f^t,$$

where $M_1 = \overline{x}_f^t - x_f^{*t-1} + d_f^{*t}$ and $M_2 = \underline{x}_f^t - x_f^{*t-1} - d_f^{*t}$ are, respectively, the upper and lower bounds of

$$x_f^t - x_f^{*t-1} - \Big(\sum_{\ell=1}^{t} d_f^{\ell} - \sum_{\ell=1}^{t-1} d_f^{*\ell}\Big)\cos(m_f^{*t-1})$$

and $M_3 = \overline{y}_f^t - y_f^{*t-1} + d_f^{*t}$ and $M_4 = \underline{y}_f^t - y_f^{*t-1} - d_f^{*t}$ are, respectively, the upper and lower bounds of

$$y_f^t - y_f^{*t-1} - \Big(\sum_{\ell=1}^{t} d_f^{\ell} - \sum_{\ell=1}^{t-1} d_f^{*\ell}\Big)\sin(m_f^{*t-1}).$$

In order to have affordable computational results for the model, once these new

constraints of equality (divided in two inequalities) are introduced, an enough positive number ε can be considered in the constraints allowing the variables x_f^t and y_f^t to be in the intervals $(x_f^t - \varepsilon, x_f^t + \varepsilon)$ and $(y_f^t - \varepsilon, y_f^t + \varepsilon)$, respectively.

3.3.3 The VCTP formulation

Now, the full formulation for the VCTP model is presented below, including all the aspects that have been studied above.

$$\min w_1 \sum_{f\in\mathcal{F}}\sum_{t\in\mathcal{T}}\left(\frac{c_{ft}^{a^+}\,a_f^{t+}}{\overline{a}_f^t - \underline{a}_f^t} + \frac{c_{ft}^{a^-}\,a_f^{t-}}{\overline{a}_f^t - \underline{a}_f^t}\right) + w_2 \sum_{f\in\mathcal{F}}\sum_{t\in\mathcal{T}} c_{ft}^d \beta_f^t \tag{3.5}$$

subject to $\forall f \in \mathcal{F}, \forall t \in \mathcal{T} : t = \{t_f^d + 1, \ldots, t_f^r\}$

$$\underline{v}_f^t \leqslant \quad v_f^{t-1} + a_f^t I_t \quad \leqslant \overline{v}_f^t \tag{3.6a}$$

$$\underline{a}_f^t \leqslant \qquad a_f^t \qquad\quad \leqslant \overline{a}_f^t \tag{3.6b}$$

$\forall f \in \mathcal{F}, \forall t \in \mathcal{T} : t = \{t_f^d + 1, \ldots, t_f^r\}$

$$d_f^t = v_f^{t-1} I_t + \frac{1}{2}(a_f^{t+} - a_f^{t-}) I_t^2 \tag{3.7}$$

$\forall i, j \in \mathcal{F} : i < j \wedge p_{ij} = 0, \forall t \in \mathcal{T} : t = \big\{ \max\{t_i^d, t_j^d\} + 1, \ldots, \min\{t_i^r, t_j^r\} - 1\big\}$

$$v_i^t\big(\cos(m_i^{*t})(1 - pc_{ij}^t) - \sin(m_i^{*t}) pc_{ij}^t\big) - v_j^t\big(\cos(m_j^{*t})(1 - pc_{ij}^t) - \sin(m_j^{*t}) pc_{ij}^t\big) \leqslant (\overline{v}_i^t + \overline{v}_j^t)(1 - \delta_{ijt}^1) \tag{3.8a}$$

$$-v_i^t\big(h_i^t(1 - pc_{ij}^t) + h_i'^t pc_{ij}^t\big) + v_j^t\big(h_j^t(1 - pc_{ij}^t) + h_j'^t pc_{ij}^t\big) \leqslant \Big(\big(\overline{v}_i^t|h_i^t| + \overline{v}_j^t|h_j^t|\big)(1 - pc_{ij}^t) + \big(\overline{v}_i^t|h_i'^t| + \overline{v}_j^t|h_j'^t|\big) pc_{ij}^t\Big)(1 - \delta_{ijt}^1) \tag{3.8b}$$

$$v_i^t\big(\cos(m_i^{*t})(1 - pc_{ij}^t) - \sin(m_i^{*t}) pc_{ij}^t\big) - v_j^t\big(\cos(m_j^{*t})(1 - pc_{ij}^t) - \sin(m_j^{*t}) pc_{ij}^t\big) \leqslant (\overline{v}_i^t + \overline{v}_j^t)(1 - \delta_{ijt}^2) \tag{3.8c}$$

$$v_i^t\big(k_i^t(1-pc_{ij}^t)+k_i^{'t}pc_{ij}^t\big)-v_j^t\big(k_j^t(1-pc_{ij}^t)+k_j^{'t}pc_{ij}^t\big)\leqslant \Big(\big(\overline{v}_i^t|k_i^t|+\overline{v}_j^t|k_j^t|\big)(1-pc_{ij}^t)+\big(\overline{v}_i^t|k_i^{'t}|+\overline{v}_j^t|k_j^{'t}|\big)pc_{ij}^t\Big)(1-\delta_{ijt}^2) \quad (3.8d)$$

$$-v_i^t\big(\cos(m_i^{*t})(1-pc_{ij}^t)-\sin(m_i^{*t})pc_{ij}^t\big)+v_j^t\big(\cos(m_j^{*t})(1-pc_{ij}^t)-\sin(m_j^{*t})pc_{ij}^t\big)\leqslant (\overline{v}_i^t+\overline{v}_j^t)(1-\delta_{ijt}^3) \quad (3.8e)$$

$$v_i^t\big(h_i^t(1-pc_{ij}^t)+h_i^{'t}pc_{ij}^t\big)-v_j^t\big(h_j^t(1-pc_{ij}^t)+h_j^{'t}pc_{ij}^t\big)\leqslant \Big(\big(\overline{v}_i^t|h_i^t|+\overline{v}_j^t|h_j^t|\big)(1-pc_{ij}^t)+\big(\overline{v}_i^t|h_i^{'t}|+\overline{v}_j^t|h_j^{'t}|\big)pc_{ij}^t\Big)(1-\delta_{ijt}^3) \quad (3.8f)$$

$$-v_i^t\big(\cos(m_i^{*t})(1-pc_{ij}^t)-\sin(m_i^{*t})pc_{ij}^t\big)+v_j^t\big(\cos(m_j^{*t})(1-pc_{ij}^t)-\sin(m_j^{*t})pc_{ij}^t\big)\leqslant (\overline{v}_i^t+\overline{v}_j^t)(1-\delta_{ijt}^4) \quad (3.8g)$$

$$-v_i^t\big(k_i^t(1-pc_{ij}^t)+k_i^{'t}pc_{ij}^t\big)+v_j^t\big(k_j^t(1-pc_{ij}^t)+k_j^{'t}pc_{ij}^t\big)\leqslant \Big(\big(\overline{v}_i^t|k_i^t|+\overline{v}_j^t|k_j^t|\big)(1-pc_{ij}^t)+\big(\overline{v}_i^t|k_i^{'t}|+\overline{v}_j^t|k_j^{'t}|\big)pc_{ij}^t\Big)(1-\delta_{ijt}^4) \quad (3.8h)$$

$$\delta_{ijt}^1+\delta_{ijt}^2+\delta_{ijt}^3+\delta_{ijt}^4=1 \quad (3.8i)$$

$\forall f\in\mathcal{F},\forall t\in\mathcal{T}: t=\{t_f^d+1,\ldots,t_f^r\}$

$$\sum_{\ell=1}^{t}d_f^{\ell}-\sum_{\ell=1}^{t}d_f^{*\ell}\leqslant\frac{d_f^{*t}}{div}\gamma_f^t \quad (3.9a)$$

$$\sum_{\ell=1}^{t}d_f^{\ell}-\sum_{\ell=1}^{t}d_f^{*\ell}-\varepsilon\geqslant(-\frac{d_f^{*t}}{div}-\varepsilon)(1-\gamma_f^t) \quad (3.9b)$$

$$x_f^t-x_f^{*t}-\Big(\sum_{\ell=1}^{t}d_f^{\ell}-\sum_{\ell=1}^{t}d_f^{*\ell}\Big)\cos(m_f^t)\leqslant(\overline{x}_f^t-x_f^{*t}+\frac{d_f^{*t}}{div})(1-\gamma_f^t) \quad (3.9c)$$

$$x_f^t-x_f^{*t}-\Big(\sum_{\ell=1}^{t}d_f^{\ell}-\sum_{\ell=1}^{t}d_f^{*\ell}\Big)\cos(m_f^{*t})\geqslant(\underline{x}_f^t-x_f^{*t}-\frac{d_f^{*t}}{div})(1-\gamma_f^t) \quad (3.9d)$$

$$y_f^t-y_f^{*t}-\Big(\sum_{\ell=1}^{t}d_f^{\ell}-\sum_{\ell=1}^{t}d_f^{*\ell}\Big)\sin(m_f^{*t})\leqslant(\overline{y}_f^t-y_f^{*t}+\frac{d_f^{*t}}{div})(1-\gamma_f^t) \quad (3.9e)$$

$$y_f^t - y_f^{*t} - \Big(\sum_{\ell=1}^{t} d_f^{\ell} - \sum_{\ell=1}^{t} d_f^{*\ell}\Big)\sin(m_f^{*t}) \geqslant (\underline{y}_f^t - y_f^{*t} - \frac{d_f^{*t}}{div})(1-\gamma_f^t) \tag{3.9f}$$

$$x_f^t - x_f^{*t-1} - \Big(\sum_{\ell=1}^{t} d_f^{\ell} - \sum_{\ell=1}^{t-1} d_f^{*\ell}\Big)\cos(m_f^{*t-1}) \leqslant (\overline{x}_f^t - x_f^{*t-1} + d_f^{*t})\gamma_f^t \tag{3.9g}$$

$$x_f^t - x_f^{*t-1} - \Big(\sum_{\ell=1}^{t} d_f^{\ell} - \sum_{\ell=1}^{t-1} d_f^{*\ell}\Big)\cos(m_f^{*t-1}) \geqslant (\underline{x}_f^t - x_f^{*t-1} - d_f^{*t})\gamma_f^t \tag{3.9h}$$

$$y_f^t - y_f^{*t-1} - \Big(\sum_{\ell=1}^{t} d_f^{\ell} - \sum_{\ell=1}^{t-1} d_f^{*\ell}\Big)\sin(m_f^{*t-1}) \leqslant (\overline{y}_f^t - y_f^{*t-1} + d_f^{*t})\gamma_f^t \tag{3.9i}$$

$$y_f^t - y_f^{*t-1} - \Big(\sum_{\ell=1}^{t} d_f^{\ell} - \sum_{\ell=1}^{t-1} d_f^{*\ell}\Big)\sin(m_f^{*t-1}) \geqslant (\underline{y}_f^t - y_f^{*t-1} - d_f^{*t})\gamma_f^t \tag{3.9j}$$

$$\sum_{\ell=1}^{t} d_f^{\ell} - \sum_{\ell=1}^{t} d_f^{*\ell} \leqslant \beta_f^t \tag{3.10a}$$

$$\sum_{\ell=1}^{t} d_f^{*\ell} - \sum_{\ell=1}^{t} d_f^{\ell} \leqslant \beta_f^t \tag{3.10b}$$

$\forall f \in \mathcal{F}, \forall t \in \mathcal{T} : t = \{t_f^d + 1, \ldots, t_f^r - 1\}$

$$\underline{d}_f^t = d_f^{*t} - \frac{d_f^{*t}}{div} \leqslant \quad d_f^t \quad \leqslant d_f^{*t} + \frac{d_f^{*t}}{div} = \overline{d}_f^t \tag{3.11a}$$

$$\underline{x}_f^t = x_f^{*t} - \frac{d_f^{*t}}{div}\cos(m_f^{*t-1}) \leqslant \quad x_f^t \quad \leqslant x_f^{*t} + \frac{d_f^{*t}}{div}\cos(m_f^{*t}) = \overline{x}_f^t \tag{3.11b}$$

$$\underline{y}_f^t = y_f^{*t} - \frac{d_f^{*t}}{div}\sin(m_f^{*t-1}) \leqslant \quad y_f^t \quad \leqslant y_f^{*t} + \frac{d_f^{*t}}{div}\sin(m_f^{*t}) = \overline{y}_f^t \tag{3.11c}$$

$\forall f \in \mathcal{F}$

$$d_f^{t_f^d} = 0 \tag{3.12a}$$

$$x_f^{t_f^d} = x_f^{*t_f^d} \tag{3.12b}$$

$$x_f^{t_f^r} = x_f^{*t_f^r} \tag{3.12c}$$

$$y_f^{t_f^d} = y_f^{*t_f^d} \tag{3.12d}$$

$$y_f^{t_f^r} = y_f^{*t_f^r} \tag{3.12e}$$

$\forall f \in \mathcal{F}, \forall t \in \mathcal{T} : t = \{t_f^d, \ldots, t_f^r\}$

$$x_f^t, y_f^t, a_f^t \in \mathbb{R} \tag{3.13a}$$

$$v_f^t, a_f^{t+}, a_f^{t-}, d_f^t, \beta_f^t \in \mathbb{R}^+ \tag{3.13b}$$

$\forall i, j \in \mathcal{F} : i < j \wedge p_{ij} = 0, \forall t \in \mathcal{T} : t = \left\{ \max\{t_i^d, t_j^d\} + 1, \ldots, \min\{t_i^r, t_j^r\} - 1 \right\}$

$$\delta_{ijt}^1, \delta_{ijt}^2, \delta_{ijt}^3, \delta_{ijt}^4 \in \{0, 1\} \tag{3.13c}$$

$\forall f \in \mathcal{F}, \forall t \in \mathcal{T} : t = \{t_f^d, \ldots, t_f^r\}$:

$$\gamma_f^t \in \{0, 1\} \tag{3.13d}$$

The objective function (3.5) gives the optimization criterion for the model. It has two terms, that were explained in section (3.2.5), where the values of the w_1 and w_2 emphasizes one term over the other. If the second term of the objective function is contemplated, it must be accompanied by constraints (3.10). Constraints (3.6) avoid the velocity and the acceleration to be bigger or smaller than the upper or lower bound, respectively. Constraints (3.7) update the covered distance by an aircraft after the changes in its configuration in time period $t \in \mathcal{T}$. Constraints (3.8) detect and solve the conflicts in the airspace, distinguishing between the four cases considered in Section 3.3.1. (Notice that anomalous cases are contemplated by using parameter pc_{ij}^t). Constraints (3.9) update the positions in each time period $t \in \mathcal{T}$, according to the previous changes in velocity made until the current time period, and after the dimension reduction shown in Section 3.3.2. Constraints (3.10) transform the objective function considered in Section 3.2.5 in a linear function, since it minimizes an absolute value. Constraints (3.11) force some variables to be into the fixed bounds as was described in Section 3.2.4. Constraints (3.12) fix the variables of positions x and y and the initial distance d to the values in the predicted configuration, forcing aircraft to arrive to the last point of the trajectory in the predicted time. Finally, constraints (3.13) give the variables' type.

Model dimensions

Table 3.1 shows the summary of the recount of all variables and constraints for the VCTP model. The total number of variables in the model depends on the objective function

Table 3.1: Dimensions of the VCTP model

v_f^t	$\sum_{f\in\mathcal{F}}(t_f^r - t_f^d + 1)$
a_f^{t+}	$\sum_{f\in\mathcal{F}}(t_f^r - t_f^d + 1)$
a_f^{t-}	$\sum_{f\in\mathcal{F}}(t_f^r - t_f^d + 1)$
x_f^t	$\sum_{f\in\mathcal{F}}(t_f^r - t_f^d + 1)$
y_f^t	$\sum_{f\in\mathcal{F}}(t_f^r - t_f^d + 1)$
d_f^t	$\sum_{f\in\mathcal{F}}(t_f^r - t_f^d + 1)$
β_f^t	$\sum_{f\in\mathcal{F}}(t_f^r - t_f^d + 1)$
γ_f^t	$\sum_{f\in\mathcal{F}}(t_f^r - t_f^d + 1)$
δ_{ijz}^n	$4\sum_{i<j\in\mathcal{F}}\big(\min\{t_i^r, t_j^r\} - \max\{t_i^d, t_j^d\} - 1\big)$

(a) Number of variables

C. (3.6)	$2\sum_{f\in\mathcal{F}}(t_f^r - t_f^d + 1)$
C. (3.7)	$\sum_{f\in\mathcal{F}}(t_f^r - t_f^d + 1)$
C. (3.8)	$9\sum_{i<j\in\mathcal{F}}\big(\min\{t_i^r, t_j^r\} - \max\{t_i^d, t_j^d\} - 1\big)$
C. (3.9)	$10\sum_{f\in\mathcal{F}}(t_f^r - t_f^d)$
C. (3.10)	$2\sum_{f\in\mathcal{F}}(t_f^r - t_f^d + 1)$
C. (3.11)	$6\sum_{f\in\mathcal{F}}(t_f^r - t_f^d)$
C. (3.12)	$5F$

(b) Number of constraints

of choice, since if the second term is added, two additional constraints must be added. Then, the total number of variables will be the sum of the corresponding values shown in the table.

The table also shows the number of constraints for the VCTP model. (Notice that it also depends on the objective function of choice, and it will be the sum of the corresponding values of the table)

3.3.4 Computational experience

In this section some computational experience is presented. First of all, notice that the model is based on mixed 0-1 nonlinear optimization (see constraints (3.8b), (3.8d), (3.8f) and (3.8h)) unlike the VAC model presented in the previous chapter. For solving this model the first step was to implement it by using the model generator engine GAMS [41] but it cannot work due to the square roots in the nonlinear inequalities since they could have negative argument. After solving this inconvenience the next one that was found is the existence of fractions that could have null denominators. However, null denominators were impossible to appear, since these ones were detected in the preprocessing phase, but

in despite of the previous detection, the solver did not continue with the optimization.

After this, the next step was linearizing the model by using Taylor polynomials for the approximation. The nonlinear constraints were approximated by their Taylor polynomial until the first degree (i.e., obtaining linear polynomials). Now, an algorithmic approach is necessary for reaching a good solution near to the optimal one of the initial model, and it is presented in the next section.

Algorithmic approach

For solving iteratively the linearized model, the algorithmic approach described in Almiñana et al. (2007) [6] inspires the work presented in this thesis. It is based on a iterative optimization by starting with the initial configuration and updating the input parameters where the derivatives are centered until a stop criterion is satisfied. However, due to the particular details of the model proposed in this thesis, the algorithm that has been developed differs from the algorithmic presented in [6]. Usually the parameters to be updated are those that are taken the derivative multiplied by a parameter $0 < \lambda < 1$. In the case of the VCTP model, if coordinates x and y are multiplied by λ, the result could be coordinates being out of the trajectory. Then, it was decided in this thesis to update the parameter d and after that, calculating the corresponding x, y and v as following.

First, the nonlinear constraints have to be linearized by using Taylor polynomials, so the new mathematical expression for each inequality ($n = 1, \ldots, 4$) can be expressed as follows,

$$\left\{ C_n + \left(\frac{\partial C_n}{\partial (v^t_{i \text{ and } j}, x^t_{i \text{ and } j}, y^t_{i \text{ and } j})} \right) \right\}_{|(\hat{v}^t_{i \text{ and } j}, \hat{x}^t_{i \text{ and } j}, \hat{y}^t_{i \text{ and } j})} \begin{pmatrix} v_{i \text{ and } j} - \hat{v}^t_{i \text{ and } j} \\ x_{i \text{ and } j} - \hat{x}^t_{i \text{ and } j} \\ y_{i \text{ and } j} - \hat{y}^t_{i \text{ and } j} \end{pmatrix} \leq M(1 - \delta^n_{ijt}).$$

The formal expressions for these nonlinear constraints and their corresponding derivatives with respect to each variable x, y and v are detailed in Appendix B.3, page 169.

The algorithm for the resolution consists of solving the linearized model and, next, updating the parameters with the obtained solution until the difference between the one value of the parameters in the given solution and the last updated parameters is less than the

fixed tolerance of choice. The algorithm starts with the parameters of the initial configuration, i.e., v_f^t, x_f^t, y_f^t. The through steps of the algorithm are as follows.

Step 1. Computing the values of the nonlinear constraints $\forall i, j \in \mathcal{F} : i < j$ and $\forall f \in \mathcal{F}$, such that $v_i^t, v_j^t, x_i^t, x_j^t, y_i^t, y_j^t$ are replaced with $\hat{v}_i^t, \hat{v}_j^t, \hat{x}_i^t, \hat{x}_j^t, \hat{y}_i^t, \hat{y}_j^t$, respectively. In the first iteration, $\hat{v}_i^t = v_i^{*t}, \hat{v}_j^t = v_j^{*t}, \hat{x}_i^t = x_i^{*t}, \hat{x}_j^t = x_j^{*t}, \hat{y}_i^t = y_i^{*t}, \hat{y}_j^t = y_j^{*t}, \hat{d}_f^t$.

Step 2. Solving the mixed zero-one model, where the nonlinear constraints are substituted by its linear approximation. Let d_f^t be the optimal values of the respective variables.

Step 3. Optimality test. If the following condition is satisfied then stop, the quasi-optimal solution has been obtained. Otherwise, go to Step 4.

$$\sum_{f \in \mathcal{F}} \sum_{t \in \mathcal{T}} (d_f^t - \hat{d}_f^t)^2 \leq \varepsilon$$

Step 4.

- Updating the covered distance

$$\hat{d}_f^t := \hat{d}_f^t + \lambda (d_f^t - \hat{d}_f^t) \forall f \in \mathcal{F}, \forall t \in \mathcal{T},$$

  where $0 < \lambda < 1$.

- Updating the acceleration

$$\hat{a}_f^t = \frac{2\hat{d}_f^t - \hat{v}_f^{t-1} I_t}{I_t^2}$$

  by taking $\hat{v}_f^{t_f^d} = v_f^{*t_f^d}$.

- Updating the velocity

$$\hat{v}_f^t = \hat{v}_f^{t-1} + \hat{a}_f^t I_t.$$

- Updating the positions (abscissa y ordinate)

$$\hat{x}_f^t = x_f^{*t-1} + \hat{d}_f^t \cos(m_f^{*t-1}) \qquad \text{if } \sum_{\ell=1}^{t} \hat{d}_f^\ell \leqslant \sum_{\ell=1}^{t} d_f^{*t}$$

$$\hat{x}_f^t = x_f^{*t} + \hat{d}_f^t \cos(m_f^{*t}) \qquad \text{if } \sum_{\ell=1}^{t} \hat{d}_f^\ell > \sum_{\ell=1}^{t} d_f^{*t}$$

$$\hat{y}_f^t = y_f^{*t-1} + \hat{d}_f^t \sin(m_f^{*t-1}) \qquad \text{if } \sum_{\ell=1}^{t} \hat{d}_f^\ell \leqslant \sum_{\ell=1}^{t} d_f^{*t}$$

$$\hat{y}_f^t = y_f^{*t} + \hat{d}_f^t \sin(m_f^{*t}) \qquad \text{if } \sum_{\ell=1}^{t} \hat{d}_f^{\ell} > \sum_{\ell=1}^{t} d_f^{*t}$$

- Updating the pc parameter with the variables $\hat{x}_f^t$.
- Go to Step 1.

When the positions are updated, the covered distance is needed to know if the aircraft arrives earlier or later to the predicted time. In the case of an earlier arrival to the predicted time (i.e., case $\sum_{\ell=1}^{t} \hat{d}_f^{\ell} > \sum_{\ell=1}^{t} d_f^{*t}$), the initial position and the angle in time period t have to be considered. Otherwise (i.e., case $\sum_{\ell=1}^{t} \hat{d}_f^{\ell} \leqslant \sum_{\ell=1}^{t} d_f^{*t}$), the initial position and the angle in the previous time period $t-1$ have to be considered.

Now, the linearized model can be solved by using the optimization engine of choice for mixed 0-1 linear models.

Preprocessing

Before solving the model by using the optimization engine, a carefully preprocessing has to be implemented in order to have a faster resolution. Firstly, all initial configuration parameters are read and then the most fragile part has to be carefully implemented, since it corresponds to the nonlinear expressions and their derivatives with respect to each variable that takes place in the expression. This terms have to be calculated centered in the current term of the iterative resolution by using Taylor approximations, $\hat{x}_i^t, \hat{x}_j^t, \hat{y}_i^t, \hat{y}_j^t, \hat{v}_i^t, \hat{v}_j^t$.

Then, parameter pc_{ijt} is calculated, being 1 if an anomalous case happens between aircraft i and j for $i, j \in \mathcal{F}$ in time period $t \in \mathcal{T}$. When a false conflict occurs, the parameter fc_{ijt} must be 1, and it has to be fixed in preprocessing. Immediately, the parameter p_{ij} will be 1 if based on some particular aspects, the ATC decides that a given pair of aircraft should not be considered in the model. The calculation of this parameters helps to reduce the dimensions of the detection and resolution constraints and, consequently, the number of variables to take into account.

In the preprocessing phase, $\min\{t_i^r, t_j^r\}$ and $\max\{t_i^d, t_j^d\}$ $\forall i, j \in \mathcal{F} : i < j$ are calculated in order to count the number of detection and resolution constraints to be added to the model, since the aircraft positions for i and j are compared in those time periods that the aircraft have in common. Finally, the terms $\hat{d}, \hat{a}, \hat{v}, \hat{x}, \hat{y}$ are updated.

A dynamic assignment of memory was used in the implementation in C++ for reducing the memory consumption, since the following computational experience was made in a standard personal computer and, due to the large dimensions of the model, the execution time could grow excessively. Notice that CPLEX [63], the optimization engine of choice, uses as much memory as possible.

Illustrative instance

Previously to the extensive computational experience that it is reported below in this thesis, the VCTP model has been tested by using the illustrative instance shown in Fig. 3.6 in order to prove that the conflicts are avoided. In this instance, 72 time periods with the same length (10 units) are considered. Notice that different length for the time periods is considered in the model. Each aircraft needs only one time period to reach its next position. There exists several crossing conflicts in order to test the model. For the resolution, only the first term of the objective function (3.5) was taken into account, being $w_1 = 1$ and $w_2 = 0$.

The computational experience was made by using the following HW/SW platform: Intel Core 2DUO P8400, 2.26GHz, 2GB RAM; Microsoft Windows 7 Professional SO. Only one iteration of the Taylor approach is presented for obtaining the results shown in Fig. 3.7, where:

- Several changes in the position have been made. The red circles with a cross denote the position after the resolution.
- The objective function value is 3.4238.
- The execution time has been 238 secs. by using CPLEX [63] (with the default options).

In this instance all conflicts have been detected and pseudo-solved since in fact, the conflicts are not solved by using only one iteration, but if the iterative algorithm continues the final solution will be feasible and will solve the problem. In this particular case, the algorithmic approach does not converge due to the multiplicity solutions in the problem. If different optimal values for the objective function exist, the algorithmic approach based on Taylor polynomials goes from one solution to other different one without reaching a favorable optimality test. Fig. 3.7 helps to test at least that the conflicts are detected.

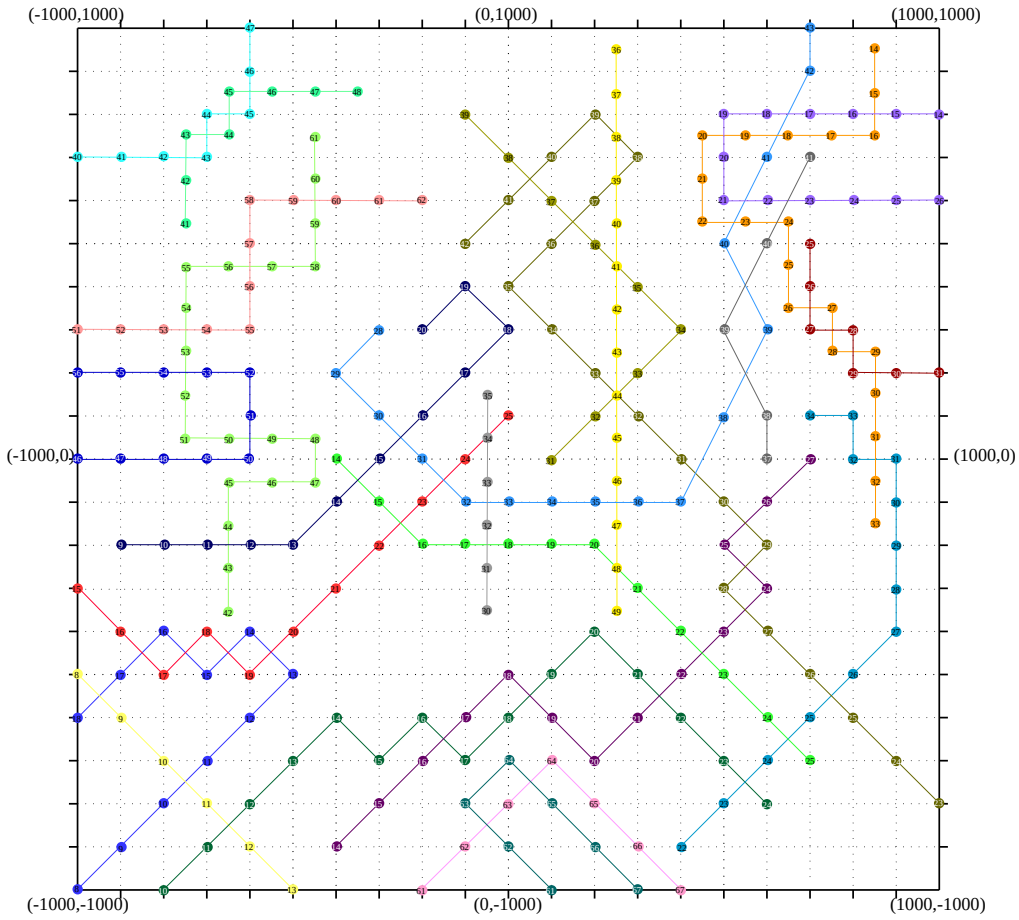

Figure 3.6: Illustrative instance for testing the VCTP model. Initial situation

In this particular case, there are a lot of changes in the signs of the cosines and sines of the angles of motion, and the convergence is not reached. However, in the extensive computational experience all the instances converge to the optimal value as shown below.

Extensive computational experience

Some computational experience for the VCTP model is reported. 25 random simulations are performed for each dimensional case (7 in total) considering 72 time periods in each case, and the result averages are presented. The next technical aspects were taken into account for the simulation:

- The number of aircraft and velocity bounds was fixed.

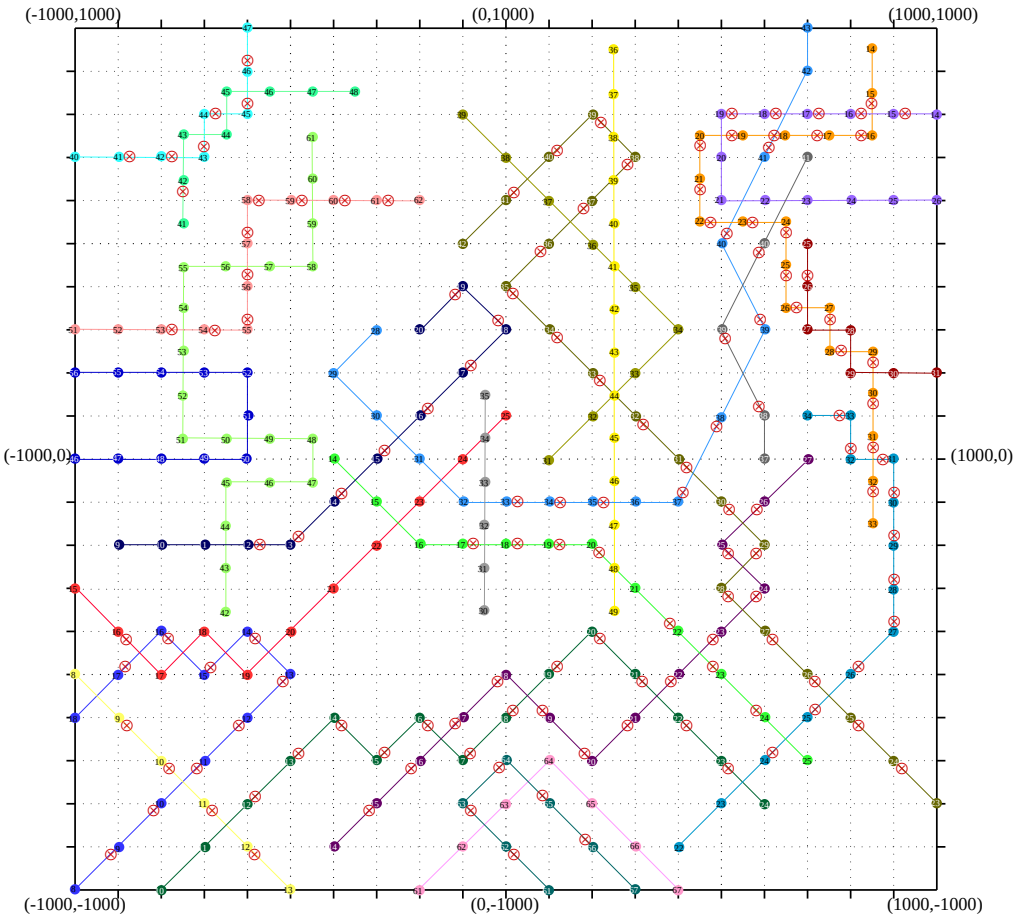

Figure 3.7: Illustrative instance for testing the VCTP model. Resolution after 1st iteration

- The number of airports considered was generated by using an Uniform distribution.
- The departure and arrival airports were generated by using an Uniform distribution.
- The trajectory of each aircraft was generated by considering the total distance between the departure and arrival airports where some angles of motion can change $\pm\frac{\pi}{16}$ or $\pm\frac{\pi}{8}$.
- The final time period for each aircraft is adjusted to force the aircraft to arrive in the predicted time.
- The velocity of each aircraft was generated by using an Uniform distribution between the bounds allowed for each aircraft.
- The number of total time periods is 72.

Table 3.2: Case dimensions

Case	m	n	nel	d	m^*	n^*	nel^*	d^*
C020	3957.9	5053.6	36294.5	0.0018	3915.8	1917.6	33209.8	0.0044
C025	4915.9	7065.4	45199.1	0.0013	4862.7	2381.4	41364.4	0.0036
C030	6007.2	10050.8	54670.5	0.0009	5945.7	2912.4	49997.6	0.0029
C035	7158.7	13508.6	66818.0	0.0007	7087.4	3473.2	61260.4	0.0025
C040	7905.9	15969.4	72116.6	0.0006	7820.2	3829.7	65950.2	0.0022
C045	9715.1	23426.0	93653.8	0.0004	9618.1	4718.4	86128.4	0.0019
C050	10368.2	26459.5	97466.0	0.0004	10262.8	5030.9	89415.7	0.0017

After this simulation, the resolution of the 175 cases of study is described in the following, taking the input parameters for the Taylor approximation, $\lambda = 0.8$ and $\varepsilon = 0.1$.

Table 3.2 shows the average of the dimensions of the model before and after the presolve made by CPLEX, where the headings are as follows:

- *Case*: Case configuration: CAAA denotes number of aircraft (AAA).
- *nit*: Number of iteration in the Taylor approximation.
- m: Number of constraints.
- n: Number of variables.
- nel: Number of non zero elements.
- d: Constraints matrix density.
- m^*, n^*, nel^* and d^*: Number of constraints, variables and constraints matrix, non zero elements and density, respectively, after the preprocessing made by CPLEX [63].

Table 3.3 shows the most important results (averages), where the headings are as follows:

- *Case*: Case configuration: CAAA denotes number of aircraft (AAA).
- *nit*: Number of iterations in the Taylor approximation.
- z_{lp}: Value of the objective function in the continuous linear relaxation.
- z_s: Value of the bound after performing the CPLEX cut identification and appending at node 0

Table 3.3: Computational results ($\lambda = 0.80$)

Case	nit	z_{lp}	z_s	z_{ip}	GAP_{lp}	GAP_s	nb	nn	t_{lp}	t_s	t_{ip}	nc
					0.6848	0.0000						
C020	3.4	0.0013	0.0184	0.0186	0.9291	0.0101	51	29.76	0.76	4.60	9.83	101.8
					1.0000	0.0957						
					0.7999	0.0000						
C025	5.0	0.0010	0.0225	0.0227	0.9572	0.0097	111	28.14	1.37	9.31	19.95	185.4
					1.0000	0.0864						
					0.8630	0.0000						
C030	4.3	0.0011	0.0264	0.0268	0.9599	0.0139	94	34.94	1.52	9.34	24.25	221.0
					1.0000	0.0609						
					0.8781	0.0000						
C035	5.6	0.0017	0.0312	0.0315	0.9463	0.0114	129	42.95	2.42	17.52	54.54	351.8
					1.0000	0.0508						
					0.6406	0.0000						
C040	6.6	0.0036	0.0369	0.0374	0.9038	0.0117	99	36.96	3.23	20.13	54.41	286.6
					1.0000	0.0584						
					0.6084	0.0000						
C045	7.2	0.0045	0.0458	0.0457	0.9011	−0.0009	157	45.18	4.70	31.43	116.55	505.0
					0.9969	0.0449						
					0.8043	0.0000						
C050	5.7	0.0034	0.0486	0.0496	0.9321	0.0189	90	47.58	4.03	27.55	81.05	510.9
					1.0000	0.0893						

- z_{ip}: Value of the objective function for the optimal solution of the problem.
- GAP_{lp}: $\frac{z_{ip}-z_{lp}}{z_{ip}}$
- GAP_s: $\frac{z_{ip}-z_s}{z_{ip}}$
- nb: Number of times that there is branching
- nn: Number of CPLEX branch-and-cut nodes
- t_{lp}: Time (secs.) to obtain the z_{lp} value
- t_s: Time (secs.) to obtain the z_s value.
- t_{ip}: Time (secs.) to obtain the z_{ip} value.
- nc: Total number of cuts performed by CPLEX.

Notice that the minimum, average and maximum GAPs are reported in Table 3.3.

And, finally, Table 3.4 shows the average of the number of cuts that CPLEX executed for solving the VAC model, where the headings are as follows:

- *Case*: Case configuration: CAAA-ZZ denotes number of aircraft (AAA).

Table 3.4: Cuts identified and appended ($\lambda = 0.80$)

Case	nit	Clique	Cover	Implied	Flow	MIR	Zero-Half	Gomory	Total
C020	3.4	0.0	0.2	3.2	71.2	0.6	0.0	26.6	101.8
C025	5.0	0.0	0.1	12.5	119.3	20.6	0.0	33.0	185.4
C030	4.3	0.0	0.2	31.2	113.2	51.2	0.0	25.2	221.0
C035	5.6	0.0	0.3	28.6	235.2	39.0	0.0	48.8	351.8
C040	6.6	0.0	0.6	33.6	183.2	34.3	0.0	35.0	286.6
C045	7.2	0.0	0.6	83.9	267.5	111.5	0.0	41.4	505.0
C050	5.7	0.0	0.3	31.6	363.6	60.7	0.0	54.7	510.9

- *nit*: Number of iterations in the Taylor approximation.
- Clique: Number of clique cuts.
- Cover: Number of Cover cuts.
- Implied: Number of Implied cuts.
- Flow: Number of Flow cuts.
- MIR: Number of Mixed Integer Rounding cuts.
- Zero-Half: Number of Zero-half cuts.
- Gomory: Number of Gomory cuts.
- Total: Total number of cuts.

As it happens in other computational reports on different problems that we are aware of, the CPLEX Gomory cuts are very strong compared with the other cuts that have been identified. Notice that neither clique nor Zero-Half cuts have been identified, what is not a surprise giving the structure of the model

In Appendix B.4, page 179, more detailed tables for the particular cases of study are shown. The whole computational experience is presented in the extended version of the thesis in the CD enclosed.

3.4 Local Branching and VNDS

As it has been shown above, the execution time for solving the VCTP model is not so large for medium dimensional problems. However, the model should be applied in a big

airspace. Unfortunately, the resolution time could be very large for this purpose, so, it is not affordable to apply the model in short or medium terms. Due to the exponential complexity of the Branch and Bound (B&B) and Branch and Cut (B&C) schemes in MILP and the large dimensions of the model, CPLEX [63] is not able to get the optimal solution in an affordable time for very large problems.

In view of the situation, one alternative consists of implementing a metaheuristic scheme able to get a good solution in an affordable time. The characteristics of this problem make the optimality to be aside, being the feasibility of the solution the first goal. With metaheuristic schemes good upper bounds for the optimal solution in the case of minimazing the objective function can be obtained, but the quality of the bound has to be measure by using another scheme that offers good lower bounds. It has been proved that Lagrangian Relaxation schemes offer good lower bounds for the optimal solution. In this section the main objective will be to implement a metaheuristic scheme able to obtain good solutions in reasonable time. The scheme of choice has been "Variable Neighbourhood Search" (VNS) combined with "Local Branching" (LB) presented in a recent published work by Lazic et al. (2010) [72], so called "Variable Neighbourhood Decomposition Search" (VNDS).

Fischetti and Lodi (2003) [38] propose the LB scheme for solving heuristically MILP problems, provided that the total time allocated to solve a given instance is not sufficient for obtaining the optimal solution or for proving its optimality. This situation is very common for $\mathcal{NP}$-Hard problems. Let P be the problem

$$
\begin{aligned}
&(P)\ \min c^T x \\
&\quad Ax \geqslant b \\
&\quad x_j \in \{0,1\} && \forall j \in \mathcal{B} \neq \emptyset \\
&\quad x_j \geqslant 0 && \forall j \in \mathcal{C}.
\end{aligned}
$$

The main observation is that the neighbourhood of a feasible MILP solution often contains better solutions (if the rectangular distance is considered). Very often, Local Branching is used as a heuristic for improving an incumbent solution. Let x' be the incumbent solution, x^* the best known solution found and $\varepsilon > 0$ a small non-negative real number,

according to the notation in [72], the LB solves the following subproblem:

$$
\begin{aligned}
(P') \min\ & c^T x \\
& Ax \geqslant b \\
& \delta(\mathcal{B}, x, x') \leqslant k \\
& c^T x \leqslant c^T x^* - \varepsilon \\
& x_j \in \{0,1\} && \forall j \in \mathcal{B} \neq \emptyset \\
& x_j \geqslant 0 && \forall j \in \mathcal{C}
\end{aligned}
$$

where $\delta(\mathcal{B}, x, x') \leqslant k$ is the distance of the solutions x and x' in the index contained in $\mathcal{B}$, i.e., $\sum_{b \in \mathcal{B}} |x_b - x'_b|$. Let X be the solution space of P, then, the neighbourhood structures $\{\mathcal{N}_k : k = k_{min}, \ldots, k_{max}\}$ where $1 \leqslant k_{min} \leqslant k_{max} \leqslant |\mathcal{B}|$ can be defined if the distance δ between any two solutions $x, y \in X$ is known. The set of all solutions in the kth neighbourhood of $x \in X$ is denoted as $\mathcal{N}_k = \{y \in Y : \delta(\mathcal{B}, x, y) \leqslant k\}$. Then, $\delta(\mathcal{B}, x, x') \leqslant k$ represents the space of solutions of the neighbourhood $\mathcal{N}_k$.

The LB combines local search with a MILP solver. After the first feasible solution x' is found (if it exists), the first subproblem P' for $k = k_{min}$ is solved (k_{min} is the minimum size of the neighbourhood, it is an input parameter). After that, if the best solution found is improved, a new subproblem is generated and solved, and the process is repeated iteratively. Diversification strategies can also be used for improving the scheme. See [38] for more details.

Hansen and Mladenovic (2006) [50] introduce a modification in the LB scheme, by using it in the VNS philosophy and, then, presenting the "Variable Neighbourhood Search Branching" scheme (VNSB). The VNS philosophy consists of exploring and changing the neighbourhoods of a given solution with the aim of reaching zones in the solution space that can improve the incumbent solution. The VNSB scheme adds constraints to the initial problem P but the neighbourhoods are changed in a systematic manner following the main ideas of the "Variable Neighbourhood Descent" (VND). In this approach the neighbourhoods are changed deterministically until a maximal number of neighbourhoods is reached or the time limit is exceeded. Then, the VNSB uses VND steps but the stop criterion is reaching the time limit.

Combining these ideas, Lazic et al. (2010) [72] proposed a VNDS approach, by using a two level VNS scheme. The algorithm starts finding an optimal solution $\bar{x}$ of the

linear relaxation of problem P. Notice that if $\bar{x}$ is integer problem P is solved and the optimal solution is $\bar{x}$. After this, the next step consists of finding a feasible solution x for the MILP problem. While the total time is not exceeded, the main body of the algorithm has to be iterated by using a subroutine for the VND scheme. The rough details of the algorithm are as follows:

1. Find $\bar{x}$, optimal solution of LR(P).
2. Find x, feasible 0-1MLP of P.
3. Set $t = 0$.
4. **while** ($t < t_{max}$)
   (a) Calculate $\delta_j = |x_j - \bar{x}_j|$ for $j \in \mathcal{B}$, and rank them so that $\delta_1 \leqslant \ldots \leqslant \delta_p$ where $p = |\mathcal{B}|$ and $\mathcal{B}$ is the set of binary index.
   (b) Set $n_d = |\{j \in \mathcal{B} : \delta_j \neq 0\}|$, $k_{step} = [\frac{n_d}{d}]$, $k = p - k_{step}$.
   (c) **while** ($t < t_{max}$) **and** ($k > 0$)
      i. x' = MIPSOLVE$\big(P(x, \{1, 2, \ldots, k\}), t_{sub}, x\big)$
      ii. **if** ($c^T x' < c^T x$) **then** x = VND-MIP$(P, t_{vnd}, t_{mip}, rhs_{max}, x')$
      iii. **else**
         A. **if** ($k - k_{step} > p - n_d$) **then** $k_{step} = \max\{[\frac{k}{2}], 1\}$
         B. $k = k - k_{step}$
         C. $t_{end} = cpuTime()$, $t = t_{end} - t_{start}$
      iv. **endif**
   (d) **endwhile**
5. **endwhile**
6. **return** x

We have chosen this algorithm for providing good feasible solutions (i.e., upper bounds for the optimal solution) of the VCTP model in order to be applied in very large-scale problems, where the optimization by using exact schemes can be very hard, being practically impossible to get a good solution in a reasonable computing time.

Table 3.5: VNDS computational results ($\lambda = 0.80$)

Case	**Tnit**	**VNDS nit**	z_{lp}	z_{best}	GAP_{lp}	t_{best}
C-020	1.7	1.0	0.0013	0.0187	0.9292	1.56
C-025	1.5	1.0	0.0010	0.0228	0.9574	2.02
C-030	1.3	1.0	0.0011	0.0269	0.9600	2.42
C-035	1.8	1.0	0.0017	0.0318	0.9465	8.73
C-040	2.7	1.0	0.0036	0.0375	0.9040	6.66
C-045	4.3	1.0	0.0045	0.0459	0.9028	18.90
C-050	3.0	1.0	0.0034	0.0498	0.9322	13.19

3.4.1 Computational experience

In this section the same testbed used in the results reported in Section 3.3.4 is also used here, so that it can be tested the quality of the solutions obtained by VNDS while comparing them with the exact resolution presented in the previous section. The input parameters for the VNDS scheme are $t_{max} = 60$, $t_{vnd} = 15$ and $t_{mip} = 15$ secs. and, $\lambda = 0.8$ where λ has been used in Section 3.3.4. Table 3.5 shows the main results of the computational experience where the headings are as follows:

- *Tnit*: Number of iterations in the Taylor approximation.
- *VNDS nit*: Number of iterations in the VNDS scheme.
- z_{lp}: Value of the objective function in the continuous linear relaxation.
- z_{best}: Best solution obtained.
- GAP_{lp}: $\frac{z_{ip}-z_{lp}}{z_{ip}}$
- t_{best}: Total time.

In Table 3.5 the values of the objective function in the continuous linear relaxation, z_{lp}, are shown in order to give a lower bound of the value of the objective function. The GAP between z_{lp} and the best solution found by using VNDS, z_{best}, is very big. It shows that the continuous linear relaxation is not near to the optimal solution of the problem. The number of VNDS iterations is 1 in all cases, where the iterations in the Taylor approximation is higher. When the number of aircraft increases, the model dimensions increase too, due to the higher probability of conflict situations. As a consequence, the number of Taylor iterations is higher for bigger instances.

Table 3.6: Results comparison ($\lambda = 0.80$)

Case	z_{ip}	z_{VNDS}	GAP_{VNDS}	t_{ip}	t_{VNDS}
C-020	0.0186	0.0187	0.0053	9.83	1.56
C-025	0.0227	0.0228	0.0044	19.95	2.02
C-030	0.0268	0.0269	0.0037	24.25	2.42
C-035	0.0315	0.0318	0.0094	54.54	8.73
C-040	0.0374	0.0375	0.0027	54.41	6.66
C-045	0.0457	0.0459	0.0044	116.55	18.90
C-050	0.0496	0.0498	0.0040	81.05	13.19

Results comparison

For comparison purposes of the VNDS solution quality, Table 3.6 shows the objective function values by plain use of the engine CPLEX for optimizing the VCTP model and, independently, by using the VNDS scheme presented in this thesis, where the headings are as follows:

- z_{ip}: Optimal solution by using CPLEX [63].
- z_{VNDS}: Best solution obtained by using VNDS.
- GAP_{VNDS}: $\frac{z_{VNDS}-z_{ip}}{z_{VNDS}}$
- t_{ip}: Time (secs.) to obtain the z_{ip} value.
- t_{VNDS}: Best time (secs.) to obtain the best solution by using VNDS.

Table 3.6 shows the small GAP between the optimal solution obtained by CPLEX and the best solution obtained by VNDS scheme. The resolution times are notably shorter by using the metaheuristic scheme instead of the exact one. It seems that for large-scale instances the metaheuristic scheme will give good solutions in short time, but this has to be proved with an extensive computational experience.

Chapter 4

Conclusions, original contributions and future research

The final observations are presented in this chapter, where some conclusions are presented, original contributions about the work developed above are detailed and, the main future research lines are outlined.

4.1 Conclusions

In the development of this work two models based on mathematical optimization have been presented. Next, the main conclusions are detailed.

Chapter 1: State of the art

In this chapter was presented an extended bibliography about the scientific literature until 2010 for the Collision Avoidance Problem. Several approaches from different research fields have studied the problem. Notice that the most part is published in engineering journals although with hight mathematical contents.

Throughout the study, the start point was the work presented in Pallottino et al. (2002) [85], such that the basis of this work is the geometric construction that they have proposed.

Chapter 2: The velocity and altitude changes model

This chapter was devoted to explain and extend the work in Pallottino et al. (2002), specifically the "velocity changes" model. This model has several weak points, and the aim of the proposed model, "Velocity and Altitude Changes", presented in this chapter is to extend the initial work including important aspects to take into account and solving specific cases that the previous work was not able to do. The most notable contribution was the inclusion of the "anomalous cases" in the model, avoiding the domino effect in the resolution of the problem and considering all situations the same model.

A simple distribution of the information between different air traffic controllers (the VAC model is applied in one aerial sector), has been presented by considering the cases depending on the aerial sector each aircraft belong to.

The detailed computational experience shows amazing results, being this model able to be applied in real time. All conflicts in the airspace were solved and the optimal value was found for all cases in the testbed.

Chapter 3: The velocity changes with time periods model

A new model was presented by extending the "Velocity Changes" including the time horizon divided in several time periods. It helps the inclusion of an acceleration term as well as the consideration of continuous velocity changes. The result was a model based on mixed 0-1 nonlinear optimization and it was tackled by iteratively linearizing the nonlinear constraints by using Taylor's polynomials.

The computational experience in the testbed reported for this thesis, by using exact schemes, shows that the resolution time was not affordable as the model dimensions are incremented. The next step was implementing a metaheuristic algoritmia based on "Variable Neighbourhood Search" and "Local Branching", so called "Variable Neighbourhood Decomposition Search" (VNDS) so that the computational time is short for reasonable problems. The inconvenience of using this metaheuristic schemes is that it is not easy to prove if the solution obtained is the optimal or not, but what it is known is that this solution is a good upper bound for the value of the objective function (the problem is minimizing).

4.2 Contributions visibility

The main results of this thesis have been presented in several national and international meetings:

- XXXI SEIO. *On the collision avoidance for air traffic management problem* (Agustín, A.; Alonso-Ayuso, A.; Escudero, L. F.; Martín-Campo, F. J.; Olaso, P.; Pizarro, C.). Murcia (Spain). February 2009.
- The Advanced School on Mathematical Modeling. *On the collision avoidance problem* (Martín-Campo, F. J.). Seville (Spain). June 2009.
- XXIII EURO. *A short term approach for the collision avoidance for air traffic management problem* (Martín-Campo, F. J.; Agustín, A.; Pizarro, C.). Bonn (Germany). July 2009.
- XXIII EURO. *On the collision avoidance for air traffic management problem, a large scale mixed 0-1 program approach* (Olaso, P.; Pizarro, C.; Martín-Campo, F. J.). Bonn (Germany). July 2009.
- Advanced Course on Optimization: Theory, Methods and Applications. *On the collision avoidance for air traffic management problem* (Martín-Campo, F. J.). Barcelona (Spain). July 2010.
- Workshop on Mixed Integer Nonlinear Programming. *Collision avoidance for the ATM problem: A mixed 0-1 nonlinear model* (Martín-Campo, F. J.; Alonso-Ayuso, A.; Escudero, L. F.). Marseille (France). April 2010.
- XXIII ECCO. *A mixed 0-1 nonlinear approach for the collision avoidance for the Air Traffic Management Problem* (Martín-Campo, F. J.; Alonso-Ayuso, A.; Escudero, L. F.). Málaga (Spain). May 2010.
- XXIV EURO. *Collision avoidance for the ATM problem: A mixed 0-1 nonlinear approach* (Martín-Campo, F. J.; Alonso-Ayuso, A.; Escudero, L. F.). Lisbon (Portugal). July 2010.
- XXXII SEIO. *A mixed 0-1 nonlinear approach for the collision avoidance problem* (Martín-Campo, F. J.; Alonso-Ayuso, A.; Escudero, L. F.). A Coruña (Spain). September 2010.

Furthermore, most part of the chapter 2 has been translated in a paper that has been accepted for publication in the journal IEEE, Transactions on Intelligent Transportation Systems and, currently, it is published online, see [8]. An extended abstract has been submitted for publication in the Proceedings of the 9th Innovative Research Workshop & Exhibition organized by Eurocontrol [9], whereas part of the chapter 3 has been published in the Proceedings of the European Workshop on Mixed Integer Nonlinear Programming (EWMINLP) [7] held in Marseille (France), 2010.

4.3 Future Research

Although our work offers another point of view for the detection and resolution of the conflicts in the airspace, new interesting research lines appear for the development of more precise models, able to solve the problem efficiently in a suitable computational time. Some future research lines are as follows:

- Firstly, one of the weak points of the VAC model detailed in Chapter 2, page 21, is that it considers velocity and altitude instantaneous changes. This is not a very important deficiency, since the times that an aircraft needs to make the maneuvers does not exceed ten seconds in the case of the velocity changes (considering a velocity change from the minimum to the maximum velocity). In the case of the altitude changes, the inconvenience is smaller than in the case of velocity changes, since the conflicts are detected with enough time to make the vertical maneuvers adequate. However, a model able to incorporate the continuity in the changes should improve the results that are obtained by using the VAC model. One of the future research lines consists of constructing a new model, perhaps in two steps, being able to include the continuity in the maneuvers. It could be an intermediate model between VAC and VCTP.

- In Chapter 3, page 77, a study of the lower bound for the objective function (in case of minimization) in the VCTP model proposed is required, since the metaheuristic algoritmia that have been inspired in “Variable Neighbourhood Decomposition Search” provides a good upper bound, but it is necessary to measure the quality of the solution. By analyzing these two bounds, a measure can be given by studying the difference between both in the problem magnitudes. For this purpose, the implementation of schemes such that they give good lower bounds for the objective function are very appropriate. We are planning to work on lower bounds provided by Lagrangian Re-

laxation schemes. These schemes are based on dualizing the hardest constraints in the model in order to penalize them in the objective function by the appropriate Lagrangian multipliers, such that the resulting Lagrangian model can be easily solved. Iteratively the multipliers in the objective function are adjusted obtaining a good lower bound of the objective function. These schemes were introduced by Held and Karp (1971) [51] while solving the "Travelling Salesman Problem" and the "Minimum Spanning Trees" problem. See the seminal work due to Geoffrion (1974) [44]. Held et al. (1974) [52], Bertsekas (1982) [13] and Guignard and Kim (1987) [48] continued the Lagrangian Relaxation research, among others. A good review of the Lagrangian Relaxation schemes has been presented in [47]. Our first evaluation for implementing these schemes in the VCTP model has been the study of the type constraints that can be dualized. It seems that they are the constraints (3.7), on page 111, since they descompose the model in three independent blocks (acceleration, velocity with the detection and resolution constraints and distance in the updating position constraints). This assumption should be implemented to be tested. If the choice is good, then, the VNDS solutions (upper bounds) can be compared with the lower bounds obtaining a good measure of the quality of the solution.

- Another important step for the VCTP model that needs to be further explored consists of including the vertical maneuvers, in a continuous way if possible, taking the advantage of the time periods used in the proposed mathematical model. In this manner, the conflicts will be tackled with two different maneuvers, giving a larger space of feasible solutions. Additionally, infeasible situations are avoided, where only velocity changes cannot avoid the conflicts (such as "head to head" cases, persecution between two different aircraft in the same direction but with different velocities, etc.).

- One inconvenience of the VNDS scheme is the time required to obtain the first integer solution. Perhaps, it is necessary to implement a scheme that helps the solver to find this first integer solution faster. In order to do this, Fischetti et al. (2005) [37] proposed a heuristic scheme for getting the first integer solution that, sometimes requires shorter computing time than CPLEX does it.

- The VCTP model is solved by iteratively linearizing the mixed 0-1 nonlinear model. One alternative scheme could be how to implement the metaheuristic VNS scheme in order to solve the nonlinear model. Liberti et al. (2009) [73] proposed a scheme based on VNS for solving mixed integer nonlinear models, although the model dimensions that they consider are not as bigger as ours.

- It is important the refinement of the objective function in the two models that have been introduced, since other considerations can be included.
- One important line of future research will be the study of the convergence where multiple local optima exist for the same instance. For these cases, we are thinking about penalize the aircraft that have not changed their configuration, in order to force the algorithmic approach based on Taylor polynomials to refine the first obtained solution.
- Finally, it is important to include in the models some other possibility to avoid conflicts. It is the implementation of heading angle changes. However, it can involve nonlinear equations, due to the nonlinear nature of this maneuvers, and much work has to be done in this topic.

Appendices

Appendix A

Detailed operations in the VAC model

A.1 Linearizing logic and nonlinear functions

Very often, when a model based on mathematical optimization is constructed, needs to include logic and nonlinear constraints. The resulting nonlinear model must be transformed in linear inequalities for solving large-scale problems. The investigation in this topic shows that the linearization can be done by introducing no so much difficult changes.

A.1.1 Or constraints

It can be observed that it was necessary to introduce a set of or-contraints in the VAC model. The transformation to linear constraints is as it is done in the following example. Notice that

$$(f_1(x) \geqslant 0 \text{ and } f_2(x) \leqslant 0) \text{ or } g(x) \leqslant 0 \text{ or } (h_1 \geqslant 0 \text{ and } h_2 \leqslant 0)$$

is equivalent to

$$\begin{aligned} f_1(x) &\geqslant \underline{f_1}(1-\delta_1) \\ f_2(x) &\leqslant \overline{f_2}(1-\delta_1) \\ g(x) &\leqslant \overline{g}(1-\delta_2) \\ h_1(x) &\geqslant \underline{h_1}(1-\delta_3) \\ h_2(x) &\leqslant \overline{h_2}(1-\delta_3) \\ \delta_1 + \delta_2 + \delta_3 &= num, \end{aligned}$$

where $\underline{f_1}$ and $\overline{f_2}$ are the lower and upper bounds of the functions f_1 and f_2 respectively; $\overline{g}$ is the upper bound of the function g; $\underline{h_1}$ and $\overline{h_2}$ are the lower and upper bounds of the functions h_1 and h_2 respectively; δ_i, with $i \in \{1, 2, 3\}$ are auxiliary 0-1 variables and num is the number of conditions that has to be checked in total.

A.1.2 Minimizing an absolute value

The absolute value of a difference $|a-b|$ is a nonlinear function. For its linearization it can be taken the maximum function between the differences $a - b$ and $b - a$ as follows,

$$|a - b| = \max\{a - b, b - a\}$$

But the maximum function is also nonlinear. However, it can easily be modeled by using two constraints as follows as it is customarily done for minimizing a maximum function $\max\{c, d\}$, being in this particular case $c = a - b$ and $d = b - a$,

$$c \geqslant a - b$$
$$d \geqslant b - a,$$

where $c = |a - b| = \max\{a - b, b - a\}$.

Notice that maximizing a minimum function is analogue. The only change to make is the sense of the inequalities in last expression.

A.2 Calculation of the α angles between aircraft with different safety radii

Section 2.3.1, page 35, is devoted to obtain α angles between aircraft i and j, being $i, j \in \mathcal{F}$ with different safety radii. The detailed explanation based on Fig. A.1 is presented in this appendix.

There are four tangent straight lines between two circumferences (if the intersection of the circles is empty) that are so-called interior and exterior tangent straight lines. Therefore, each circumference has four tangent points. It is necessary to find the slope of the interior tangent straight line that has positive value.

Let two different safety circumferences be for two aircraft i and j, with $i, j \in \mathcal{F}$. It can be considered that the ordinate of each aircraft is 0 since the final expression only depends on the radii r_i and r_j, and the distance between the two aircraft. The equations of the circumferences are as follows,

$$(x - x_i)^2 + y^2 = r_i^2 \tag{A.1a}$$

$$(x - x_j)^2 + y^2 = r_j^2. \tag{A.1b}$$

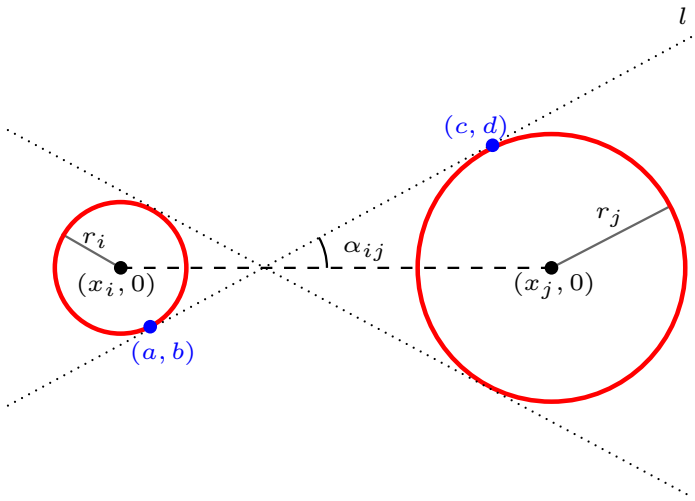

Figure A.1: Interior tangent straight lines construction

Now, the derivative of y with respect to x is calculated as follows,

$$2(x - x_i) + 2y'y = 0 \Rightarrow y = \frac{(x_i - x)}{y'} \tag{A.2a}$$

$$2(x - x_j) + 2y'y = 0 \Rightarrow y = \frac{(x_j - x)}{y'}. \tag{A.2b}$$

Let the straight line l be as in Fig. A.1. The straight line crosses points $(\hat{x}^0, \hat{y}^0) \in C_i$ and $(\hat{x}^1, \hat{x}^1) \in C_j$ (being C_i and C_j the circumferences centered in $(x_i, 0)$ and $(x_j, 0)$, respectively). The slope of this straight line will be $y' = m > 0$. For $(\hat{x}^0, \hat{y}^0)$ and $(\hat{x}^1, \hat{y}^1)$ equations (A.1) and (A.2) must be satisfied. The slope of the straight line can be calculated by using two points, obtaining that $m = y' = \frac{\hat{y}^1 - \hat{y}^0}{\hat{x}^1 - \hat{x}^0}$. Therefore, the linear system (A.3) with five equations and five unknowns has been obtained as follows,

$$(\hat{x}^0 - x_i)^2 + (\hat{y}^0)^2 = r_i^2 \tag{A.3a}$$

$$(\hat{x}^1 - x_j)^2 + (\hat{y}^1)^2 = r_j^2 \tag{A.3b}$$

$$\hat{y}^0 = \frac{x_i - \hat{x}^0}{m} \tag{A.3c}$$

$$\hat{y}^1 = \frac{x_j - \hat{x}^1}{m} \tag{A.3d}$$

$$m = \frac{\hat{y}^1 - \hat{y}^0}{\hat{x}^1 - \hat{x}^0}. \tag{A.3e}$$

By using (A.3c) in (A.3a), it results that

$$(\hat{x}^0 - x_i)^2 + \frac{(x_i - \hat{x}^0)^2}{m^2} = r_i^2 \Rightarrow (1 + m^2)(x_i - \hat{x}^0)^2 = m^2 r_i^2$$

Taking the positive square root in the expression, it results that

$$\sqrt{1 + m^2}(x_i - \hat{x}^0) = m r_i \Rightarrow x_i - \hat{x}^0 = \frac{m r_i}{\sqrt{1 + m^2}}$$

and $\hat{x}^0$ results

$$\hat{x}^0 = x_i - \frac{m r_i}{\sqrt{1 + m^2}}. \tag{A.4}$$

By using (A.3d) in (A.3b), it is obtained the same results above, but the negative

square root has to be taken, so, it results,

$$\sqrt{1+m^2}(x_j-\hat{x}^1)=m^2r_j^2 \Rightarrow x_j-\hat{x}^1=-\frac{mr_j}{\sqrt{1+m^2}},$$

where $\hat{x}^1$ results

$$\hat{x}^1=x_j+\frac{mr_j}{\sqrt{1+m^2}}. \tag{A.5}$$

By using (A.3c) and (A.3d) in (A.3e) it results,

$$m=\frac{\frac{x_j-\hat{x}^1}{m}-\frac{x_i-\hat{x}^0}{m}}{\hat{x}^1-\hat{x}^0}=\frac{x_j-\hat{x}^1-x_i+\hat{x}^0}{m(\hat{x}^1-\hat{x}^0)}.$$

As $x_j-x_i=dist(x_i,x_j)=d_{ij}$, the above expression can be simplified as follows,

$$m=\frac{d_{ij}+(\hat{x}^0-\hat{x}^1)}{m(\hat{x}^1-\hat{x}^0)} \Rightarrow m^2(\hat{x}^1-\hat{x}^0)=d_{ij}+(\hat{x}^0-\hat{x}^1),$$

where

$$1+m^2=\frac{d_{ij}}{\hat{x}^1-\hat{x}^0}. \tag{A.6}$$

Now, by using (A.4) and (A.5) in (A.6), it results

$$1+m^2=\frac{d_{ij}}{x_j+\frac{mr_j}{\sqrt{1+m^2}}-x_i+\frac{mr_i}{\sqrt{1+m^2}}}=\frac{\sqrt{1+m^2}d_{ij}}{\sqrt{1+m^2}x_j+mr_j-\sqrt{1+m^2}x_i+mr_i} \Rightarrow$$

$$\sqrt{1+m^2}d_{ij}=(1+m^2)\Big(\sqrt{1+m^2}(x_j-x_i)+m(r_i+r_j)\Big).$$

Dividing by $\sqrt{1+m^2}$ and taking $(x_j-x_i)=d_{ij}$, it results,

$$d_{ij}=\sqrt{1+m^2}\Big(\sqrt{1+m^2}d_{ij}+m(r_i+r_j)\Big) \Rightarrow -m^2d_{ij}=m\sqrt{1+m^2}(r_i+r_j).$$

Dividing by m and squaring, it results

$$(1+m^2)(r_i+r_j)^2=m^2d_{ij}^2 \Rightarrow (r_i+r_j)^2=m^2\big(d_{ij}^2-(r_i+r_j)^2\big),$$

where

$$m^2=\frac{(r_i+r_j)^2}{d_{ij}^2-(r_i+r_j)^2} \Rightarrow m=\pm\frac{r_i+r_j}{\sqrt{d_{ij}^2-(r_i+r_j)^2}}.$$

Now, the α_{ij} angle can be easily obtained by using the archtangent of the obtained slope as follows,

$$\alpha_{ij} = \arctan\left(\frac{r_i + r_j}{\sqrt{d_{ij}^2 - (r_i + r_j)^2}} \right).$$

In the following, it is compared the approach presented in this thesis with the method proposed by Pallottino (2002) [85]. It is considered in the VC model, that the radii are $\frac{s}{2}$ for all aircraft. If $r_i, r_j = \frac{s}{2}$ are taken in the expression and $\arctan(x) = \arcsin\left(\frac{x}{\sqrt{x^2+1}}\right)$ is used, it results,

$$\alpha_{ij} = \arctan\left(\frac{s}{\sqrt{d_{ij}^2 - s^2}} \right) = \arcsin\left(\frac{\frac{s}{\sqrt{d_{ij}^2 - s^2}}}{\sqrt{\frac{s^2}{d_{ij}^2 - s^2} + 1}} \right) =$$

$$= \arcsin\left(\frac{\frac{s}{\sqrt{d_{ij}^2 - s^2}}}{\frac{d_{ij}}{\sqrt{d_{ij}^2 - s^2}}} \right) = \arcsin\left(\frac{s}{d_{ij}}\right) = \alpha_{ij},$$

what is the same expression.

A.3 Going out from the aerial sector in the predicted time

One of the main objectives of the models iVAC and VAC consists of returning to the initial configuration, causing as less as possible perturbations between the predicted and the new plans where all conflicts in the airspace are avoided. For returning to the velocity in the initial plan, it is required to penalize the difference between the predicted time and the new time for leaving the aerial sector, so that, the geometric construction shown in Fig. A.2 is taken into account.

The distance between points (x_f, y_f) and (x_f^1, y_f^1) can be known in two ways, namely,

$$\begin{aligned} dist((x_f, y_f), (x_f^1, y_f^1)) &= \hat{v}_f(t_f^1 - t) \\ &\text{and} \\ dist((x_f, y_f), (x_f^1, y_f^1)) &= \sqrt{(x_f^1 - x_f)^2 + (y_f^1 - y_f)^2}. \end{aligned}$$

Hence,

$$\hat{v}_f(t_f^1 - t) = \sqrt{(x_f^1 - x_f)^2 + (y_f^1 - y_f)^2},$$

where the velocity that an aircraft might have to arrive at the destination point in the predicted time is as follows,

$$\widehat{v}_f = \frac{\sqrt{(x_f^1 - x_f)^2 + (y_f^1 - y_f)^2}}{t_f^1 - t}.$$

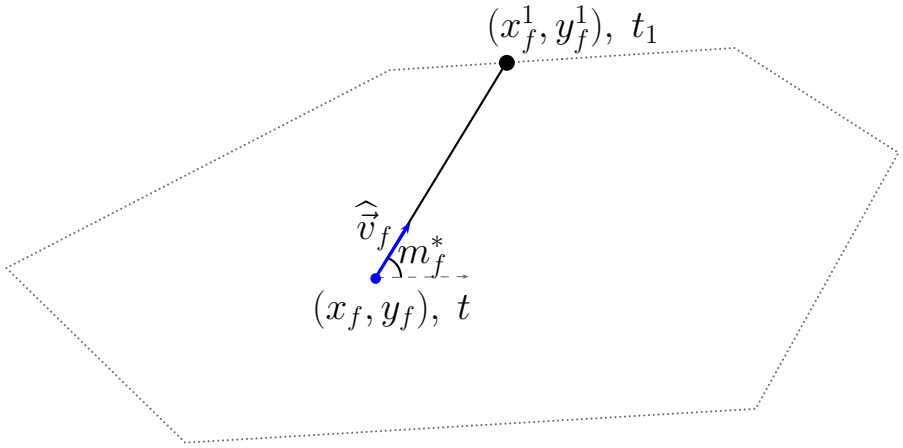

Figure A.2: Return to the initial configuration time

A.4 Intersection point calculation

It is needed in section 2.3.9, page 52, to calculate the intersection point between two different straight lines. In what follows, the calculations are presented by using some geometric properties. As a first step, the straight line equation that goes through the (x_0, y_0) point and has the director vector $\overrightarrow{v} = (v_1, v_2)$ has to be calculated as follows,

$$\frac{x - x_0}{v_1} = \frac{y - y_0}{v_2},$$

where

$$y = \frac{v_2}{v_1}x + \left(y_0 - \frac{v_2}{v_1}x_0\right)$$

is the straight line equation that is looked for.

In the general case, let $y = ax + b$ and $y = cx + d$ be two straight lines, then the abscissa of the intersection point can be calculated by making equal the two ordinates, such that

$$x = \frac{d - b}{a - c}.$$

With this expression the ordinate of the intersection point can be calculated replacing the x with the previous expression in one straight line equation, resulting

$$y = \frac{ad - bc}{a - c}.$$

For the particular case considered in Section 2.3.9, page 52, let (x_1, y_1), (x_2, y_2), (v_1, v_2) and (w_1, w_2) be the initial points and the director vectors of two different aircraft. Then, the intersection point between both trajectories by using the previous concepts can be calculated as follows,

$$\begin{aligned} y &= \left(\frac{v_2}{v_1}\right)x + \left(y_1 - \frac{v_2}{v_1}x_1\right) \\ &\text{and} \\ y &= \left(\frac{w_2}{w_1}\right)x + \left(y_2 - \frac{w_2}{w_1}x_2\right), \end{aligned}$$

such that the intersection point looked for can be expressed

$$\left(\frac{y_2 - \frac{w_2}{w_1}x_2 - y_1 + \frac{v_2}{v_1}x_1}{\frac{v_2}{v_1} - \frac{w_2}{w_1}} \quad , \frac{\frac{v_2}{v_1}\left(y_2 - \frac{w_2}{w_1}x_2\right) - \frac{w_2}{w_1}\left(y_1 - \frac{v_2}{v_1}x_1\right)}{\frac{v_2}{v_1} - \frac{w_2}{w_1}}. \right) \tag{A.7}$$

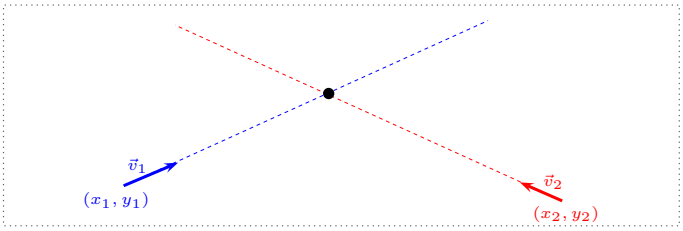

Figure A.3: Intersection point in the sector

See in Fig. A.3 the situation of interest with two aircraft that have intersection point of the trajectories inside the aerial sector.

A.5 Computational results for the VAC model

In this section, part of the computational experience is presented in detail. Three types of tables are presented for each dimensional case, namely,

- The model dimensions where the headings are as follows:
  - *Case*: Gives the case configuration: CAAA-ZZ denotes number of aircraft (AAA) and levels (ZZ).
  - m: Number of constraints.
  - n: Number of variables.
  - d: Constraints matrix density.
  - m^*, n^* and d^*: the number of constraints, variables and constraints matrix density, respectively, after the preprocessing made by CPLEX [63].
- The results of the model where the headings are as follows:
  - *Case*: Gives the case configuration: CAAA-ZZ denotes number of aircraft (AAA) and levels (ZZ).
  - z_{lp}: Value of the objective function in the continuous linear relaxation.
  - z_s: Value of the bound after performing the CPLEX cut identification and appending at node 0
  - z_{ip}: Value of the objective function for the optimal solution of the problem.
  - GAP_{lp}: $\frac{z_{ip}-z_{lp}}{z_{ip}}$
  - GAP_s: $\frac{z_{ip}-z_s}{z_{ip}}$
  - nb: Number of times that there is branching
  - nn: Number of CPLEX branch-and-cut nodes
  - t_{lp}: Time (secs.) to obtain the z_{lp} value
  - t_s: Time (secs.) to obtain the z_s value.
  - t_{ip}: Time (secs.) to obtain the z_{ip} value.
  - nc: Total number of cuts performed by CPLEX.
- The number of cuts identified and appended by CPLEX [63] where the headings are as follows:

- *Case*: Gives the case configuration: CAAA-ZZ denotes number of aircraft (AAA) and levels (ZZ).
- Clique: Number of clique cuts.
- Cover: Number of Cover cuts.
- Implied: Number of Implied cuts.
- Flow: Number of Flow cuts.
- MIR: Number of Mixed Integer Rounding cuts.
- Zero-Half: Number of Zero-half cuts.
- Gomory: Number of Gomory cuts.
- Total: Total number of cuts.

Only the results for the cases with 20 aircraft and 10 levels are presented. However, the results for the other cases in the testbed reported in this thesis can be found in the extended version of the thesis in the CD enclosed with this thesis.

Table A.1: Dimensions for 20 aircraft and 10 levels

Case	m	n	d	m^*	n^*	d^*
C020-10-001	21100	9820	0.0005	2838	1700	0.0028
C020-10-002	21100	9820	0.0005	2018	1240	0.0037
C020-10-003	21100	9820	0.0005	3146	1809	0.0026
C020-10-004	21100	9820	0.0005	3044	1740	0.0027
C020-10-005	21100	9820	0.0005	2567	1530	0.0031
C020-10-006	21100	9820	0.0005	1957	1269	0.0035
C020-10-007	21100	9820	0.0005	1523	1039	0.0043
C020-10-008	21100	9820	0.0005	2606	1559	0.0029
C020-10-009	21100	9820	0.0005	2927	1700	0.0028
C020-10-010	21100	9820	0.0005	2307	1470	0.0030
C020-10-011	21100	9820	0.0005	3166	1829	0.0026
C020-10-012	21100	9820	0.0005	2578	1498	0.0031
C020-10-013	21100	9820	0.0005	1321	858	0.0053
C020-10-014	21100	9820	0.0005	2510	1508	0.0031
C020-10-015	21100	9820	0.0005	3952	2249	0.0021
C020-10-016	21100	9820	0.0005	3517	2060	0.0023
C020-10-017	21100	9820	0.0005	3827	2190	0.0021
C020-10-018	21100	9820	0.0005	1398	1000	0.0043
C020-10-019	21100	9820	0.0005	3509	2060	0.0023
C020-10-020	21100	9820	0.0005	2118	1360	0.0034
C020-10-021	21100	9820	0.0005	2008	1290	0.0036
C020-10-022	21100	9820	0.0005	2675	1580	0.0029
C020-10-023	21100	9820	0.0005	2199	1380	0.0034
C020-10-024	21100	9820	0.0005	3460	2060	0.0023
C020-10-025	21100	9820	0.0005	2906	1699	0.0027
C020-10	21100.0	9820.0	0.0005	2643.1	1587.1	0.0029

Table A.2: Results for 20 aircraft and 10 levels

Case	z_{lp}	z_s	z_{ip}	GAP_{lp}	GAP_s	**nn**	t_{lp}	t_s	t_{ip}
C020-10-001	0.0000	0.0000	0.0000	0.0000	0.0000	0	0.06	0.22	0.14
C020-10-002	0.0000	0.0000	0.0000	0.0000	0.0000	0	0.06	0.14	0.14
C020-10-003	5.6451	6.2357	6.4451	12.4124	3.2504	0	0.06	0.70	0.47
C020-10-004	0.0000	0.0000	0.0000	0.0000	0.0000	0	0.09	0.16	0.14
C020-10-005	13.2102	13.4957	13.4957	2.1153	0.0000	0	0.06	0.16	0.23
C020-10-006	12.0681	13.1106	13.1106	7.9514	0.0000	0	0.08	0.16	0.14
C020-10-007	0.0000	0.0000	0.0000	0.0000	0.0000	0	0.05	0.11	0.13
C020-10-008	0.0000	0.0000	0.0000	0.0000	0.0000	0	0.06	0.22	0.23
C020-10-009	0.0000	0.0000	0.0000	0.0000	0.0000	0	0.05	0.17	0.14
C020-10-010	0.0000	0.0000	0.0000	0.0000	0.0000	0	0.09	0.25	0.16
C020-10-011	0.0000	0.0000	0.0000	0.0000	0.0000	12	0.05	0.39	0.50
C020-10-012	0.0000	0.0000	0.0000	0.0000	0.0000	0	0.06	0.13	0.20
C020-10-013	24.0218	24.0218	24.0218	0.0000	0.0000	0	0.06	0.14	0.11
C020-10-014	9.0377	9.0377	9.0377	0.0000	0.0000	0	0.06	0.16	0.14
C020-10-015	7.8889	8.4649	8.8500	10.8600	4.3516	26	0.06	0.45	0.41
C020-10-016	10.9267	10.9267	10.9267	0.0000	0.0000	0	0.06	0.23	0.23
C020-10-017	12.1492	12.4843	12.4843	2.6847	0.0000	0	0.06	0.17	0.17
C020-10-018	8.6044	9.0044	9.0044	4.4423	0.0000	0	0.06	0.23	0.22
C020-10-019	0.0000	0.0000	0.0000	0.0000	0.0000	16	0.06	0.25	0.50
C020-10-020	0.0000	0.0000	0.0000	0.0000	0.0000	5	0.06	0.23	0.41
C020-10-021	0.0000	0.0000	0.0000	0.0000	0.0000	0	0.06	0.17	0.14
C020-10-022	0.0000	0.0000	0.0000	0.0000	0.0000	0	0.05	0.20	0.34
C020-10-023	0.0000	0.0000	0.0000	0.0000	0.0000	0	0.08	0.14	0.13
C020-10-024	0.0000	0.0000	0.0000	0.0000	0.0000	0	0.06	0.20	0.28
C020-10-025	0.0000	0.0000	0.0000	0.0000	0.0000	0	0.13	0.16	0.16
C020-10	4.1421	4.2713	4.2951	3.5615	0.5538	2.4	0.07	0.22	0.23

Table A.3: CPLEX cuts for 20 aircraft and 10 levels

Case	Clique	Cover	Implied	Flow	MIR	Zero-half	Gomory	Total
C020-10-001	0	0	0	0	0	0	0	0
C020-10-002	0	0	0	0	0	0	0	0
C020-10-003	8	26	19	15	1	3	27	99
C020-10-004	0	0	0	0	0	0	0	0
C020-10-005	0	0	0	0	0	0	0	0
C020-10-006	9	47	19	0	0	0	36	111
C020-10-007	0	0	0	0	0	0	0	0
C020-10-008	0	0	0	0	0	0	0	0
C020-10-009	0	0	0	0	0	0	0	0
C020-10-010	0	0	0	0	0	0	0	0
C020-10-011	0	0	0	4	0	1	1	6
C020-10-012	0	0	0	0	0	0	0	0
C020-10-013	0	0	0	0	0	0	0	0
C020-10-014	0	0	0	0	0	0	0	0
C020-10-015	20	41	29	3	1	1	41	136
C020-10-016	0	0	0	0	0	0	0	0
C020-10-017	0	0	0	0	0	0	0	0
C020-10-018	0	0	0	1	0	2	1	4
C020-10-019	0	4	0	1	0	0	1	6
C020-10-020	0	0	0	5	0	1	1	7
C020-10-021	0	0	0	0	0	0	0	0
C020-10-022	0	0	1	1	1	1	1	5
C020-10-023	6	40	17	0	1	0	32	96
C020-10-024	0	2	0	0	0	0	0	2
C020-10-025	0	0	0	0	0	0	0	0
C020-10	1.7	6.4	3.4	1.2	0.2	0.4	5.6	18.9

Appendix B

Detailed operations in the VCTP model

B.1 Calculation of the tangent of l and g angles

It is presented in this section the calculations of the tangent of l and g angles for the VCTP model. Firstly, four trigonometric properties that will be used to calculate the respective tangents are proved.

Lemma 1. $\sin(a \pm b) = \sin(a)\cos(b) \pm \cos(a)\sin(b))$.

Lemma 2. $\cos(a \pm b) = \cos(a)\cos(b) \mp \sin(a)\sin(b)$.

These two previous lemmas are important properties that are frequently used in trigonometric relations.

Lemma 3. $\tan(a \pm b) = \frac{\tan(a) \pm \tan(b)}{1 \mp \tan(a)\tan(b)}$

It is used in the the Lemmas 1 and 2 that have been introduced above.

$$\tan(a \pm b) = \frac{\sin(a \pm b)}{\cos(a \pm b)} = \frac{\sin(a)\cos(b) \pm \cos(a)\sin(b)}{\cos(a)\cos(b) \mp \sin(a)\sin(b)} = \frac{\frac{\sin(a)\cos(b) \pm \cos(a)\sin(b)}{\cos(a)\cos(b)}}{\frac{\cos(a)\cos(b) \mp \sin(a)\sin(b)}{\cos(a)\cos(b)}} = \frac{\tan(a) \pm \tan(b)}{1 \mp \tan(a)\tan(b)}.$$

Lemma 4. $\tan\big(\arcsin(x)\big) = \frac{x}{\sqrt{1-x^2}}$

The proof is as follows,

$$\tan\big(\arcsin(x)\big) = \frac{\sin\big(\arcsin(x)\big)}{\cos\big(\arcsin(x)\big)} = \frac{x}{\sqrt{1 - \sin^2\big(\arcsin(x)\big)}} = \frac{x}{\sqrt{1-x^2}}.$$

It is used in the second equality the relation $\sin^2(x) + \cos^2(x) = 1$, resulting $\cos(x) = \sqrt{1 - \sin^2(x)}$.

Now, with these results, the calculation of $\tan(l_{ij}^t)$ is as follows. It can be seen in the VC model that $l_{ij} = \omega_{ij} + \alpha$, where $\omega_{ij} = \arctan\left(\frac{y_i - y_j}{x_i - x_j}\right)$ and $\alpha_{ij} = \arcsin\left(\frac{s}{d_{ij}}\right)$. These parameters are assumed for the current time period $t \in \mathcal{T}$.

$$\tan(l_{ij}^t) = \tan(\omega_{ij}^t + \alpha_{ij}^t) = \tan\left(\arctan\left(\frac{y_i^t - y_j^t}{x_i^t - x_j^t}\right) + \arcsin\left(\frac{s}{d_{ijt}}\right)\right)$$

And from Lemma 3, it results,

$$\tan(l_{ij}^t) = \frac{\tan\left(\arctan\left(\frac{y_i^t - y_j^t}{x_i^t - x_j^t}\right)\right) + \tan\left(\arcsin\left(\frac{s}{d_{ijt}}\right)\right)}{1 - \tan\left(\arctan\left(\frac{y_i^t - y_j^t}{x_i^t - x_j^t}\right)\right)\tan\left(\arcsin\left(\frac{s}{d_{ijt}}\right)\right)}.$$

From Lemma 4, it results

$$\tan(l_{ij}^t) = \frac{\frac{y_i^t - y_j^t}{x_i^t - x_j^t} + \frac{s/d_{ijt}}{\sqrt{1 - s^2/d_{ijt}^2}}}{1 - \left(\frac{y_i^t - y_j^t}{x_i^t - x_j^t}\right)\left(\frac{s/d_{ijt}}{\sqrt{1 - s^2/d_{ijt}^2}}\right)} = \frac{\frac{y_i^t - y_j^t}{x_i^t - x_j^t} + \frac{s}{\sqrt{d_{ijt}^2 - s^2}}}{1 - \left(\frac{y_i^t - y_j^t}{x_i^t - x_j^t}\right)\left(\frac{s}{\sqrt{d_{ijt}^2 - s^2}}\right)} =$$

$$\frac{\frac{(y_i^t - y_j^t)\sqrt{d_{ijt}^2 - s^2} + (x_i^t - x_j^t)s}{(x_i^t - x_j^t)\sqrt{d_{ijt}^2 - s^2}}}{\frac{(x_i^t - x_j^t)\sqrt{d_{ijt}^2 - s^2} - (y_i^t - y_j^t)s}{(x_i^t - x_j^t)\sqrt{d_{ijt}^2 - s^2}}} = \frac{(x_i^t - x_j^t)s + (y_i^t - y_j^t)\sqrt{d_{ijt}^2 - s^2}}{(x_i^t - x_j^t)\sqrt{d_{ijt}^2 - s^2} - (y_i^t - y_j^t)s} =$$

$$\frac{(x_i^t - x_j^t)s + (y_i^t - y_j^t)\sqrt{(x_i^t - x_j^t)^2 + (y_i^t - y_j^t)^2 - s^2}}{(x_i^t - x_j^t)\sqrt{(x_i^t - x_j^t)^2 + (y_i^t - y_j^t)^2 - s^2} - (y_i^t - y_j^t)s}.$$

Now the g angle can be calculated in a similar way as follows,

$$\tan(g_{ij}^t) = \tan(\omega_{ij}^t - \alpha_{ij}^t) = \tan\left(\arctan\left(\frac{y_i^t - y_j^t}{x_i^t - x_j^t}\right) - \arcsin\left(\frac{s}{d_{ijt}}\right)\right).$$

And from Lemma 3, it results

$$\tan(g_{ij}^t) = \frac{\tan\left(\arctan\left(\frac{y_i^t - y_j^t}{x_i^t - x_j^t}\right)\right) - \tan\left(\arcsin\left(\frac{s}{d_{ijt}}\right)\right)}{1 + \tan\left(\arctan\left(\frac{y_i^t - y_j^t}{x_i^t - x_j^t}\right)\right)\tan\left(\arcsin\left(\frac{s}{d_{ijt}}\right)\right)}.$$

From Lemma 4, it results

$$\tan(g_{ij}^t) = \frac{\frac{y_i^t - y_j^t}{x_i^t - x_j^t} - \frac{s/d_{ijt}}{\sqrt{1 - s^2/d_{ijt}^2}}}{1 + \left(\frac{y_i^t - y_j^t}{x_i^t - x_j^t}\right)\left(\frac{s/d_{ijt}}{\sqrt{1 - s^2/d_{ijt}^2}}\right)} = \frac{\frac{y_i^t - y_j^t}{x_i^t - x_j^t} - \frac{s}{\sqrt{d_{ijt}^2 - s^2}}}{1 + \left(\frac{y_i^t - y_j^t}{x_i^t - x_j^t}\right)\left(\frac{s}{\sqrt{d_{ijt}^2 - s^2}}\right)} =$$

$$\frac{\frac{(y_i^t-y_j^t)\sqrt{d_{ijt}^2-s^2}-(x_i^t-x_j^t)s}{(x_i^t-x_j^t)\sqrt{d_{ijt}^2-s^2}}}{\frac{(x_i^t-x_j^t)\sqrt{d_{ijt}^2-s^2}+(y_i^t-y_j^t)s}{(x_i^t-x_j^t)\sqrt{d_{ijt}^2-s^2}}} = \frac{-(x_i^t-x_j^t)s+(y_i^t-y_j^t)\sqrt{d_{ijt}^2-s^2}}{(x_i^t-x_j^t)\sqrt{d_{ijt}^2-s^2}+(y_i^t-y_j^t)s} =$$

$$\frac{-(x_i^t-x_j^t)s+(y_i^t-y_j^t)\sqrt{(x_i^t-x_j^t)^2+(y_i^t-y_j^t)^2-s^2}}{(x_i^t-x_j^t)\sqrt{(x_i^t-x_j^t)^2+(y_i^t-y_j^t)^2-s^2}+(y_i^t-y_j^t)s}.$$

Notice that these two expressions have null denominator if and only if $s=|x_i^t-x_j^t|$.

B.2 Cases of the new aircraft positions in the VCTP model

Four different cases were presented in Section 3.2, page 81, to model the new aircraft positions along the polygonal of the aircraft positions in fixed time periods. It is presented the calculation in this appendix.

Excess-Excess position situation

For this case see Fig. B.1. Let (x_f^{*t-1}, y_f^{*t-1}) and (x_f^{*t}, y_f^{*t}) be the initial configuration position for aircraft $f \in \mathcal{F}$ in time periods $t-1$ and $t \in \mathcal{T}$, respectively. In this case, the aircraft arrives early to the predicted position in $t-1$ and $t \in \mathcal{T}$, since it has to avoid a previous conflict situation, being (x_f^t, y_f^t) the new configuration position for the aircraft after the resolution.

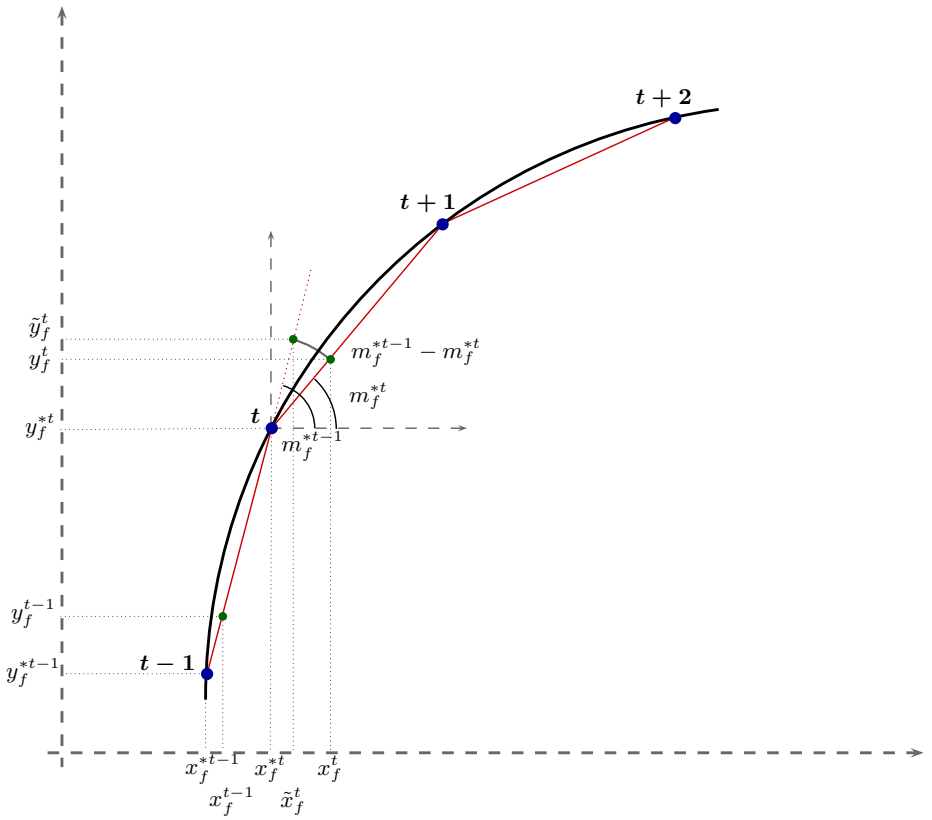

Figure B.1: Excess-Excess position situation

Let $(\tilde{x}_f^t, \tilde{y}_f^t)$ be the aircraft position in time period $t \in \mathcal{T}$ if the aircraft flies along a straight line. These parameters can be expressed

$$\begin{aligned} \tilde{x}_f^t &= x_f^{t-1} + \Big((v_f^{t_d} + \sum_{\ell=1}^{t-1} a_f^t I_\ell) I_t + \frac{1}{2} a_i^t I_t^2 \Big) \cos(m_f^{*t-1}) \\ \text{and} & \\ \tilde{y}_f^t &= y_f^{t-1} + \Big((v_f^{t_d} + \sum_{\ell=1}^{t-1} a_f^t I_\ell) I_t + \frac{1}{2} a_i^t I_t^2 \Big) \sin(m_f^{*t-1}) \end{aligned}$$

by using equation (3.1b) on page 78.

This position must be translated to the segment between time periods t and $t-1 \in \mathcal{T}$ by turning this point clockwise $m_f^{*t-1} - m_f^{*t}$ degrees. Notice that if the turn is not clockwise, then, $m_f^{*t-1} - m_f^{*t}$ will be negative. Firstly, the position (x_f^{*t}, y_f^{*t}) must be centered in the origin of the reference system, such that the point $(\tilde{x}_f^t, \tilde{y}_f^t)$ in the new reference will be

$$(\tilde{x}_f^t - x_f^{*t}, \tilde{y}_f^t - y_f^{*t})$$

and, then, making the turn by using the turn-matrix

$$\begin{pmatrix} \cos\vartheta & \sin\vartheta \\ -\sin\vartheta & \cos\vartheta \end{pmatrix},$$

where $\vartheta = m_f^{*t-1} - m_f^{*t}$.

After the turn, the return to the initial reference must be satisfied, and the new position will be

$$\begin{aligned} x_f^t =& (\tilde{x}_f^t - x_f^{*t}) \cos(m_f^{*t-1} - m_f^{*t}) + (\tilde{y}_f^t - y_f^{*t}) \sin(m_f^{*t-1} - m_f^{*t}) + x_f^{*t} \\ y_f^t =& -(\tilde{x}_f^t - x_f^{*t}) \sin(m_f^{*t-1} - m_f^{*t}) + (\tilde{y}_f^t - y_f^{*t}) \cos(m_f^{*t-1} - m_f^{*t}) + y_f^{*t}. \end{aligned}$$

Defect-Defect position situation

For this case see Fig. B.2. Let (x_f^{*t-1}, y_f^{*t-1}) and (x_f^{*t}, y_f^{*t}) be the initial configuration positions for aircraft $f \in \mathcal{F}$ in time periods $t-1$ and $t \in \mathcal{T}$, respectively. In this case, the aircraft arrives later to the predicted position in $t-1$ and $t \in \mathcal{T}$. Let $(\tilde{x}_f^t, \tilde{y}_f^t)$ be the aircraft position in the straight line of the segment that joins the positions in time periods $t-2$ and $t-1$.

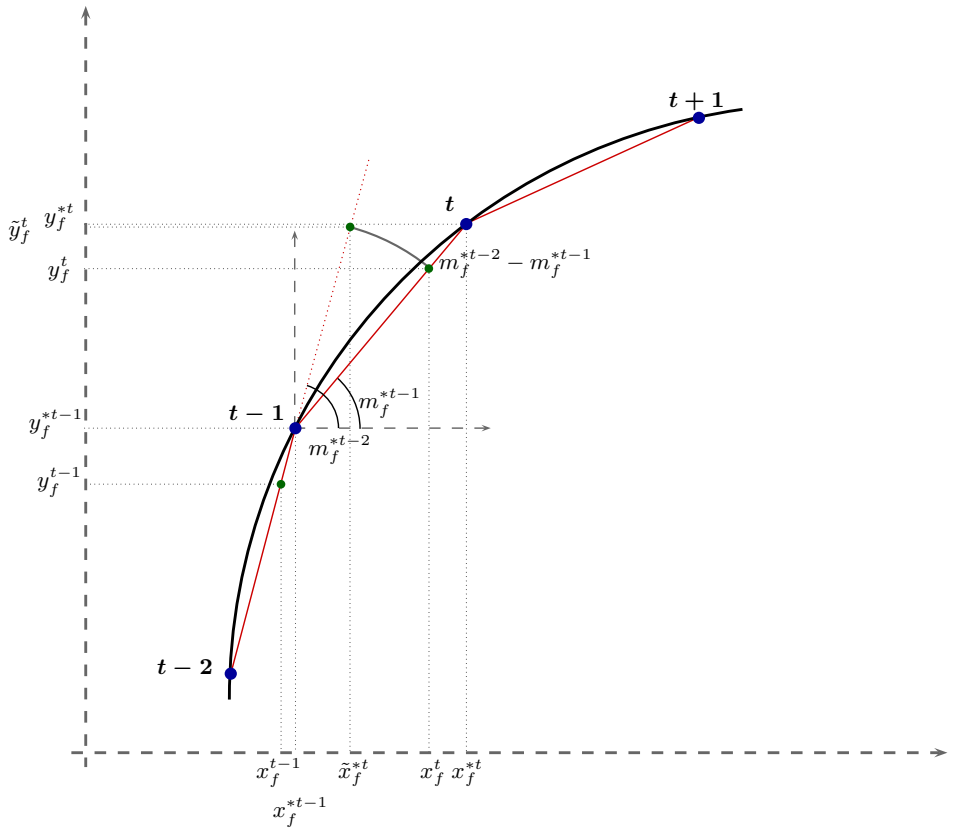

Figure B.2: Defect-Defect position situation

This case for the calculations is similar to the first one, and, simple changes must be done. The point to center in the origin of the reference system is (x_f^{*t-1}, y_f^{*t-1}). It must be turned $m_f^{*t-2} - m_f^{*t-1}$ degrees. So, doing the appropriate calculations over it results,k

$$x_f^t = (\tilde{x}_f^t - x_f^{*t-1})\cos(m_f^{*t-2} - m_f^{*t-1}) + (\tilde{y}_f^t - y_f^{*t-1})\sin(m_f^{*t-2} - m_f^{*t-1}) + x_f^{*t-1}$$
$$y_f^t = -(\tilde{x}_f^t - x_f^{*t-1})\sin(m_f^{*t-2} - m_f^{*t-1}) + (\tilde{y}_f^t - y_f^{*t-1})\cos(m_f^{*t-2} - m_f^{*t-1}) + y_f^{*t-1}.$$

Defect-Excess position situation

For this case see Fig. B.3. Let (x_f^{*t-1}, y_f^{*t-1}) and (x_f^{*t}, y_f^{*t}) be the initial configuration positions for aircraft $f \in \mathcal{F}$ in time periods $t-1$ and $t \in \mathcal{T}$ respectively. This case considers the situation in which an aircraft arrives later in time period $t-1$ and arrives early in time period $t \in \mathcal{T}$. It is more difficult than the two cases considered above, since a double translation and turn is necessary to force the aircraft to fly along the polygonal. Let

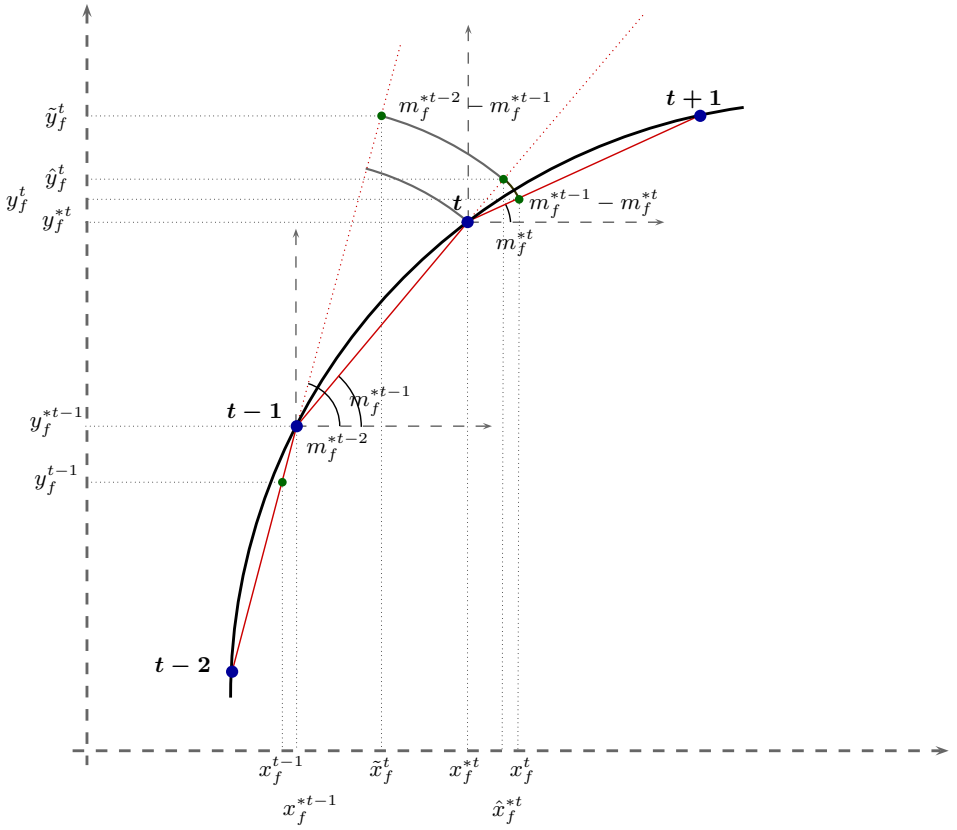

Figure B.3: Defect-Excess position situation

$(\tilde{x}_f^t, \tilde{y}_f^t)$ be the position if the aircraft flies along the segment of the polygonal between time periods $t-2$ and $t-1$. Then, the point (x_f^{*t-1}, y_f^{*t-1}) has to be translated to the origin in the reference system and, then, the point (x_f^t, y_f^t) must be clockwise turned $m_f^{*t-2} - m_f^{*t-1}$ degrees. After the return to the initial position, the point in the segment between time periods $t-1$ and $t \in \mathcal{T}$ is $(\hat{x}_f^t, \hat{y}_f^t)$ can be expressed

$$\begin{aligned}\hat{x}_f^t =& (\tilde{x}_f^t - x_f^{*t-1})\cos(m_f^{*t-2} - m_f^{*t-1}) + (\tilde{y}_f^t - y_f^{*t-1})\sin(m_f^{*t-2} - m_f^{*t-1}) + x_f^{*t-1} \\ \hat{y}_f^t =& -(\tilde{x}_f^t - x_f^{*t-1})\sin(m_f^{*t-2} - m_f^{*t-1}) + (\tilde{y}_f^t - y_f^{*t-1})\cos(m_f^{*t-2} - m_f^{*t-1}) + y_f^{*t-1}.\end{aligned}$$

Once again, a translation and a turn must be done. After the translation of the point (x_f^{*t}, y_f^{*t}) to the origin in the reference system and the clockwise turn $m_f^{*t-1} - m_f^{*t}$ degrees of the point $(\hat{x}_f^t, \hat{y}_f^t)$, the final point obtained in the segment between the time periods t and

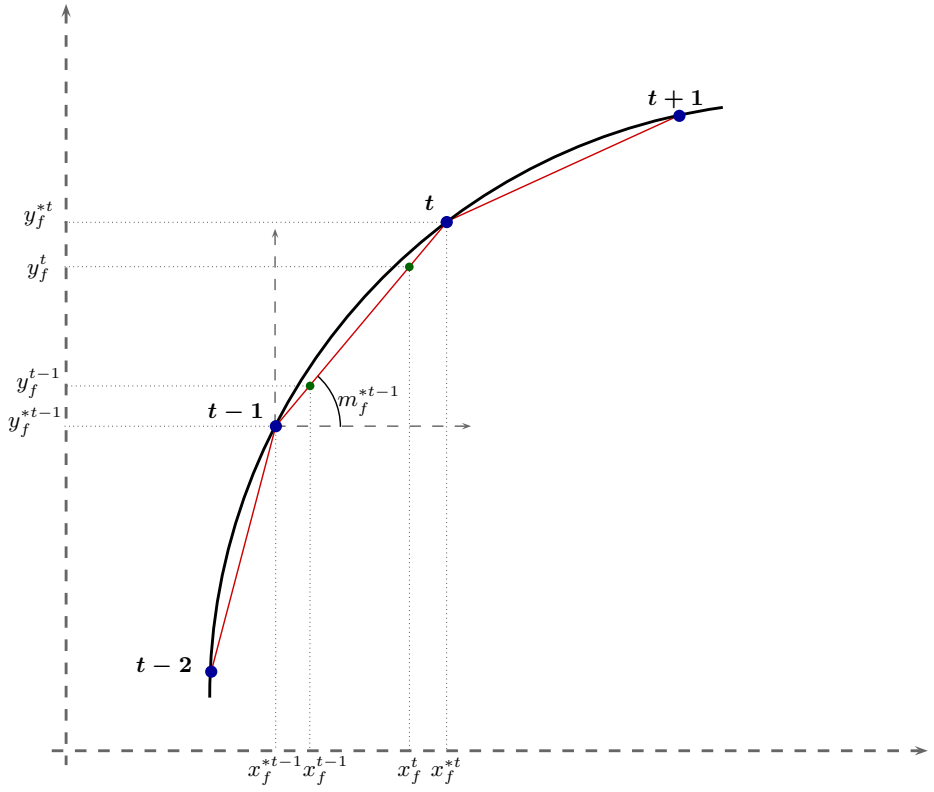

Figure B.4: Excess-Defect position situation

$t+1 \in \mathcal{T}$ can be

$$x_f^t = \Big((\tilde{x}_f^t - x_f^{*t-1})\cos(m_f^{*t-2} - m_f^{*t-1}) + (\tilde{y}_f^t - y_f^{*t-1})\sin(m_f^{*t-2} - m_f^{*t-1}) + x_f^{*t-1}\Big)$$
$$\cos(m_f^{*t-1} - m_f^{*t}) + \Big(-(\tilde{x}_f^t - x_f^{*t-1})\sin(m_f^{*t-2} - m_f^{*t-1}) + (\tilde{y}_f^t - y_f^{*t-1})\cos(m_f^{*t-2} - m_f^{*t-1})$$
$$+ y_f^{*t-1}\Big)\sin(m_f^{*t-1} - m_f^{*t}) + x_f^{*t}$$

$$y_f^t = -\Big((\tilde{x}_f^t - x_f^{*t-1})\cos(m_f^{*t-2} - m_f^{*t-1}) + (\tilde{y}_f^t - y_f^{*t-1})\sin(m_f^{*t-2} - m_f^{*t-1}) + x_f^{*t-1}\Big)$$
$$\sin(m_f^{*t-1} - m_f^{*t})$$
$$+ \Big(-(\tilde{x}_f^t - x_f^{*t-1})\sin(m_f^{*t-2} - m_f^{*t-1}) + (\tilde{y}_f^t - y_f^{*t-1})\cos(m_f^{*t-2} - m_f^{*t-1}) + y_f^{*t-1}\Big)$$
$$\cos(m_f^{*t-1} - m_f^{*t}) + y_f^{*t}.$$

Excess-Defect position situation

For this case see Fig. B.4. Let (x_f^{*t-1}, y_f^{*t-1}) and (x_f^{*t}, y_f^{*t}) be the initial configuration position for aircraft $f \in \mathcal{F}$ in time periods $t-1$ and $t \in \mathcal{T}$, respectively. This case considers the situation in which an aircraft arrives early in time period $t-1$ and later in time period $t \in \mathcal{T}$. This case is the easiest, since the translation and turn are not necessary. The final point is as follows,

$$\begin{aligned} x_f^t &= \tilde{x}_f^t \\ y_f^t &= \tilde{x}_f^t. \end{aligned}$$

B.3 Analytic results in partial derivatives

The analytic expressions for the partial derivatives are presented in this section as well as the original functions to be taken derivative. Eight nonlinear constraints are considered in the first VCTP model and four ones in the compact version of the model, after the reduction of the model dimensions. It is presented in this section the eight nonlinear expressions, since although the final VCTP model has only four nonlinear constraints, the nonlinear terms take place in the four final constraints.

The notation in the following pages in order to reduce the expressions is as follows:

- C_i for $i = 1, \ldots, 8$ denotes each set of nonlinear constraints of the VCTP model, by considering the initial approach presented in Section 3.2.1, page 82. These constraints are defined for all $t \in \mathcal{T} : t = \left\{ \max\{t_i^d, t_j^d\}, \ldots, \min\{t_i^r, t_j^r\} \right\}$, and forall $i, j \in \mathcal{F} : i < j \wedge p_{ij} = 0$.
- $R = \sqrt{(x_i^t - x_j^t)^2 + (y_i^t - y_j^t)^2 - s^2}$.

Then, the following pages present all derivatives of the nonlinear constraints with respect to variables v_i, v_j, x_i, x_j, y_i and y_j.

The initial nonlinear constraints functions are presented in this page:

$$C_1 = - v_i^t \left(\frac{(y_i^t - y_j^t)R + s(x_i^t - x_j^t)}{(x_i^t - x_j^t)R - s(y_i^t - y_j^t)} \cos(m_i^{*t}) - \sin(m_i^{*t}) \right) + v_j^t \left(\frac{(y_i^t - y_j^t)R + s(x_i^t - x_j^t)}{(x_i^t - x_j^t)R - s(y_i^t - y_j^t)} \cos(m_j^{*t}) - \sin(m_j^{*t}) \right)$$

$$C_2 = v_i^t \left(\frac{(y_i^t - y_j^t)R - s(x_i^t - x_j^t)}{(x_i^t - x_j^t)R + s(y_i^t - y_j^t)} \cos(m_i^{*t}) - \sin(m_i^{*t}) \right) - v_i^t \left(\frac{(y_i^t - y_j^t)R - s(x_i^t - x_j^t)}{(x_i^t - x_j^t)R + s(y_i^t - y_j^t)} \cos(m_j^{*t}) - \sin(m_j^{*t}) \right)$$

$$C_3 = v_i^t \left(\frac{(y_i^t - y_j^t)R + s(x_i^t - x_j^t)}{(x_i^t - x_j^t)R - s(y_i^t - y_j^t)} \cos(m_i^{*t}) - \sin(m_i^{*t}) \right) - v_j^t \left(\frac{(y_i^t - y_j^t)R + s(x_i^t - x_j^t)}{(x_i^t - x_j^t)R - s(y_i^t - y_j^t)} \cos(m_j^{*t}) - \sin(m_j^{*t}) \right)$$

$$C_4 = - v_i^t \left(\frac{(y_i^t - y_j^t)R - s(x_i^t - x_j^t)}{(x_i^t - x_j^t)R + s(y_i^t - y_j^t)} \cos(m_i^{*t}) - \sin(m_i^{*t}) \right) + v_j^t \left(\frac{(y_i^t - y_j^t)R - s(x_i^t - x_j^t)}{(x_i^t - x_j^t)R + s(y_i^t - y_j^t)} \cos(m_j^{*t}) - \sin(m_j^{*t}) \right)$$

$$C_5 = - v_i^t \left(\frac{(y_i^t - y_j^t)R + s(x_i^t - x_j^t)}{(x_i^t - x_j^t)R - s(y_i^t - y_j^t)} \sin(m_i^{*t}) - \cos(m_i^{*t}) \right) + v_j^t \left(\frac{(y_i^t - y_j^t)R + s(x_i^t - x_j^t)}{(x_i^t - x_j^t)R - s(y_i^t - y_j^t)} \sin(m_j^{*t}) - \cos(m_j^{*t}) \right)$$

$$C_6 = v_i^t \left(\frac{(y_i^t - y_j^t)R - s(x_i^t - x_j^t)}{(x_i^t - x_j^t)R + s(y_i^t - y_j^t)} \sin(m_i^{*t}) - \cos(m_i^{*t}) \right) - v_i^t \left(\frac{(y_i^t - y_j^t)R - s(x_i^t - x_j^t)}{(x_i^t - x_j^t)R + s(y_i^t - y_j^t)} \sin(m_j^{*t}) - \cos(m_j^{*t}) \right)$$

$$C_7 = v_i^t \left(\frac{(y_i^t - y_j^t)R + s(x_i^t - x_j^t)}{(x_i^t - x_j^t)R - s(y_i^t - y_j^t)} \sin(m_i^{*t}) - \cos(m_i^{*t}) \right) - v_j^t \left(\frac{(y_i^t - y_j^t)R + s(x_i^t - x_j^t)}{(x_i^t - x_j^t)R - s(y_i^t - y_j^t)} \sin(m_j^{*t}) - \cos(m_j^{*t}) \right)$$

$$C_8 = - v_i^t \left(\frac{(y_i^t - y_j^t)R - s(x_i^t - x_j^t)}{(x_i^t - x_j^t)R + s(y_i^t - y_j^t)} \sin(m_i^{*t}) - \cos(m_i^{*t}) \right) + v_j^t \left(\frac{(y_i^t - y_j^t)R - s(x_i^t - x_j^t)}{(x_i^t - x_j^t)R + s(y_i^t - y_j^t)} \sin(m_j^{*t}) - \cos(m_j^{*t}) \right)$$

In this page, the parcial derivatives of the first set of nonlinear constraints with respect to variables v_i, v_j, x_i, x_j, y_i and y_j are presented:

$$\frac{\partial C_1}{\partial v_i^t} = \sin(m_i^{*t}) - \frac{(y_i^t - y_j^t)R + s(x_i^t - x_j^t)}{(x_i^t - x_j^t)R - s(y_i^t - y_j^t)} \cos(m_i^{*t})$$

$$\frac{\partial C_1}{\partial v_j^t} = \sin(m_j^{*t}) - \frac{(y_i^t - y_j^t)R + s(x_i^t - x_j^t)}{(x_i^t - x_j^t)R - s(y_i^t - y_j^t)} \cos(m_j^{*t})$$

$$\frac{\partial C_1}{\partial x_i^t} = \left(\frac{s + \frac{(x_i^t - x_j^t)(y_i^t - y_j^t)}{R}}{(x_i^t - x_j^t)R - s(y_i^t - y_j^t)} - \frac{\left((y_i^t - y_j^t)R + s(x_i^t - x_j^t)\right)\left(R + \frac{(x_i^t - x_j^t)^2}{R}\right)}{\left((x_i^t - x_j^t)R - s(y_i^t - y_j^t)\right)^2} \right) \left(v_j^t \cos(m_j^{*t}) - v_i^t \cos(m_i^{*t}) \right)$$

$$\frac{\partial C_1}{\partial x_j^t} = \left(\frac{s + \frac{(x_i^t - x_j^t)(y_i^t - y_j^t)}{R}}{(x_i^t - x_j^t)R - s(y_i^t - y_j^t)} - \frac{\left((y_i^t - y_j^t)R + s(x_i^t - x_j^t)\right)\left(R + \frac{(x_i^t - x_j^t)^2}{R}\right)}{\left((x_i^t - x_j^t)R - s(y_i^t - y_j^t)\right)^2} \right) \left(v_i^t \cos(m_i^{*t}) - v_j^t \cos(m_j^{*t}) \right)$$

$$\frac{\partial C_1}{\partial y_i^t} = \left(\frac{R + \frac{(y_i^t - y_j^t)^2}{R}}{(x_i^t - x_j^t)R - s(y_i^t - y_j^t)} + \frac{\left((y_i^t - y_j^t)R + s(x_i^t - x_j^t)\right)\left(s - \frac{(y_i^t - y_j^t)(x_i^t - x_j^t)}{R}\right)}{\left((x_i^t - x_j^t)R - s(y_i^t - y_j^t)\right)^2} \right) \left(v_j^t \cos(m_j^{*t}) - v_i^t \cos(m_i^{*t}) \right)$$

$$\frac{\partial C_1}{\partial y_j^t} = \left(\frac{R + \frac{(y_i^t - y_j^t)^2}{R}}{(x_i^t - x_j^t)R - s(y_i^t - y_j^t)} + \frac{\left((y_i^t - y_j^t)R + s(x_i^t - x_j^t)\right)\left(s - \frac{(y_i^t - y_j^t)(x_i^t - x_j^t)}{R}\right)}{\left((x_i^t - x_j^t)R - s(y_i^t - y_j^t)\right)^2} \right) \left(v_i^t \cos(m_i^{*t}) - v_j^t \cos(m_j^{*t}) \right)$$

In this page, the parcial derivatives of the second set of nonlinear constraints with respect to variables v_i, v_j, x_i, x_j, y_i and y_j are presented:

$$\frac{\partial C_2}{\partial v_i^t} = \sin(m_i^{*t}) - \frac{(y_i^t - y_j^t)R - s(x_i^t - x_j^t)}{(x_i^t - x_j^t)R + s(y_i^t - y_j^t)} \cos(m_i^{*t})$$

$$\frac{\partial C_2}{\partial v_j^t} = \sin(m_j^{*t}) - \frac{(y_i^t - y_j^t)R - s(x_i^t - x_j^t)}{(x_i^t - x_j^t)R + s(y_i^t - y_j^t)} \cos(m_j^{*t})$$

$$\frac{\partial C_2}{\partial x_i^t} = \left(\frac{s - \frac{(x_i^t - x_j^t)(y_i^t - y_j^t)}{R}}{(x_i^t - x_j^t)R + s(y_i^t - y_j^t)} + \frac{\left((y_i^t - y_j^t)R - s(x_i^t - x_j^t)\right)\left(R + \frac{(x_i^t - x_j^t)^2}{R}\right)}{\left((x_i^t - x_j^t)R + s(y_i^t - y_j^t)\right)^2} \right) \left(v_j^t \cos(m_j^{*t}) - v_i^t \cos(m_i^{*t}) \right)$$

$$\frac{\partial C_2}{\partial x_j^t} = \left(\frac{s - \frac{(x_i^t - x_j^t)(y_i^t - y_j^t)}{R}}{(x_i^t - x_j^t)R + s(y_i^t - y_j^t)} + \frac{\left((y_i^t - y_j^t)R - s(x_i^t - x_j^t)\right)\left(R + \frac{(x_i^t - x_j^t)^2}{R}\right)}{\left((x_i^t - x_j^t)R + s(y_i^t - y_j^t)\right)^2} \right) \left(v_i^t \cos(m_i^{*t}) - v_j^t \cos(m_j^{*t}) \right)$$

$$\frac{\partial C_2}{\partial y_i^t} = \left(\frac{R + \frac{(y_i^t - y_j^t)^2}{R}}{(x_i^t - x_j^t)R + s(y_i^t - y_j^t)} - \frac{\left((y_i^t - y_j^t)R - s(x_i^t - x_j^t)\right)\left(s + \frac{(y_i^t - y_j^t)(x_i^t - x_j^t)}{R}\right)}{\left((x_i^t - x_j^t)R + s(y_i^t - y_j^t)\right)^2} \right) \left(v_i^t \cos(m_i^{*t}) - v_j^t \cos(m_j^{*t}) \right)$$

$$\frac{\partial C_2}{\partial y_j^t} = \left(\frac{R + \frac{(y_i^t - y_j^t)^2}{R}}{(x_i^t - x_j^t)R + s(y_i^t - y_j^t)} - \frac{\left((y_i^t - y_j^t)R - s(x_i^t - x_j^t)\right)\left(s + \frac{(y_i^t - y_j^t)(x_i^t - x_j^t)}{R}\right)}{\left((x_i^t - x_j^t)R + s(y_i^t - y_j^t)\right)^2} \right) \left(v_j^t \cos(m_j^{*t}) - v_i^t \cos(m_i^{*t}) \right)$$

In this page, the parcial derivatives of the third set of nonlinear constraints with respect to variables v_i, v_j, x_i, x_j, y_i and y_j are presented:

$$\frac{\partial C_3}{\partial v_i^t} = \sin(m_i^{*t}) - \frac{(y_i^t - y_j^t)R + s(x_i^t - x_j^t)}{(x_i^t - x_j^t)R - s(y_i^t - y_j^t)} \cos(m_i^{*t})$$

$$\frac{\partial C_3}{\partial v_j^t} = \sin(m_j^{*t}) - \frac{(y_i^t - y_j^t)R + s(x_i^t - x_j^t)}{(x_i^t - x_j^t)R - s(y_i^t - y_j^t)} \cos(m_j^{*t})$$

$$\frac{\partial C_3}{\partial x_i^t} = \left(\frac{s + \frac{(x_i^t - x_j^t)(y_i^t - y_j^t)}{R}}{(x_i^t - x_j^t)R - s(y_i^t - y_j^t)} - \frac{\left((y_i^t - y_j^t)R + s(x_i^t - x_j^t)\right)\left(R + \frac{(x_i^t - x_j^t)^2}{R}\right)}{\left((x_i^t - x_j^t)R - s(y_i^t - y_j^t)\right)^2} \right) \left(v_i^t \cos(m_i^{*t}) - v_j^t \cos(m_j^{*t}) \right)$$

$$\frac{\partial C_3}{\partial x_j^t} = \left(\frac{s + \frac{(x_i^t - x_j^t)(y_i^t - y_j^t)}{R}}{(x_i^t - x_j^t)R - s(y_i^t - y_j^t)} - \frac{\left((y_i^t - y_j^t)R + s(x_i^t - x_j^t)\right)\left(R + \frac{(x_i^t - x_j^t)^2}{R}\right)}{\left((x_i^t - x_j^t)R - s(y_i^t - y_j^t)\right)^2} \right) \left(v_j^t \cos(m_j^{*t}) - v_i^t \cos(m_i^{*t}) \right)$$

$$\frac{\partial C_3}{\partial y_i^t} = \left(\frac{R + \frac{(y_i^t - y_j^t)^2}{R}}{(x_i^t - x_j^t)R - s(y_i^t - y_j^t)} + \frac{\left((y_i^t - y_j^t)R + s(x_i^t - x_j^t)\right)\left(s - \frac{(y_i^t - y_j^t)(x_i^t - x_j^t)}{R}\right)}{\left((x_i^t - x_j^t)R - s(y_i^t - y_j^t)\right)^2} \right) \left(v_i^t \cos(m_i^{*t}) - v_j^t \cos(m_j^{*t}) \right)$$

$$\frac{\partial C_3}{\partial y_j^t} = \left(\frac{R + \frac{(y_i^t - y_j^t)^2}{R}}{(x_i^t - x_j^t)R - s(y_i^t - y_j^t)} + \frac{\left((y_i^t - y_j^t)R + s(x_i^t - x_j^t)\right)\left(s - \frac{(y_i^t - y_j^t)(x_i^t - x_j^t)}{R}\right)}{\left((x_i^t - x_j^t)R - s(y_i^t - y_j^t)\right)^2} \right) \left(v_j^t \cos(m_j^{*t}) - v_i^t \cos(m_i^{*t}) \right)$$

In this page, the parcial derivatives of the fourth set of nonlinear constraints with respect to variables v_i, v_j, x_i, x_j, y_i and y_j are presented:

$$\frac{\partial C_4}{\partial v_i^t} = \sin(m_i^{*t}) - \frac{(y_i^t - y_j^t)R - s(x_i^t - x_j^t)}{(x_i^t - x_j^t)R + s(y_i^t - y_j^t)} \cos(m_i^{*t})$$

$$\frac{\partial C_4}{\partial v_j^t} = \sin(m_j^{*t}) - \frac{(y_i^t - y_j^t)R - s(x_i^t - x_j^t)}{(x_i^t - x_j^t)R + s(y_i^t - y_j^t)} \cos(m_j^{*t})$$

$$\frac{\partial C_4}{\partial x_i^t} = \left(\frac{s - \frac{(x_i^t - x_j^t)(y_i^t - y_j^t)}{R}}{(x_i^t - x_j^t)R + s(y_i^t - y_j^t)} + \frac{\left((y_i^t - y_j^t)R - s(x_i^t - x_j^t)\right)\left(R + \frac{(x_i^t - x_j^t)^2}{R}\right)}{\left((x_i^t - x_j^t)R + s(y_i^t - y_j^t)\right)^2} \right) \left(v_i^t \cos(m_i^{*t}) - v_j^t \cos(m_j^{*t}) \right)$$

$$\frac{\partial C_4}{\partial x_j^t} = \left(\frac{s - \frac{(x_i^t - x_j^t)(y_i^t - y_j^t)}{R}}{(x_i^t - x_j^t)R + s(y_i^t - y_j^t)} + \frac{\left((y_i^t - y_j^t)R - s(x_i^t - x_j^t)\right)\left(R + \frac{(x_i^t - x_j^t)^2}{R}\right)}{\left((x_i^t - x_j^t)R + s(y_i^t - y_j^t)\right)^2} \right) \left(v_j^t \cos(m_j^{*t}) - v_i^t \cos(m_i^{*t}) \right)$$

$$\frac{\partial C_4}{\partial y_i^t} = \left(\frac{R + \frac{(y_i^t - y_j^t)^2}{R}}{(x_i^t - x_j^t)R + s(y_i^t - y_j^t)} - \frac{\left((y_i^t - y_j^t)R - s(x_i^t - x_j^t)\right)\left(s + \frac{(y_i^t - y_j^t)(x_i^t - x_j^t)}{R}\right)}{\left((x_i^t - x_j^t)R + s(y_i^t - y_j^t)\right)^2} \right) \left(v_j^t \cos(m_j^{*t}) - v_i^t \cos(m_i^{*t}) \right)$$

$$\frac{\partial C_4}{\partial y_j^t} = \left(\frac{R + \frac{(y_i^t - y_j^t)^2}{R}}{(x_i^t - x_j^t)R + s(y_i^t - y_j^t)} - \frac{\left((y_i^t - y_j^t)R - s(x_i^t - x_j^t)\right)\left(s + \frac{(y_i^t - y_j^t)(x_i^t - x_j^t)}{R}\right)}{\left((x_i^t - x_j^t)R + s(y_i^t - y_j^t)\right)^2} \right) \left(v_i^t \cos(m_i^{*t}) - v_j^t \cos(m_j^{*t}) \right)$$

In this page, the parcial derivatives of the fifth set of nonlinear constraints with respect to variables v_i, v_j, x_i, x_j, y_i and y_j are presented:

$$\frac{\partial C_5}{\partial v_i^t} = \cos(m_i^{*t}) - \frac{(x_i^t - x_j^t)R - s(y_i^t - y_j^t)}{(y_i^t - y_j^t)R + s(x_i^t - x_j^t)} \sin(m_i^{*t})$$

$$\frac{\partial C_5}{\partial v_j^t} = \cos(m_j^{*t}) - \frac{(x_i^t - x_j^t)R - s(y_i^t - y_j^t)}{(y_i^t - y_j^t)R + s(x_i^t - x_j^t)} \sin(m_j^{*t})$$

$$\frac{\partial C_5}{\partial x_i^t} = \left(\frac{R + \frac{(x_i^t - x_j^t)^2}{R}}{(y_i^t - y_j^t)R + s(x_i^t - x_j^t)} - \frac{\left((x_i^t - x_j^t)R - s(y_i^t - y_j^t)\right)\left(s + \frac{(x_i^t - x_j^t)(y_i^t - y_j^t)}{R}\right)}{\left((y_i^t - y_j^t)R + s(x_i^t - x_j^t)\right)^2} \right) \left(v_j^t \sin(m_j^{*t}) - v_i^t \sin(m_i^{*t}) \right)$$

$$\frac{\partial C_5}{\partial x_j^t} = \left(\frac{R + \frac{(x_i^t - x_j^t)^2}{R}}{(y_i^t - y_j^t)R + s(x_i^t - x_j^t)} - \frac{\left((x_i^t - x_j^t)R - s(y_i^t - y_j^t)\right)\left(s + \frac{(x_i^t - x_j^t)(y_i^t - y_j^t)}{R}\right)}{\left((y_i^t - y_j^t)R + s(x_i^t - x_j^t)\right)^2} \right) \left(v_i^t \sin(m_i^{*t}) - v_j^t \sin(m_j^{*t}) \right)$$

$$\frac{\partial C_5}{\partial y_i^t} = \left(\frac{s - \frac{(y_i^t - y_j^t)(x_i^t - x_j^t)}{R}}{(y_i^t - y_j^t)R + s(x_i^t - x_j^t)} + \frac{\left((x_i^t - x_j^t)R - s(y_i^t - y_j^t)\right)\left(R + \frac{(y_i^t - y_j^t)^2}{R}\right)}{\left((y_i^t - y_j^t)R + s(x_i^t - x_j^t)\right)^2} \right) \left(v_i^t \sin(m_i^{*t}) - v_j^t \sin(m_j^{*t}) \right)$$

$$\frac{\partial C_5}{\partial y_j^t} = \left(\frac{s - \frac{(y_i^t - y_j^t)(x_i^t - x_j^t)}{R}}{(y_i^t - y_j^t)R + s(x_i^t - x_j^t)} + \frac{\left((x_i^t - x_j^t)R - s(y_i^t - y_j^t)\right)\left(R + \frac{(y_i^t - y_j^t)^2}{R}\right)}{\left((y_i^t - y_j^t)R + s(x_i^t - x_j^t)\right)^2} \right) \left(v_j^t \sin(m_j^{*t}) - v_i^t \sin(m_i^{*t}) \right)$$

In this page, the parcial derivatives of the sixth set of nonlinear constraints with respect to variables v_i, v_j, x_i, x_j, y_i and y_j are presented:

$$\frac{\partial C_6}{\partial v_i^t} = \cos(m_i^{*t}) - \frac{(x_i^t - x_j^t)R + s(y_i^t - y_j^t)}{(y_i^t - y_j^t)R - s(x_i^t - x_j^t)} \sin(m_i^{*t})$$

$$\frac{\partial C_6}{\partial v_j^t} = \cos(m_j^{*t}) - \frac{(x_i^t - x_j^t)R + s(y_i^t - y_j^t)}{(y_i^t - y_j^t)R - s(x_i^t - x_j^t)} \sin(m_j^{*t})$$

$$\frac{\partial C_6}{\partial x_i^t} = \left(\frac{R + \frac{(x_i^t - x_j^t)^2}{R}}{(y_i^t - y_j^t)R - s(x_i^t - x_j^t)} + \frac{\left((x_i^t - x_j^t)R + s(y_i^t - y_j^t)\right)\left(s - \frac{(x_i^t - x_j^t)(y_i^t - y_j^t)}{R}\right)}{\left((y_i^t - y_j^t)R - s(x_i^t - x_j^t)\right)^2} \right) \left(v_i^t \sin(m_i^{*t}) - v_j^t \sin(m_j^{*t}) \right)$$

$$\frac{\partial C_6}{\partial x_j^t} = \left(\frac{R + \frac{(x_i^t - x_j^t)^2}{R}}{(y_i^t - y_j^t)R - s(x_i^t - x_j^t)} + \frac{\left((x_i^t - x_j^t)R + s(y_i^t - y_j^t)\right)\left(s - \frac{(x_i^t - x_j^t)(y_i^t - y_j^t)}{R}\right)}{\left((y_i^t - y_j^t)R - s(x_i^t - x_j^t)\right)^2} \right) \left(v_j^t \sin(m_j^{*t}) - v_i^t \sin(m_i^{*t}) \right)$$

$$\frac{\partial C_6}{\partial y_i^t} = \left(\frac{s + \frac{(y_i^t - y_j^t)(x_i^t - x_j^t)}{R}}{(y_i^t - y_j^t)R - s(x_i^t - x_j^t)} - \frac{\left((x_i^t - x_j^t)R + s(y_i^t - y_j^t)\right)\left(R + \frac{(y_i^t - y_j^t)^2}{R}\right)}{\left((y_i^t - y_j^t)R - s(x_i^t - x_j^t)\right)^2} \right) \left(v_i^t \sin(m_i^{*t}) - v_j^t \sin(m_j^{*t}) \right)$$

$$\frac{\partial C_6}{\partial y_j^t} = \left(\frac{s + \frac{(y_i^t - y_j^t)(x_i^t - x_j^t)}{R}}{(y_i^t - y_j^t)R - s(x_i^t - x_j^t)} - \frac{\left((x_i^t - x_j^t)R + s(y_i^t - y_j^t)\right)\left(R + \frac{(y_i^t - y_j^t)^2}{R}\right)}{\left((y_i^t - y_j^t)R - s(x_i^t - x_j^t)\right)^2} \right) \left(v_j^t \sin(m_j^{*t}) - v_i^t \sin(m_i^{*t}) \right)$$

In this page, the parcial derivatives of the seventh set of nonlinear constraints with respect to variables v_i, v_j, x_i, x_j, y_i and y_j are presented:

$$\frac{\partial C_7}{\partial v_i^t} = \cos(m_i^{*t}) - \frac{(x_i^t - x_j^t)R - s(y_i^t - y_j^t)}{(y_i^t - y_j^t)R + s(x_i^t - x_j^t)} \sin(m_i^{*t})$$

$$\frac{\partial C_7}{\partial v_j^t} = \cos(m_j^{*t}) - \frac{(x_i^t - x_j^t)R - s(y_i^t - y_j^t)}{(y_i^t - y_j^t)R + s(x_i^t - x_j^t)} \sin(m_j^{*t})$$

$$\frac{\partial C_7}{\partial x_i^t} = \left(\frac{R + \frac{(x_i^t - x_j^t)^2}{R}}{(y_i^t - y_j^t)R + s(x_i^t - x_j^t)} - \frac{\left((x_i^t - x_j^t)R - s(y_i^t - y_j^t)\right)\left(s + \frac{(x_i^t - x_j^t)(y_i^t - y_j^t)}{R}\right)}{\left((y_i^t - y_j^t)R + s(x_i^t - x_j^t)\right)^2} \right) \left(v_i^t \sin(m_i^{*t}) - v_j^t \sin(m_j^{*t}) \right)$$

$$\frac{\partial C_7}{\partial x_j^t} = \left(\frac{R + \frac{(x_i^t - x_j^t)^2}{R}}{(y_i^t - y_j^t)R + s(x_i^t - x_j^t)} - \frac{\left((x_i^t - x_j^t)R - s(y_i^t - y_j^t)\right)\left(s + \frac{(x_i^t - x_j^t)(y_i^t - y_j^t)}{R}\right)}{\left((y_i^t - y_j^t)R + s(x_i^t - x_j^t)\right)^2} \right) \left(v_j^t \sin(m_j^{*t}) - v_i^t \sin(m_i^{*t}) \right)$$

$$\frac{\partial C_7}{\partial y_i^t} = \left(\frac{s - \frac{(y_i^t - y_j^t)(x_i^t - x_j^t)}{R}}{(y_i^t - y_j^t)R + s(x_i^t - x_j^t)} + \frac{\left((x_i^t - x_j^t)R - s(y_i^t - y_j^t)\right)\left(R + \frac{(y_i^t - y_j^t)^2}{R}\right)}{\left((y_i^t - y_j^t)R + s(x_i^t - x_j^t)\right)^2} \right) \left(v_j^t \sin(m_j^{*t}) - v_i^t \sin(m_i^{*t}) \right)$$

$$\frac{\partial C_7}{\partial y_j^t} = \left(\frac{s - \frac{(y_i^t - y_j^t)(x_i^t - x_j^t)}{R}}{(y_i^t - y_j^t)R + s(x_i^t - x_j^t)} + \frac{\left((x_i^t - x_j^t)R - s(y_i^t - y_j^t)\right)\left(R + \frac{(y_i^t - y_j^t)^2}{R}\right)}{\left((y_i^t - y_j^t)R + s(x_i^t - x_j^t)\right)^2} \right) \left(v_i^t \sin(m_i^{*t}) - v_j^t \sin(m_j^{*t}) \right)$$

In this page, the parcial derivatives of the eighth set of nonlinear constraints with respect to variables v_i, v_j, x_i, x_j, y_i and y_j are presented:

$$\frac{\partial C_8}{\partial v_i^t} = \cos(m_i^{*t}) - \frac{(x_i^t - x_j^t)R + s(y_i^t - y_j^t)}{(y_i^t - y_j^t)R - s(x_i^t - x_j^t)} \sin(m_i^{*t})$$

$$\frac{\partial C_8}{\partial v_j^t} = \cos(m_j^{*t}) - \frac{(x_i^t - x_j^t)R + s(y_i^t - y_j^t)}{(y_i^t - y_j^t)R - s(x_i^t - x_j^t)} \sin(m_j^{*t})$$

$$\frac{\partial C_8}{\partial x_i^t} = \left(\frac{R + \frac{(x_i^t - x_j^t)^2}{R}}{(y_i^t - y_j^t)R - s(x_i^t - x_j^t)} + \frac{\left((x_i^t - x_j^t)R + s(y_i^t - y_j^t)\right)\left(s - \frac{(x_i^t - x_j^t)(y_i^t - y_j^t)}{R}\right)}{\left((y_i^t - y_j^t)R - s(x_i^t - x_j^t)\right)^2} \right) \left(v_j^t \sin(m_j^{*t}) - v_i^t \sin(m_i^{*t}) \right)$$

$$\frac{\partial C_8}{\partial x_j^t} = \left(\frac{R + \frac{(x_i^t - x_j^t)^2}{R}}{(y_i^t - y_j^t)R - s(x_i^t - x_j^t)} + \frac{\left((x_i^t - x_j^t)R + s(y_i^t - y_j^t)\right)\left(s - \frac{(x_i^t - x_j^t)(y_i^t - y_j^t)}{R}\right)}{\left((y_i^t - y_j^t)R - s(x_i^t - x_j^t)\right)^2} \right) \left(v_i^t \sin(m_i^{*t}) - v_j^t \sin(m_j^{*t}) \right)$$

$$\frac{\partial C_8}{\partial y_i^t} = \left(\frac{s + \frac{(y_i^t - y_j^t)(x_i^t - x_j^t)}{R}}{(y_i^t - y_j^t)R - s(x_i^t - x_j^t)} - \frac{\left((x_i^t - x_j^t)R + s(y_i^t - y_j^t)\right)\left(R + \frac{(y_i^t - y_j^t)^2}{R}\right)}{\left((y_i^t - y_j^t)R - s(x_i^t - x_j^t)\right)^2} \right) \left(v_j^t \sin(m_j^{*t}) - v_i^t \sin(m_i^{*t}) \right)$$

$$\frac{\partial C_8}{\partial y_j^t} = \left(\frac{s + \frac{(y_i^t - y_j^t)(x_i^t - x_j^t)}{R}}{(y_i^t - y_j^t)R - s(x_i^t - x_j^t)} - \frac{\left((x_i^t - x_j^t)R + s(y_i^t - y_j^t)\right)\left(R + \frac{(y_i^t - y_j^t)^2}{R}\right)}{\left((y_i^t - y_j^t)R - s(x_i^t - x_j^t)\right)^2} \right) \left(v_i^t \sin(m_i^{*t}) - v_j^t \sin(m_j^{*t}) \right)$$

B.4 Computational results for the VCTP model (by using exact schemes)

Part of the computational experience for the VCTP is presented in detail in this section. This optimization engine CPLEX [63] is used. Three types of tables are presented for each dimensional case, namely,

- The model dimensions where the headings are as follows:
  - *Case*: Case configuration: CAAA denotes number of aircraft (AAA).
  - *nit*: Number of iteration in the Taylor approximation.
  - m: Number of constraints.
  - n: Number of variables.
  - nel: Number of non zero elements.
  - d: Constraints matrix density.
  - m^*, n^*, nel^* and d^*: Number of constraints, variables and constraints matrix, non zero elements and density, respectively, after the preprocessing made by CPLEX.
- The results where the headings are as follows:
  - *Case*: Case configuration: CAAA denotes number of aircraft (AAA).
  - *nit*: Number of iterations in the Taylor approximation.
  - z_{lp}: Value of the objective function in the continuous linear relaxation.
  - z_s: Value of the bound after performing the CPLEX cut identification and appending at node 0
  - z_{ip}: Value of the objective function for the optimal solution of the problem.
  - GAP_{lp}: $\frac{z_{ip}-z_{lp}}{z_{ip}}$
  - GAP_s: $\frac{z_{ip}-z_s}{z_{ip}}$
  - nb: Number of times that there is branching
  - nn: Number of CPLEX branch-and-cut nodes
  - t_{lp}: Time (secs.) to obtain the z_{lp} value
  - t_s: Time (secs.) to obtain the z_s value.

  - t_{ip}: Time (secs.) to obtain the z_{ip} value.
  - nc: Total number of cuts performed by CPLEX.

- The number of cuts done identified and appended to the model by CPLEX where the headings are as follows:

  - *Case*: Case configuration: CAAA-ZZ denotes number of aircraft (AAA).
  - *nit*: Number of iterations in the Taylor approximation.
  - Clique: Number of clique cuts.
  - Cover: Number of Cover cuts.
  - Implied: Number of Implied cuts.
  - Flow: Number of Flow cuts.
  - MIR: Number of Mixed Integer Rounding cuts.
  - Zero-Half: Number of Zero-half cuts.
  - Gomory: Number of Gomory cuts.
  - Total: Total number of cuts.

Only the cases for 20 aircraft are presented. The rest of the cases in the testbed reported in this thesis can be found in the extended version of the thesis in the CD enclosed with this thesis.

Table B.1: Dimensions for 20 aircrafts ($\lambda = 0.80$).

Case	**nit.**	m	n	nel	d	m^*	n^*	nel^*	d^*
C020-001	1	3876	5270	35730	0.0017	3836	1878	32710	0.0045
Averages:	1	3876.0	5270.0	35730.0	0.0017	3836.0	1878.0	32710.0	0.0045
C020-002	1	4549	5502	45524	0.0018	4508	2214	42020	0.0042
	2	4549	5502	45524	0.0018	4508	2214	42020	0.0042
	3	4549	5502	45524	0.0018	4508	2214	42020	0.0042
	4	4549	5502	45524	0.0018	4508	2214	42020	0.0042
	5	4549	5502	45524	0.0018	4508	2214	42020	0.0042
	6	4549	5502	45524	0.0018	4508	2214	42020	0.0042
	7	4549	5502	45524	0.0018	4508	2214	42020	0.0042
	8	4549	5502	45524	0.0018	4508	2214	42020	0.0042
	9	4549	5502	45524	0.0018	4508	2214	42020	0.0042
	10	4549	5502	45524	0.0018	4508	2214	42020	0.0042

(It is continued in the next page)

Dimensions table for 20 aircrafts ($\lambda = 0.80$).

Case	Iter.	m	n	nel	d	m^*	n^*	nel^*	d^*
Averages:	10	4549.0	5502.0	45524.0	0.0018	4508.0	2214.0	42020.0	0.0042
C020-003	1	3512	4768	29550	0.0018	3472	1696	26790	0.0045
Averages:	1	3512.0	4768.0	29550.0	0.0018	3472.0	1696.0	26790.0	0.0045
C020-004	1	3568	3676	31410	0.0024	3528	1724	28610	0.0047
Averages:	1	3568.0	3676.0	31410.0	0.0024	3528.0	1724.0	28610.0	0.0047
C020-005	1	3400	3704	28770	0.0023	3360	1640	26090	0.0047
Averages:	1	3400.0	3704.0	28770.0	0.0023	3360.0	1640.0	26090.0	0.0047
C020-006	1	4296	6196	41710	0.0016	4242	2082	38352	0.0043
	2	4296	6196	41710	0.0016	4242	2082	38352	0.0043
	3	4296	6196	41710	0.0016	4242	2082	38352	0.0043
	4	4296	6196	41710	0.0016	4242	2082	38352	0.0043
	5	4296	6196	41710	0.0016	4242	2082	38352	0.0043
	6	4296	6196	41710	0.0016	4242	2082	38352	0.0043
	7	4296	6196	41710	0.0016	4242	2082	38352	0.0043
	8	4296	6196	41710	0.0016	4242	2082	38352	0.0043
	9	4296	6196	41710	0.0016	4242	2082	38352	0.0043
	10	4296	6196	41710	0.0016	4242	2082	38352	0.0043
Averages:	10	4296.0	6196.0	41710.0	0.0016	4242.0	2082.0	38352.0	0.0043
C020-007	1	3176	3928	24230	0.0019	3136	1528	21710	0.0045
Averages:	1	3176.0	3928.0	24230.0	0.0019	3136.0	1528.0	21710.0	0.0045
C020-008	1	3960	4800	34680	0.0018	3914	1914	31580	0.0042
Averages:	1	3960.0	4800.0	34680.0	0.0018	3914.0	1914.0	31580.0	0.0042
C020-009	1	3918	5215	36570	0.0018	3875	1896	33510	0.0046
	2	3918	5215	36570	0.0018	3875	1896	33510	0.0046
	3	3918	5215	36570	0.0018	3875	1896	33510	0.0046
	4	3918	5215	36570	0.0018	3875	1896	33510	0.0046
	5	3918	5215	36570	0.0018	3875	1896	33510	0.0046
	6	3918	5215	36570	0.0018	3875	1896	33510	0.0046
	7	3918	5215	36570	0.0018	3875	1896	33510	0.0046
	8	3918	5215	36570	0.0018	3875	1896	33510	0.0046
	9	3918	5215	36570	0.0018	3875	1896	33510	0.0046
	10	3918	5215	36570	0.0018	3875	1896	33510	0.0046
Averages:	10	3918.0	5215.0	36570.0	0.0018	3875.0	1896.0	33510.0	0.0046
C020-010	1	5164	7110	56640	0.0015	5124	2522	52700	0.0041
Averages:	1	5164.0	7110.0	56640.0	0.0015	5124.0	2522.0	52700.0	0.0041
C020-011	1	3610	4313	31000	0.0020	3556	1739	28132	0.0045
	2	3610	4313	31000	0.0020	3556	1739	28132	0.0045
	3	3610	4313	31000	0.0020	3556	1739	28132	0.0045

(It is continued in the next page)

Dimensions table for 20 aircrafts ($\lambda = 0.80$).

Case	Iter.	m	n	nel	d	m^*	n^*	nel^*	d^*
	4	3610	4313	31000	0.0020	3556	1739	28132	0.0045
	5	3610	4313	31000	0.0020	3556	1739	28132	0.0045
	6	3610	4313	31000	0.0020	3556	1739	28132	0.0045
	7	3610	4313	31000	0.0020	3556	1739	28132	0.0045
Averages:	7	3610.0	4313.0	31000.0	0.0020	3556.0	1739.0	28132.0	0.0045
C020-012	1	4310	5699	41090	0.0017	4264	2089	37740	0.0042
Averages:	1	4310.0	5699.0	41090.0	0.0017	4264.0	2089.0	37740.0	0.0042
C020-013	1	5024	8716	51100	0.0012	4981	2449	47250	0.0039
	2	5024	8716	51100	0.0012	4981	2449	47250	0.0039
Averages:	2	5024.0	8716.0	51100.0	0.0012	4981.0	2449.0	47250.0	0.0039
C020-014	1	3946	4457	37220	0.0021	3906	1913	34150	0.0046
Averages:	1	3946.0	4457.0	37220.0	0.0021	3906.0	1913.0	34150.0	0.0046
C020-015	1	3708	4198	32800	0.0021	3668	1794	29900	0.0045
Averages:	1	3708.0	4198.0	32800.0	0.0021	3668.0	1794.0	29900.0	0.0045
C020-016	1	3610	4421	32270	0.0020	3570	1745	29440	0.0047
	2	3610	4421	32270	0.0020	3570	1745	29440	0.0047
	3	3610	4421	32270	0.0020	3570	1745	29440	0.0047
	4	3610	4421	32270	0.0020	3570	1745	29440	0.0047
	5	3610	4421	32270	0.0020	3570	1745	29440	0.0047
	6	3610	4421	32270	0.0020	3570	1745	29440	0.0047
	7	3610	4421	32270	0.0020	3570	1745	29440	0.0047
	8	3610	4421	32270	0.0020	3570	1745	29440	0.0047
	9	3610	4421	32270	0.0020	3570	1745	29440	0.0047
Averages:	9	3610.0	4421.0	32270.0	0.0020	3570.0	1745.0	29440.0	0.0047
C020-017	1	4114	5053	37880	0.0018	4074	1997	34690	0.0043
Averages:	1	4114.0	5053.0	37880.0	0.0018	4074.0	1997.0	34690.0	0.0043
C020-018	1	3891	5305	34104	0.0017	3850	1885	31070	0.0043
Averages:	1	3891.0	5305.0	34104.0	0.0017	3850.0	1885.0	31070.0	0.0043
C020-019	1	3722	4389	32460	0.0020	3682	1801	29550	0.0045
Averages:	1	3722.0	4389.0	32460.0	0.0020	3682.0	1801.0	29550.0	0.0045
C020-020	1	4338	5561	41210	0.0017	4298	2109	37860	0.0042
	2	4338	5561	41210	0.0017	4298	2109	37860	0.0042
	3	4338	5561	41210	0.0017	4298	2109	37860	0.0042
	4	4338	5561	41210	0.0017	4298	2109	37860	0.0042
	5	4338	5561	41210	0.0017	4298	2109	37860	0.0042
	6	4338	5561	41210	0.0017	4298	2109	37860	0.0042
	7	4338	5561	41210	0.0017	4298	2109	37860	0.0042
	8	4338	5561	41210	0.0017	4298	2109	37860	0.0042

(It is continued in the next page)

Dimensions table for 20 aircrafts ($\lambda = 0.80$).

Case	Iter.	m	n	nel	d	m^*	n^*	nel^*	d^*
	9	4338	5561	41210	0.0017	4298	2109	37860	0.0042
	10	4338	5561	41210	0.0017	4298	2109	37860	0.0042
Averages:	10	4338.0	5561.0	41210.0	0.0017	4298.0	2109.0	37860.0	0.0042
C020-021	1	4199	5791	39194	0.0016	4158	2039	35940	0.0042
Averages:	1	4199.0	5791.0	39194.0	0.0016	4158.0	2039.0	35940.0	0.0042
C020-022	1	4086	5003	35820	0.0018	4046	1983	32650	0.0041
Averages:	1	4086.0	5003.0	35820.0	0.0018	4046.0	1983.0	32650.0	0.0041
C020-023	1	3316	3982	27710	0.0021	3276	1598	25090	0.0048
Averages:	1	3316.0	3982.0	27710.0	0.0021	3276.0	1598.0	25090.0	0.0048
C020-024	1	4128	5192	39770	0.0019	4085	2001	36560	0.0045
	2	4128	5192	39770	0.0019	4085	2001	36560	0.0045
	3	4128	5192	39770	0.0019	4085	2001	36560	0.0045
	4	4128	5192	39770	0.0019	4085	2001	36560	0.0045
	5	4128	5192	39770	0.0019	4085	2001	36560	0.0045
	6	4128	5192	39770	0.0019	4085	2001	36560	0.0045
	7	4128	5192	39770	0.0019	4085	2001	36560	0.0045
	8	4128	5192	39770	0.0019	4085	2001	36560	0.0045
	9	4128	5192	39770	0.0019	4085	2001	36560	0.0045
Averages:	9	4128.0	5192.0	39770.0	0.0019	4085.0	2001.0	36560.0	0.0045
C020-025	1	3526	4091	28920	0.0020	3486	1703	26150	0.0044
Averages:	1	3526.0	4091.0	28920.0	0.0020	3486.0	1703.0	26150.0	0.0044
C020	3.4	3957.9	5053.6	36294.5	0.0018	3915.8	1917.6	33209.8	0.0044

(Table end.)

Table B.2: Results for 20 aircrafts ($\lambda = 0.80$).

Case	Iter.	z_{lp}	z_s	z_{ip}	GAP_{lp}	GAP_s	nn	t_{lp}	t_s	t_{ip}
C020-001	1	0.0007	0.0162	0.0162	0.9564	0.0000	0	0.23	0.86	0.86
F. Solution:	1	0.0007	0.0162	0.0162	0.9564	0.0000	0	0.23	0.86	0.86
C020-002	1	0.0001	0.0159	0.0156	0.9936	0.0000	334	0.28	1.56	8.38
C020-002	2	0.0001	0.0159	0.0156	0.9936	0.0000	334	0.26	1.56	8.30
C020-002	3	0.0001	0.0159	0.0156	0.9936	0.0000	334	0.26	1.58	8.36
C020-002	4	0.0001	0.0159	0.0156	0.9936	0.0000	334	0.25	1.56	8.33
C020-002	5	0.0001	0.0159	0.0156	0.9936	0.0000	334	0.27	1.61	8.28
C020-002	6	0.0001	0.0159	0.0156	0.9936	0.0000	334	0.27	1.55	8.56
C020-002	7	0.0001	0.0159	0.0156	0.9936	0.0000	334	0.25	1.56	8.35
C020-002	8	0.0001	0.0159	0.0156	0.9936	0.0000	334	0.27	1.56	8.39
C020-002	9	0.0001	0.0159	0.0156	0.9936	0.0000	334	0.25	1.56	8.14

(It is continued in the next page)

Results table for 20 aircrafts ($\lambda = 0.80$).

Case	Iter.	z_{lp}	z_s	z_{ip}	GAP_{lp}	GAP_s	nn	t_{lp}	t_s	t_{ip}
C020-002	10	0.0001	0.0159	0.0156	0.9936	0.0000	334	0.27	1.58	8.27
F. Solution:	10	0.0001	0.0159	0.0156	0.9936	0.0000	334	2.62	15.66	83.37
C020-003	1	0.0001	0.0134	0.0134	0.9931	0.0000	0	0.17	0.23	0.22
F. Solution:	1	0.0001	0.0134	0.0134	0.9931	0.0000	0	0.17	0.23	0.22
C020-004	1	0.0019	0.0183	0.0183	0.8938	0.0000	0	0.17	0.22	0.22
F. Solution:	1	0.0019	0.0183	0.0183	0.8938	0.0000	0	0.17	0.22	0.22
C020-005	1	0.0000	0.0115	0.0115	1.0000	0.0000	0	0.17	0.20	0.20
F. Solution:	1	0.0000	0.0115	0.0115	1.0000	0.0000	0	0.17	0.20	0.20
C020-006	1	0.0082	0.0264	0.0261	0.6848	0.0000	369	0.25	1.79	3.15
C020-006	2	0.0082	0.0264	0.0261	0.6848	0.0000	369	0.23	1.84	3.15
C020-006	3	0.0082	0.0264	0.0261	0.6848	0.0000	369	0.23	1.86	3.20
C020-006	4	0.0082	0.0264	0.0261	0.6848	0.0000	369	0.23	1.79	3.14
C020-006	5	0.0082	0.0264	0.0261	0.6848	0.0000	369	0.23	1.79	3.25
C020-006	6	0.0082	0.0264	0.0261	0.6848	0.0000	369	0.23	1.78	3.14
C020-006	7	0.0082	0.0264	0.0261	0.6848	0.0000	369	0.23	1.82	3.15
C020-006	8	0.0082	0.0264	0.0261	0.6848	0.0000	369	0.27	1.79	3.17
C020-006	9	0.0082	0.0264	0.0261	0.6848	0.0000	369	0.25	1.83	3.17
C020-006	10	0.0082	0.0264	0.0261	0.6848	0.0000	369	0.25	1.87	3.17
F. Solution:	10	0.0082	0.0264	0.0261	0.6848	0.0000	369	2.42	18.18	31.67
C020-007	1	0.0000	0.0149	0.0149	1.0000	0.0000	0	0.23	0.28	0.31
F. Solution:	1	0.0000	0.0149	0.0149	1.0000	0.0000	0	0.23	0.28	0.31
C020-008	1	0.0043	0.0262	0.0262	0.8363	0.0000	0	0.22	0.30	0.28
F. Solution:	1	0.0043	0.0262	0.0262	0.8363	0.0000	0	0.22	0.30	0.28
C020-009	1	0.0023	0.0207	0.0218	0.8950	0.0527	421	0.22	1.42	2.67
C020-009	2	0.0023	0.0207	0.0218	0.8950	0.0527	421	0.23	1.45	2.75
C020-009	3	0.0023	0.0207	0.0218	0.8950	0.0527	421	0.22	1.42	2.76
C020-009	4	0.0023	0.0207	0.0218	0.8950	0.0527	421	0.22	1.40	2.67
C020-009	5	0.0023	0.0207	0.0218	0.8950	0.0527	421	0.22	1.40	2.72
C020-009	6	0.0023	0.0207	0.0218	0.8950	0.0527	421	0.20	1.45	2.71
C020-009	7	0.0023	0.0207	0.0218	0.8950	0.0527	421	0.22	1.42	2.70
C020-009	8	0.0023	0.0207	0.0218	0.8950	0.0527	421	0.22	1.42	2.70
C020-009	9	0.0023	0.0207	0.0218	0.8950	0.0527	421	0.22	1.42	2.70
C020-009	10	0.0023	0.0207	0.0218	0.8950	0.0527	421	0.22	1.44	2.73
F. Solution:	10	0.0023	0.0207	0.0218	0.8950	0.0527	421	2.18	14.24	27.10
C020-010	1	0.0007	0.0209	0.0231	0.9682	0.0957	0	0.31	2.84	2.26
F. Solution:	1	0.0007	0.0209	0.0231	0.9682	0.0957	0	0.31	2.84	2.26
C020-011	1	0.0006	0.0149	0.0150	0.9572	0.0105	0	0.17	1.00	0.76
C020-011	2	0.0006	0.0149	0.0150	0.9572	0.0105	0	0.19	1.01	0.78
C020-011	3	0.0006	0.0149	0.0150	0.9572	0.0105	0	0.19	1.03	0.78
C020-011	4	0.0006	0.0149	0.0150	0.9572	0.0105	0	0.19	1.01	0.78
C020-011	5	0.0006	0.0149	0.0150	0.9572	0.0105	0	0.19	1.00	0.80
C020-011	6	0.0006	0.0149	0.0150	0.9572	0.0105	0	0.17	1.00	0.92
C020-011	7	0.0006	0.0149	0.0150	0.9572	0.0105	0	0.17	1.03	0.81
F. Solution:	7	0.0006	0.0149	0.0150	0.9572	0.0105	0	1.26	7.08	5.63

(It is continued in the next page)

Results table for 20 aircrafts ($\lambda = 0.80$).

Case	Iter.	z_{lp}	z_s	z_{ip}	GAP_{lp}	GAP_s	nn	t_{lp}	t_s	t_{ip}
C020-012	1	0.0045	0.0279	0.0279	0.8402	0.0000	0	0.25	0.91	0.97
F. Solution:	1	0.0045	0.0279	0.0279	0.8402	0.0000	0	0.25	0.91	0.97
C020-013	1	0.0022	0.0258	0.0263	0.9177	0.0191	35	0.31	1.98	2.60
C020-013	2	0.0022	0.0258	0.0263	0.9177	0.0191	35	0.31	1.97	2.62
F. Solution:	2	0.0022	0.0258	0.0263	0.9177	0.0191	35	0.62	3.95	5.23
C020-014	1	0.0000	0.0174	0.0174	0.9978	0.0000	0	0.20	0.94	0.95
F. Solution:	1	0.0000	0.0174	0.0174	0.9978	0.0000	0	0.20	0.94	0.95
C020-015	1	0.0000	0.0149	0.0149	1.0000	0.0000	0	0.19	0.67	0.52
F. Solution:	1	0.0000	0.0149	0.0149	1.0000	0.0000	0	0.19	0.67	0.52
C020-016	1	0.0000	0.0130	0.0129	1.0000	0.0000	40	0.19	0.53	1.59
C020-016	2	0.0000	0.0130	0.0129	1.0000	0.0000	40	0.19	0.53	1.58
C020-016	3	0.0000	0.0130	0.0129	1.0000	0.0000	40	0.17	0.53	1.59
C020-016	4	0.0000	0.0130	0.0129	1.0000	0.0000	40	0.17	0.55	1.57
C020-016	5	0.0000	0.0130	0.0129	1.0000	0.0000	40	0.19	0.53	1.59
C020-016	6	0.0000	0.0130	0.0129	1.0000	0.0000	40	0.19	0.56	1.59
C020-016	7	0.0000	0.0130	0.0129	1.0000	0.0000	40	0.17	0.55	1.56
C020-016	8	0.0000	0.0130	0.0129	1.0000	0.0000	40	0.25	0.55	1.62
C020-016	9	0.0000	0.0130	0.0129	1.0000	0.0000	40	0.17	0.55	1.56
F. Solution:	9	0.0000	0.0130	0.0129	1.0000	0.0000	40	1.69	4.87	14.26
C020-017	1	0.0020	0.0209	0.0209	0.9032	0.0000	0	0.22	0.86	0.86
F. Solution:	1	0.0020	0.0209	0.0209	0.9032	0.0000	0	0.22	0.86	0.86
C020-018	1	0.0000	0.0139	0.0139	1.0000	0.0000	0	0.20	0.31	0.25
F. Solution:	1	0.0000	0.0139	0.0139	1.0000	0.0000	0	0.20	0.31	0.25
C020-019	1	0.0000	0.0144	0.0144	1.0000	0.0000	0	0.20	0.56	0.56
F. Solution:	1	0.0000	0.0144	0.0144	1.0000	0.0000	0	0.20	0.56	0.56
C020-020	1	0.0001	0.0206	0.0206	0.9969	0.0000	319	0.23	1.64	5.79
C020-020	2	0.0001	0.0206	0.0206	0.9969	0.0000	319	0.26	1.64	5.74
C020-020	3	0.0001	0.0206	0.0206	0.9969	0.0000	319	0.23	1.64	5.77
C020-020	4	0.0001	0.0206	0.0206	0.9969	0.0000	319	0.23	1.64	5.83
C020-020	5	0.0001	0.0206	0.0206	0.9969	0.0000	319	0.23	1.61	5.79
C020-020	6	0.0001	0.0206	0.0206	0.9969	0.0000	319	0.23	1.64	5.76
C020-020	7	0.0001	0.0206	0.0206	0.9969	0.0000	319	0.23	1.62	5.87
C020-020	8	0.0001	0.0206	0.0206	0.9969	0.0000	319	0.23	1.61	5.87
C020-020	9	0.0001	0.0206	0.0206	0.9969	0.0000	319	0.23	1.61	5.83
C020-020	10	0.0001	0.0206	0.0206	0.9969	0.0000	319	0.23	1.65	5.84
F. Solution:	10	0.0001	0.0206	0.0206	0.9969	0.0000	319	2.37	16.29	58.08
C020-021	1	0.0009	0.0226	0.0228	0.9604	0.0120	0	0.22	2.39	0.97
F. Solution:	1	0.0009	0.0226	0.0228	0.9604	0.0120	0	0.22	2.39	0.97
C020-022	1	0.0002	0.0167	0.0167	0.9853	0.0000	0	0.20	0.27	0.28
F. Solution:	1	0.0002	0.0167	0.0167	0.9853	0.0000	0	0.20	0.27	0.28
C020-023	1	0.0000	0.0152	0.0152	0.9990	0.0000	0	0.16	0.19	0.22
F. Solution:	1	0.0000	0.0152	0.0152	0.9990	0.0000	0	0.16	0.19	0.22

(It is continued in the next page)

Results table for 20 aircrafts ($\lambda = 0.80$).

Case	Iter.	z_{lp}	z_s	z_{ip}	GAP_{lp}	GAP_s	nn	t_{lp}	t_s	t_{ip}
C020-024	1	0.0041	0.0203	0.0212	0.8081	0.0435	0	0.25	2.51	1.11
C020-024	2	0.0041	0.0203	0.0212	0.8081	0.0435	0	0.23	2.50	1.09
C020-024	3	0.0041	0.0203	0.0212	0.8081	0.0435	0	0.23	2.50	1.11
C020-024	4	0.0041	0.0203	0.0212	0.8081	0.0435	0	0.25	2.50	1.11
C020-024	5	0.0041	0.0203	0.0212	0.8081	0.0435	0	0.31	2.50	1.11
C020-024	6	0.0041	0.0203	0.0212	0.8081	0.0435	0	0.23	2.53	1.19
C020-024	7	0.0041	0.0203	0.0212	0.8081	0.0435	0	0.23	2.50	1.08
C020-024	8	0.0041	0.0203	0.0212	0.8081	0.0435	0	0.23	2.50	1.11
C020-024	9	0.0041	0.0203	0.0212	0.8081	0.0435	0	0.23	2.48	1.12
F. Solution:	9	0.0041	0.0203	0.0212	0.8081	0.0435	0	2.22	22.50	10.02
C020-025	1	0.0000	0.0183	0.0183	1.0000	0.0000	0	0.17	0.25	0.36
F. Solution:	1	0.0000	0.0183	0.0183	1.0000	0.0000	0	0.17	0.25	0.36
C020	3.4	0.0013	0.0184	0.0186	0.9291	0.0101	60.7	0.76	4.60	9.83

(Table end.)

Table B.3: CPLEX cuts for 20 aircrafts ($\lambda = 0.80$).

Case	Iter.	Clique	Cover	Implied	Flow	MIR	Zero-half	Gomory	Total
C020-001	1	0	0	2	41	0	0	7	50
Averages:	1	0.0	0.0	2.0	41.0	0.0	0.0	7.0	50.0
C020-002	1	0	0	13	195	13	0	62	283
C020-002	2	0	0	13	195	13	0	62	283
C020-002	3	0	0	13	195	13	0	62	283
C020-002	4	0	0	13	195	13	0	62	283
C020-002	5	0	0	13	195	13	0	62	283
C020-002	6	0	0	13	195	13	0	62	283
C020-002	7	0	0	13	195	13	0	62	283
C020-002	8	0	0	13	195	13	0	62	283
C020-002	9	0	0	13	195	13	0	62	283
C020-002	10	0	0	13	195	13	0	62	283
Averages:	10	0.0	0.0	13.0	195.0	13.0	0.0	62.0	283.0
C020-003	1	0	0	0	0	0	0	0	0
Averages:	1	0.0	0.0	0.0	0.0	0.0	0.0	0.0	0.0
C020-004	1	0	0	0	0	0	0	0	0
Averages:	1	0.0	0.0	0.0	0.0	0.0	0.0	0.0	0.0
C020-005	1	0	0	0	0	0	0	0	0
Averages:	1	0.0	0.0	0.0	0.0	0.0	0.0	0.0	0.0

(It is continued in the next page)

CPLEX cuts table for 20 aircrafts ($\lambda = 0.80$).

Case	Iter.	Clique	Cover	Implied	Flow	MIR	Zero-half	Gomory	Total
C020-006	1	0	0	0	95	0	0	13	108
C020-006	2	0	0	0	95	0	0	13	108
C020-006	3	0	0	0	95	0	0	13	108
C020-006	4	0	0	0	95	0	0	13	108
C020-006	5	0	0	0	95	0	0	13	108
C020-006	6	0	0	0	95	0	0	13	108
C020-006	7	0	0	0	95	0	0	13	108
C020-006	8	0	0	0	95	0	0	13	108
C020-006	9	0	0	0	95	0	0	13	108
C020-006	10	0	0	0	95	0	0	13	108
Averages:	10	0.0	0.0	0.0	95.0	0.0	0.0	13.0	108.0
C020-007	1	0	0	0	0	0	0	0	0
Averages:	1	0.0	0.0	0.0	0.0	0.0	0.0	0.0	0.0
C020-008	1	0	0	0	0	0	0	0	0
Averages:	1	0.0	0.0	0.0	0.0	0.0	0.0	0.0	0.0
C020-009	1	0	0	1	90	0	0	17	108
C020-009	2	0	0	1	90	0	0	17	108
C020-009	3	0	0	1	90	0	0	17	108
C020-009	4	0	0	1	90	0	0	17	108
C020-009	5	0	0	1	90	0	0	17	108
C020-009	6	0	0	1	90	0	0	17	108
C020-009	7	0	0	1	90	0	0	17	108
C020-009	8	0	0	1	90	0	0	17	108
C020-009	9	0	0	1	90	0	0	17	108
C020-009	10	0	0	1	90	0	0	17	108
Averages:	10	0.0	0.0	1.0	90.0	0.0	0.0	17.0	108.0
C020-010	1	0	0	10	273	0	0	91	374
Averages:	1	0.0	0.0	10.0	273.0	0.0	0.0	91.0	374.0
C020-011	1	0	0	2	65	0	0	10	77
C020-011	2	0	0	2	65	0	0	10	77
C020-011	3	0	0	2	65	0	0	10	77
C020-011	4	0	0	2	65	0	0	10	77
C020-011	5	0	0	2	65	0	0	10	77
C020-011	6	0	0	2	65	0	0	10	77
C020-011	7	0	0	2	65	0	0	10	77
Averages:	7	0.0	0.0	2.0	65.0	0.0	0.0	10.0	77.0
C020-012	1	0	0	0	54	0	0	4	58
Averages:	1	0.0	0.0	0.0	54.0	0.0	0.0	4.0	58.0

(It is continued in the next page)

CPLEX cuts table for 20 aircrafts ($\lambda = 0.80$).

Case	Iter.	Clique	Cover	Implied	Flow	MIR	Zero-half	Gomory	Total
C020-013	1	0	1	2	39	0	0	7	49
C020-013	2	0	1	2	39	0	0	7	49
Averages:	2	0.0	1.0	2.0	39.0	0.0	0.0	7.0	49.0
C020-014	1	0	1	13	182	0	0	132	328
Averages:	1	0.0	1.0	13.0	182.0	0.0	0.0	132.0	328.0
C020-015	1	0	0	0	7	0	0	10	17
Averages:	1	0.0	0.0	0.0	7.0	0.0	0.0	10.0	17.0
C020-016	1	0	1	0	66	0	0	6	73
C020-016	2	0	1	0	66	0	0	6	73
C020-016	3	0	1	0	66	0	0	6	73
C020-016	4	0	1	0	66	0	0	6	73
C020-016	5	0	1	0	66	0	0	6	73
C020-016	6	0	1	0	66	0	0	6	73
C020-016	7	0	1	0	66	0	0	6	73
C020-016	8	0	1	0	66	0	0	6	73
C020-016	9	0	1	0	66	0	0	6	73
Averages:	9	0.0	1.0	0.0	66.0	0.0	0.0	6.0	73.0
C020-017	1	0	0	0	56	0	0	6	62
Averages:	1	0.0	0.0	0.0	56.0	0.0	0.0	6.0	62.0
C020-018	1	0	0	0	0	0	0	0	0
Averages:	1	0.0	0.0	0.0	0.0	0.0	0.0	0.0	0.0
C020-019	1	0	0	2	47	0	0	16	65
Averages:	1	0.0	0.0	2.0	47.0	0.0	0.0	16.0	65.0
C020-020	1	0	1	8	178	2	0	82	271
C020-020	2	0	1	8	178	2	0	82	271
C020-020	3	0	1	8	178	2	0	82	271
C020-020	4	0	1	8	178	2	0	82	271
C020-020	5	0	1	8	178	2	0	82	271
C020-020	6	0	1	8	178	2	0	82	271
C020-020	7	0	1	8	178	2	0	82	271
C020-020	8	0	1	8	178	2	0	82	271
C020-020	9	0	1	8	178	2	0	82	271
C020-020	10	0	1	8	178	2	0	82	271
Averages:	10	0.0	1.0	8.0	178.0	2.0	0.0	82.0	271.0
C020-021	1	0	0	11	180	0	0	108	299
Averages:	1	0.0	0.0	11.0	180.0	0.0	0.0	108.0	299.0
C020-022	1	0	0	0	0	0	0	0	0

(It is continued in the next page)

CPLEX cuts table for 20 aircrafts ($\lambda = 0.80$).

Case	Iter.	Clique	Cover	Implied	Flow	MIR	Zero-half	Gomory	Total
Averages:	1	0.0	0.0	0.0	0.0	0.0	0.0	0.0	0.0
C020-023	1	0	0	0	0	0	0	0	0
Averages:	1	0.0	0.0	0.0	0.0	0.0	0.0	0.0	0.0
C020-024	1	0	0	16	213	0	0	94	323
C020-024	2	0	0	16	213	0	0	94	323
C020-024	3	0	0	16	213	0	0	94	323
C020-024	4	0	0	16	213	0	0	94	323
C020-024	5	0	0	16	213	0	0	94	323
C020-024	6	0	0	16	213	0	0	94	323
C020-024	7	0	0	16	213	0	0	94	323
C020-024	8	0	0	16	213	0	0	94	323
C020-024	9	0	0	16	213	0	0	94	323
Averages:	9	0.0	0.0	16.0	213.0	0.0	0.0	94.0	323.0
C020-025	1	0	0	0	0	0	0	0	0
Averages:	1	0.0	0.0	0.0	0.0	0.0	0.0	0.0	0.0
C020	1	0.0	0.2	3.2	71.2	0.6	0.0	26.6	101.8

(Table end.)

B.5 Computational results for the VCTP model (by using the metaheuristic scheme)

Part of the computational experience for the VCTP is presented in detail in this section, by using VNDS. In this reduced version of the thesis, only the results for the cases with 20 aircraft are presented. The rest of the tested cases can be found in the extended version of the thesis in the CD enclosed with this thesis. Additionally, a detailed output of the study cases is also included in the CD. The headings of the table are as follows:

- *Tnit*: Current Taylor iteration.
- *VNDS nit*: Number of VNDS iterations.
- z_{lp}: Value of the objective function for the relaxed model.
- z_{best}: Value of the best solution obtained.
- GAP_{lp}: $\frac{z_{best}-z_{lp}}{z_{best}}$
- t_{best}: Elapsed time to obtain the best solution.

Table B.4: VNDS results for 20 aircrafts, ($\lambda = 0.80$)

Case	Tnit	VNDS nit	z_{lp}	z_{best}	GAP_{lp}	t_{best}
C020-001	1	1	0.0007	0.0162	0.9564	0.78
F. Solution:	1	1.0	0.0007	0.0162	0.9564	0.78
C020-002	1	1	0.0001	0.0159	0.9937	1.37
F. Solution:	1	1.0	0.0001	0.0159	0.9937	1.37
C020-003	1	1	0.0001	0.0134	0.9931	0.33
F. Solution:	1	1.0	0.0001	0.0134	0.9931	0.33
C020-004	1	1	0.0019	0.0183	0.8938	0.38
F. Solution:	1	1.0	0.0019	0.0183	0.8938	0.38
C020-005	1	1	0.0000	0.0115	1.0000	0.37
F. Solution:	1	1.0	0.0000	0.0115	1.0000	0.37

(It is continued in the next page)

VNDS results for 20 aircrafts, ($\lambda = 0.80$) continuation.

Case	Tnit	VNDS nit	z_{lp}	z_{best}	GAP_{lp}	t_{best}
C020-006	1	1	0.0082	0.0264	0.6874	1.61
	2	1	0.0082	0.0264	0.6874	1.56
	3	1	0.0082	0.0264	0.6874	1.54
	4	1	0.0082	0.0264	0.6874	1.56
	5	1	0.0082	0.0264	0.6874	1.56
	6	1	0.0082	0.0264	0.6874	1.58
	7	1	0.0082	0.0264	0.6874	1.56
	8	1	0.0082	0.0264	0.6874	1.55
F. Solution:	8	1.0	0.0082	0.0264	0.6874	12.51
C020-007	1	1	0.0000	0.0149	1.0000	0.23
F. Solution:	1	1.0	0.0000	0.0149	1.0000	0.23
C020-008	1	1	0.0043	0.0262	0.8363	0.36
F. Solution:	1	1.0	0.0043	0.0262	0.8363	0.36
C020-009	1	1	0.0023	0.0220	0.8960	1.01
F. Solution:	1	1.0	0.0023	0.0220	0.8960	1.01
C020-010	1	1	0.0007	0.0231	0.9682	1.86
F. Solution:	1	1.0	0.0007	0.0231	0.9682	1.86
C020-011	1	1	0.0006	0.0150	0.9572	0.30
C020	2	1	0.0006	0.0150	0.9572	0.30
C020	3	1	0.0006	0.0150	0.9572	0.31
C020	4	1	0.0006	0.0150	0.9572	0.31
C020	5	1	0.0006	0.0150	0.9572	0.28
C020	6	1	0.0006	0.0150	0.9572	0.31
F. Solution:	6	1.0	0.0006	0.0150	0.9572	1.81
C020-012	1	1	0.0045	0.0279	0.8402	1.03
F. Solution:	1	1.0	0.0045	0.0279	0.8402	1.03
C020-013	1	1	0.0022	0.0263	0.9177	1.84
F. Solution:	1	1.0	0.0022	0.0263	0.9177	1.84
C020-014	1	1	0.0000	0.0174	0.9978	0.75

(It is continued in the next page)

VNDS results for 20 aircrafts, ($\lambda = 0.80$) continuation.

Case	Tnit	VNDS nit	z_{lp}	z_{best}	GAP_{lp}	t_{best}
F. Solution:	1	1.0	0.0000	0.0174	0.9978	0.75
C020-015	1	1	0.0000	0.0149	1.0000	0.33
F. Solution:	1	1.0	0.0000	0.0149	1.0000	0.33
C020-016	1	1	0.0000	0.0130	1.0000	0.31
F. Solution:	1	1.0	0.0000	0.0130	1.0000	0.31
C020-017	1	1	0.0020	0.0209	0.9032	0.75
F. Solution:	1	1.0	0.0020	0.0209	0.9032	0.75
C020-018	1	1	0.0000	0.0139	1.0000	0.41
F. Solution:	1	1.0	0.0000	0.0139	1.0000	0.41
C020-019	1	1	0.0000	0.0144	1.0000	0.34
F. Solution:	1	1.0	0.0000	0.0144	1.0000	0.34
C020-020	1	1	0.0001	0.0206	0.9969	1.14
F. Solution:	1	1.0	0.0001	0.0206	0.9969	1.14
C020-021	1	1	0.0009	0.0228	0.9604	1.42
F. Solution:	1	1.0	0.0009	0.0228	0.9604	1.42
C020-022	1	1	0.0002	0.0167	0.9853	0.36
F. Solution:	1	1.0	0.0002	0.0167	0.9853	0.36
C020-023	1	1	0.0000	0.0152	0.9990	0.30
F. Solution:	1	1.0	0.0000	0.0152	0.9990	0.30
C020-024	1	1	0.0041	0.0212	0.8081	1.23
	2	1	0.0041	0.0212	0.8081	1.23
	3	1	0.0041	0.0212	0.8081	1.23
	4	1	0.0041	0.0212	0.8081	1.23
	5	1	0.0041	0.0212	0.8081	1.20
	6	1	0.0041	0.0212	0.8081	1.23
	7	1	0.0041	0.0212	0.8081	1.20
F. Solution:	7	1.0	0.0041	0.0212	0.8081	8.57
C020-025	1	1	0.0000	0.0183	1.0000	0.33
F. Solution:	1	1.0	0.0000	0.0183	1.0000	0.33

(It is continued in the next page)

VNDS results for 20 aircrafts, ($\lambda = 0.80$) continuation.

Case	**Tnit**	**VNDS nit**	z_{lp}	z_{best}	GAP_{lp}	t_{best}
Averages:	1.7	1.0	0.0013	0.0187	0.9292	1.56

(Table end.)

Bibliography

[1] *An adaptive learning method for SOM based navigation system and its application to an underwater robot*, Kitakyushu, Japan, 2003.

[2] S. Alam, H.A. Abbass, C.J. Lokan, M. Ellejmi, and S. Kirby. Computational red teaming to investigate failure patterns in medium term conflict detection. 8th Innovative Research Workshop & Exhibition, 2009.

[3] S. Alam, M. McPartland, M. Barlow, P. Lindsay, and H.A. Abbass. Neural evolution for collision detection & resolution in a 2d free flight environment. Technical Report TR-ALAR-200507012, The Artificial Life and Adaptative Robotics Laboratory, University of New South Wales, 2005.

[4] S. Alam, K. Shafi, H.A. Abbass, and M. Barlow. Forming an intelligent ensemble of conflict detection algorithms in free flight by data mining the scenario space. Technical Report TR-ALAR-200802003, The Artificial Life and Adaptative Robotics Laboratory, University of New South Wales.

[5] S. Alam, K. Shafi, H.A. Abbass, and M. Barlow. An ensemble approach for conflict detection in free flight by data mining. *Transportation Research Part C*, 17(3):298–317, 2009.

[6] M. Almiñana, L.F. Escudero, M. Landete, J.F. Monge, A. Rabasa, and J. Sánchez-Soriano. On a mixed 0-1 separable nonlinear approach for water irrigation scheduling. *IIE Transactions*, 44(4):398–405, 2008.

[7] A. Alonso-Ayuso, L.F. Escudero, and F.J. Martín-Campo. Collision avoidance for the atm problem: A mixed 0-1 nonlinear model. In Andrew J. Miller Annick Sartenaer Pierre Bonami, Leo Liberti, editor, *Proceedings of the Workshop on Mixed Integer Nonlinear Programming*, pages 95–102, Marseille, France, 2010.

[8] A. Alonso-Ayuso, L.F. Escudero, and F.J. Martín-Campo. Collision avoidance in the air traffic management: A mixed integer linear optimization approach. *IEEE Transactions on Intelligent Transportation Systems, DOI: 10.1109/TITS.2010.2061971*, 2010.

[9] A. Alonso-Ayuso, L.F. Escudero, and F.J. Martín-Campo. On optimizing the collision avoidance in the air traffic management. In *Proceedings of the 9th Innovative Research Workshop & Exhibition (Submitted for publication)*, Brétigny-Sur-Orge (Paris), France, 2010.

[10] A. Alonso-Ayuso, L.F. Escudero, P. Olaso, and C. Pizarro. Conflict avoidance: 0-1 linear models for conflict detection & resolution. *Submitted for publication*.

[11] N. Barnier and C. Allignol. 4d-trajectory deconfliction through departure time adjustment. 8th USA/Europe air traffic management research and development seminar (ATM2009), 2009.

[12] A. M. Bayen, P. Grieder, G. Meyer, and C. J. Tomlin. Lagrangian delay predictive model for sector-based air traffic flow. *Journal of Guidance, Control and Dynamics*, 28(5):1015–1026, 2005.

[13] D.P. Bertsekas. *Constrained Optimization and Lagrange Multiplier Methods*. Academic Press, 1982.

[14] A. Bicchi and L. Pallottino. On optimal cooperative conflict resolution for air traffic management systems. *IEEE Transactions on Intelligent Transportation Systems*, 1(4):221–232, 2000.

[15] K.D. Bilimoria. A geometric optimization approach to aircraft conflict resolution. AIAA Guidance, Navigation, and Control Conference and Exhibit, Denver (USA), 2001.

[16] B. Carpenter and J. Kuchar. Probability-based collision alerting logic for closely-spaced parallel approach. In *35th AIAA Aerospace Sciences Meeting Exhibit*, Reno, NV, 1997.

[17] C.Cetek. Realistic speed change maneuvers for air traffic conflict avoidance and their impact on aircraft economics. *International Journal of Civil Aviation*, 1(1):62–73, 2009.

[18] G. Chaloulos, G. P. Roussos, J. Lygeros, and K.J. Kyriakopoulos. Mid and short term conflict resolution in autonomous aircraft operations. In *Proceedings of the 8th Innovative Research Workshop & Exhibition*, Eurocontrol, Brétigny-Sur-Orge (Paris), France, 2009.

[19] Y. Chiang, J. T. Klosowski, C. Lee, and J. S. B. Mitchell. Geometric algorithms for conflict detection/resolution in air traffic management. In *In 36th IEEE Conference on Decision and Control.*, pages 10–12, 1997.

[20] M. A. Christodoulou and C. Costoulakis. Nonlinear mixed integer programming for aircraft collision avoidance in free flight. *IEEE Melecon 2004, Dubrovnik, Croacia*, 1:327–330, 2004. ISBN: 0-7803-8271-4.

[21] M. A. Christodoulou and S. G. Kodaxakis. Automatic commercial aircraft-collision avoidance in free flight: The three-dimensional problem. *IEEE Transactions on Intelligent Transportation Systems*, 7(2):242–249, 2006.

[22] M.A. Christodoulou and C. Kontogeorgou. Automatic collision avoidance in commercial aircraft three dimensional flights, using neural networks and non-linear programming. In C.H. Skiadas, editor, *Chaotic Modeling and Simulation*, 2008.

[23] R.A. Coppenbarger, R. Lanier, D. Sweet, and S. Dorsky. Design and development of the en route descent advisor (eda) for conflict-free arrival metering. AIAA GN&C conference, 2004.

[24] P. Dell'Olmo and G. Lulli. A new hierarchical architecture for air traffic management: Optimization of airway capacity in a free flight scenario. *European Journal of Operational Research*, 144:179–193, 2003.

[25] D. V. Dimarogonas and K. J. Kyriakopoulos. Inventory of decentralized conflict detection and resolution systems in air traffic, 2003.

[26] A. Doshi. *Aircraft Position Prediction Using Neural Networks*. PhD thesis, Department of Electrical Engineering and Computer Science, Massachusetts Institute of Technology (CA), USA, 2005.

[27] G. Dowek, A. Geser, and C. Muñoz. Tactical conflict detection and resolution in a 3-d airspace. 4th USA/Europe Air Traffic Management R&D Seminar Santa Fe. (AZ), USA, 2001.

[28] G. Dowek and C. Muñoz. Conflict detection and resolution for 1,2,...,n aircraft. Seventh AIAA Aviation Technology, Integration and Operations conference, Belfast (Northern Ireland), 2007.

[29] F. Drogoul, P. Averty, and R. Weber. Erasmus strategic deconfliction to benefit sesar. 8th USA/Europe air traffic management research and development seminar (ATM2009), 2009.

[30] V. N. Duong and E. G. Hoffman. Conflict resolution advisory service in autonomous aircraft operations. In *16th Digital Avion. Syst. Conf.*, pages 9.3–10–9.3–17, Irvine, (CA), USA, 1997.

[31] N. Durand and J.M. Alliot. Ant colony optimization for air traffic conflict resolution. 8th USA/Europe air traffic management research and development seminar (ATM2009), 2009.

[32] N. Durand, J.M. Alliot, and F. Médioni. Neural nets trained by genetic algorithms for collision avoidance. *Applied Intelligence*, (13):205–213, 2000.

[33] H. Erzberger and R. Paielli. Conflict probability estimation for free flight. *AIAA Journal of Guidance, Control, and Dynamics*, 20, 1997.

[34] H. Erzberger, R. A. Paielli, D. R. Isaacson, and M. M. Eshow X. Conflict detection and resolution in the presence of prediction error, 1997. prepared for the 1st USA/Europe Air Traffic Management RD Seminar, Saclay, France.

[35] EUROCONTROL. *Fasti ATC Manual*. http://www.eurocontrol.int/fasti last access was in October, 2009.

[36] FICO. *XPRESS-MP. User's Manual for XPRESS-MP*. 2009.

[37] M. Fischetti, F. Glover, and A. Lodi. The feasibility pump. *Mathematical Programming*, 104:91–104, 2005.

[38] M. Fischetti and A. Lodi. Local branching. *Mathematical Programming Series B*, 98:23–47, 2003.

[39] E. Frazzoli, Z.-H. Mao, J.-H. Oh, and E. Feron. Resolution of conflicts involving many aircraft via semidefinite programming. *AIAA Journal of Guidance, Control and Dynamics*, pages 79–86, 1999.

[40] A.L. Galdino, C. Muñoz, and M. Ayala-Rincón. Formal verification of an optimal air traffic conflict resolution and recovery algorithm. Proceedings of the 11th working conference on correct hardware design and verification methods. CHARME 2001, 2001.

[41] GAMS INC. *GAMS. User's Manual for GAMS 23.5.2*. 2009.

[42] T. Gandhi, M.T. Yang, R. Kasturi, O.I. Camps, L. Coraor, and J. McCandless. Detection of obstacles in the flight path of an aircraft. In *IEEE Transactions on Aerospace and Electronic Systems*, volume 39, pages 176–191, 2000.

[43] S. Gaukrodger, W. Wong, B. Fields, M. Loomes, F. Han, M. Muñoz, F. Reiter, and A. Monteleone. The multi-conflict display. Eurocontrol, Brétigny-Sur-Orge (Paris), France, 2009. 8th Innovative Research Workshop & Exhibition.

[44] A.M. Geoffrion. Lagrangean relaxation for integer programming. *Mathematical Programming*, 2:82–114, 1974.

[45] A. Geser and C. Muñoz. A geometric approach to strategic conflict detection and resolution. pages 6B1.1 – 6B1.11. Proceedings of the digital avionics systems conference, 2002.

[46] C. Goodchild, M. A. Vilaplana, and S. Elefante. Co-operative optimal airborne separation assurance in free flight airspace. Third USA/Europe Air Trafic Management RD seminar, Napoli (Italy), 2000.

[47] M. Guignard. Lagrangean relaxation. *TOP*, 11:151–228, 2003.

[48] M. Guignard and S. Kim. Lagrangean decomposition. a model yielding stronger lagrangean bounds. *Mathematical Programming*, 39:215–228, 1987.

[49] GUROBI Optimization. *User's Manual for GUROBI*. 2010.

[50] P. Hansen and N. Mladenović. First improvement may be better than best improvement: An empirical study. *Discrete Applied Mathematics*, 154:802–817, 2006.

[51] M. Held and R.M. Karp. The traveling salesman problem and minimum spanning trees: part ii. *Mathematical Programming*, 6:62–88, 1971.

[52] M. Held, P. Wolfe, and H. Crowder. Validation of subgradient optimization. *Mathematical Programming*, 6:62–88, 1974.

[53] J. Hoekstra, R. van Gent, and R. Ruigrok. Conceptual design of free flight with airborne separation assurance. In *AIAA Guidance, Navigation, Control Conference*, volume AIAA-98-4239, pages 807–817, Boston, (MA), USA, 1998.

[54] J. Hu. *A Study of Conflict Detection and Resolution in Free Flight*. M.s. thesis, Department of EECS, University of California, USA, 1999.

[55] J. Hu. *On Optimal Collision Avoidance and Formation Switching on Riemannian Manifolds*. M.a. thesis, Mathematics Department, University of California, USA, 2002.

[56] J. Hu, M. Prandini, and S. Sastry. Optimal coordinated maneuvers for three dimensional aircraft conflict resolution. *AIAA Journal of Guidance, Control and Dynamics*, 25(5):888–900, 2002.

[57] J. Hu, M. Prandini, and S. Sastry. Optimal coordinated motions for multiple agents moving on a plane. *SIAM Journal on Control and Optimization*, 42(2):637–668, 2003.

[58] J. Hu, M. Prandini, and S. Sastry. Probabilistic safety analysis in three dimensional aircraft flight. In *Decision and Control, 2003. Proceedings 42nd IEEE Conference on*, volume 5, pages 5335–5340, 2003.

[59] J. Hu, M. Prandini, and S. Sastry. Aircraft conflict detection in presence of a spatially correlated wind field. *IEEE Trans. on Intelligent Transportation Systems*, 6(3):326–340, 2005.

[60] J. Hu, M. Prandini, and C. Tomlin. Interesting conjugate points in formation constrained optimal multi-agent coordination. *American Control Conference, 2005. Proceedings of the 2005*, 3:1871– 1876, 2005.

[61] J. Hu, M. Prandini, and C. Tomlin. Conjugate points in formation constrained optimal multi-agent coordination: A case study. *SIAM Journal on Control and Optimization*, 45:2119–2137, 2007. Submitted for publication. Available upon request.

[62] J. Hu and S. Sastry. Optimal collision avoidance and formation switching on riemanian manifolds. In *Decision and Control, 2001. Proceedings of the 40th IEEE Conference on*, volume 2, pages 1071–1076, 2001.

[63] IBM ILOG. *CPLEX v12.1. User's Manual for CPLEX*. 2009.

[64] INFORMS. *COIN-OR. User's Manual for COIN-OR*. 2009.

[65] K. Ishii, S. Nishida, K. Watanabe, and T. Ura. A collision avoidance system based on self-organizing map and its application to an underwater vehicle. *7th International Conference on Control, Automation, Robotics and Vision, ICARCV*, 2:602–607, 2002.

[66] M. R. Jardin. Real-time conflict-free trajectory optimization. Fifth USA/Europe Air Trafic Management RD seminar, Budapest (Hungary), 2003.

[67] M. R. Jardin. *Toward Real-Time en Route Air Traffic Control Optimization.* PhD thesis, Stanord University, Palo Alto (CA), USA, 2003.

[68] M. R. Jardin. Grid-based strategic air traffic conflict detection. In *2005 AIAA Guidance, Navigation, and Control Conference and Exhibition*, San Francisco (CA), USA, 2005.

[69] J.H. Kim, S. Hayakawa, T. Suzuki, K. Hayashi, S. Okuma, N. Tsuchida, M. Shimizu, and S. Kido. Modeling of driver's collision avoidance maneuver based on controller switching model. *Systems, Man, and Cybernetics, Part B: Cybernetics, IEEE Transactions on*, 35(6):1131–1143, 2005.

[70] J. Krozel and M. Peters. Strategic conflict detection and resolution for free flight. In *Proceedings of the 36th Conference on Decision & Control*, pages 1822–1828, 1997.

[71] J. K. Kuchar and L. C. Yang. A review of conflict detection and resolution modeling methods. *IEEE Transactions on Intelligent Transportation Systems*, 1:179–189, 2000.

[72] J. Lazić, S. Hanafi, N. Mladenović, and D. Urošević. Variable neighbourhood decomposition search for 0-1 mixed integer programs. *Computers & Operations Research*, 37:1055–1067, 2010.

[73] L. Liberti, G. Nannicini, and N. Mladenović. A good recipe for solving minlps. *Matheuristics: Annals of Information Systems, DOI: 10.1007-978-1-4419-1306-7-9*, 10:231–244, 2009.

[74] C.S. Ma and R. H. Miller. Mixed integer linear programming trajectory generation for autonomous nap-of-the earth flight in a threat environment. *Aerospace Conference, 2005 IEEE*, pages 1–9, 2005.

[75] T. Magister. Conflict detection and resolution in the vecinity of the top of descent point. *Promet*, 14(6):269–275, 2002.

[76] T. Magister. Avoidance maneuvering in the vecinity of the top of descent. *J. Aerospace Engineering*, 17(4):176–181, 2004.

[77] Z.-H. Mao, D. Dugail, and E. Feron. Space partition for conflict resolution of intersecting flows of mobile agents. *IEEE Transactions on Intelligent Transportation Systems*, 8(3):512–527, 2007.

[78] Z.-H. Mao, E. Feron, and K. Bilimoria. Stability and performance of intersecting aircraft flows under decentralized conflict avoidance rules. *IEEE Transactions on Intelligent Transportation Systems*, 2(2):101–109, 2001.

[79] Z.H. Mao, D. Dugail, E. Feron, and K. Bilimoria. Stability of intersecting aircraft flows using heading-change maneuvers for conflict avoidance. *IEEE Transactions on Intelligent Transportation Systems*, 6(4):357–369, 2005.

[80] M. Mukai, T. Kawabe, H. Nishira, Y. Takagi, and Y. Deguchi. On vehicle path generation method for collision avoidance using mixed integer programming. In *Proc. of the 2007 IEEE Conference on Control Applications*, Singapore, 2007.

[81] M. Mukai, J. Murata, T. Kawabe, H. Nisira, Y. Takagi, and Y. Deguchi. Optimal path generation for automotive collision avoidance using mixed integer programming. *SICE Journal of Control, Measurement and System Integration*, 1(3):222–226, 2008.

[82] NASA. Workshop flight deck centered parallel runway approaches in instrument meteorological conditions. In M. Waller and C. Scanlon, editors, *Proceedings of the NASA Workshop on Flight Deck Centered Parallel Runway Approaches in Instrument Meteorological Conditions*, pages 8–19, Hampton, VA (USA), 1996. NASA Conf. Pub. 10191.

[83] S. Nishida, K. Ishii, and T. Furukawa. An adaptive controller system using mnsom. *International Congress Series*, 1291:181–184, 2006.

[84] L. Pallottino. *Aircraft Conflict Resolution in "FREE FLIGHT" Air Traffic Management Systems: Models and Optimal Solutions*. PhD thesis, Automation and Industrial Robotics, Università di Pisa (Italy), 2002.

[85] L. Pallottino, E. Feron, and A. Bicchi. Conflict resolution problems for air traffic management systems solved with mixed integer programming. *IEEE Transactions on Intelligent Transportation Systems*, 3(1):3–11, 2002.

[86] J. J. Pannequin, A. M. Bayen, I. M. Mitchell, H. Chung, and S. Sastry. Multiple aircraft deconflicted path planning with weather avoidance constraints. In *AIAA Guidance, Navigation and Control Conference*, Hilton Head, USA, 2007.

[87] L. Peng and Y. Lin. Study on the model for horizontal escape maneuvers in tcas. *Transactions on intelligent transportation systems*, 2:392–398, 2010.

[88] M. Prandini and J. Hu. Application of reachability analysis for stochastic hybrid systems to aircraft conflict prediction. Technical report, IEEE Transactions on Automatic Control, 2008.

[89] M. Prandini, J. Hu, J. Lygeros, and S. Sastry. A probabilistic approach to aircraft conflict detection. *IEEE Trans. on Intelligent Transportation Systems. Special issue on Air Traffic Control*, 1(4):199–220, 2000.

[90] M. Prandini, J. Lygeros, A. Nilim, and S. Sastry. A probabilistic framework for aircraft conflict detection. In *AIAA Guidance, Navigation and Control*, Portland (OR), USA, 1999.

[91] T. Prevot, V. Batiste, E. Palmer, and S. Shelden. Air traffic concept utilizing 4d trajectories and airborne separation assistance. AIAA, Reston (Virginia), USA, 2003.

[92] J. J. Rebollo, I. Maza, and A. Ollero. A two step velocity planning method for real-time collision avoidance of multiple aerial robots in dynamic enviroments. Seventeenth World Congress. The International Federation of Automatic Control, Seoul (Korea), 2008.

[93] A. G. Richards and J. P. How. Aircraft trajectory planning with collision avoidance using mixed integer linear programming. American Control Conference, Anchorage (Alaska), USA, 2002.

[94] A. G. Richards and J. P. How. Model predictive control of vehicle maneuvers with guaranteed completion time and robust feasibility. IEEE American Control Conference, 2003.

[95] G.P. Roussos, D.V. Dimarogonas, and K.J. Kyriakopoulos. Distributed 3d navigation and collision avoidance for nonholonomic aircraft-like vehicles. Budapest, Hungary, 2009. European Control Conference.

[96] Radio Technical Committee on Aeronautics RTCA. Minimum performance specifications for tcas airborne equipment. Document No. RTCA/DO185, Washington, DC, USA, 1983.

[97] T. Schouwenaars, M. Valenti, E. Feron, and J. How. Implementation and flight test results of milp-based uav guidance. In *Aerospace Conference, 2005 IEEE*, pages 1–13, 2005.

[98] T. Sharma, P. Williams, C. Bil, and A. Eberhard. Optimal three dimensional aircraft terrain following and collision avoidance. *Anziam J.*, (47):C695–C711, 2007.

[99] J.M. Shewchun, Oh Jae-Hyuk, and E. Feron. Linear matrix inequalities for free flight conflict problems. In *Proceedings of the 36th IEEE Conference on Decision and Control, 1997*, volume 3, pages 2417–2422, San Diego, (CA), USA, 1997.

[100] K. Sigurd and J. How. Uav trajectory design using total field collision avoidance. AIAA Guidance, Navigation and Control conference, 2003.

[101] C. Tomlin, G. J. Pappas, and S. Sastry. Conflict resolution for air traffic management: A study in multiagent hybrid systems. *IEEE Transactions on Automatic Control*, 43(4):509–521, 1998.

[102] K. Treleaven. *Conflict Resolution and Traffic Complexity of Multiple Intersecting Flows of Aircraft*. PhD thesis, Faculty of the School of Engineering, University of Pittsburgh, Pittsburgh, (PA), USA, 2007.

[103] K. Zeghal and E. Hoffman. Design of cockpit displays for limited delegation of separation assurance. In *18th Digital Avion. Syst. Conf.*, St. Louis, (MO), USA, 1999.

[104] Z. Zhong and Zhang Xuejun. An improved geometric approach to conflict resolution in curve trajectory. Beijing, China, 2009. 9th International Conference on Electronic Measurement & Instruments.

[105] ZIBerlin. *SCIP. User's Manual for SCIP*. 2009.